Winter 2002

Modeling the Biogeochemical Cycle of Selenium in the San Francisco Bay

Shannon L. Meseck
Old Dominion University

MODELING THE BIOGEOCHEMICAL CYCLE OF SELENIUM IN THE SAN FRANCISCO BAY

by

Shannon L. Meseck
B.S. June 1997, State University of New York at Plattsburgh

A Dissertation Submitted to the Faculty of
Old Dominion University in Partial Fulfillment of the
Requirement for the Degree of

DOCTOR OF PHILOSOPHY

OCEANOGRAPHY

OLD DOMINION UNIVERSITY
December 2002

Approved by:

Gregory A. Cutter (Director)

Eileen Hofmann (Member)

Samuel N. Luoma (Member)

James G. Sanders (Member)

ABSTRACT

MODELING THE BIOGEOCHEMICAL CYCLE OF SELENIUM IN THE SAN FRANCISCO BAY

Shannon L. Meseck
Old Dominion University, 2002
Director: Gregory A. Cutter

Due to recent concerns about selenium toxicity in the San Francisco Bay and the roles of refinery and San Joaquin River inputs on the selenium cycle, the model ECoS 3 (distributed from Plymouth Marine Laboratory, United Kingdom) was modified to simulate the biogeochemical cycle of selenium in the Northern Reach. The model is designed to simulate salinity, total suspended material, phytoplankton concentrations, dissolved selenium and its speciation (selenite, selenate, and organic selenide), and particulate selenium and its speciation (selenite+selenate, elemental selenium, and organic selenide). Actual data from 1999 were used to calibrate the model, while data from other sampling periods (1986-1988 and 1997-1998) were then compared to model simulations to verify its accuracy. The sensitivity of the model to specific inputs of selenium was also determined. These results indicate that dissolved selenium is largely controlled by riverine and refinery inputs, while particulate selenium is a function of phytoplankton productivity and riverine inputs of sediment. Forecasting simulations included increasing the San Joaquin River discharge to the Delta and varying refinery discharges to the Bay. These simulation results indicate that total particulate selenium concentrations may increase in the entire Bay to 1 $\mu g\ g^{-1}$ if the San Joaquin Flow is increased. This concentration is twice as high as the current estuarine average particulate selenium and at the level where the concentration of selenium in *Potomocorbula*

amurensis becomes problematic for estuarine predators. Furthermore, simulations suggest that doubling the current refinery loads as selenate have little effect on the particle-associated selenium in the estuary. Simulated data from the model can be used in other models to predict selenium concentrations in higher trophic levels. Furthermore the model can be used as a template to study the biogeochemical cycle of other elements in well-mixed estuaries, and in restoration projects, pollution control and other trophic transfer scenarios.

This thesis is dedicated to my parents Arthur and Carol Meseck.

ACKNOWLEDGMENTS

I would like to thank my committee members Gregory A. Cutter, Eileen E. Hofmann, Samuel N. Luoma, and James G. Sanders who have provided advice and guidance along the way.

The work presented here would not be possible without help from Lynda Cutter and Martina Dublin. I want to thank the many students, Paul Richardson, Aaron Goodman, and Jason Beck who over the years prepared samples for this dissertation. I would like to also thank Katherine Filippino who helped me remain calm when I wanted to see if the computer could fly and Isaac Schroeder and Hae-Cheol Kim who helped me along the way with the modeling.

I especially thank my husband, Jean-Paul Simjouw, who always provided encouragement along the way. My family has provided the encouragement I have needed during my stay here at Old Dominion University.

Over the last 5 years I have had the opportunity to have contact with many students and I would like to thank them for providing friendship to me over the years. I would also like to thank my running partners who have provided an outlet to release my stress.

TABLE OF CONTENTS

Page

LIST OF TABLES

LIST OF FIGURES

CHAPTER I

GENERAL INTRODUCTION

1.1. INTRODUCTION

When a trace element is introduced into an aquatic ecosystem, chemical reactions occur that produce a variety of chemical forms including: organic complexes (e.g., CuL_1), inorganic complexes (e.g., $ZnCl^+$,$ZnCl_2$), and different oxidation states (e.g., Hg^{+2}, Hg^0). The chemical form, or speciation, of a trace element determines its chemical and biochemical reactivity (Sunda, 1988; Bruland et al., 1991). Trace elements undergo chemical and biological reactions as they are transported by rivers to the ocean through estuaries. Estuaries are defined as "semi-enclosed coastal bodies of water which have free connections to the open sea, extending into the river as far as the limit of tidal influence, and within which sea water is measurably diluted with fresh water derived from land drainage" (Dyer, 1997). The mixing of fresh water with sea water causes a change in ionic strength, which can affect the speciation of an element. For example, dissolved cadmium in river water is predominantly found as free Cd^{2+}, but as river water mixes with seawater, the speciation of cadmium is altered to cadmium sulfate complexes (Comans and Van Dijk, 1988). Because estuaries are highly dynamic areas with enhanced biological productivity (Kennish, 1990), removal of a trace element can occur due to biological uptake during estuarine transport (e.g., iron; Gobler et al., 2002).

Past studies of trace elements in estuaries have focused on the speciation of an

---

The model journal for this dissertation was Marine Chemistry

element in the dissolved phase (e.g., Boughriet et al., 1992; Kozelka and Bruland, 1998; Michel et al., 1999), and total concentrations in the particulate phase (e.g., Guentzel et al., 1996; Michel et al, 1999, Zwolsman and van Eck, 1999), in sediments (e.g., Robbe et al., 1985; Jones and Turki, 1997), and in organisms (e.g., Fowler and Benayoun, 1976; Sunda, 1988; Luoma et al., 1992). Additionally, extensive research has been done on modeling how either the physical, biological, or chemical parameters in an estuary individually affect the distribution and speciation of a trace element (e.g., Paucot and Wollast, 1997; Baeyens et al., 1998; Mwanuzi and De Smedt, 1999), but little work has been done in using models to simulate the complete biogeochemical cycle of a trace element (i.e., coupling physical, biological and chemical processes). With recent advances in estuarine modeling, more extensive simulations of the biogeochemical cycle of an element are now possible.

This study used estuarine modeling to simulate the biogeochemical cycle of the metalloid element selenium in the San Francisco Bay estuary, concentrating on its different chemical species. Selenium was chosen because it is essential for all organisms, but can become toxic depending on its chemical speciation and concentration (e.g., Lindstrom and Rodhe, 1978; Wehr and Brown, 1985; Price et al., 1987; Doblin et al., 1999). Added benefits to studying selenium are that there are no contamination problems during sampling and analysis as with some trace metals (e.g., mercury and zinc), and the methodology used to determine the speciation of selenium is well developed (Cutter, 1978; 1983; 1992). The San Francisco Bay is an ideal study area because extensive research has been done to understand its physical characteristics (i.e., its flow regime and

morphology; Walter and Gartner, 1985; Smith et al., 1991; Uncles and Peterson, 1996), how selenium affects benthic organisms (e.g., *Macoma balthica*; Johns et al., 1988), and processes controlling the chemical speciation of selenium in the dissolved and particulate phases (Cutter, 1989a; Cutter and San Diego-McGlone, 1990). Specific objectives of this study were to:

1) Determine the concentration, distribution, and speciation of selenium in San Francisco Bay sediments. These results are presented in Chapter II.

2) Modify an existing biogeochemical model so that it simulates the estuarine cycle of selenium, including its speciation. The sensitivity analysis and calibration of the model are discussed in Chapter III. Validation of the model is presented in Chapter IV.

3) Predict how a change in physical, biological, or chemical parameters will affect the concentration, distribution, and speciation of selenium in the San Francisco Bay. These predictions are discussed in Chapter IV.

4) Evaluate the limitations of the model and research knowledge about the biogeochemical cycle of selenium. This assessment will be discussed in Chapter V.

The remainder of this Chapter is focused on a review of the biogeochemistry of selenium, what is already known about selenium in the San Francisco Bay, and a description of the model.

1.2. BIOGEOCHEMISTRY OF SELENIUM

1.2.1 Selenium Biogeochemistry Review

Selenium is an essential element for plants, animals, and humans (Schwarz and Foltz, 1957; Kolbl, 1995) since it is required in several enzymes and proteins (Stadtman, 1990; Wendel, 1992). Selenium can be found in many different environments, including soils, fresh water, seawater, and sediments, with concentrations varying from 10^{-7} to several thousand mmol kg^{-1} (Kolbl, 1995). Even though selenium is found naturally in the environment, its mobility has increased due to human activities (i.e., irrigation, petroleum refining, power production and mining; Nriagu and Pacyna, 1988). This increase in mobility may have contributed to elevated concentrations in waterfowl, fish, and bivalves of some estuaries (Ohlendorf et al., 1986).

Selenium is a Group VI element (atomic number 34, mass 78.962) and is in the same family as oxygen, sulfur, tellurium and polonium. Selenium can exist in four oxidation states (-II, O, IV, and VI; Geering et al., 1968; Cutter and Bruland, 1984; Cutter, 1992), and in different chemical forms (e.g., organic and inorganic) within these oxidation states (Cutter 1989b). An Eh versus pH diagram for selenium in an aqueous environment predicts that in oxygenated water of an estuary, dissolved selenium should be present exclusively as selenate, while in anoxic water elemental selenium is the stable form (Fig. 1). The problem with using an Eh versus pH diagram is that it does not take into account kinetic effects and biologically-mediated reactions (Stumm and Morgan, 1981). As an illustration, in oxygenated marine and fresh waters, dissolved selenium is

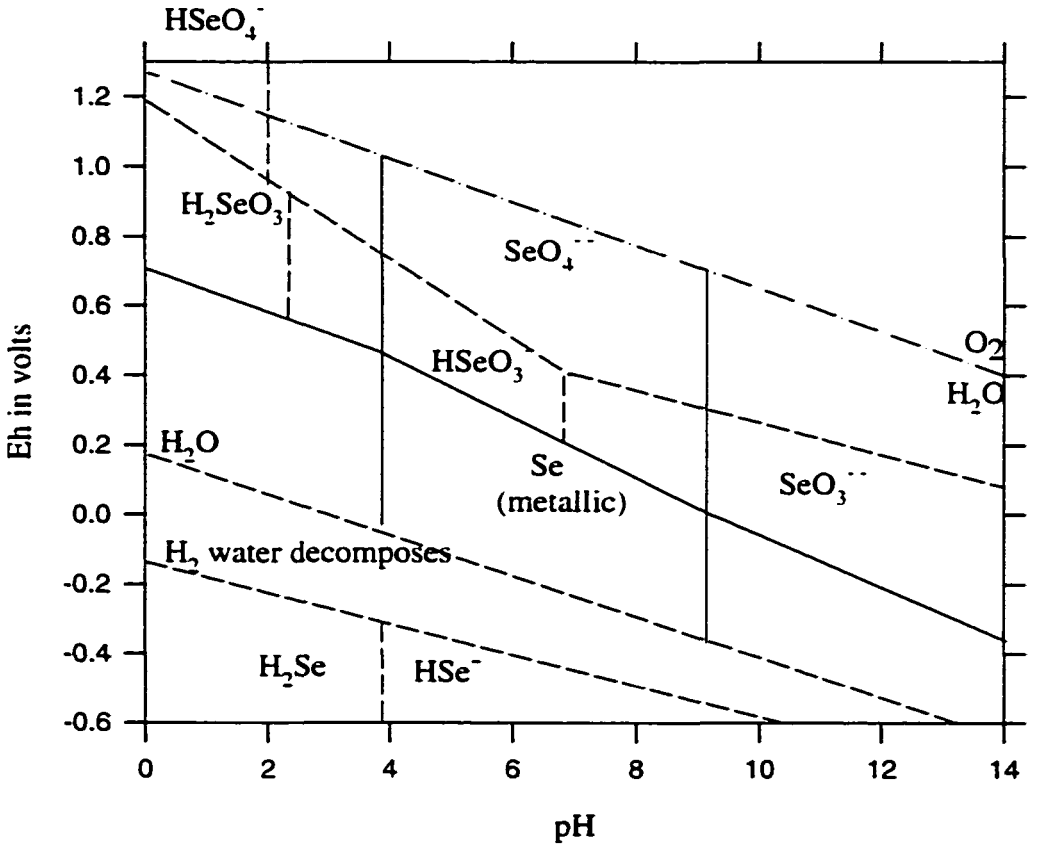

Fig. 1. Eh versus pH of selenium at 25°C, 1 atm, and a selenium concentrations of 10^{-6}M. (From Coleman and Delevaus, 1957).

found as selenite (i.e., 35% of the total selenium; Measures et al., 1980), selenate, and organic selenides (Apte et al., 1986), contrary to thermodynamic predictions. An explanation of why thermodynamically unstable species are present in oxygenated waters is that selenium (primarily in the form of organic selenides) is regenerated from biogenic particles in multiple steps, producing the thermodynamically unstable species, and slow rates of inter-conversion then allow them to persist (Cutter, 1992). Understanding this chemical speciation of selenium in aquatic environments is important since the biotic and abiotic reactivity of selenium is a function of its chemical form (Wrench and Measures, 1982; Cutter and Bruland, 1984).

1.2.2. Dissolved Selenium in Marine Environments

The biogeochemical cycle of selenium in an estuary is dependent upon its speciation and concentration at the freshwater and seawater end members. Dissolved selenium concentrations at the freshwater end member range from 0.5 to 4.9 nmol L^{-1} (Measures and Burton, 1978; Takayanagi and Wong, 1984 ; Takayanagi and Cossa, 1985; Cutter, 1989a). In rivers, approximately 7 to 60% of the total dissolved selenium is selenite, 20 to 87% is selenate, and less than 10% is organic selenide (Cutter, 1989a). In the James River, Takayanagi and Wong (1984), determined that selenite and organic selenide were the dominant species, while in the St. Lawrence River selenite was the dominant species (i.e., 70% of the total dissolved selenium, Takayanagi and Cossa, 1985).

The behavior of selenium in estuarine waters has been studied by many

researchers (Measures and Burton, 1978; Takayanagi and Wong, 1984; Takayanagi and Cossa, 1985; van der Sloot et al., 1985; Cutter, 1989b). In partially mixed estuaries like the St. Lawrence (Takayanagi and Cossa, 1985) and the Chesapeake Bay (Takayanagi and Wong, 1984), total dissolved selenium displayed conservative behavior during estuarine mixing (Fig. 2; Takayanagi and Cossa, 1985). In well-mixed estuaries like the San Francisco Bay, total dissolved selenium also behaves conservativly (Cutter, 1989b). Even though total dissolved selenium is conservative, dissolved selenite, selenate, or organic selenide often display non-conservative behavior in both partially-mixed and well-mixed estuaries. At low salinity (< 4), removal of selenite has been reported in the James River (Takayanagi and Wong, 1984) and the St. Lawrence River estuaries (Takayanagi and Cossa, 1985). In the James River, Takayanagi and Wong (1984) suggested that chemical conditions may favor the oxidation of selenite to selenate, thus causing a removal of selenite. As with selenite, non-conservative behavior of selenate has also been observed in the Chesapeake Bay (Takayanagi and Wong, 1984) and the San Francisco Bay (Cutter, 1989b). In the San Francisco Bay, selenate displayed non-conservative behavior with removal in the salinity range of 6 to 12 (Cutter, 1989b), while in Chesapeake Bay there was production of selenate (Takayanagi and Wong, 1984). Like inorganic selenium, organic selenide can behave non-conservatively or conservatively. For example, in the San Francisco Bay dissolved organic selenide behaves non-conservatively and is approximately 35 to 45% of the total selenium (Cutter, 1989b), while in the St. Lawrence estuary organic selenide is conservative and 10 to 30% of the total selenium (Takayanagi and Cossa, 1985). Organic selenide maxima in the San Francisco Bay correlate with

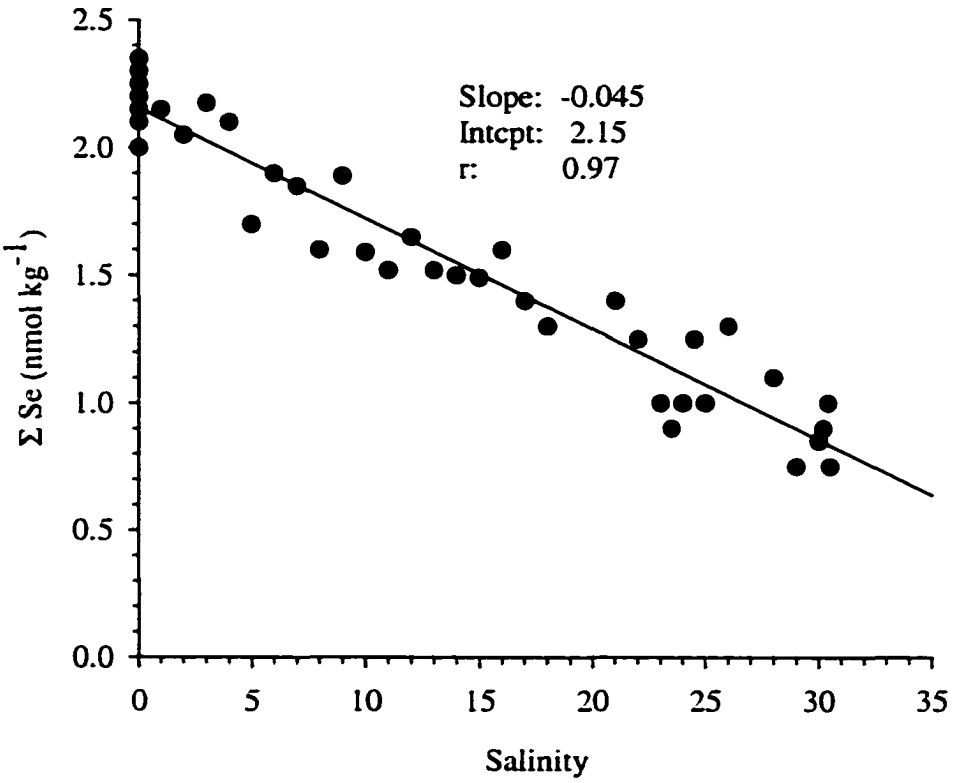

Fig. 2. Dissolved selenium from the St. Lawrence Estuary. The selenium data are from Takayanagi and Cossa (1985).

chlorophyll-a concentrations, suggesting that the non-conservative behavior of organic selenide is from biological activity (Cutter, 1989b).

In highly polluted estuaries (e.g., Scheldt River estuary, Belgium) the speciation of selenium tends to be different than in less polluted estuaries. In the Scheldt, 85% of the total dissolved selenium is in the form of selenite (van der Sloot et al., 1985), but in the less polluted River Test estuary (Measures and Burton, 1978), selenite averages less than 10% of the total dissolved selenium. Thus, the difference between the speciation of selenium in highly polluted and "non-polluted" estuaries makes it possible to use the speciation as a "signature" of specific inputs and cycling processes.

The seawater end member usually has a lower concentration of total dissolved selenium than the fresh water end member. Total dissolved selenium in sea water is approximately 1 nmol L^{-1} in surface waters, and 80% of the total dissolved selenium is organic selenide (Cutter and Bruland, 1984). Selenate is the next most predominant species in surface seawater, while selenite concentrations remain uniformly low (Cutter and Bruland, 1984). The transport of river water to the ocean results in a change in concentration of selenium and its speciation. Thus, estuaries are important in the *in situ* production and removal of dissolved selenium forms.

1.2.3. Particulate Selenium

Little research has been done on particulate selenium in estuaries, where it can be from riverine inputs, sea water inputs, sediment resuspension, and *in situ* production (e.g., phytoplankton). The latter term is important in the transfer of selenium to other estuarine

trophic levels. Decho and Luoma (1996) found that consumers (e.g., clams) assimilate particulate selenium of biological origin (e.g., bacteria and phytoplankton) faster than from sedimentary particles. Furthermore, Schelkat et al. (2000) found that elemental selenium created by microbial reduction (i.e., in estuarine sediments) is assimilated at a greater rate than abiotically produced elemental selenium. Therefore, sources of particulate selenium are important in the uptake, assimilation, and trophic transfer of selenium.

The only available data for particulate selenium in an estuary is that of Cutter (1989b) who measured total particulate selenium concentrations in the San Francisco Bay (no speciation data). The range of total particulate selenium was between 0.04 to 0.39 nmol L^{-1} (7% of the total selenium in the water column), with an estuarine distribution that was similar to the total suspended material (Cutter, 1989b).

1.2.4. Sedimentary Selenium

Only a few researchers have examined sedimentary selenium in oceanic (Sokolova and Pilipchuk, 1973; Tamari, 1978) or estuarine waters (Belzile and Lebel, 1988; Takayanagi and Belzile, 1988; Velinsky and Cutter, 1991). In both oceanic and estuarine sediments, a positive relationship between total sedimentary selenium and organic carbon (OC) and iron have been reported (Sokolova and Pilipchuck, 1973; Tamari, 1978; Belzile and Lebel, 1988). The correlation between selenium and organic carbon indicates that selenium may be biologically removed from the water column (i.e., incorporation by phytoplankton), while the iron-selenium relationship may be due to its

association with iron-sulfide minerals (e.g., pyrite or ferroselite).

The solubility of sedimentary selenium is dependent on its oxidation state, and can thus affect its mobility (Velinsky and Cutter, 1991). Both biotically and abiotically controlled reactions can change the oxidation state and/or phase of selenium. For example, dissimilatory reduction of selenite or selenate to elemental selenium may be a mechanism by which selenium is incorporated and retained in sediments (Rosenfeld and Beath, 1964; Elrashidi et al., 1989). Other possible reactions include the release or oxidation of particulate organic selenide, the oxidation of elemental selenium to dissolved selenite, scavenging of dissolved selenite by iron or manganese oxides, and the formation of solid phase selenium minerals such as achavalite (FeSe) or ferroselite ($FeSe_2$) (Velinsky and Cutter, 1991; Belzile et al., 2000).

In marine sediments, total sedimentary selenium concentrations range from 4.6 nmol g^{-1} to 16.2 nmol g^{-1} (Takayanagi and Belzile, 1988;Velinsky and Cutter, 1991; Peters et al. 1999; Belzile et al. 2000). A typical solid-phase depth profile of total selenium (Takayanagi and Belzile, 1988) shows that concentrations remain relatively constant with depth (Fig. 3). Velinsky and Cutter (1991) and Peters et al. (1999) found a similar trend, with some sites occasionally showing a decrease in total selenium with depth. According to Eh/pH stability field diagrams (Fig. 1), elemental selenium should be the dominant form of selenium in anoxic sediments (Geering et al., 1968; Lakin, 1973;

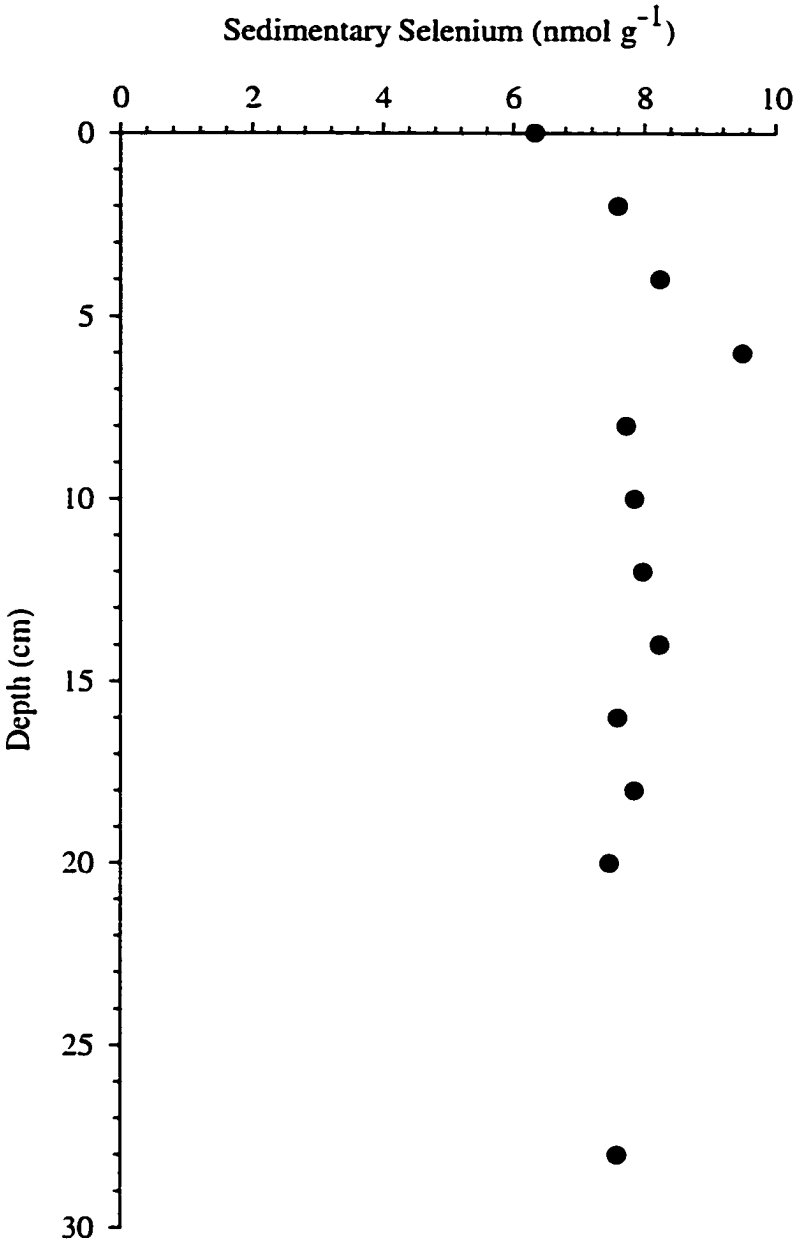

Fig. 3. Sedimentary selenium in sediments from the St. Lawrence Estuary. The selenium data are from Takayanagi and Belzile (1998).

Howard, 1977; Elrashidi et al., 1987). The speciation of selenium in sediments from a Delaware salt marsh (Fig. 4A) shows that elemental selenium at the surface ranged from 58 to 71% of the total selenium (Velinsky and Cutter, 1991), somewhat confirming these predictions for anoxic sediments. When these sediments become oxic, a slight decrease in elemental selenium near the surface may be found due to the oxidation of elemental selenium via abiotic and/or biotic processes. The abiotic oxidation of elemental selenium is slow (Geering et al., 1968; Howard, 1977), suggesting that any decrease in elemental selenium may be from the biologically mediated oxidation of elemental selenium to selenite (Sarathchandra and Watkinson, 1981).

Particulate (adsorbed) selenite + selenate account for a maximum of 30% of total sedimentary selenium and decreased with depth in salt marsh sediments (Fig. 4B, Velinsky and Cutter, 1991). Decreases in selenite + selenate can be related to biological uptake, conversion to either elemental selenium or other selenium phases, or remobilization to pore waters (Velinsky and Cutter, 1991). Unlike the inorganic sedimentary selenium, organic selenide had no consistent trend with depth (Fig. 4C) and was as high as 70% of the total sedimentary selenium in salt marsh sediments (Velinsky and Cutter, 1991).

Pore water determinations provide information on the remineralization of solid phase sedimentary selenium. Limited speciation data from a Delaware salt marsh indicate that in the oxidizing portion of pore water, selenite + selenate accounted for 50% of the total dissolved selenium (Velinsky and Cutter, 1991). The concentration of

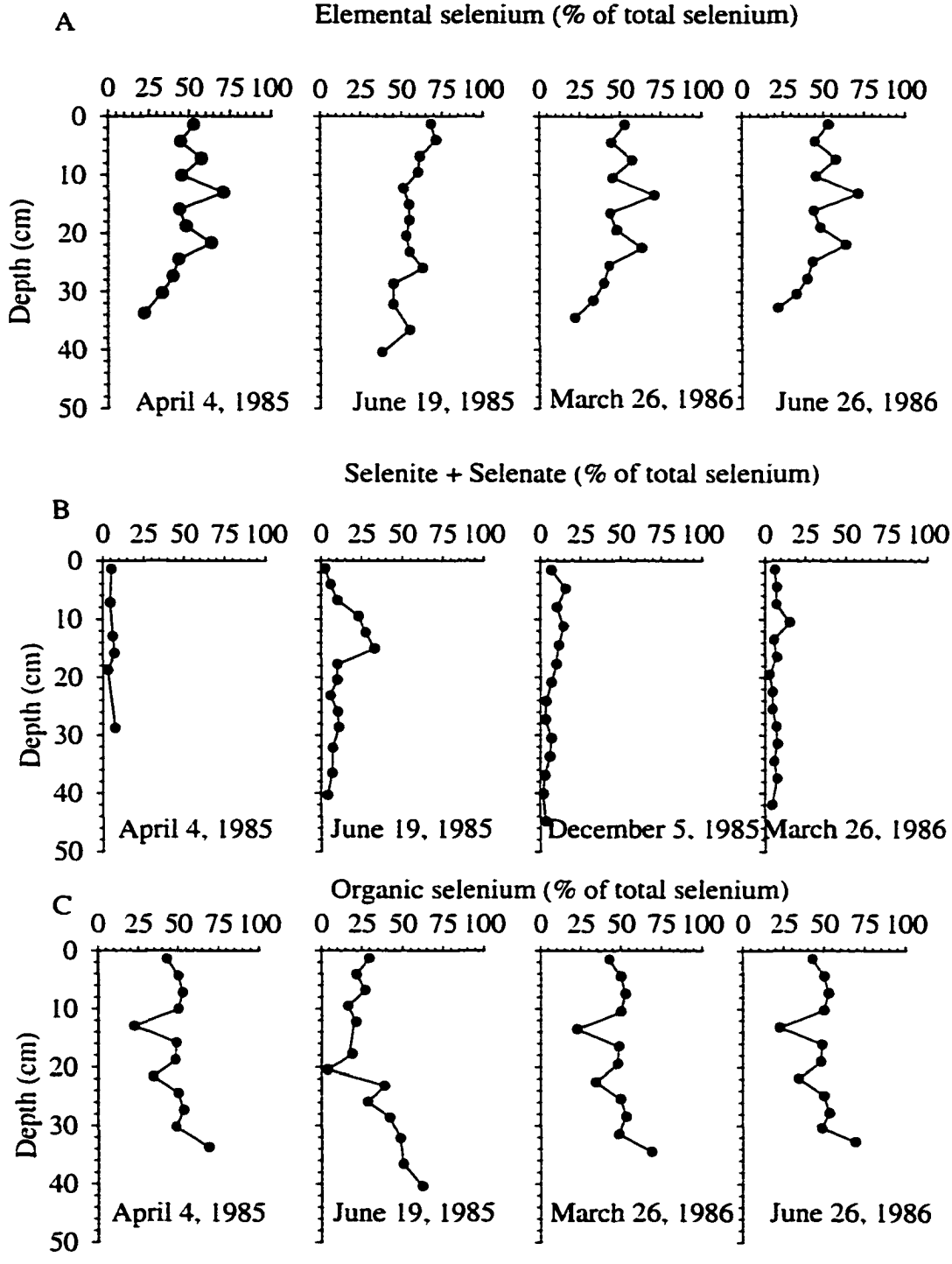

Fig. 4. Sedimentary selenium speciation from a salt marsh in Delaware. The selenium data are from Velinsky and Cutter (1991).

pore water selenite + selenate decreased with depth (and degree of anoxia) until dissolved organic selenide accounted for 100% of the total dissolved selenium in the Delaware salt marsh. Belzile et al. (2000) also reported that dissolved organic selenide was the dominant form in pore water from fresh water sediments, but after 5 cm the organic selenide concentration dropped. Belzile et al. (2000) suggested that the maximum of dissolved organic selenide at 5 cm was probably due to decomposition of particulate organic matter, while the decrease may be due to the formation of particulate elemental selenium by bacteria.

Takayanagi and Belzile (1988) and Belzile et al. (2000) found that the flux across the sediment-water interface might be important in the transfer of sedimentary selenium to the overlying water. In the St. Lawrence Estuary, the loss of leachable sedimentary selenium in the sediments matched the upward flux of dissolved selenium out of the sediments (Takayanagi and Belzile, 1988), suggesting that diagenetic processes were responsible for the mobilization of sedimentary selenium. The various chemical and biological reactions occurring in sediments can change the mobility and speciation of selenium. Therefore, more research needs to be done on sedimentary selenium to better evaluate the exchange pathways between the dissolved and particulate phases.

1.2.5. Selenium in Phytoplankton and Higher Trophic Levels

Phytoplankton plays an important role in the biogeochemical cycle of selenium by biologically mediating the transformation of selenium from one chemical form to another (Wrench, 1978; Cutter, 1982; Cooke and Bruland, 1987), by utilizing dissolved selenium

for growth, and by acting as a food source to higher organisms (i.e., responsible for selenium transfer to other trophic levels). Selenium is both essential and toxic for several species of dinoflagellates (Lindstrom and Rodhe, 1978; Lindstrom, 1980; Ishimaru et al., 1989; Doblin et al., 1999), diatoms (Price et al., 1987), and chrysophytes (Wehr and Brown, 1985). The utilization of selenium by phytoplankton is dependent on the speciation of selenium. For example, the marine diatom *Thalassiosira pseudonana* requires trace amounts (0.1 to 1 nmol L^{-1}) of selenite for growth and it will not grow even if other forms of selenium are present at concentrations greater than 10 nmol L^{-1} (Price et al., 1987). Furthermore, Hu et al. (1996) demonstrated that the diatom *Chaetoceros calcitrans* and green algae *Chlorella vulgaris* are able to distinguish between inorganic and organic selenium species; they preferentially incorporated selenite. For most phytoplankton, selenite is assimilated more rapidly than selenate (Kumar and Prakash, 1971; Price et al., 1987; Riedel et al., 1996). Thus, the speciation of selenium affects phytoplankton growth.

The toxicity of selenium is also dependent on the speciation of selenium (Kumar and Prakash, 1971; Price et al., 1987; Boisson et al., 1995; Riedel et al., 1996). Effects of toxicity on phytoplankton can include a decrease in phytoplankton growth (Bennett, 1988; Wong and Oliveira, 1991a,b), morphological affects (Wong and Oliveira, 1991a,b), changes in respiratory and photosynthetic rates (Wong and Oliveira, 1991a,b), and changes in nucleus, mitochondria, and chloroplasts of the cells (Wong and Oliveria, 1991b). At concentrations greater than 10^{-4} mol L^{-1} of selenite the growth of several phytoplankton species (*Dunaliella tertiolecta, Agemenellum quadruplicatum,*

Nannochloropsis oculata, Povlova lutheri) is inhibited, but at concentrations of 10^{-5} mol L^{-1} growth is stimulated for these species (Wong and Oliveria, 1991a). For selenate, at concentrations of 10^{-2} to 10^{-3} mol L^{-1} growth is completely inhibited for several freshwater algae (*Dunaliella tertiolecta, Agemenellum quadruplicatum, Nannochloropsis oculata, Chaetoceros vixvisibilis*). The toxicity of selenium to phytoplankton are dependent on the phytoplankton species but several researchers have reported higher toxicity for selenate than selenite (Price et al., 1987; Bennett, 1988; Wong and Oliveira, 1991a,b). Concentrations in seawater are in the range of 10^{-8} to 10^{-10} mol L^{-1} indicating that in natural marine environment toxicity affects are minor.

Once phytoplankton take up selenium, it can be incorporated into various biochemical components such as amino acids, proteins, soluble carbohydrates, lipids and polysaccharides (Bottino et al., 1984; Vandermeulen and Foda, 1988). Wrench (1978) and Bottino et al. (1984) found that most of the selenium in phytoplankton was found in seleno amino acids. The ability of phytoplankton to incorporate selenium into biochemical components may be important in the transfer of selenium through the food web because it can be transferred to the next trophic level with great efficiency. For example, calanoid copepods are able to assimilate 97% of the ingested selenium from *T. pseudonana* (a diatom; Fisher and Reinfelder, 1991) and other herbivores such as mollusk and crustacean larvae assimilate 61 to 100% of the selenium ingested from phytoplankton (Reinfelder and Fisher, 1994). Thus, one of the possible routes for the transfer of selenium to higher trophic levels (e.g., fish and clams) is through phytoplankton.

The ability of higher trophic levels to directly take up selenium from the dissolved

phase has also been investigated. Past research indicates that the direct uptake of dissolved selenium to clams, fish, and waterfowl appears to be minimal. Luoma et al. (1992) found that the direct uptake of selenium was extremely slow for the clam *Macoma balthica*. Furthermore, a food-chain experiment by Sandholm et al. (1973) showed that high selenium concentrations reported in fish resulted from high selenium content in plankton on which they feed, not on direct water uptake. Direct uptake is minimal compared to trophic-level transfer because of the low epithelial adsorption or blood adsorption through the gills (Sandholm et al., 1973). As a result, the uptake of selenium through food web components, with phytoplankton being the first step, is a key factor for higher trophic levels.

1.3. SAN FRANCISCO BAY

1.3.1. Hydrology and Morphology

San Francisco Bay is considered the largest estuary in the United States to be modified by human activities (Nichols et al., 1986). Since the early 1900s, the surface area and depth of the Bay have decreased, marshes have been destroyed, fresh water diverted for irrigation, exotic plants and animals introduced, and the effects of sewage and refinery effluents have become apparent (Nichols et al., 1986). The San Francisco Bay has a total surface area of 1240 km^2, with an average depth of 6.1 m (Conomos et al., 1985) and is divided into what is known as the "Northern Reach" and the South Bay. The Northern Reach includes Central Bay, San Pablo Bay, and Suisun Bay (Fig. 5). Seawater enters the Bay through the Golden Gate and can either proceed north into the Northern

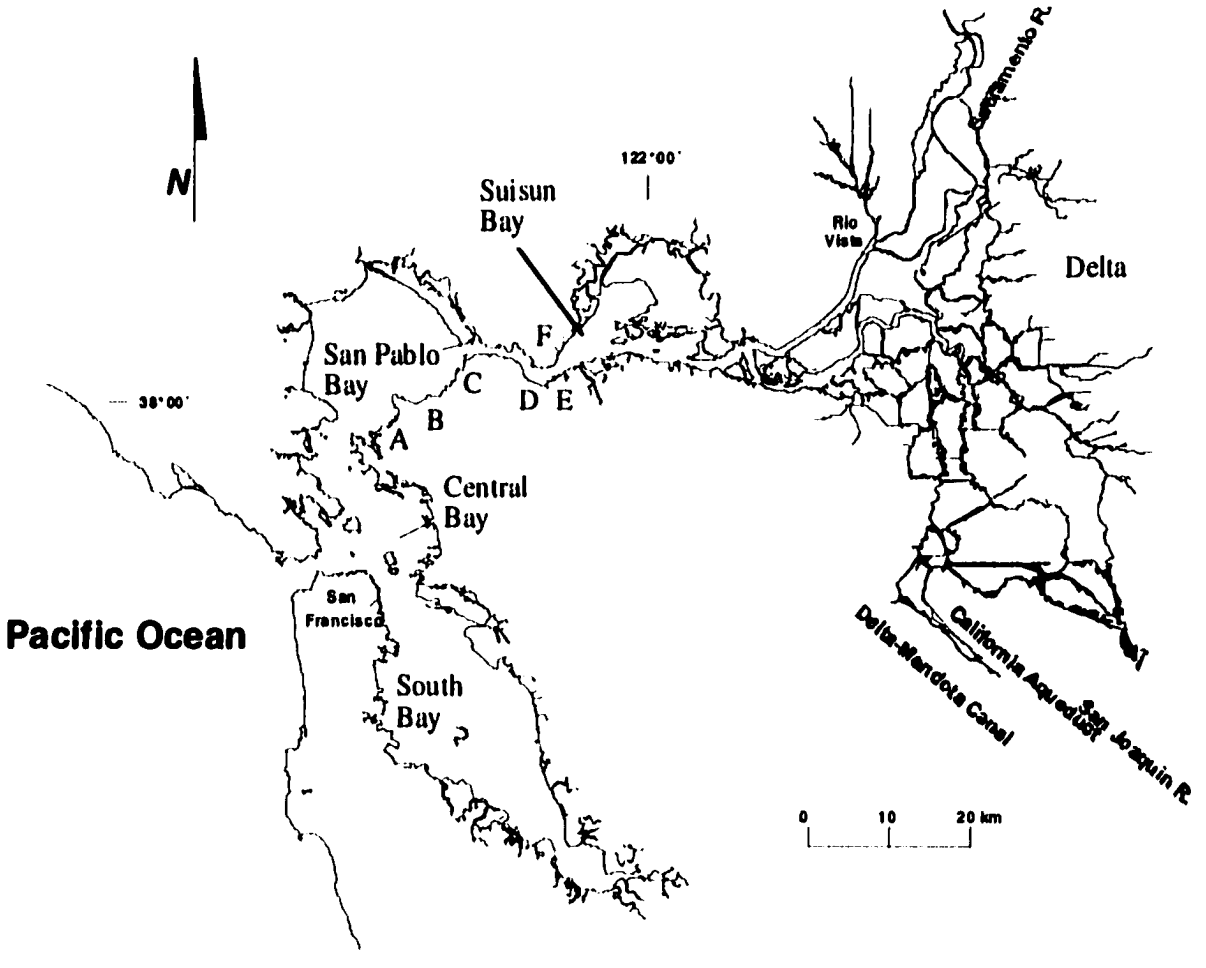

Fig. 5. The San Francisco Bay and Sacramento-San Joaquin Delta and the location of six major refineries. Letter A is the Chevron USA Richmond, B is Pacific Refining Co. Hercules, C is Unocal Corp. Rodeo, D is Shell Oil Co. Martinez, E is Tosco Refining Co. Martinez, and F is Exxon USA Benicia.

Reach or south into the South Bay. The Northern Reach is a strongly tidal, well to partially mixed estuary, while the South Bay is a strongly tidal, lagoon-type estuary with a small freshwater inflow (Uncles and Peterson, 1996). My research focused on the Northern Reach since it has many features common to other estuaries (e.g., short residence time, strong tidal influences, well to partially mixed, and natural and anthropogenic inputs of selenium), and I will thus omit further discussion of the South San Francisco Bay.

Two major rivers enter the Northern Reach of the San Francisco Bay, the northward-flowing San Joaquin River and the southward-flowing Sacramento River. These rivers carry runoff from 153,000 km^2 of land, which is 40% of the surface area in California (Nichols et al., 1986), and join at the San Francisco Bay 'Delta' (Fig. 5). The average freshwater residence time in the Northern Reach is 2 to 160 days depending on the discharge from the Sacramento-San Joaquin Rivers (Cutter, 1989b). Historical data (Conomos et al., 1979) show that discharge into the Delta varies seasonally, with maximum river discharge occurring in January-February and minimum discharge during July-August. During most of the year, the San Joaquin discharge rate is low, with little or no water entering the estuary (Arthur and Ball, 1979). In fact, from 1984 to 1987 the San Joaquin River only discharged into the Bay during April and May 1986 (Cutter, 1989b). Approximately 98% of the flow from the San Joaquin River is diverted for irrigation practices, which leaves the lower part of the river dependent on fresh water disposal from agricultural drainage (Presser and Piper, 1998). Thus, the Sacramento River largely defines the riverine input of selenium into the Northern Reach.

1.3.2. Dissolved Selenium in the Northern Reach

The concentration of selenium in the Northern Reach is dependent upon the input from the Sacramento River and San Joaquin River (when flowing), petroleum refinery effluents, and the Pacific Ocean. Comparison of the discharge from the Sacramento River and total selenium and selenate concentrations, show a positive linear correlation (Cutter, 1989b). Thus, during the winter months when the discharge is high more total dissolved selenium fluxes into the Bay than in the summer months when the discharge is low (Cutter, 1989b). From July 1984 to June 1988, total dissolved selenium concentration in the Sacramento River ranged from 0.5 to 1.40 nmol L^{-1}, with an average total selenium concentration of 0.86 nmol L^{-1}, with selenate representing 48% of the total dissolved selenium, organic selenide 40%, and selenite less than 12% (Cutter, 1989b). Recent data from November 1998 to May 2000 suggests that the input of selenium from the Sacramento has not changed since 1984 (Cutter and Cutter, in prep.). The range of total dissolved selenium was 0.67 to 1.37 nmol L^{-1} with an average concentration of 0.94 nmol L^{-1}. The percentage of each species has also remained the same, suggesting that the input of selenium from the Sacramento River is stable on decadal time scales.

Even though the San Joaquin River rarely discharges into the Northern Reach, the EPA and other state, federal, and local agencies in the State of California have been developing an integrated ecosystem-based approach to restoring the ecological health of the estuary and the San Joaquin River (http://calfed.water.ca.gov). These approaches include restoring freshwater tidal marshes, riparian habitats, reversing subsidence on Delta islands, providing adequate flows to replicate natural hydrological patterns,

removing barriers (e.g., obsolete dams), and reducing pollutant loading in the San Joaquin watershed (http://calfed.water.ca.gov). Restoration of the San Joaquin flow could affect the estuarine concentration of selenium due to high concentrations in this river. Between July 1984 and June 1988, the San Joaquin River had total dissolved selenium concentrations ranging from 1.7 to 59.4 nmol L^{-1} (average 20.3 nmol L^{-1}), with selenate being 74% of the total dissolved selenium, organic selenide 19%, and selenite 7% (Cutter, 1989b). Recent data from November 1998 to April 2000 indicate that total dissolved selenium concentrations have decreased to 4.6 to 13.7 nmol L^{-1} (average 8.6 nmol L^{-1}; Cutter and Cutter, in prep.). The speciation data was slightly different than in the 1980's, with selenate being 66% of the total, organic selenide 31%, and selenite 3%. The decadal variation and high concentrations of dissolved selenium in the San Joaquin River suggest that it is important to understand how restoring its flow would affect the distribution of selenium in the Bay.

Estuarine transects in the Northern Reach during April 1986 (high flow conditions), with a third end member (the San Joaquin River), shows that total dissolved selenium was nearly conservative in the Bay, with concentrations ranging between 1.4 to 3.0 nmol L^{-1} (Fig. 6A). The selenite estuarine profile however shows non-conservative behavior, with a dissolved selenite maximum concentration at a salinity of 9 where it is 23% of the total dissolved selenium (Fig. 6B, Cutter, 1989b). Selenate, on the other hand, displayed non-conservative removal between a salinity of 6 to 12 (Fig. 6C). In most of the Northern Reach, selenate averaged 49% of the total dissolved selenium, except at the top of the estuary where it averaged 82% (Cutter, 1989b). Organic selenide

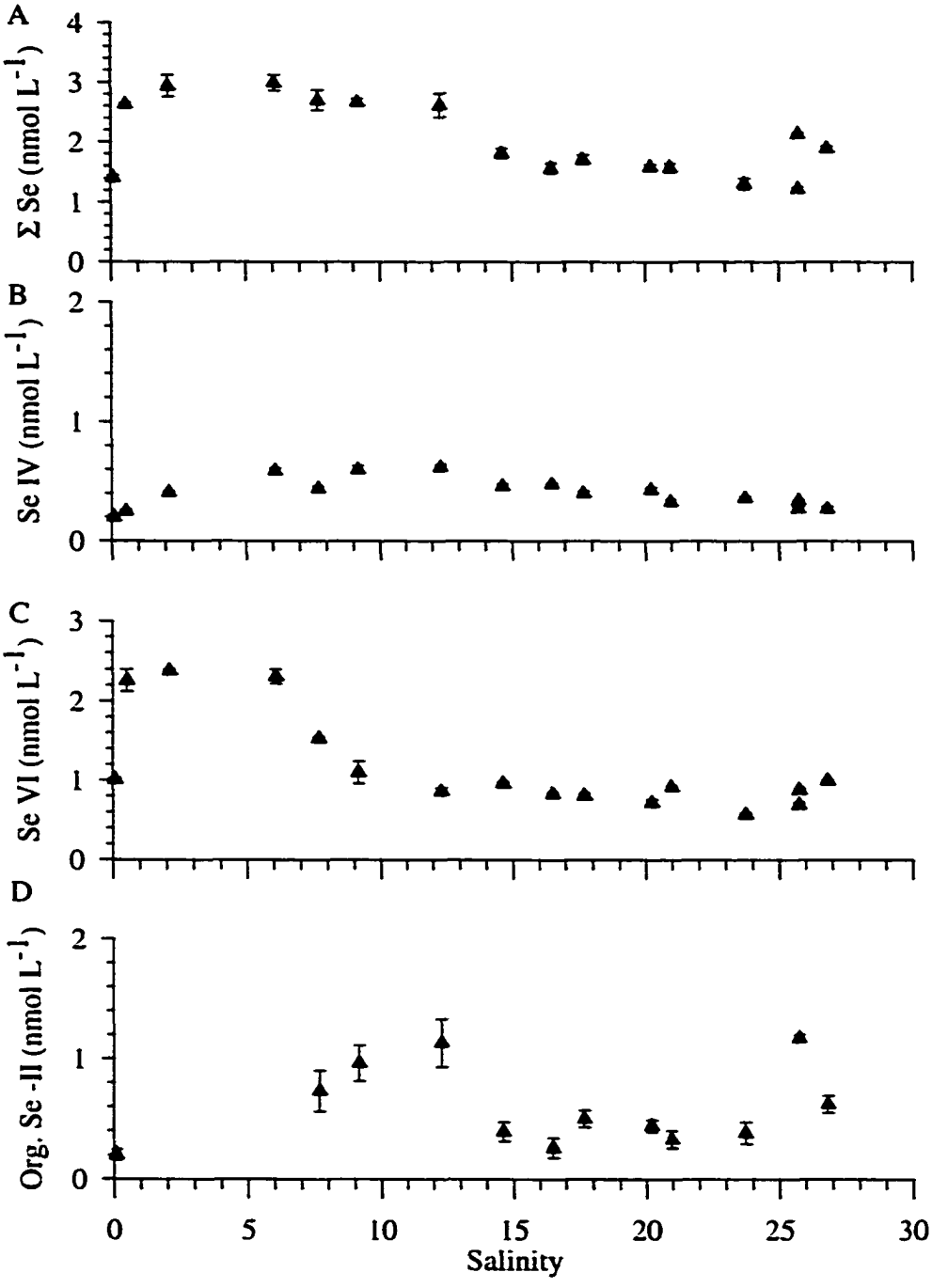

Fig. 6. Dissolved selenium in the San Francisco Bay, April 23, 1986. Total selenium (A), selenite (B), selenate (C), and organic selenide (D) data are from Cutter and Cutter (in prep).

was 35 to 44% of the total dissolved selenium within the Bay, and displayed non-conservative behavior, with the maximum organic selenide concentration occurring at a salinity of 10 and at the Golden Gate (Fig. 6D).

The total dissolved selenium data for low flow conditions in September1986 were significantly different than those in April 1986. The total selenium concentration in September was non-conservative and ranged between 1.6 to 3.6 nmol L^{-1} (Fig. 7A), with a maximum occurring at a salinity between 10 to 20 (Cutter 1989b). Cutter (1989b) found during low flow selenite was still non-conservative, but the selenite maximum between the salinity of 9 to 20 increased to 41% of the total dissolved selenium (Fig. 7B).

The selenate versus salinity profile during low flow was different than that in high flow. There was still a slight maximum between a salinity of 10 to 14, but overall it was largely conservative and approximately 33% of the total dissolved selenium (Fig. 7B). As with the April 1986 data, organic selenide was non-conservative and had a maximum that corresponded with the location of elevated concentrations of chlorophyll-a. Organic selenide was 31 to 48% of the total dissolved selenium, with a higher percentage located at the top of the estuary (Fig. 7D, Cutter 1989b).

Cutter (1989b) and Cutter and San Diego-McGlone (1990) reported dissolved selenite maxima in the vicinity of Carquinez Strait taken where six oil refineries are located (Fig. 5). At this time, refinery effluents had total dissolved selenium concentrations of 100 to 2600 nmol L^{-1}, with 64% of the total selenium being selenite and 25% selenate. Using estuarine modeling, Cutter (1989b) calculated the input fluxes at Carquinez Strait during low flow conditions. By comparing the calculated fluxes to the

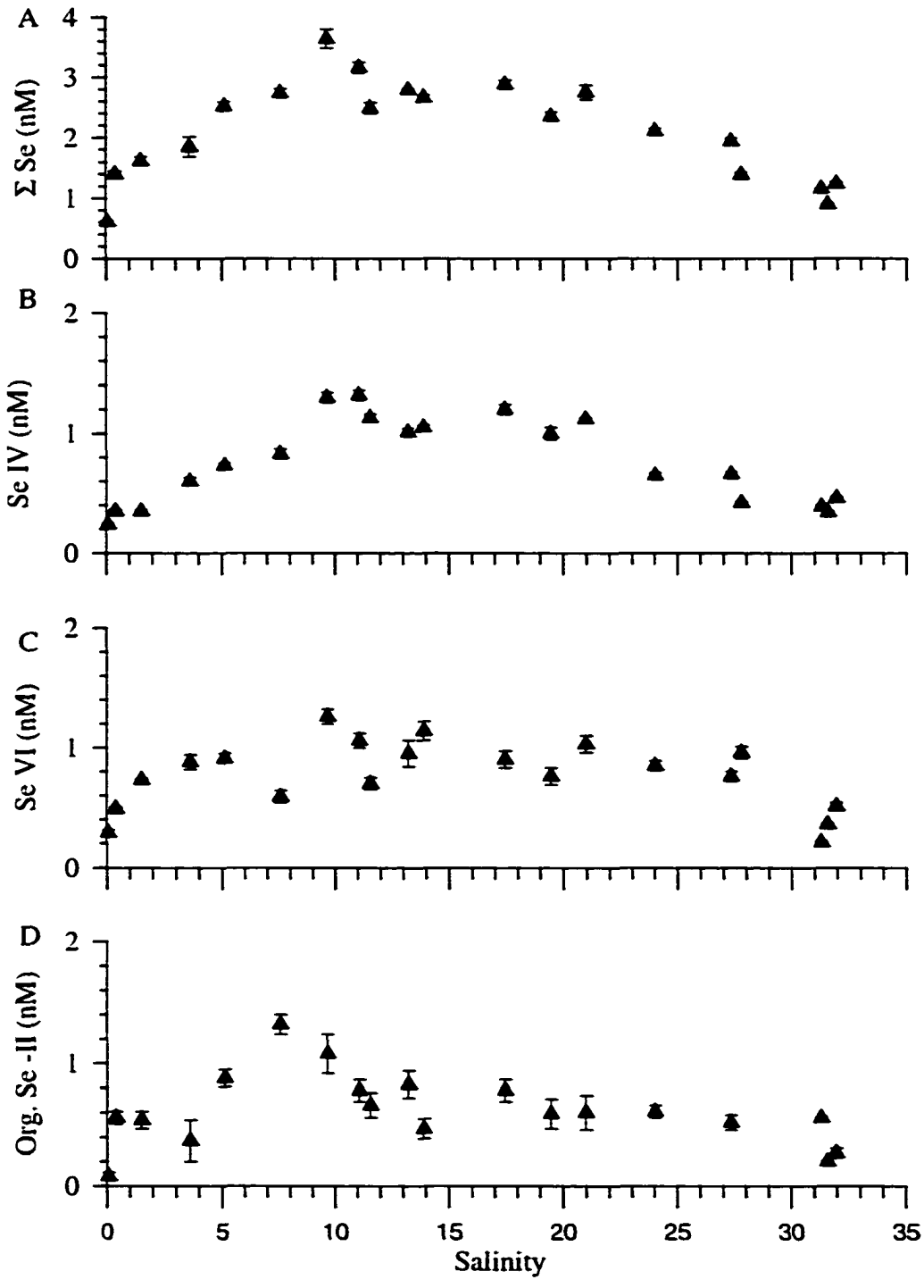

Fig. 7. Dissolved selenium in the San Francisco Bay, September 23, 1986. Total selenium (A), selenite (B), selenate (C) and organic selenide (D) data are from Cutter (1989b).

measured fluxes from oil refinery effluents, it was determined that 60% of the total selenium flux, virtually all of the selenite flux, 40% of the selenate flux, and 24% of the organic selenide flux could be traced to refinery effluents (Cutter 1989b).

From 1997 to 2000, estuarine transects in the San Francisco Bay were taken in the fall and spring to determine if dissolved selenium profiles had changed from the 1980's. Cutter and Cutter (in prep.) found that in November 1999 total dissolved selenium was between 0.9 to 1.5 nmol L^{-1} (Fig. 8A), which is lower than the total dissolved selenium concentrations previously reported by Cutter (1989b). Estuarine profiles of selenite still show non-conservative behavior, but the selenite concentration decreased from a maximum value of 1.32 nmol L^{-1} in 1986 to 0.24 nmol L^{-1} in 1999 (Fig. 8B). Selenite was now 9 to 25% of the total selenium. Selenate also behaved non-conservatively (Fig. 8C) and averaged 65% of the total dissolved selenium in the estuary, with a higher percentage in the salinity range of 15 to 20. Organic selenide had a maximum between a salinity of 10 to 20, which corresponded with higher chlorophyll-a concentrations (Fig. 8D). Organic selenide was 10 to 30% of the total dissolved selenium. In 1999, compared to 1986, there has been an observed change in the speciation and concentration of dissolved selenium in the Bay.

Refinery effluent data in 1999 indicate that total dissolved selenium concentrations dropped from 100 to 2600 nmol L^{-1} (an average of 689 ± 592 nmol L^{-1}) in 1986 to 90 to 390 nmol L^{-1} (an average of 207 ± 131 nmol L^{-1}) in 1999, with selenite being 14% of the total dissolved selenium and selenate 61% of the total. Cutter and Cutter (in prep.) found that the concentration of the Sacramento River has not varied in

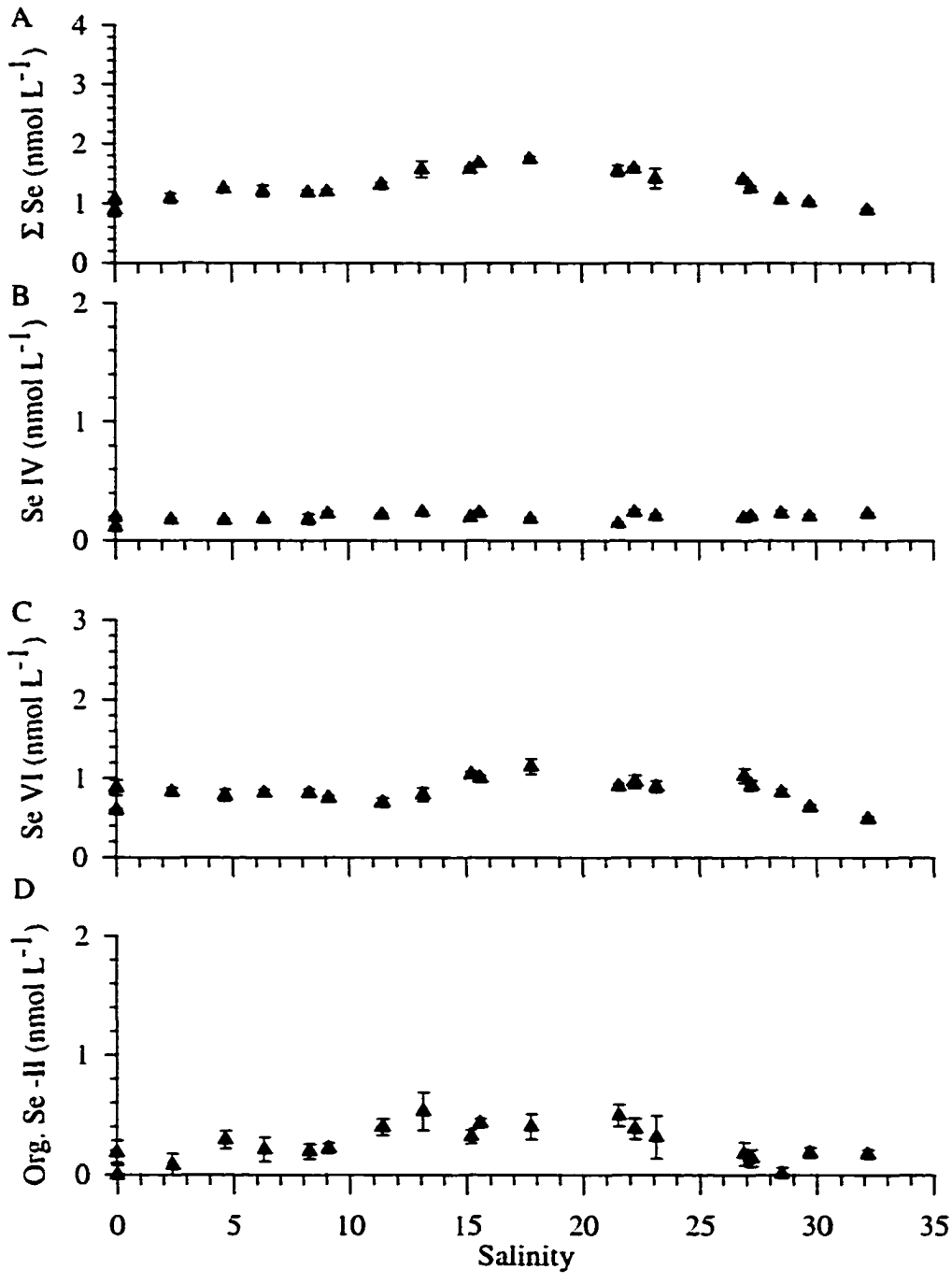

Fig. 8. Dissolved selenium in the San Francisco Bay, November 10, 1999. Total selenium (A), selenite (B), selenate (C), and organic selenide (D) data are from Cutter and Cutter (in prep).

the last decade, suggesting that the decreased dissolved selenium concentrations in the estuary may be due to the decrease in inputs by the refineries (i.e., a 30% reduction since 1986).

1.3.3. Particulate Selenium in the Northern Reach

Cutter (1989b) found that total particulate selenium concentration regardless of whether it was high flow or low flow ranged from 0.15 nmol L^{-1} to 0.39 nmol L^{-1} (corresponding to 0.42 μg g^{-1} to 0.72 μg g^{-1}) during April and September of 1986 (Fig. 9A and Fig. 9B, respectively). During high flow and low flow (Fig. 9) the suspended particulate selenium estuarine profiles were similar to that of the total suspended material. Recent work by Doblin et al. (in prep.) found that total particulate concentrations in 1999 (Fig. 9C and Fig. 9D) were similar to those of Cutter (1989b).

Little research is available on the speciation of suspended particulate material in the Northern Reach. Speciation analysis on the particulate material (Doblin et al., in prep.) show that 37 to 50% of the particulate material was organic selenide, 19 to 38% was elemental selenium, and 12 to 44% was selenate + selenite. These speciation data are useful in tracing particulate inputs (i.e., elemental selenium is from resuspended sediments and riverine inputs, while organic selenide comes from phytoplankton, resuspended sediments, and riverine inputs).

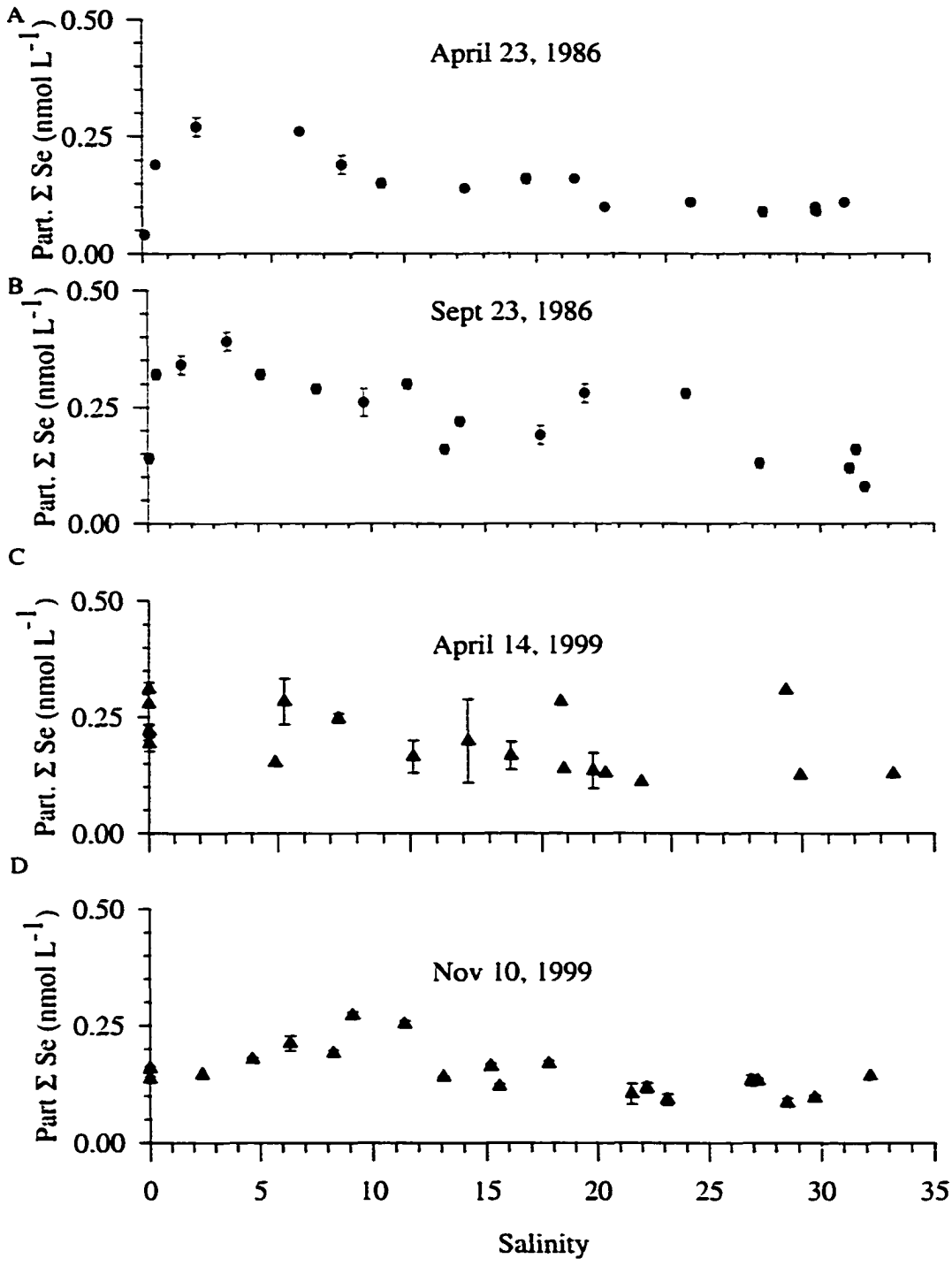

Fig. 9. Particulate selenium for various years and flow conditions in the San Francisco Bay. The data for 1986 are from Cutter (1989b) and the data for 1999 are from Doblin et al. (in prep).

1.3.4. Biogeochemical Cycle of Selenium in the Northern Reach

Figure 10 illustrates the biogeochemical cycle of selenium in the Northern Reach of the San Francisco Bay. Dissolved selenium is introduced in the Bay via rivers, refineries, and exchange with the open ocean. Transport of selenium in the estuary is due to advection and diffusion. During transport, internal transformation of dissolved selenium can occur through biotic and abiotic reactions. The abiotic reactions include the oxidation of dissolved organic selenide to selenite and the oxidation of dissolved selenite to selenate. Biotic reactions include dissolved selenite, selenate, and organic selenide uptake by phytoplankton, and incorporation into various biochemical components as discussed above.

The sources of particulate selenium to the Northern Reach are particulate selenium from the rivers (biogenic and mineral detritus), biogenic particles produced in the water column (organic phytoplankton detritus), and sediment resuspension. *In situ* particulate organic selenide can undergo remineralization to dissolved organic selenide or it can sink and become part of the sedimentary record. In the sediments, particulate selenium can undergo a variety of oxidation-reduction reactions that may cause the selenium to become mobile or permanently buried. For example, particulate selenium in the bed of the estuary can undergo regeneration to dissolved organic selenide. In this way, sediments can become a source of dissolved selenium to the estuary via pore water exchange with the overlying water. Any simulation model of the biogeochemical cycle of selenium needs to include all of the processes in Fig. 10.

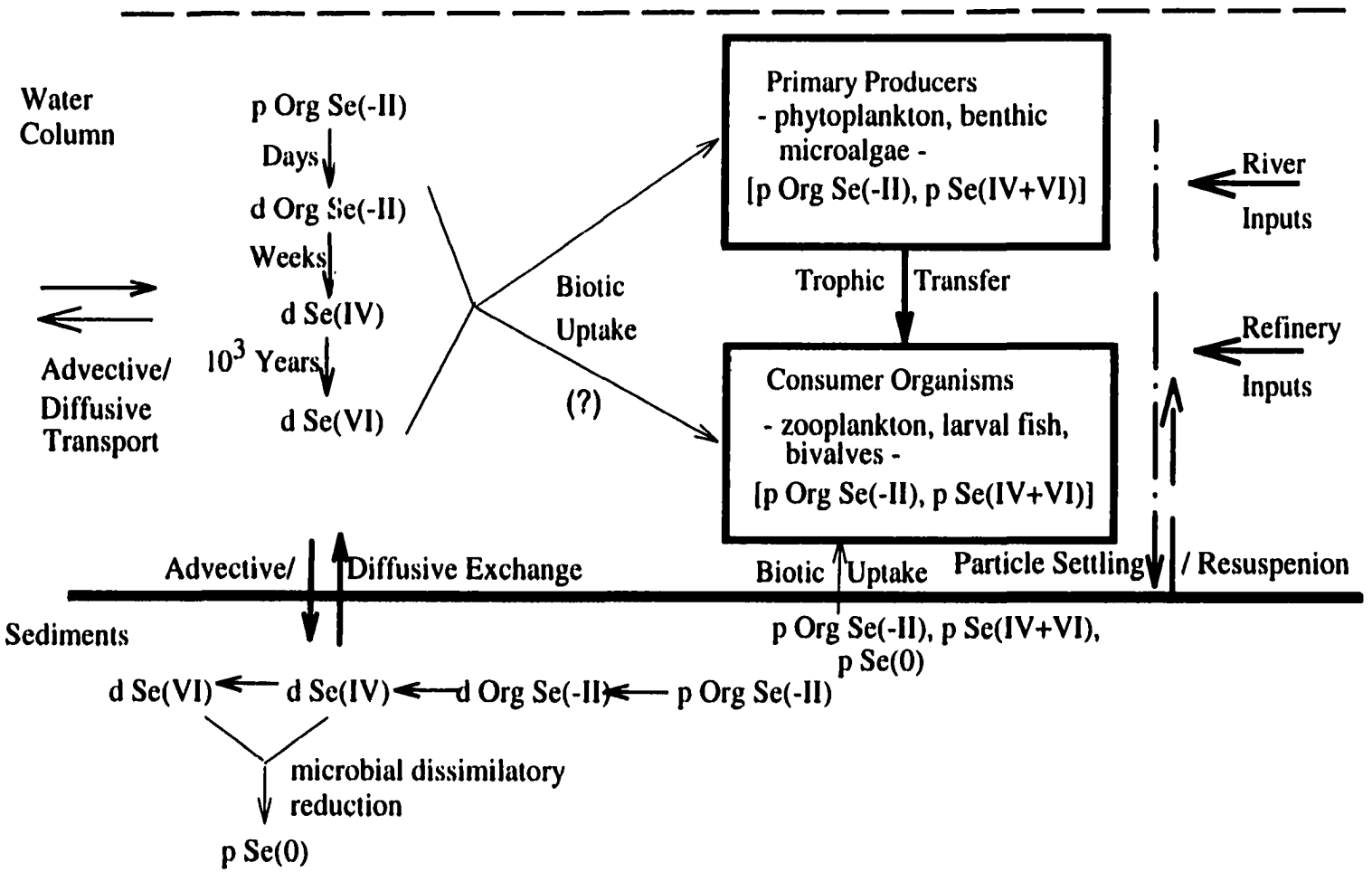

Fig. 10. The biogeochemical cycle of selenium in an estuary.

1.4. MODELING

1.4.1. Estuarine Classification

Estuaries are classified according to their topography and/or salinity structure and this affects the choice of models. The topographic classification of an estuary, as defined by Pritchard (1952), are drowned river valleys (e.g., Chesapeake Bay), fjords (e.g., Sogne Fjord, Norway), bar-built estuaries (e.g., Roanoke River), and tectonically-produced estuaries (e.g., San Francisco Bay). Estuaries can also be classified as vertically well-mixed, partially-mixed, or highly stratified according to their salinity structure.

Conomos (1979) found that the water column in the Northern Reach is typically well-mixed due to wind and tides. The well-mixed water column in the Northern Reach allowed Selleck (1968) and Cifuentes et al. (1990) to simulate the distribution of salinity in the San Francisco Bay using a one layer, advection-dispersion model. Uncles and Peterson (1996), on the other hand, used a two-layer, width-averaged, multi-segmented model for salinity. Their two-layer model was chosen to simulate the layer-averaged salinity and mixing within each level (Uncles and Peterson, 1996). However, all of these models have generated salinity profiles that agreed with measured data (Selleck, 1968; Cifuentes et al. 1990; Uncles and Peterson, 1996).

Using the continuity equation for water, the movement of a solute in an estuary can be described by

$$\frac{\partial s}{\partial t} = u\frac{\partial s}{\partial x} + v\frac{\partial s}{\partial y} + w\frac{\partial s}{\partial z} - \frac{\partial}{\partial x}(K_x\frac{\partial s}{\partial x}) - \frac{\partial}{\partial y}(K_y\frac{\partial s}{\partial y}) - \frac{\partial}{\partial z}(K_z\frac{\partial s}{\partial z}) - \Gamma \quad (1.1)$$

where s is the solute, t is time, u is the tidal velocity, v is the lateral velocity, w is the

vertical velocity, K_x is the coefficient of longitudinal eddy diffusion, K_y is the coefficient of lateral eddy diffusion, K_z is the coefficient of vertical eddy diffusion, and Γ is other processes/reactions (e.g., biological uptake) that may affect the transport of constituent *s*.

Dimensionless classification parameters can be used to determine which parameters in Equation 1.1 are important in the transport of a constituent in the Northern Reach of the San Francisco Bay. There are many different classification schemes that have been developed (e.g., Simmons, 1955; Ippen and Harleman, 1961; Hansen and Rattray, 1966;Fischer, 1972; Uncles et al., 1983; Prandle, 1985; Jay and Smith, 1988), with the main differences being between the type of data needed. For example, Simmons (1955) classified estuaries based on the ratio of river flow per tidal cycle to the tidal prism, while Fisher (1972) used salinity, velocity measurements, and the breadth of the estuary to construct a stratification-circulation diagram that can be used under a wide range of conditions.

To determine if the San Francisco Bay can be classified as a well-mixed estuary, the classification scheme of Simmons (1955) and the stratification-circulation diagram of Fisher (1972) were applied to the San Francisco Bay. Simmons (1955) stated that when the flow ratio (ratio of river flow per tidal cycle to the tidal prism) is greater than 1, the estuary is stratified, for 0.25 it is partially-mixed, and when the ratio is less than 0.1 it is well-mixed. Conomos (1979) reported a tidal prism of 1.50×10^9 m^3 at the Golden Gate, but using this number could be misleading since it includes flow from the South Bay. Cheng et al. (1993) determined the tidal prism of the San Francisco Bay at various locations in the Northern Reach for neap and spring tides. During spring tide, the tidal

prism ranged from 2.1 X 10^9 m^3 at the Golden Gate to 0.45 X 10^9 m^3 in Suisun Bay. The tidal prism was less during neap tide, with the Golden Gate having a tidal prism of 0.93 X 10^9 m^3 and 0.19 X 10^9 m^3 in Suisun Bay. Due to this large range in the tidal prism, it is important to determine if the entire estuary is well-mixed during a complete tidal cycle. To account for yearly differences in discharge from the Delta, the average Delta discharge of 776 m^3 s^{-1} from 1957 to 1999, (Dayflow Interagency Ecological Program, http://iep.water.ca.gov/dayflow/) was used in calculating the flow ratio. Flow ratios (Table 1) indicate the estuary is well-mixed from the Golden Gate to Suisun Bay for spring tide. During neap tide, the flow ratio in Suisun Bay is slightly greater than that of a well-mixed estuary (0.1), but less than that of a partially-mixed estuary (0.25). Thus, the classification scheme by Simmons (1955) indicates that the Northern Reach is a well-mixed estuary for most of the year.

Table 1
The flow ratio for the San Francisco Bay

Area	Flow Ratio	Tidal Prism (m^3)
Golden Gate		
Spring	0.02	2.10 x 10^9
Neap	0.04	0.93 x 10^9
Central Bay		
Spring	0.05	0.75 x 10^9
Neap	0.09	0.40 x 10^9
San Pablo Bay		
Spring	0.07	0.50 x 10^9
Neap	0.10	0.35 x 10^9
Suisun Bay		
Spring	0.08	0.45 x 10^9
Neap	0.18	0.19 x 10^9

An estuary stratification-circulation diagram was used to further confirm if the San Francisco Bay could be modeled as a well-mixed estuary. Fischer (1972) calculated stratification using the estuarine Richardson number, which is defined as:

$$R_{ie} = \frac{\Delta\rho}{\rho} * \frac{g u_f}{b u_t^3} \tag{1.2}$$

where b is the estuary width, ρ is the water density, u_f is the velocity of fresh water flow, u_t is the root mean square tidal current, and g is gravitational acceleration. Using this equation, when R_{ie} is greater than 0.8 the estuary is highly stratified and for a R_{ie} less than 0.08, the estuary is well-mixed; anything in-between is classified as a partially-mixed estuary. Using flow data from Peterson and Conomos (1975) and Peterson et al. (1978), the stratification-circulation diagram (Fig. 11) indicates that the R_{ie} is less than 0.08 in the Northern Reach of the San Francisco Bay. Therefore, the stratification-circulation diagram also classifies the Northern Reach as a well-mixed estuary. Therefore Equation 1.1 can be reduced to

$$\frac{\partial s}{\partial t} = u\frac{\partial s}{\partial x} - \frac{\partial}{\partial x}(K_x \frac{\partial s}{\partial x}) - \Gamma \tag{1.3}$$

and the San Francisco Bay can be modeled as a one-dimensional estuary.

1.4.2. Biogeochemical Model Description

The Center for Coastal and Marine Sciences at the Plymouth Marine Laboratory, United Kingdom, developed a biogeochemical model, ECoS 3, that simulates the transport of a solute in the well-mixed Tamar Estuary, England. In the Tamar Estuary,

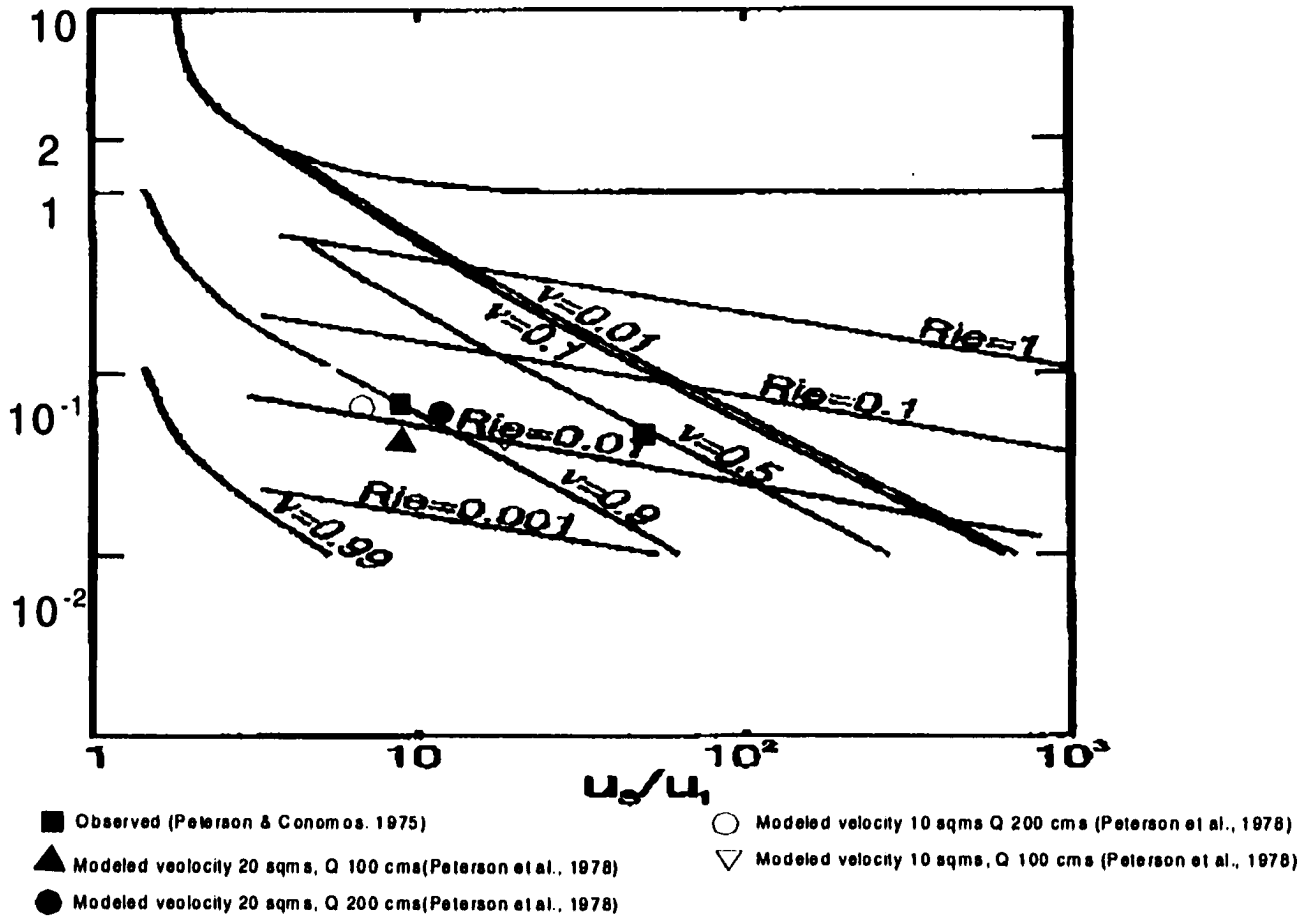

Fig. 11. Stratification-circulation diagram for the Northern Reach.

ECoS 3 simulates phytoplankton growth, sediment transport, and biological uptake of nutrients. ECoS 3 was chosen over other estuarine models because it has been proven to work an estuary that has hydrodynamics similar to the Northern Reach, it can simulate biological productivity, total suspended material, salinity, and nutrients, and it can be easily adapted to include dissolved and particulate selenium reactions. Thus, using this model only requires adjusting ECoS 3 to the San Francisco Bay and coding the processes of selenium transport and transformation. The models of Uncles and Peterson (1996), McDonald and Cheng (1997) or Cole and Cloern (1987), even though designed for the San Francisco Bay, were not chosen since they only handle one process in the estuary (i.e., salinity transport, sediment movement, phytoplankton growth) instead of the multiple interactions of a solute in the Bay.

In ECoS 3, the transport and transformation of a solute is calculated using a step-wise approach. First, the changes due to *in situ* processes, Γ, are calculated and then the changes due to transport are calculated. ECoS solves the changes in the concentration of a solute due to Γ in Equation 1.3 as:

$$c_n^{\Delta} - c_n^{\#} = \sum_i c_i g_{i,n}(c_1^{\#}, c_2^{\#} \ldots c_s^{\#}) - c_n^{\Delta} \sum_i g_{n,i}(c_1^{\#}, c_2^{\#} \ldots c_s^{\#}) \qquad (1.4)$$

where for the time step, Δt, the initial concentration of nth species, $c^{\#}_n$, and the final concentration without being transported, c^{Δ}_n, are solved, with the solute concentration being updated continuously. The transport of the solute is then calculated using the concentration of the solute at the last time step. Therefore, for each species the transport and any of the Γ terms are solved as:

$$c - c^{\Delta} = (-\frac{\Delta(uc)_x}{\Delta x} + \frac{\Delta(\frac{k_x \Delta c_x}{\Delta x})}{\Delta x})\Delta t \qquad (1.5)$$

where c is solved for the final concentration, and becomes the initial concentration for the next time step (Harris and Gorley, 1998).

In ECoS 3, the estuary can be modeled as one complete box or subdivided into a series of multiple boxes. By using multiple boxes, the concentration of the solute in a box is solved and used to predict the concentration in the next box as described in Equation 1.4 and 1.5. For each box, a solute (e.g., selenium) undergoes the same Γ processes as in the previous box. Uncles and Peterson (1996) divided the Northern Reach into 33 boxes and found that the box model approach was able to simulate salinity in the Bay with reasonable agreement between their simulations and field data. Therefore the same 33 boxes of Uncles and Peterson (1996) were used in ECoS 3.

1.4.3. Modeling Morphology and Hydrology

The shape of the estuary defines the flow of water within the estuary. To produce an accurate estuarine shape, depths at fixed points within the estuary are used to determine its bathymetry. The area of the each estuarine segment is determined from a quadratic function where:

$$A = a_o + a_1 x + a_2 x^2 \qquad (1.6)$$

where A is the area of each segment, a_o to a_2 are ratios of the cross-sectional area and water depth at suitable points along the estuary, and x is the segment length; the total

estuarine area is the sum of each segment area.

During high flow, the Sacramento-San Joaquin discharge accounts for 90% of the freshwater entering the Bay. As discussed above (in Section 1.3.2), the Sacramento River largely defines the input of fresh water into the Bay from the month of June to November (low flow months). Therefore, the Sacramento River at Rio Vista is the freshwater end member. The Pacific Ocean at Golden Gate is the seaward end member. The river end member is defined as a closed system (inputs only), while the Pacific Ocean is defined as an open end member where exchange occurs. The San Joaquin River is treated as a point source into a specific box since it only has appreciable flow during the winter months.

Discharge from the Sacramento-San Joaquin Rivers are classified into three categories, wet, dry or intermediate according to their combined discharge into the Delta. When the summer discharge is greater than 400 $m^3 s^{-1}$, it is a wet year, and a dry year is when the mean summer flow is less than 200 $m^3 s^{-1}$, but greater than 120 $m^3 s^{-1}$ (Peterson et al., 1985). The discharge from each river varies significantly between a wet, dry and intermediate year (Fig. 12). During a wet year the discharge from the Sacramento River can be 1000 $m^3 s^{-1}$ greater than that during an intermediate year (Fig. 12A). Furthermore, during a dry year the San Joaquin can have no discharge for 5 to 6 months (Fig. 12B). Due to the variability in riverine discharge, flow from each river is obtained from the Interagency Ecological Program (http://iep.water.ca.gov/dayflow/). The Interagency Ecological Program continuously monitors and quality checks the discharge data to ensure accuracy.

The rest of the Northern Reach water budget includes direct rainfall and

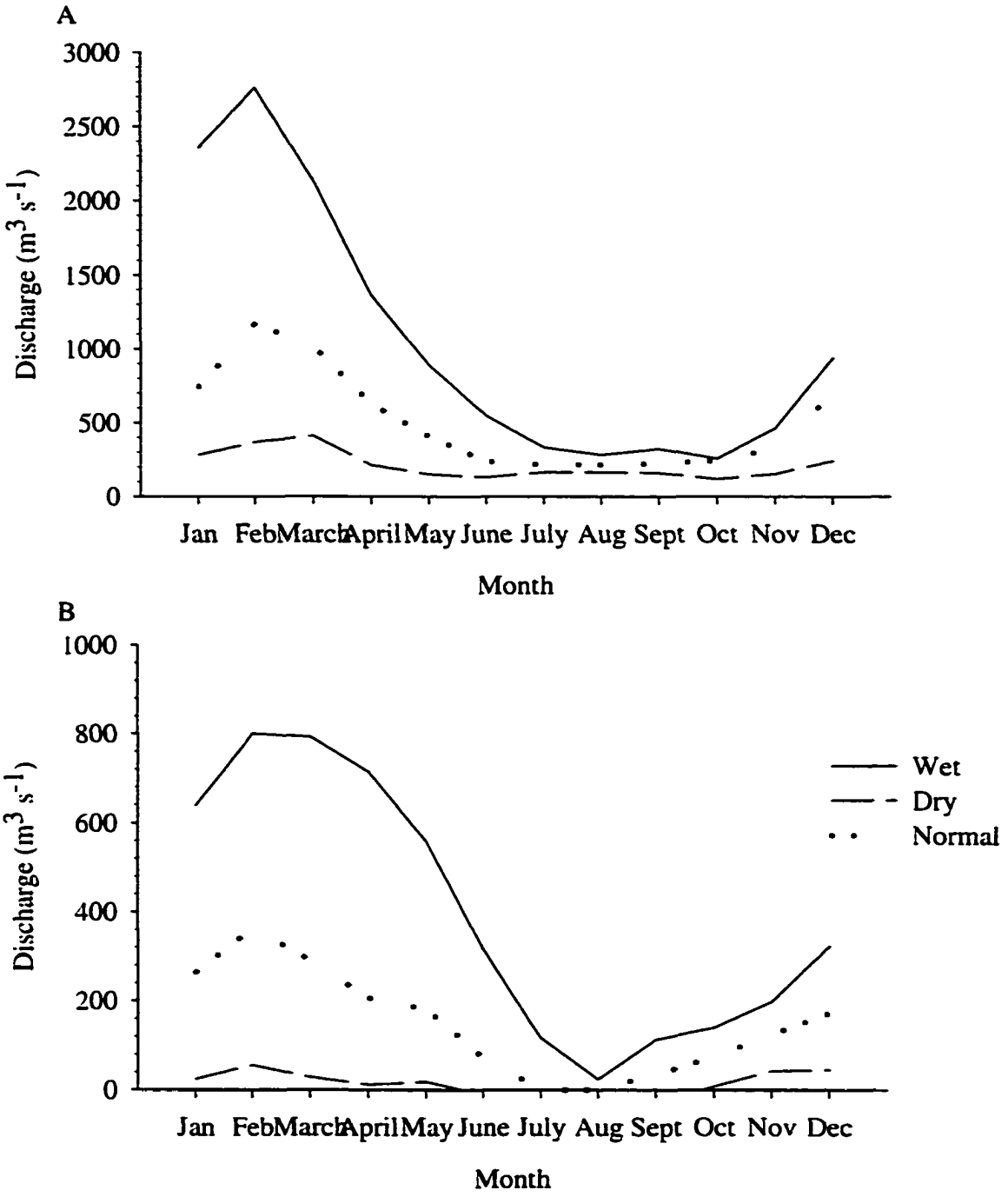

Fig. 12. Annual discharge from the Sacramento River (A) and the San Joaquin River (B) for different flow conditions. The data are from www.iep.ca.gov.

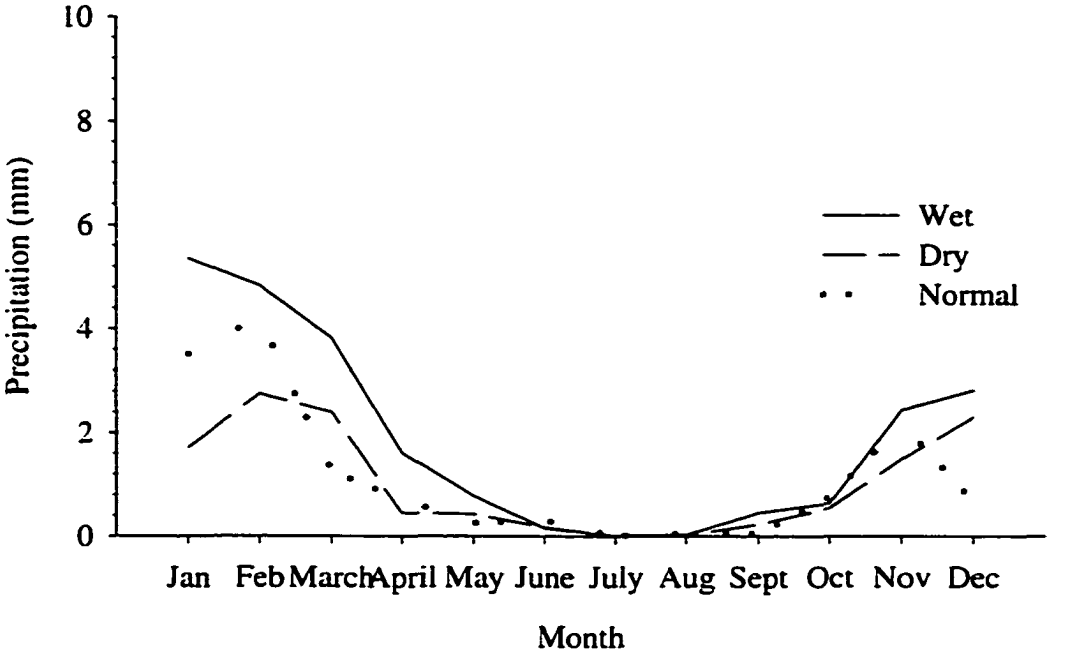

Fig. 13. Monthly precipitation averages for the San Francisco Bay.

evaporation measurements. Monthly averaged precipitation rates since 1982 can be obtained from the California Weather Database Station Davis CIMIS # 6 (http://www.ipm.ucdavis.edu/calludt.cgi/WXSTATIONDATA?STN=DAVIS.A). The precipitation between wet and dry years does not vary significantly (Fig. 13) compared to river inputs, and thus the average precipitation from 1982 to present is used for precipitation inputs. Since few researchers have measured evaporation rates in the Bay, the rates that Uncles and Peterson (1996) calculated are used. A minimum evaporation of 0.95×10^{-8} m s^{-1} occurs during December, while in July the maximum evaporation is 6.2×10^{-8} m s^{-1}. For the model, daily evaporation rates are linearly interpolated between the minimum and maximum of Uncles and Peterson (1996).

1.4.4. Tides

In the Northern Reach, the diurnal component of the tide in the San Francisco Bay is strong, and thus there is a large difference between successive low-water and high-water levels (Uncles and Peterson, 1996). The spring-neap variation in the Bay can be very pronounced, with spring tide being 1.55 times the mean amplitude at the Golden Gate, and neap tide being 0.58 times (Uncles and Peterson, 1996). Additionally, Walters and Gartner (1985) found that water circulation in the Bay is strongly driven by Pacific tides propagating through the Golden Gate. Tidal variation is simulated using a six component tidal model defined as

$$TIDE = M_2 + S_2 + K_2 + O_1 + M_4 + M_6 \tag{1.7}$$

where each component is defined as

$$TC(i) = TA(i) * COS((TP(i) - TF(i)) * \pi / 180) \quad (1.8)$$

where TC_i is the tidal constituent (e.g., M_2,S_2, K_2, etc.), TA is the tidal amplitude (m), TP is the tidal phase (degrees), TF is the tidal frequency (degrees), $\pi/180$ converts the angles of the tidal frequency and phase to radians, and COS is the cosine function.

According to Cheng et al. (1993) and Uncles and Peterson (1996), the main components of tides in the Bay are the M_2 (0.58 m), K_1 (0.37 m) and O_1 (0.23 m) constituents. Using the method of least squares harmonic analysis, tidal data from January 1999 produced amplitudes similar to those found by Cheng et al. (1993) and Uncles and Peterson (1996). Since Cheng et al. (1993) and Uncles and Peterson (1996) components were determined over a longer time period (i.e., 20 yrs), their amplitudes, phases, and frequencies are used.

1.4.5. Conservative Tracer

A conservative tracer is a constituent that is transported through an estuary without any losses or gains. Salinity is used as a conservative tracer since it does not undergo any biological or chemical reactions in an estuary (Dyer, 1997). For a conservative solute, the concentration gradient in the estuary represents a balance of advection and dispersion. The transport of a conservative solute is described by

$$\frac{\partial C}{\partial t} = -U\frac{\partial C}{\partial x} + K_w \frac{\partial^2 C}{\partial x^2} \quad (1.9)$$

where U is the water velocity, C is the conservative tracer, and K_w is the dispersion coefficient along the axis (x) of the estuary. A negative U indicates that the water is

going out of the estuary, while a positive U indicates that the water is coming into the estuary. Dyer (1997) defines the water velocity as the total freshwater input above a point in the estuary divided by the cross-sectional area of the estuary, and the dispersion coefficient as

$$K_w = \frac{Q * S}{A * (\frac{\partial S}{\partial x})} \tag{1.10}$$

where Q is the total freshwater input (m^3/s), A is the cross-sectional area (m^2), S is salinity, and $\partial S/\partial x$ is the axial salinity gradient (m^{-1}). The input of fresh water to the estuary, Q, is defined by the discharge from the Sacramento River, the San Joaquin River, precipitation, and evaporation. The initial salinity gradient at time zero is specified so that Equation 1.10 can be solved for the first day, otherwise a mathematical error occurs (cannot divide by zero).

1.4.6. Suspended Material

Total suspended material (TSM) in an estuary consists of permanently suspended material, resuspended sediment from the bed of the estuary, and particles produced *in situ* (e.g., phytoplankton). In the San Francisco Bay, the TSM concentration has an estuarine turbidity maximum (ETM) that can be formed through gravitational circulation or tidal asymmetry of velocity (Jay and Musiak, 1994; Schoellhamer, 2001). The ETM usually forms in Suisun Bay at a surface salinity between 1 and 6 (Arthur and Ball, 1979; Schoellhamer, 2001). TSM is defined as

$$TSM = PSM + BEPS + B \tag{1.11}$$

where PSM is the permanently suspended material (mg L^{-1}), BEPS is the sediment resuspended from the bed of the estuary (mg L^{-1}), and B is the phytoplankton biomass (mg L^{-1}). The inputs of PSM and BEPS and their transport are discussed below followed by the model description on how phytoplankton is produced and transported in the estuary (Section 1.4.7).

Permanently suspended material is sediment that enters the Bay through river discharge and does not sink. The velocity and dispersion of PSM can therefore be treated as a conservative solute (Harris et al., 1984) and thus the change in PSM with time becomes:

$$\frac{\partial PSM}{\partial t} = -U\frac{\partial PSM}{\partial x} + K_w\frac{\partial^2 PSM}{\partial x^2} + PSM_{river} \tag{1.12}$$

where U and K_w are defined above (Equation 1.9) and PSM_{river} is the riverine input of permanently suspended material.

Dinehart and Schoellhamer (1999) found that the Sacramento River discharges seven times more suspended sediment to the Bay than other tributaries to the Bay, including the San Joaquin River. Therefore, the primary input of PSM is through the Sacramento and the sea water end members. Harris et al. (1984) define the riverine end member input of PSM as

$$PSM_{river} = a + (b * Q_{Sac}{}^{c}) \tag{1.13}$$

where PSM_{river} is the sediment load (g d^{-1}), a is the concentration of bed-exchangeable sediment in the river water (g d^{-1}), b is the concentration of suspended sediment (g L^{-1}) , c

is an adjustable parameter, and Q_{Sac} is the discharge from the Sacramento River (L d^{-1}). The seawater end member of PSM set to a constant value as in Harris et al. (1984).

Modeling BEPS is often difficult due to little data on the concentration of sediment in the water column due to resuspension and the amount of sediment available for resuspension. The transfer of sediment between the bed of the estuary and the water column occurs during the tidal cycle (e.g., erosion during flood tide). Uncles (1981) found that a tidal asymmetry causes an up-estuary movement of particulate material. This up-estuary movement is balanced by river discharge. A resulting estuary turbidity maximum in the Northern Reach is a function of tides and salinity (Schoellhamer, 2001). Therefore, BEPS is

$$\frac{\partial BEPS}{\partial t} = -U_{BEPS}\frac{\partial BEPS}{\partial x} + K_{BEPS}\frac{\partial^2 BEPS}{\partial x^2} - \frac{\partial}{\partial z}V_s BEPS \qquad (1.14)$$

where U_{BEPS} is the transport velocity of BEPS (m d^{-1}), K_{BEPS} is the dispersion of BEPS (m^2 d^{-1}), z is depth, and V_s is the sinking velocity. The transport velocity of BEPS (U_{BEPS}) is defined as

$$U_{BEPS} = d * U - e * TIDE * S \qquad (1.15)$$

where *d* is a constant that determines the response time of the suspended particles to changes in tides and water flow, *e* is a constant that scales tidal range and salinity, TIDE is given in Equation 1.7, U is the water velocity (m d^{-1}), and S is the salinity. Equation 1.14 causes a maximum BEPS to form by allowing the net seaward velocity to increase in response to the increase in net water flow (Harris and Gorley, 1998).

The dispersion of BEPS is described by Harris and Gorley (1998) as

$$K_{BEPS} = \varepsilon * U + \psi * TIDE * S \quad (1.16)$$

where K_{BEPS} is the dispersion coefficient ($m^2 d^{-1}$), and ε and ψ are constants (m). A BEPS maximum will occur when U_{BEPS} equals zero (Harris and Gorely, 1998).

Information about basic processes governing erosion and deposition are limited due to the extreme difficulty in obtaining field measurements (McDonald and Cheng, 1997). To further complicate the matter, the Bay is periodically dredged in order to maintain navigational channels (Shoellhamer, 2002). To account for limited data on these processes, it is assumed that the total flux of sediment from the estuarine bed to the water column is balanced by a return (deposition) as in the Tamar Estuary (Harris et al., 1984). The sinking of particles, V_s, is set to a constant rate of 86.4 m d^{-1} based on measurements by McDonald and Cheng (1997). Since little is known about the sea water or riverine end member concentration of BEPS, the end members were set to those values used in other well-mixed estuaries. For the sea water end member, BEPS was set to zero, and the riverine end member concentration of BEPS was set to a constant value of 0.004 g L^{-1} (Harris et al, 1984).

1.4.7. Phytoplankton Dynamics

Modeling phytoplankton biomass is difficult due to seasonal variations in community composition and productivity within an estuary (Cloern et al., 1985). In a well-mixed estuary, phytoplankton biomass is modeled as

$$\frac{\partial B}{\partial t} = -U\frac{\partial B}{\partial x} + K_w \frac{\partial^2 B}{\partial x^2} + u_n B - GB - P_b B - \frac{\partial}{\partial z}(w_s B) - RB - B_{river} Q \quad (1.17)$$

where B is the phytoplankton biomass (g chl L^{-1}), μ_n is the net biomass-specific growth rate of phytoplankton (d^{-1}), G (d^{-1}) is loss rate due to zooplankton grazing (Koseff et al., 1993; Lucas et al., 1998), P_b (d^{-1})is a loss due to benthic grazing (Koseff et al., 1993; Lucas et al., 1998), z is the depth (m), w_s is the sinking rate, and R is the loss of phytoplankton due to respiration, and B_{river} is the riverine input of phytoplankton. Sinking of phytoplankton tends to be small (0.5 m d^{-1} to 0.9 m d^{-1}) and is set to a constant value based on literature values of Cloern (1991), Kosseff et al., (1993), and Lucas et al. (1998) for the San Francisco Bay (0.5 m d^{-1}).

The net biomass-specific growth rate, u_n, is

$$u_n = \frac{P}{C : Chlorophyll} \quad (1.18)$$

where P is the biomass specific rate of photosynthesis (mg C mg chl^{-1} d^{-1}), and C:Chlorophyll is the carbon to chlorophyll-a ratio. This ratio is 51 mg C (mg chl)$^{-1}$ based on measurements by Cloern and Alpine (1991) in the San Francisco Bay.

The biomass specific rate of photosynthesis, (B in Equation 1.17) can be a function of nutrients, light availability, respiration losses, and grazing. Past research by Cole and Cloern (1984,1987), Peterson et al. (1987), and Alpine and Cloern (1988) have shown that in the San Francisco Bay nutrient concentrations are greater than those needed to limit phytoplankton growth. High turbidity in the estuary makes growth a function of light availability (Cole and Cloern, 1984; Peterson and Festa, 1984), and phytoplankton growth is based on the photosynthesis-irradiance equation of Platt and Jassby (1976):

$$P = P_m \tanh(\alpha I) \quad (1.19)$$

where P is the biomass-specific rate of photosynthesis (see above), P_m is the maximum rate of photosynthesis at optimal light intensity (mg C (mg chl)$^{-1}$ d^{-1}), α is the initial slope of the light-saturation curve divided by P_m (m^2 d^1 Einst.$^{-1}$) , and I is the photosynthetically active radiation (PAR, Einst. m^{-2} d^{-1}). In the Northern Reach, P_m varies from 24 to 219 mg C (mg chl)$^{-1}$ d^{-1} (Cloern and Alpine, 1991), with alpha value of 0.002 to 0.009 Einst. m^2 d^{-1} (Peterson and Festa, 1984; Lucas et al., 1998). These values are the ranges of P_m and α used in the model .

Photosynthetically active radiation (I in Equation 1.19) is absorbed and scattered by dissolved and suspended matter in the water (Parsons et al., 1984). The irradiance of light at depth, z, is expressed as

$$I(z,\lambda) = I_\lambda e^{-kz} \quad (1.20)$$

where λ is the wavelength of light, k is the attenuation coefficient of light within the water column (m^{-1}), and z is the depth in meters (Miller and Zepp, 1979). In a well-mixed water column, it is assumed that biomass is within the photic zone, and thus every molecule in the water column is exposed to an equal amount of sunlight during a given period (Miller and Zepp, 1979). In a well-mixed estuary Equation 1.20 then becomes

$$I = I_\lambda \left(\frac{1 - e^{(-kz)}}{kz}\right) \quad (1.21)$$

where I_λ in the model is defined as the photosynthetically active radiation (PAR, Einst. m^{-2} d^{-1}).

PAR is calculated using an empirical equation that Jim Cloern (personal

communication) developed using historical sunlight data from the California Weather Database at Davis (http://www.ipm.ucdavis.edu/calludt.cgi/WXSTATIONDATA?STN=DAVIS.A):

$$I_\lambda = 13.8237 + 47.608 * \sin^2\left(\frac{JulianDay * \pi}{365}\right) \quad (1.22)$$

Cloern (personal communication) found that the linear correlation coefficient, r, between the observed PAR and the calculated PAR using Equation 1.22 was 0.992.

The attenuation coefficient, (k in Equation 1.21) is defined by Parsons et al. (1984) as

$$k = k_w + k_d + k_p + k_s * TSM \quad (1.23)$$

where k_w is the scattering of light due to water (m^{-1}), k_d is due to dissolved matter (m^{-1}), k_p is due to phytoplankton (m^{-1}), and k_s is due to non-living suspended material (L g^{-1} m^{-1}). The attenuation of light due to phytoplankton is less than 5% of the total light attenuation in the San Francisco Bay (Cole and Cloern, 1987), and thus k_b is set to zero. The sum of k_w and k_d is set to 0.1 m^{-1} based on calculations by Miller and Zepp (1979). In fresh water systems k_s can be as high as 500 L g^{-1} m^{-1} (Miller and Zepp, 1979) if the photic depth is less than 0.1 m. In the San Francisco Bay, Cloern and Alpine (1991) reported a photic depth between 0.5 and 2 m. Therefore, k_s may need to be adjusted during calibration to represent the conditions in the San Francisco Bay. The above equations (1.19 through 1.23) are needed to simulate u_n for Equation 1.18.

Phytoplankton mortality in the San Francisco Bay is due to respiration losses and grazing effects (benthic and zooplankton). Mortality due to respiration (R in Equation

1.17) can be up to 10% of P_m (Cole and Cloern, 1984) and is held at a constant value (10% of P_m) in the model.

Grazing in the San Francisco Bay includes zooplankton grazing and benthic grazing. The zooplankton grazing rate (G in Equation 1.17) is simulated by the model using mean zooplankton biomass and a modified Ivlev function that predicts the ingestion of phytoplankton per animal (Cloern et al., 1985). The later is a function of temperature (Conover, 1956; Ikeda, 1974; Vidal, 1980) and zooplankton weight (Paffenhoefer, 1971, Nival and Nival, 1976; Vidal, 1980). Parson and LeBrasseur (1970) define daily ingestion of phytoplankton by zooplankton, F, (mg C animal^{-1}) as

$$F = 9.5x10^{-4} * W^{0.8} * e^{0.069*(T-10)} * (1 - e^{-0.01*B}) \quad (1.24)$$

with T being temperature (^{0}C), W is the zooplankton mass (μg C animal^{-1}), and B is the biomass of phytoplankton in units of carbon. The weight of zooplankton varies among species and ranges from 7 to 63 µg C animal^{-1} (Hutchinson, 1981). The temperature of the water is the estuarine averaged temperature from the USGS monitoring program (http://sfbay.wr.usgs.gov/access/wqdata/webbib.html). The phytoplankton biomass is converted to units of carbon with a carbon to chlorophyll-a ratio. The total daily zooplankton ingestion, I, (mg C m^{-3}) is calculated using

$$I = F * Z \quad (1.25)$$

where Z is the average zooplankton abundance (m^{-3}). Zooplankton biomass in the San Francisco Bay varies seasonally, but species composition is similar for each season in 1978 to 1981 (Ambler et al., 1985). Zooplankton communities within the San Francisco Bay are comprised of *Acartia claus.*, *Acartia californiensis*, *Oithona davisae*,

harpacticoid copepods, *Eurytemora affinis*, *Sinocalanus doerrii*, cyclopoid copepods, *Bosmina sp.*, *Daphnia pulex*, *Brachionus sp.*, and bivalve veligers (Ambler et al., 1985). Mean zooplankton abundance for each season was obtained from Ambler et al. (1985) and Purkerson et al. (accepted) with 10 animal L^{-1} during the winter to 850 animal L^{-1} during the spring/summer. Linear interpolation to estimate biomass between these extremes was used.

Using the above equation (1.25), the specific loss of phytoplankton per day by zooplankton grazing (G in Equation 1.17) is simulated from Cloern et al. (1985)

$$G = \frac{-\ln(B - I)}{B} \tag{1.26}$$

with B being the phytoplankton biomass in units of carbon.

Benthic grazing of phytoplankton (P_b in Equation 1.17) is largely due to the presence of the benthic clam, *Potomocorbula amurensis*. Prior to the introduction of *P. amurensis*, the main control on phytoplankton populations was zooplankton grazing (Cloern et al., 1985). In 1987, *P. amurensis* colonized the Bay, causing a significant decrease in phytoplankton biomass (Cloern and Alpine, 1992). The introduction of *P. amurensis* resulted in a decrease in the average summer chlorophyll-a concentration from 20 μg chl L^{-1} to less than 2 μg chl L^{-1} (Cloern and Alpine, 1992). Based on measurements by Werner and Hollibaugh (1993), *P. amurensis* has the potential to graze phytoplankton at rates greater than the specific growth rate of phytoplankton. Since the San Francisco Bay is well-mixed, potentially all the phytoplankton are available to the benthos (Werner and Hollibaugh, 1993). Food availability to *P. amurensis* is affected by

water movement and food depletion within the benthic boundary layer and is still under investigation (Frechette and Bourget, 1985a,b; Frechette et al., 1989). Samplings in the Northern Reach indicate that a large number of benthic grazers are located in Suisun Bay (Thompson, 2000); therefore, grazing rates were increased by 25% for this region. Although few data on benthic grazing rates for the Northern Reach are available, the rates were compared to those in the South Bay (Cloern, 1982), with Kosseff et al., (1993), and Lucas et al (1998).

The concentration of phytoplankton added to the estuary via the Sacramento River is defined as

$$\frac{\partial B_{input}}{\partial t} = B_{river} * Q \qquad (1.27)$$

where B is the riverine concentration of phytoplankton (μg chl L^{-1}), with B varying with time, and Q is the freshwater discharge from theh river. The same equation is used to define the input of phytoplankton from the San Joaquin River. Due to limited data availability, chlorophyll-a concentrations at the sea water end member of phytoplankton are held constant based on measurements by Cutter and Cutter (in prep.) at the Golden Gate (2.3 ± 1.0 μg chl L^{-1}).

1.4.8. Dissolved Selenium Speciation

Dissolved selenium is introduced to the estuary through the Sacramento River, the San Joaquin River, refinery effluents, and sediment pore water fluxes. Total dissolved selenium is defined as the sum of selenite, selenate and organic selenide. As discussed

above (Section 1.3.2.), selenite, selenate and organic selenide profiles from the San Francisco Bay suggest that there are production and removal of each of these species in the Bay. Therefore, the time dependent behavior of any dissolved selenium species is given by:

$$\frac{\partial Se_i}{\partial t} = -U\frac{\partial Se_i}{\partial x} + K_w\frac{\partial^2 x}{\partial x^2} - \Gamma \qquad (1.28)$$

where Se_i is the selenium species of interest.

The input of selenium from the Sacramento River has remained fairly constant over the last 10 years (Cutter and Cutter, in prep.) and shows minor variability with time (Cutter and San Diego-McGlone, 1990). Thus, the concentration of selenite, selenate, and organic selenium were plotted against Julian days and a sine wave was fit to the data. The following equation is used to fit the selenium speciation in the Sacramento River and the San Joaquin River:

$$y = y_o + a * \sin(\frac{2 * \pi * T}{b} + c) \qquad (1.29)$$

where y_o is the initial selenium concentration at June 1, 1986, a, b, and c are fitting constants, and T is the time in Julian days. The constants for a, b, and c for each selenium species are found in Table 2.

Table 2
Constants for Equation 1.29 for the Sacramento and San Joaquin River

	a	b	c	y_o	r
Sacramento River					
Selenite	0.03	75	0.41	0.11	0.48
Selenate	0.29	1556	3.77	0.60	0.76
Organic Selenide	0.06	312	1.32	0.35	0.36
San Joaquin River					
Selenite	0.15	125	4.87	0.24	0.62
Selenate	1.69	622	5.30	5.49	0.57
Organic Selenide	1.42	76	5.49	2.77	0.69

Speciation data used in Equation 1.29 for the San Joaquin River were taken from Vernalis, which is approximately 60 km from where the San Joaquin River enters the Delta. During the transport of selenium through the Delta biogeochemical processes could cause removal/production of selenium. Cruise samples taken in the San Joaquin River (Fall, 1998, Summer 2000; Cutter, unpublished data) indicate that the concentration of selenium at Vernalis is reduced by 60 to 80% as it is being transported from San Joaquin River through the Delta and into the estuary at Antioch. Based on these findings, the predicted selenium concentrations at Vernalis from Equation 1.29 for the San Joaquin River is reduced in order to represent the actual input of selenium at Antioch (referred to as "Delta removal effect" in the following Chapters), using the above percentages to account for any removal of selenium in the Delta.

As stated earlier, refineries are a source of selenium in the Northern Reach. Total selenium input to the Northern Reach from each refinery is monitored due to

environmental regulations. Output fluxes of total selenium were obtained from each refinery for the years of interests (San Francisco Bay Regional Water Quality Control Board, personal communication). Cutter and Cutter (in prep.) and Cutter and San Diego-McGlone (1990) determined speciation data from these refinery effluents. Refinery inputs of dissolved selenium are treated as point sources in the model and the fluxes are held constant with time for each.

Exchange with the open ocean can also be a source of selenium to the estuary. Observations by Cutter and Bruland (1984) show that total selenium in the Pacific Ocean is approximately 1 nmol L^{-1}, and of this 80% is in the form of organic selenide. Based on their findings, the sea water end member concentration were specified and held constant over time.

The production and removal terms, Γ (Equation 1.28), that affect selenium include biological uptake and oxidation/reduction reactions (Fig. 10). Phytoplankton are able to influence the speciation of dissolved and particulate selenium by selectively taking up dissolved selenium species and producing particulate organic selenide. Figure 14 shows the biotic and abiotic reactions that occur in oxygenated waters. The rate constants k_4, k_5,and k_6 are functions of biological activity, while the rate constants k_2 and k_3 are a function of oxygen concentrations (Fig. 14).

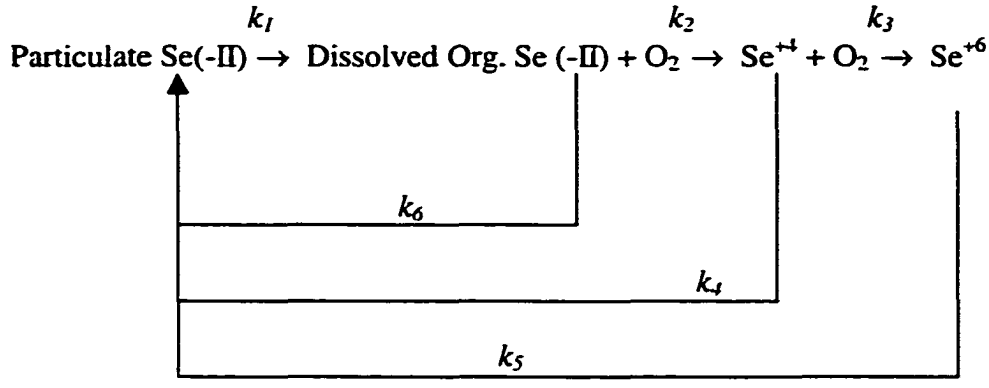

Fig. 14. Possible reaction pathways for selenium in oxic seawater and associated first order rate constants.

The time dependency of selenate, selenite, and organic selenide concentrations (Γ in Equation 1.28) are described by:

$$\frac{\partial Se(VI)}{\partial t} = k_3[Se(IV)] - k_5[SeI(VI)] \quad (1.30)$$

$$\frac{\partial Se(IV)}{\partial t} = k_2[\partial DSe(-II)] - k_3[Se(IV)] - k_4 Se(IV) \quad (1.31)$$

$$\frac{\partial DSe-II}{\partial t} = k_1[PSe(-II)] - k_2[DSe(-II)] - k_6[DSe(-II)] \quad (1.32)$$

The transformation of particulate selenide to dissolved organic selenide, k_1, is biologically controlled and probably of a complex order, but regeneration experiments (Cutter, 1982) show that the reaction is fast and pseudo first order (Cutter and Bruland, 1984). The oxidation of dissolved organic selenide to selenite, k_2, and selenite to selenate, k_3, are also pseudo first order since dissolved oxygen concentrations are high relative to dissolved organic selenide and selenite concentrations (Cutter and Bruland,

1984; Cutter, 1992). The oxidation rate constants for selenium (k_2 and k_3) have been previously determined (Table 3).

As noted in the preceding discussion, the rate constant k_4, k_5, and k_6 are controlled by phytoplankton, but Michaelis-Menton uptake parameters for selenite, selenate, and organic selenide in marine phytoplankton are limited and have some problems. For selenite, Baines and Fisher (2001) determined a half-saturation value of 0.2 nmol L^{-1} for the diatom, *Thalassiorsira pseudonana*. Vandermeulen and Foda (1988) found a selenite half-saturation of 15 nmol L^{-1} for the diatom *Thalassiorsira nordenskoldii*. For freshwater phytoplankton (a chlorophyte, *Ankistrodesmus* sp., a cyanophyte *Merismopedia* sp., and algae *Anabaena flos-aquae*, *Chlamydomonas reinhardtii*, and *Cyclotella meneghiani*), Riedel et al. (1991) observed linear uptake of selenite for concentrations of 12 to 633 nmol L^{-1}. These studies indicate that there can be a large difference in selenite uptake by phytoplankton that is dependent on the species present. In the San Francisco Bay, the phytoplankton community is mostly dominated by diatoms (Cloern et al., 1985, Lehman, 2000). In the winter, phytoplankton biomass in the upper estuary is comprised of freshwater diatoms (*Melosira* spp., *Fragilaria crotonensis*, *Amphora* sp., *Skeletonema costatum* and *Thalasiosira rotula;* Cloern et al., 1985). Marine centric diatoms (*Thalassiosira* spp. and *Coscinodiscus* spp.; Cloern et al 1985; Lehman, 2000) dominate the spring blooms. Due to the large range in phytoplankton uptake rates and the fact that the Bay is dominated by fresh water diatoms, the first order uptake rate constants for selenite of Riedel et al. (1996) will be used instead of Michaelis-Menton kinetics (Table 3). This will also be discussed later.

Table 3
First order rate constants for selenium

Constant	Process	Value	Unit	Reference
k_1	P Se(-II) →D Se (-II)	1.3×10^{-5} - 5×10^{-2}	d^{-1}	Cutter (1991)
k_2	D Se(-II) →D Se (IV)	1.0×10^{-3} - 81.0	d^{-1}	Cutter (1991)
k_3	D Se(IV) →D Se (VI)	2.4×10^{-6}	d^{-1}	Cutter & Bruland (1984)
k_4	D Se(IV) → P Se (-II)	2.02-2.41	µmol (g chl)$^{-1}$ hr^{-1}	Riedel et al. (1996)
k_5	D Se(VI) → P Se (-II)	0.43-0.58	µmol (g chl)$^{-1}$ hr^{-1}	Riedel et al. (1996)
k_6	D Se(-II) → P Se (-II)	0.5 k_4	µmol (g chl)$^{-1}$ hr^{-1}	Baines et al. (2001)

For selenate, Vandermeulen and Foda (1988) found that the uptake rate by marine phytoplankton is linear, but minimal until concentrations are in the millimolar range. Riedel et al. (1996) found freshwater phytoplankton take up 21% less selenate than selenite, but that it is also linear for concentrations ranging from 12 to 633 nmol L^{-1}. The above results suggest selenate uptake cannot be defined by Michaelis-Menton kinetics. Therefore, the selenate uptake rate constants of Riedel et al. (1996) will be used (Table 3).

Like inorganic selenium uptake, the uptake of organic selenide is still under investigation. Baines et al. (2001) found that the uptake of organic selenide is complex and is about half the rate of selenite uptake. Based on this finding the uptake rate constant of organic selenide was set at half of selenite value in the model. Clearly, more rate measurements are needed for estuarine phytoplankton species; this is discussed in future studies in Chapter V.

Pore water exchange can be a significant source or sink of dissolved selenium to the estuary (see above discussion and Chapter II). Pore water exchange is modeled as

$$\frac{\partial Se_{porewater}}{\partial t} = A * J_{Se} \tag{1.33}$$

where A is the area (m^2) of the sediment and J_{Se} is the diffusive flux (nmol m^{-2} yr^{-1}). The pore water fluxes from Chapter II indicate that dissolved selenite + selenate are fluxing into the sediments and dissolved organic selenide is fluxing out of the sediments. Mass balance calculations show that there may have been a change in pore water fluxes in the past 10 years. To account for this, diffusive fluxes are calculated based on the overlying

water concentration. The axial gradient of pore water concentrations for selenite + selenate and organic selenide are specified based on the measurements in Chapter II.

1.4.9. Particulate Selenium Speciation

Particulate selenium in the water column is derived from sediment resuspension, sediment loading from the Sacramento River, and *in situ* production (e.g., phytoplankton uptake of selenium). Total particulate selenium is defined as the sum of particulate elemental selenium, selenite + selenate, and organic selenide.

Elemental selenium can only be generated through dissimilatory selenite + selenate degradation in anoxic systems (Oremland et al., 1989). The water column in the San Francisco Bay is oxic, and therefore the presence of particulate elemental selenium must be through either sediment resuspension or riverine inputs. The input of elemental selenium to the water column is described by:

$$\frac{\partial PSe_o}{\partial t} = Se_{o.SED} * \frac{\partial BEPS}{\partial t} + Se_{o.river} * \frac{\partial PSM}{\partial t} \tag{1.34}$$

where PSe_O is the particulate elemental concentration (nmol L^{-1}) in the water column, $Se_{o.\,BED}$ is the elemental selenium concentration on the bed of the estuary (nmol g^{-1}), $Se_{o.river}$ is the riverine concentration of selenium (nmol g^{-1}), PSM is defined by Equation 1.12 and BEPS is defined by Equation 1.14.

The particulate selenite + selenate concentrations are represented by

$$\frac{\partial PSe_{IV+VI}}{\partial t} = Se_{IV+VI.SED} * \frac{\partial BEPS}{\partial t} + Se_{IV+VI.river} * \frac{\partial PSM}{\partial t} - \Gamma \tag{1.35}$$

where PSe_{IV+VI} is the particulate selenite + selenate concentration in the water column

(nmol L^{-1}), $Se_{IV+VI,\ SED}$ is the particulate selenite + selenate concentration in the sediments (nmol g^{-1}), $Se_{o,river}$ is the riverine concentration of selenium (nmol g^{-1}), and the other variables have been previously described, and Γ is adsorption/desorption.

Adsorption of selenite and selenate onto minerals have been extensively studied in soils (Balistrieri and Chao, 1986; Ahlrichs and Hossner, 1987; Bar-Yosef and Meek, 1987; Neal et al., 1987; Zhang and Sparks, 1990). Selenate adsorption is non-specific and is an outer sphere complex that can be represented by Fig. 15 (Zhang and Sparks, 1990).

$$SeO_4^{2-} + XOH + H^+ \underset{b}{\overset{a}{\rightleftharpoons}} XOH_2^+\text{-}SeO_4^{2-}$$

Fig. 15. The adsorption/desorption of selenate onto particles, where XOH is the neutral surface site.

However, ligand exchange is responsible for selenite adsorption (Balistrieri and Chao, 1987; Zhang and Sparks, 1990) and can be expressed by Fig. 16. In both figures, the rate constant for adsorption is *a* and rate constant for desorption is b.

$$SeO_3^{2-} + XOH + 2H^+ \underset{b}{\overset{a}{\rightleftharpoons}} XHSeO_3^0 + H_2O$$

$$SeO_3^{2-} + XOH + H^+ \underset{b}{\overset{a}{\rightleftharpoons}} XSeO_3^- + H_2O$$

Fig. 16. The adsorption/desorption of selenite onto particles, where XOH is the ligand.

Neal et al. (1987) found that when the ionic strength in saturated sediments was increased from 0.05 M to 0.1 M the change in selenite adsorption was minimal. However, increasing the pH or increasing the concentration of phosphate in the soils resulted in a decrease in selenite adsorption by one-half (Neal et al., 1987). Ahlrichs and Hossner (1987) and Balistrieri and Chao (1987) found similar results when increasing pH on low ionic strength solutions (0.1M). Selenite adsorption decreases with pH until it is undetectable at a pH of 8.3 (Zhang and Sparks, 1990). In fresh water, Zhang and Sparks (1990) suggests that selenite adsorption may be complex, but occurs rapidly (i.e., within 60 seconds).

For selenate, in sediments the primary factor controlling the rate of adsorption is pH (Ahlrichs and Hossner, 1987; Balistrieri and Chao, 1987; Zhang and Sparks, 1990). At a pH of 6, the adsorption of selenate is non-detectable (Balistrieri and Chao, 1987; Zhang and Sparks, 1990). These findings also suggest that the adsorption of selenate is weaker than that of selenite. Based on these findings, selenate adsorption in an estuary would be minimal due to the high pH. Thus, it is assumed that any adsorption only involves selenite.

All of the available studies of selenite adsorption have only been in low ionic strength waters, thus making it difficult to apply the above findings to an estuarine environment. In an estuary, a change in pH, salinity, and turbidity often affects the adsorption of a metal to particles (Salomon and Forstner, 1984). For cadmium (Bale, 1987), nickel and zinc (Liu et al., 1998), and copper and manganese (Millward and Moore, 1982), studies found that even though adsorption decreased with pH, the effects

of salinity were greater. Freundlich and Langmuir equations cannot be used to model metal adsorption due to salinity effects (Chen and Lin, 2001). However, the adsorption of selenite onto particles can be characterized by the distribution coefficient (K_d)

$$K_d = \frac{a'}{b} \tag{1.36}$$

where a' is the intrinsic adsorption rate constant (L g^{-1} d^{-1}), and b is rate constant (d^{-1}) of desorption in Fig. 16 (Nyffeler et al., 1984). For fresh water, Lemly (1985) determined a fresh water partition coefficient of 0.3 L g^{-1}, while Zhang and Moore (1996a, 1996b) determined a K_d that ranged from 0.5 L g^{-1} to 2.5 L g^{-1}. Studies by Zhang and Sparks (1990) indicate that at a pH of 8.3, adsorption of selenite is minimal, therefore K_d in seawater is zero. Based on the adsorption behavior of other metals in an estuary and reported K_d values for selenite, the decrease in K_d for selenite with increasing salinity is modeled as

$$K_d = k_o * (S+1)^{-\Xi} \tag{1.37}$$

where k_o is the distribution coefficient in fresh water (L kg^{-1}), and Ξ is the power that dictates how the distribution coefficient declines with increasing salinity (Bale, 1987). Equation 1.37 was fitted to the literature data described above to obtain the coefficients k_o and Ξ.

It is often difficult to measure the rate constants a and b in Fig. 16, but they can be determined from the K_d value. Nyffeler et al. (1984) found that reaction rate constant can be quantified as

$$a = a' * BEPS + a' * PSM \tag{1.38}$$

where a is the reaction rate constant of adsorption, a' is the rate coefficient of adsorption (L g^{-1} d^{-1}), BEPS and PSM are described above. Nyffeler et al. (1984) and Zhang and Sparks (1990) found that a' for selenite ranged from 0.1 L g^{-1} d^{-1} to 0.8 L g^{-1} d^{-1}. By rearranging Equation 1.36, b can be solved as (Nyffeler et al., 1984; Bale, 1987)

$$b = \frac{a'}{K_d} \tag{1.39}$$

with K_d defined above. This is a kinetic approach that Nyffeler et al. (1984) used to investigate the adsorption/desorption of selenite in sediments. The values of Nyffeler et al. (1984) are used for a' in the model.

The concentration of particulate organic selenide is a function of BEPS, PSM, and *in situ* production. Once phytoplankton take up dissolved selenium, as defined by the uptake rates (k_4, k_5, and k_6 described earlier), it is converted into particulate organic selenide. Particulate organic selenium is defined as

$$\frac{\partial PSe_{-II}}{\partial t} = Se_{-II.SED} * \frac{\partial BEPS}{\partial t} + Se_{-II.river} * \frac{\partial PSM}{\partial t} + P_{uptake} - k_1[PSe(-II)] \tag{1.40}$$

where $Se_{org.SED}$ is the organic selenide concentration in the sediment (nmol g^{-1}), $Se_{org.river}$ is the riverine concentration of organic selenide (nmol g^{-1}), BEPS and PSM (g L^{-1}) are defined above (Section 1.4.6), k_1 is the oxidation of particulate organic selenide to dissolved organic selenide, and uptake is defined as

$$P_{Uptake} = k_4 * [Se(IV)] + k_5[Se(VI)] + k_6[DSe(-II)] \tag{1.41}$$

with the k values described above (Section 1.4.8.). The concentration and speciation of sedimentary selenium is discussed in Chapter II. Using the sediment data from Chapter

II, the selenium concentration in the bed of the sediment for each species (Equations 1.34, 1.35 and 1.40) is quantified. Doblin et al. (in prep.) determined the PSM concentration at the riverine end member and those concentrations ranges are used to define PSM selenium (elemental selenium ranged from 1.04 to 5.01 nmol g^{-1}, selenite + selenate from non-detectable to 3.21 nmol g^{-1}, and organic selenide concentrations from 0.20 to 9.35 nmol g^{-1}).

The above equations define the biogeochemical cycle of selenium in the Northern Reach. The next chapter discusses the geochemistry of selenium in the sediments from the San Francisco Bay. Once the speciation of selenium in the sediments is quantified, the above model can be calibrated to observed dissolved and particulate data from 1999 as presented in Chapter III. A sensitivity analysis, presented in Chapter III, of the model will indicate which of the above parameters are controlling the dissolved and particulate concentrations and distribution of selenium in the Bay. Once the model is successfully calibrated, validation of the model using dissolved and particulate selenium data from 1986, 1987, 1988, 1997, and 1998 will determine the ability of the model to predict selenium in the Bay under different environmental conditions. Upon successful validation, future predictions on how changing the flow from the San Joaquin River and changing refinery inputs would affect particulate and dissolved selenium concentrations are presented.

CHAPTER II

SEDIMENTARY SELENIUM IN THE SAN FRANCISCO BAY

2.1. SEDIMENT INTRODUCTION

The speciation of dissolved selenium in estuarine waters (Measures and Burton, 1978; Takayanagi and Wong, 1984; Takayanagi and Cossa, 1985; van der Sloot et al., 1985; Cutter, 1989b; Cutter and Cutter, in prep.) and its bioavailability (Price et al., 1987; Fisher and Reinfelder, 1991; Luoma et al., 1992; Hu et al., 1996; Doblin et al., 1999) have been extensively studied, but only a few researchers (Belzile and Lebel, 1988; Takayanagi and Belzile, 1988; Velinsky and Cutter, 1991; Peters et al., 1999) have examined the speciation of selenium in marine sediments (discussed in Chapter I). In estuarine sediments, diagentetic processes can change the speciation or phase (dissolved/particulate) of a trace element, and thus cause the sediments to act as an important source or sink to an estuary. For example, in the Chesapeake Bay methyl mercury is formed within estuarine sediments and released to the overlying water column during seasonal anoxia (Mason et al., 1999). Research by Takayanagi and Belzile (1988) showed that phase changes of selenium are occurring in sediments from the St. Lawrence Estuary. In these sediments the loss of solid phase selenium was balanced by an upward flux of pore water selenium to the overlying water (Takayanagi and Belzile, 1988). Determining the speciation of selenium in estuarine sediments provides additional information on biogeochemical reactions within the sediments, and their role as

sources/sinks to the San Francisco Bay; the later was included in the estuarine selenium model described in Chapter I. This chapter discusses the geochemistry of sedimentary selenium in the Northern Reach of the San Francisco Bay.

2.2. METHODS

2.2.1. Sample Collection

The criteria for sediment sampling included finding areas where high selenium concentrations were reported in clams (e.g., *Macoma balthica* and *Corbicula* sp., Johns et al., 1988), taking cores in areas of sediment accumulation, and locating sites close to refinery effluent discharges. Sediment samples were taken in San Pablo Bay, Suisun Bay, the Delta, and a mudflat and marsh located in Martinez (Fig. 17).

Sediment and pore water samples were collected on 7 November 1997, 18 June 1998, 7-8 October 1998, and 4-5 November 1999 using the R.V. David Johnson and a box corer. From each box core, one sub-core was taken for sediment sectioning and two sub-cores were taken to obtain pore water samples. Sediment sub-cores (20 cm deep) were obtained with an acrylic core tube (o.d. of 5.7 cm). Within an hour of collection, the sediment sub-core was sectioned in 1 cm intervals up to 5 cm, and below this depth, in 2 cm intervals. All sediment samples were placed in polyethylene whirl pak bags and immediately frozen until processing.

High-resolution pore water samples were collected using the whole-core squeezer method described by Bender et al. (1987). The acrylic sub-core tube (o.d. of 7.7 cm) was inserted into the box core sediments, and the top piston, fitted with a 3.5 cm porous

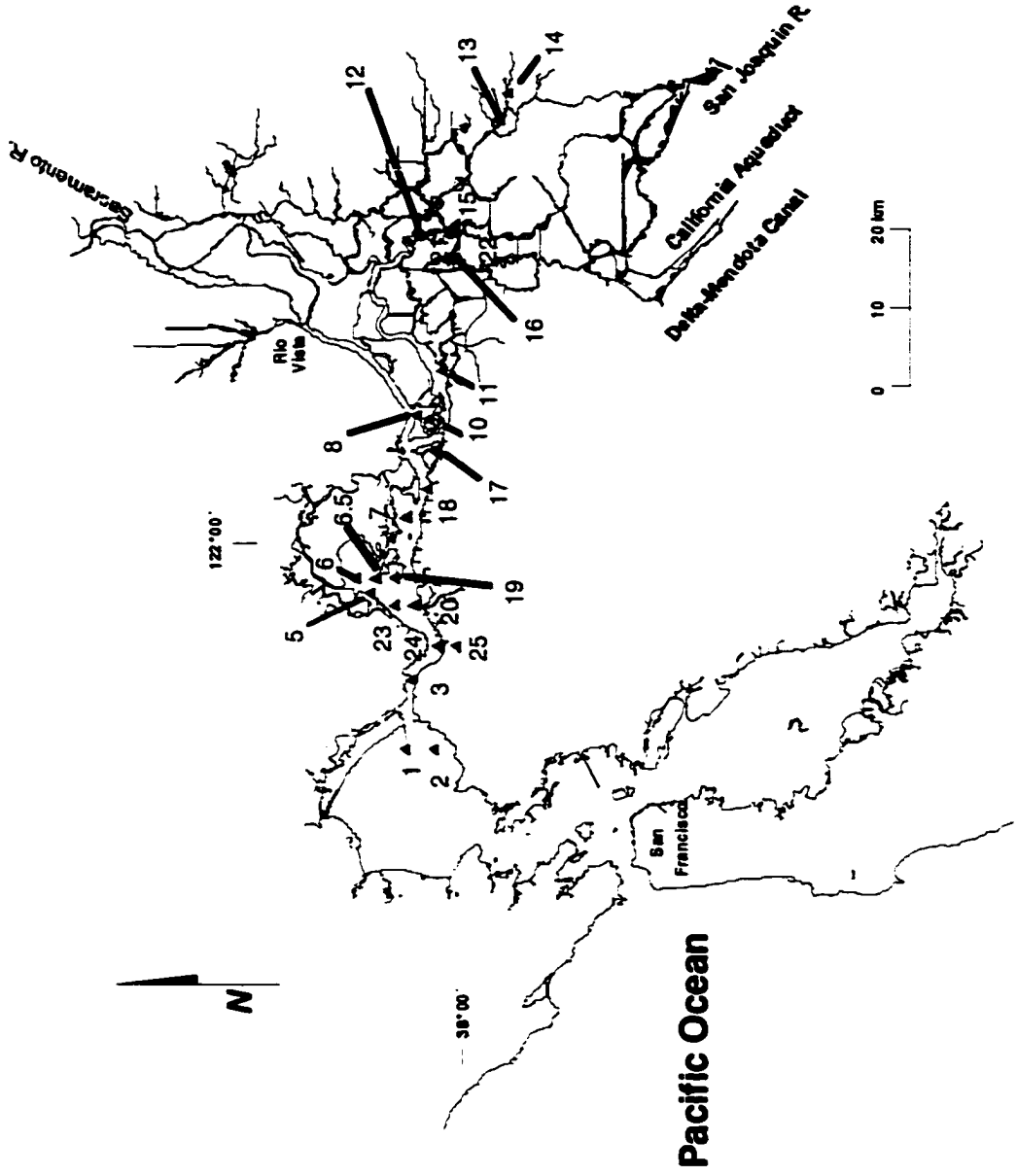

Fig. 17. Sediment sampling sites in the Northern Reach and the Delta.

polyethylene disk on the bottom, and three-way valve to extract pore water was placed in the top of the sub-core tube before removal. Once removed, the bottom piston was quickly inserted into the bottom of the core. The sub-core was placed in a rack that held the core tube and top piston in place, while a hydraulic jack pushed the bottom piston up, causing the sediment to move to the upper piston of the squeezer. Water was pre-filtered through the porous polyethylene disk before it was transferred through a three-way valve into a gas-tight glass syringe (Zhang et al., 1998). After 10 mL of pore water were taken, the three-way value was closed, another syringe attached, and the sample was directly filtered through a 0.4 μm membrane filter into pre-cleaned glass vials. Due to low concentrations of dissolved selenium, pore waters from two sub-cores were combined. Pore water samples were immediately acidified to pH of 1.5 and refrigerated. Sub-cores were also taken to determine sediment porosity in order to convert the volume of pore water collected to depth intervals (Bender et al., 1987).

2.2.2. Analytical Methods

Sediment samples were dried at 50 ^{0}C, ground with an agate mortar and pestle, and sieved through a 150 μm nylon mesh screen; these sediments were stored in 30 mL polyethylene bottles. Processed samples were used to determine total sedimentary selenium and organic carbon, organic nitrogen, and sulfur (CNS). A Carlo Erba 1500 Elemental Analyzer was used to determine CNS (Cutter and Radford-Knoery, 1991).

Total sedimentary selenium was determined using a three-step nitric-perchloric acid digestion on dried sediment as described by Cutter (1985). The method was

modified so that after the final digestion and addition of hydrochloric acid, the sample solutions were passed through Bio-Rad AG 1 X 8 anion exchange resin (chloride form, 100-200 mesh); the eluent was collected. This removed any iron that might interfere in the subsequent determinations. The resin was rinsed with 10 mL of 4 M HCl and this eluent was combined with the previous one in 30 mL polyethylene bottles. To measure digestion accuracy, a NIST standard (NIST SRM 2704, Buffalo River Sediment) was digested with the samples. The recovery of the SRM was 97.3 ± 5.3% (1.09 ± 0.06 μg g^{-1}, n=13) of the total selenium.

Elemental selenium was determined using a sodium sulfite extraction and oxidation with nitric acid as described by Velinsky and Cutter (1990) on wet sediments. The eluent was stored in 30 mL polyethylene bottles until analysis. Sedimentary selenite + selenate was determined using a modified sodium hydroxide leaching technique developed by Cutter (1985). After the sodium hydroxide leach (Cutter, 1985), the supernatant was adjusted to pH 6 to 7 with hydrochloric acid and passed through Bio-Rad AG 1 X 8 anion exchange resin (100-200 mesh) which retains selenite + selenate. After the leachate was passed through the resin columns, they were rinsed with 15 mL of milli-Q water to ensure that only selenite + selenate were retained and the flow-through was discarded. Five milliliters of a 1 M solution of formic acid were added to the resin and the eluent was collected. The resin was then rinsed with 15 mL of 4 M HCl and this eluent was combined with the previous one. The eluent was stored in 30 mL poly-ethylene bottles until analyzed.

Pore water samples were analyzed for total selenium, and if enough sample was

left, selenite + selenate. Digested sediments and pore water samples were analyzed for dissolved selenium as described by Cutter (1978; 1983; 1985) and Velinsky and Cutter (1990) using selective hydride generation. Briefly, this involves the selective generation of hydrogen selenide from dissolved selenite using sodium borohydride and acidification, liquid nitrogen-cooled trapping, and atomic absorption detection with a quartz tube burner and an air-hydrogen flame.

The standard additions method of calibration was used to ensure accuracy (in addition to the analyses of SRM) and all digests were done in duplicate, with determinations made in triplicate. The detection limit for pore water was 0.06 nmol L^{-1} and the precision was generally better than 15% (relative standard deviation). Total sedimentary selenium and its speciation had a detection limit of 0.01 nmol g^{-1} when 0.3 g were digested, with the precision better than 10% (relative standard deviation).

2.3. RESULTS

2.3.1. General Sediment Characteristics

Estuarine sites (Stns. 1 through 7, 18 to 20, and 23; Fig. 17) were predominately fine grain silt and clay. Conomos and Peterson (1977) found that the channels of the estuary were composed of poorly sorted silty clay, clayey silt and sand-silt-clay. All estuarine sites had clams in the upper 2 cm, suggesting that bioturbation was occurring. The porosity and dry sediment density among estuarine sites was similar and averaged 0.69 ± 0.05 (n=88) and 2.15 ± 0.10 g cm^{-3} (n=88), respectively, which agrees with values reported by van Geen and Luoma (1999). The sedimentation rate in the depositional

zones of the estuary can range from 0.45 cm yr^{-1} to 4.5 cm yr^{-1} (Fuller et al., 1999), with an estuarine average sedimentation rate of 0.9 cm yr^{-1} (van Geen and Luoma, 1999). Organic carbon in the estuary did not vary with depth and was 1.35 ± 0.50% by weight (n =88) in the upper 5 cm. Organic nitrogen and sulfur averaged 0.11 ± 0.01% by weight (n = 88) and 0.11 ± 0.01% by weight (n = 88), respectively, and both were constant with depth in the estuary.

The mudflat and salt marsh sites were located in the Martinez salt marsh (Stns. 24 and 25; Fig. 17). Approximately 200 m of the mudflat site is exposed during low tide. The salt marsh flora is pre-dominantly *Spartina alterniflora*. Both the mud flat and the salt marsh site had fine grain, silty-clay compositions. The average porosity for the mud flat site was 0. 68 ± 0.03 (n =11), with a dry density of 2.21 ± 0.03 g cm^{-3} (n=11). The sedimentation rate is currently unknown in these sediments. The concentrations of organic carbon, organic nitrogen, and sulfur were constant with depth and averaged 1.25 ± 0.02% organic carbon (n = 22), 0.10 ± 0.02 % of organic nitrogen (n=22), and 0.14 ± 0.04 % (n=22) sulfur.

The Delta stations (Stns. 8, and 10 through 17; Fig. 17) had a clay and silt composition, with a 0.5 cm flocculent layer on top. As with the estuarine sites, there were clams in the upper 2 cm, suggesting that bioturbation was present. The average porosity was 0.69 ± 0.04, with a dry density of 2.21 ± 0.08 g cm^{-3} (n=99). In 1999, sediments in the Delta at Mildred Island (Stns. 21 and 22, Fig. 17) were collected. Mildred Island was farmland prior to a dyke breaking in 1983 and it was allowed to stay flooded. Approximately 6 cm from the top of the cores in Mildred, a change in sediment

texture, and organic carbon, nitrogen, and sulfur were observed, suggesting that this is the soil horizon. Thus, assuming that the Delta has a similar sedimentation rate as Mildred Island, the rate is estimated to be 0.38 cm yr^{-1}. Excluding those depths below 6 cm in Mildred Island, the organic carbon, nitrogen and sulfur concentrations did not greatly vary and averaged 6.09 ± 0.11% (n=99), 0.43 ± 0.01% (n=99), and 0.12 ± 0.02% (n=99), respectively.

2.3.2. Solid Phase Total Selenium

Total sedimentary selenium in the upper 2 cm at all the stations ranged between 2.0 and 7.9 nmol g^{-1}, with concentrations in the Delta twice as high as those in the Bay and the salt marsh (Fig. 18). A statistical analysis of the data for total selenium in the upper 2 cm of estuarine, salt marsh, and Delta sites shows that there were significant differences (p=0.001) between surface total selenium concentrations in the Delta and the estuary, and between the Delta and salt marsh (p=0.019). There was little statistical difference in surface selenium concentrations between the estuarine and salt marsh sites (p=0.082). Johns et al. (1988) reported total sedimentary selenium concentrations of 1 to 6 nmol g^{-1} from six stations in Suisun Bay, which are consistent with our results. However, total selenium concentrations in the Northern Reach were 2 times lower than those reported by Takayanagi and Belzile (1988) for estuarine sediments and Velinsky and Cutter (1991) for salt marsh sediments.

Due to the number of stations, it is unfeasible to show the depth distribution for each one, and thus representative depth profiles from a station in San Pablo Bay (Stn. 1),

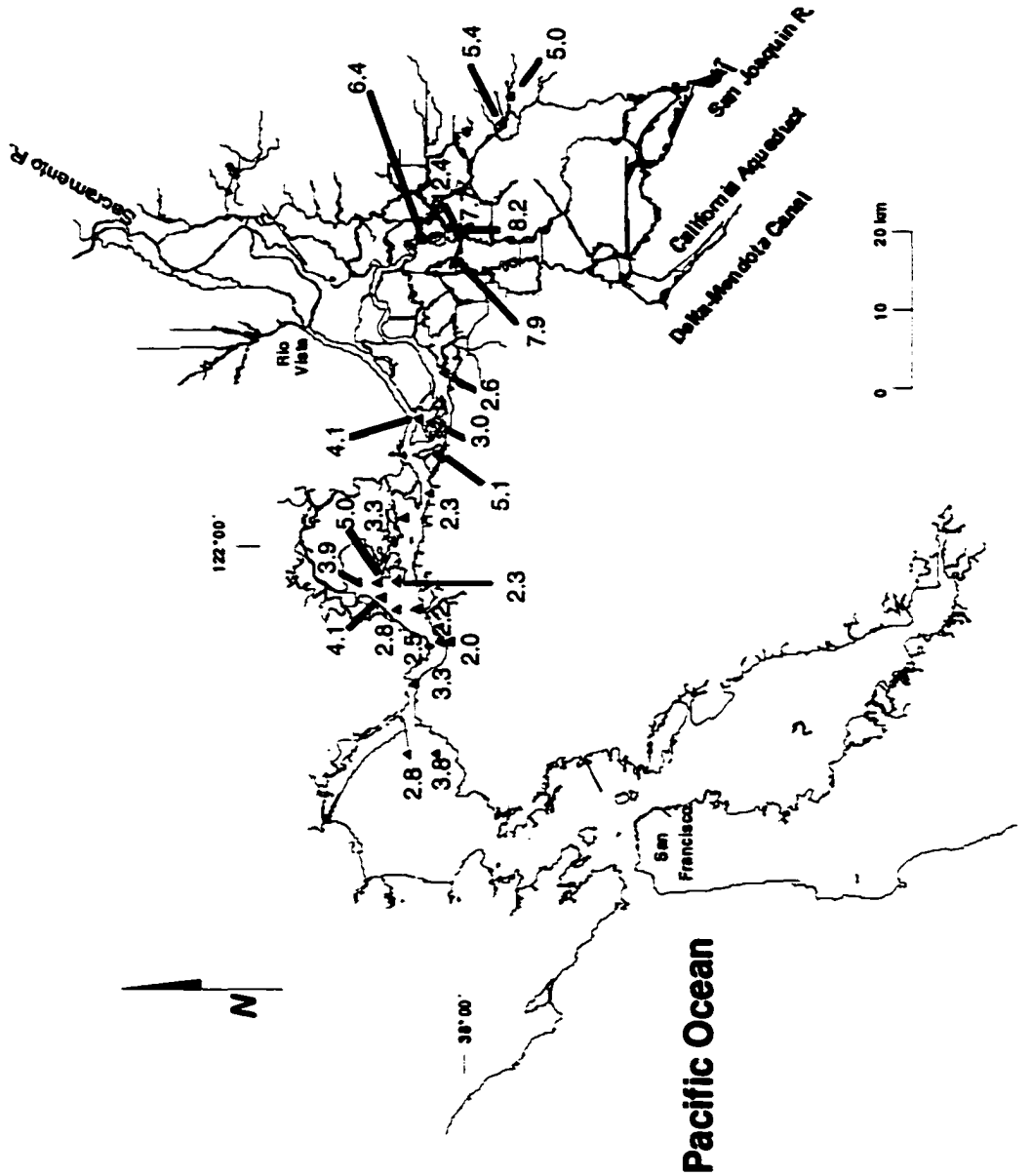

Fig. 18. Total sedimentary selenium (nmol g^{-1}) in the upper 2 cm.

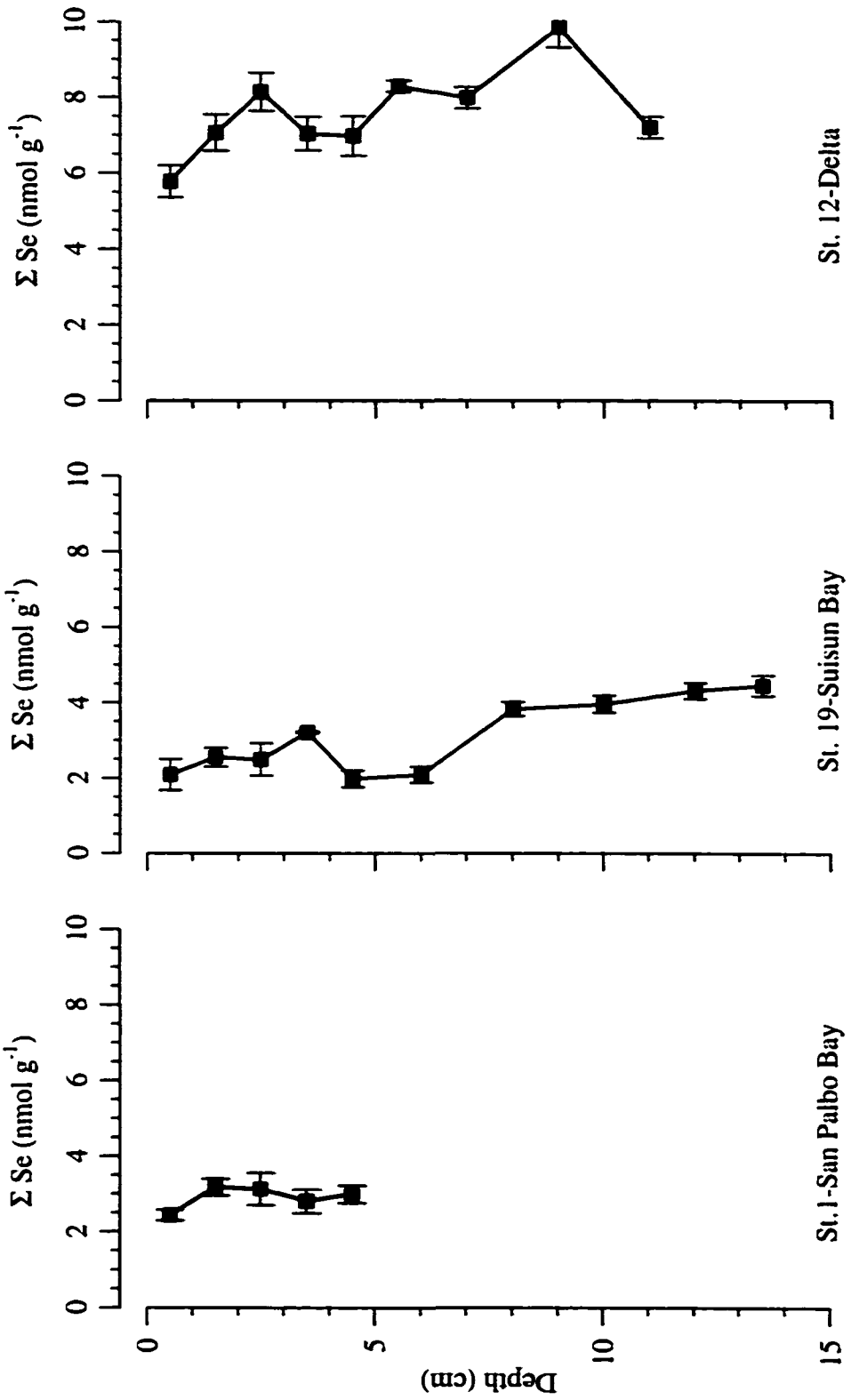

Fig. 19. The depth profile of total sedimentary selenium in the Northern Reach and the Delta.

Suisun Bay (Stn. 19), and the Delta (Stn. 12) are presented (Fig. 19). For the estuarine sites, there was a slight increase in total selenium with depth, while in the Delta it had a constant concentration with depth (Fig. 19). The observed estuarine sediment behavior is contrary to what has been observed in most marine sediments, where total selenium is either constant or decreases with depth (Takayanagi and Belzile, 1988; Velinsky and Cutter 1991).

2.3.3. Solid Phase Selenium Speciation

The concentration of elemental selenium at all sites ranged from 0.29 to 9.55 nmol g^{-1}. The estuarine sites had an average elemental concentration in the upper 2 cm of 1.65 ± 0.45 nmol g^{-1} (n = 34), or 52% of the total. The surface concentrations of elemental selenium in the Delta were greater than the estuary (3.19 ± 0.53 nmol g^{-1}, n = 24), but the percentage of elemental selenium relative to the total was the same as the estuarine sites (52% of the total). The surface elemental selenium concentration in the salt marsh was 0.92 ± 0.02 nmol g^{-1} (n=4), or 47% of the total. There was no statistical difference in the percentage of elemental selenium between the Delta and the estuarine sites (p=0.317). For all sediment sites, the percentage of elemental selenium was consistent with other salt marsh (49 to 68%, Velinsky and Cutter, 1991) and fresh water sediments (40 to 95%, Belzile et al. 2000). The vertical distribution of elemental selenium as a percentage of total selenium was constant with depth for the estuarine sites, and a slight decrease with depth for the Delta (Fig. 20). This decrease with depth has been observed in marine sediments (Velinsky and Cutter, 1991)

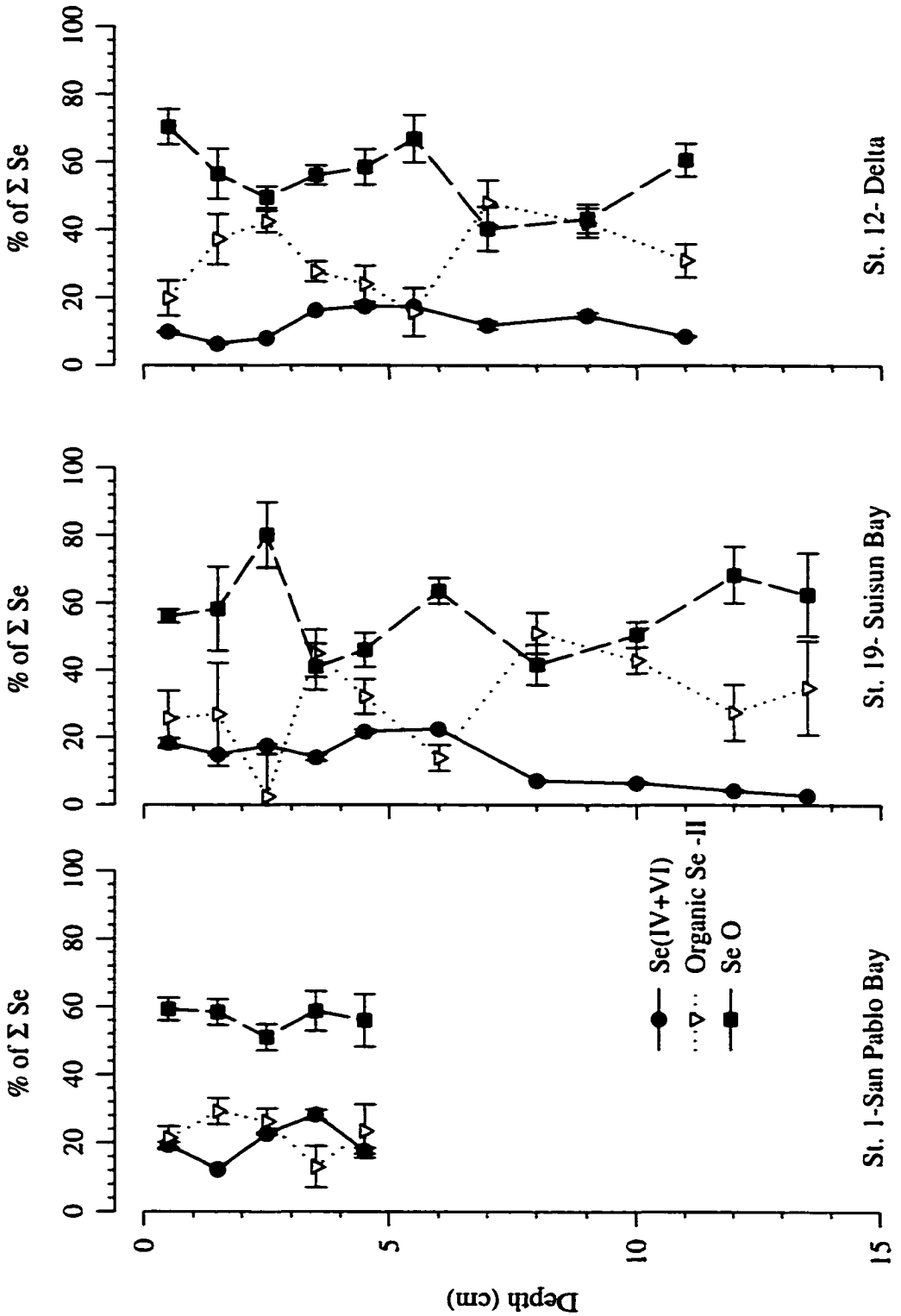

Fig. 20. Speciation of sedimentary selenium in the Northern Reach and Delta.

and an increase with depth has been observed in fresh water sediments (Belzile et al. 2000).

Sedimentary selenite + selenate ranged from 0.03 to 1.99 nmol g^{-1} for all the sediment sites. The Delta sediments had a higher concentration of selenite + selenate (0.98 ± 0.37 nmol g^{-1}) than the estuarine (0.41 ± 0.09 nmol g^{-1}) and salt marsh sites (0.16 ± 0.04 nmol g^{-1}) in the upper 2 cm, but once normalized to total selenium, the percentages of selenite + selenate in the Delta were similar to those in the estuary ($16.0 \pm 6\%$ n=22 for the Delta and $13 \pm 3\%$, n=9 for the estuary). As with elemental selenium, there was little statistical difference in the percentage of selenite+selenate between the estuarine and Delta sites (p=0.421). The salt marsh had the lowest percentage of selenite + selenate at the surface ($8 \pm 2\%$ of the total, n=4). The percentage of selenite + selenate (Fig. 20) remained constant with depth for the Delta, while in Suisun Bay there was a decreased with depth. The later trend is consistent with other marine sites (Velinsky and Cutter, 1991).

For the entire data set, organic selenide in the upper 2 cm ranged from 0.07 to 8.70 nmol g^{-1}. In the Delta, the upper 2 cm had an average organic selenide concentration of 1.96 ± 0.31 nmol g^{-1}, 1.08 ± 0.35 nmol g^{-1} for the estuarine sites, and 0.91 ± 0.14 nmol g^{-1} for the salt marsh. When normalized to total selenium, organic selenide in the upper 2 cm was $34 \pm 11\%$ (n=9) of the total selenium for the estuarine sites, and $32 \pm 5\%$ (n = 22) in the Delta, and there was little statistical difference (p =0.693) between the estuarine and Delta sites. The salt marsh had the highest percentage of organic selenide compared to the other stations ($46 \pm 7\%$, n=4), but it was not statistically significant compared to

the other sites (p=0.113). The percentage of organic selenide varied considerably with depth and showed no consistent trend (Fig. 20). Similarly, Velinsky and Cutter (1991) reported an organic selenide concentration that ranged between 0.9 to 7.5 nmol g^{-1} (47 ± 11% of the Σ Se), with no consistent trend with depth.

2.3.4. Dissolved Selenium in Pore Waters

Total dissolved selenium in pore waters ranged from 1 nmol L^{-1} to 6 nmol L^{-1} in the upper 2 cm of the San Francisco Bay sediments. The average pore water concentration for the Delta was 2.3 ± 0.2 nmol L^{-1} (n=24), with the estuarine sites having similar concentrations (2.7 ± 0.3 nmol L^{-1}, n =56). The average concentration for the salt marsh was slightly higher at 3.4 ± 0.2 nmol L^{-1} (n=7). Vertical profiles of total dissolved selenium in pore waters increased with depth (Fig. 21) for San Pablo and the Delta, and remained constant in Suisun. Total dissolved selenium concentrations in pore water were similar to those reported by Takayanagi and Belize (1988) in the St. Lawrence Estuary (approximately 2.1 nmol L^{-1}). Zawislanski and McGrath (1998) reported a total dissolved selenium pore water concentration of approximately 50 nmol L^{-1} for the Martinez mudflat in 1995, which is inconsistent with the data shown here and other marine (Velinsky and Cutter, 1991) and fresh water (Belzile et al., 2000) sediments. The difference between their pore water concentrations and those reported here cannot be easily explained.

For all stations, selenite + selenate was 60 to 80% of the total dissolved selenium in the top 1 cm, but was non-detectable below 2 cm (Fig. 22). Organic selenide was

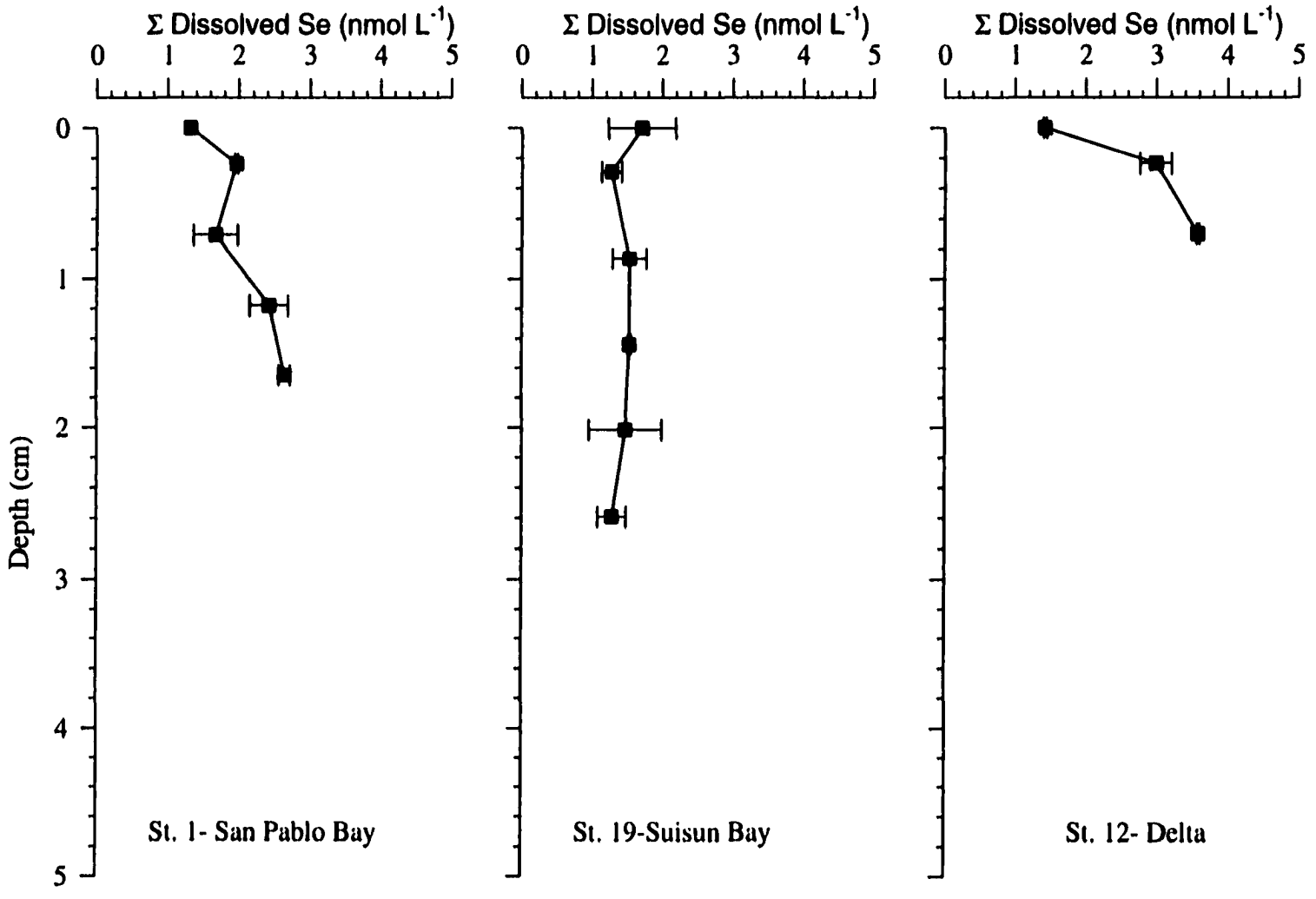

Fig. 21. Pore water total dissolved selenium in the Northern Reach and Delta.

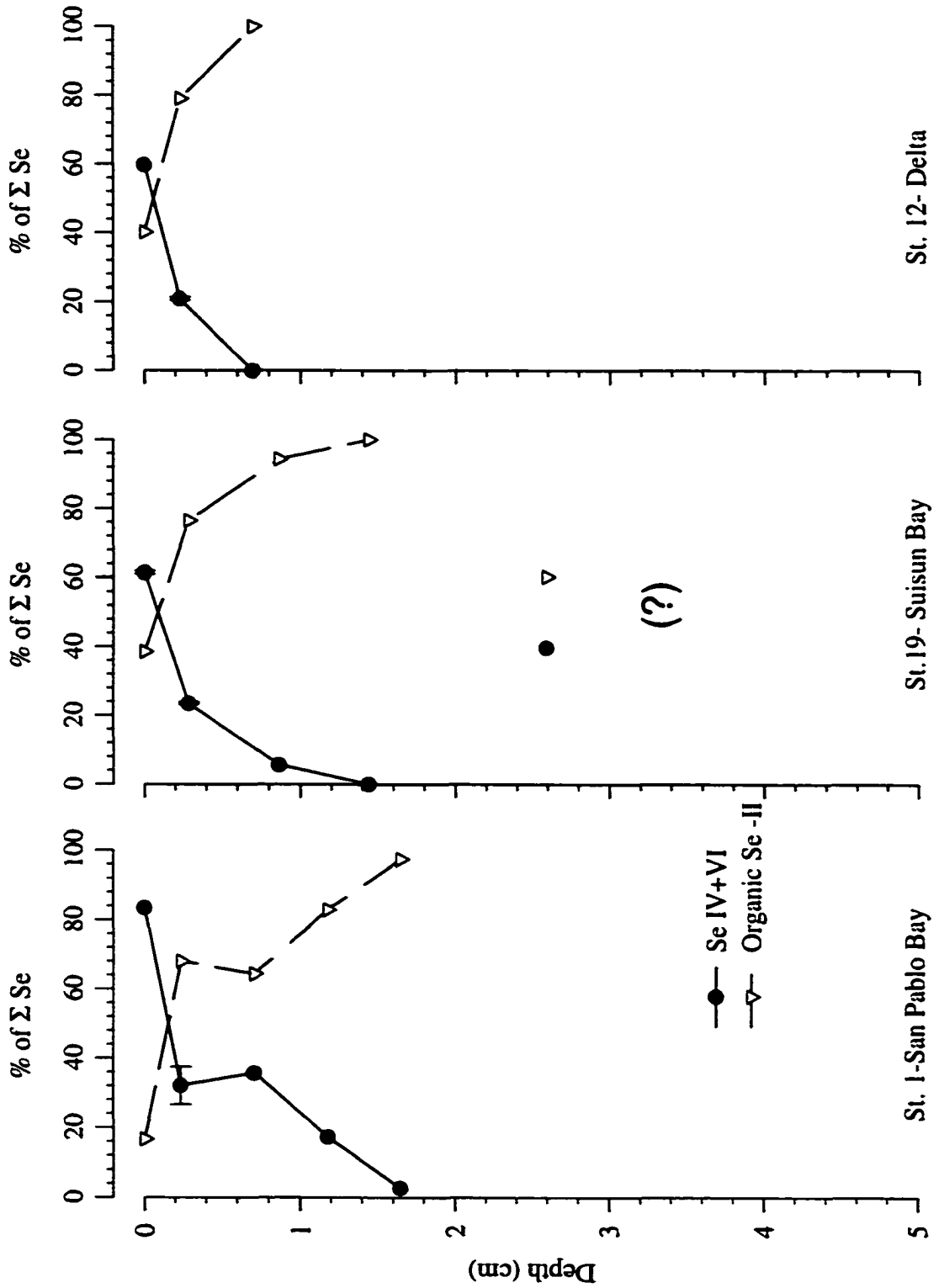

Fig. 22. Speciation of pore water selenium in the Northern Reach and Delta.

approximately 20 to 40% of the total dissolved selenium in the top 1 cm and increased with depth (Fig. 22). Velinsky and Cutter (1991) found similar results for pore water selenite + selenate and organic selenide. Belzile et al. (2000) also found that there was a net increase of organic selenide with depth in pore water samples from freshwater sediments. However, in anoxic freshwater sediments, selenite was the most important fraction of the dissolved selenium (Belzile et al., 2000), which was not seen in these sediments.

2.4. DISCUSSION

2.4.1. Solid Phase Selenium and Carbon Relationship

In other marine sediments, a correlation between solid phase total selenium and organic carbon has been found (Sokolova and Pilipchuk, 1973; Belzile and Lebel, 1988; Velinsky, 1987). Sokolova and Pilipchuck (1973) suggest that the positive correlation between selenium and organic matter may be due to biological uptake of dissolved selenium in the overlying water or scavenging of dissolved selenium onto particulate organic matter. Even though the concentrations of solid phase total selenium were different between the estuarine and the Delta sites, the total selenium to carbon atomic ratios were similar (Delta Σ Se:C was $1.1 \pm 0.5 \times 10^{-6}$, n=99; estuarine Σ Se:C was $2.5 \pm 0.8 \times 10^{-6}$, n=88). The linear regression using all stations and depths (except those in Mildred Island greater than 6 cm) resulted in a strong positive correlation between total selenium and organic carbon (Fig. 23; Σ Se:C $1.3 \pm 1.0 \times 10^{-6}$, r =0.846, n=187).

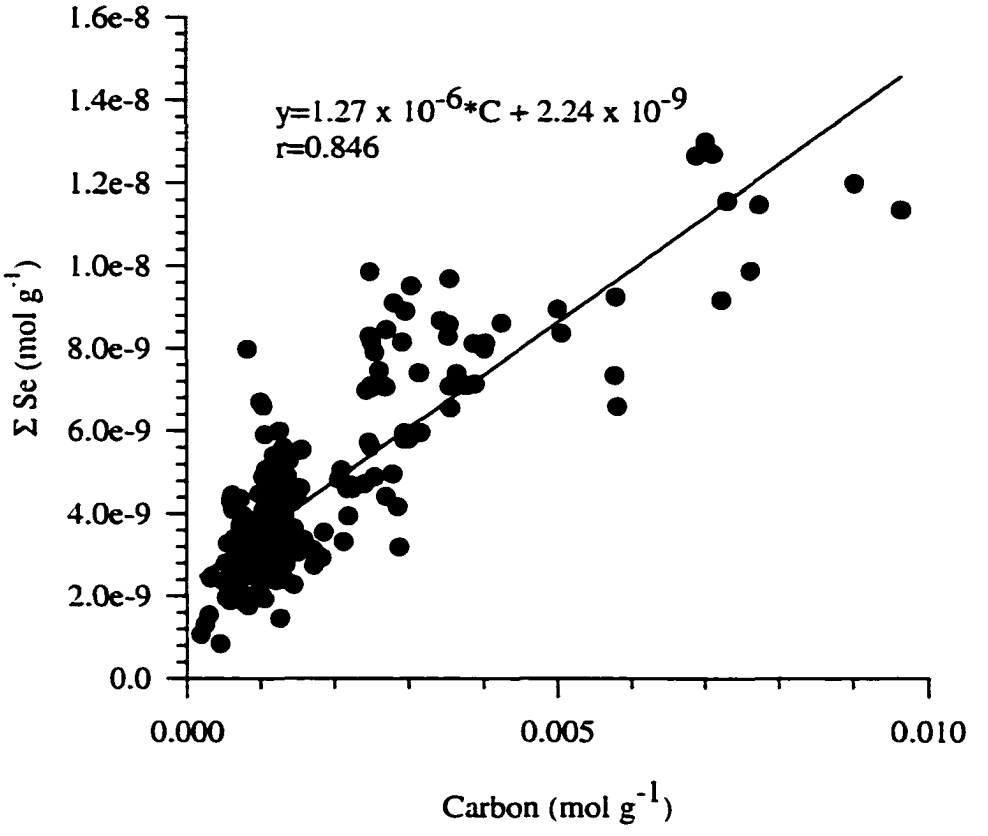

Fig. 23. Total selenium and organic carbon sediment concentration for all sediment sites. All depths are used except those below 6 cm in Mildred Island which were believed to be from the old soil horizon.

Estuarine sediments from the Chesapeake Bay have a total sedimentary selenium concentration of 15 nmol g^{-1}, which is five times greater than what was observed in the San Francisco Bay. However, the total selenium to carbon atomic ratio of 5.1 x 10^{-6} in the Chesapeake Bay (Cutter, unpublished data) is within the range of these in the San Francisco Bay sediments. These observations suggest that the mechanism causing the positive correlation between total selenium and organic carbon is the actual incorporation of selenium into organic matter (e.g., seleno amino acids in proteins of phytoplankton). Indeed, these Σ Se:C ratios are almost identical to those in phytoplankton cultures (3.2 ± 6.2 x 10^{-6}; Baines and Fisher, 2001; Doblin et al., in prep.). Thus, organic selenium can be delivered to sediments in phytoplankton detritus, as are additional particulate selenium forms in other detrital particles (e.g., elemental selenium in sediment particles). Other means of incorporating selenium in San Francisco Bay sediments (e.g., *in situ* reduction of selenite + selenate to elemental selenium) will be discussed below.

2.4.2. Diffusion of Pore Water Selenium

The internal cycle of sedimentary selenium in the San Francisco Bay can include: the oxidation of elemental (Geering et al., 1968, Velinsky and Cutter, 1991) and organic selenium (Velinsky and Cutter, 1991); the biotic reduction of selenite and selenate to elemental selenium (Shamberger, 1983; Oremland et al., 1989); and the biotic conversion to gaseous selenium (Reamer and Zoller, 1980, Amouroux et al., 2001). These transformations include changes between the solid and dissolved phases (i.e., pore water intermediates).

Dissolved selenium in pore waters can be a source or sink of solid phase selenium, and thus the exchange with the overlying water was calculated. However, the presence of clams in the sediments, suggests that irrigation could affect the exchange of dissolved selenium with the overlying water. To account for possible irrigation in the sediments, the flux can be calculated using a modification of Fick's First Law of Diffusion (Berner, 1980) that Emerson et al. (1984) and Hammond et al. (1995) used for shallow water estuarine sediments:

$$J = -\phi * D_s * \frac{\partial Se}{\partial z} + \sum^{i} z_i \lambda_i (C_w - C_i) \qquad (2.1)$$

where J is the flux, ϕ is the porosity, D_s is the effective diffusion coefficient, $\partial Se/\partial z$ is the observed concentration gradient of pore water selenium, z_i is the depth of zone i (cm), λ_i is the irrigation coefficient (s^{-1}), C_w is the overlying water concentration, and C_i is the average pore water concentration at depth i. A negative J indicates that the dissolved selenium is fluxing out of the sediments, while a positive J results from dissolved selenium fluxing into the sediments.

Irrigation coefficients for nutrients (e.g., phosphate) and some metals (e.g., iron, copper, nickel and cadmium) in shallow water estuaries range from 1×10^{-7} s^{-1} to 20×10^{-7} s^{-1} (Emerson et al., 1984; Hammond et al., 1995). My study did not investigate what the irrigation coefficient of selenium was, but to ensure that irrigation processes are not underestimated, the maximum irrigation rate was used in Equation 2.1. The overlying water concentration at each sediment sites was not always determined, but Cutter and Cutter (in prep.) determined the surface water concentrations of selenium in the Northern

Reach. Due to the well-mixed water column in the Northern Reach (Conomos et al., 1979; Chapter I), the proximity of sediment sites to the estuarine dissolved selenium sites (less than 3 km), and little variation in total dissolved selenium in the estuary between sites (Cutter and Cutter, in prep.), the estuarine dissolved selenium values from Cutter and Cutter (in prep.) were used for C_w when data were not available for the actual sediment sites. Li and Gregory (1974) give the molecular diffusion coefficient, D, for selenium as 8.45 X 10^{-6} cm^2 s^{-1} at 18 °C. Correcting for tortuosity effects as described by Ullman and Aller (1982), the effective diffusion coefficient is 5.83 X 10^{-6} cm^2 s^{-1}.

The average flux due to diffusion and irrigation for total dissolved selenium is -0.03 ± 0.02 nmol cm^{-2} yr^{-1} for the estuary and -0.15 ± 0.02 nmol cm^{-2} yr^{-1} for the Delta. The importance of diffusion versus irrigation can be investigated using Equation 2.1, with the first term in the equation being the diffusional fluxes and the second term is the irrigation flux. In this manner, less than 3% of the total flux to the overlying water was due to irrigation (Table 4). When examining the upper 2 cm of irrigated sediments, Emerson et al. (1984) found that the exchange between pore water and overlying water is primarily controlled by diffusion. These results are consistent with that finding. The total dissolved selenium fluxes from San Francisco Bay sediments are comparable to fluxes from other marine and fresh water sediments (-0.01nmol cm^{-2} yr^{-1} to -0.11 nmol cm^{-2} yr^{-1}; Takayanagi and Belzile, 1988; Velinsky and Cutter, 1991; Belzile et al., 2000). Therefore, these sediments are a source of total dissolved selenium to the estuary and the flux is controlled by diffusion.

Using Equation 2.1, the fluxes of dissolved selenite + selenate and organic

Table 4
Pore water fluxes in sediments from the Northern Reach

Area	Diffusion (nmol cm^{-2} yr^{-1})[a]	Irrigation (nmol cm^{-2} yr^{-1})[a]	Total Flux (nmol cm^{-2} yr^{-1})[a]
Estuarine Sites			
Solid Phase (n=15)			
Sedimentary			
Σ Se	NA	NA	+0.3 ± 0.1
Se O	NA	NA	+0.4 ± 0.2
Se IV+VI	NA	NA	+0.0 ± 0.1
Org. Se -II	NA	NA	-0.1 ± 0.1
Dissolved			
Pore water			
Σ Se (n=12)	-0.03 ± 0.02	-0.002 ± 0.001	-0.03 ± 0.02
Se IV+VI (n=3)	+0.06 ± 0.01	-0.001 ± 0.001	+0.06 ± 0.01
Org. Se -II (n=3)	-0.09 ± 0.01	-0.001 ± 0.002	-0.09 ± 0.01
Delta Sites			
Dissolved			
Pore water			
Σ Se (n=8)	-0.15 ± 0.02	-0.005 ± 0.004	-0.15 ± 0.02
Se IV+VI (n=4)	+0.14 ± 0.02	-0.002 ± 0.001	+0.14 ± 0.02
Org Se -II (n=4)	-0.30 ± 0.02	-0.003 ± 0.002	-0.30 ± 0.02

[a] "-" sign indicate a flux out of the sediments, while a " +" sign indicates input to the sediments

selenide were also calculated for those stations where there was enough sample to do speciation analyses (n =3 in the estuary, n = 4 in the Delta). For both the estuary and Delta, dissolved selenite + selenate is fluxing into the sediments, while dissolved organic selenide is fluxing out of the sediments (Table 4). The average estuarine flux of selenite + selenate is $+0.06 \pm 0.01$ nmol cm^{-2} yr^{-1} and $+0.14 \pm 0.02$ nmol cm^{-2} yr^{-1} in the Delta, while the organic selenide flux is -0.09 ± 0.01 nmol cm^{-2} yr^{-1} and -0.30 ± 0.02 nmol cm^{-2} yr^{-1} for the estuary and Delta, respectively. As with total dissolved selenium, irrigation is a minor part of the flux of dissolved selenite + selenate and organic selenide (Table 4). Pore water speciation data for other estuaries are nonexistent, and thus the results from Belzile et al. (2000) are used as a comparison. Using their pore water profiles at Clearwater Lake, Canada, the estimated flux was -0.05 nmol cm^{-2} yr^{-1} for selenite + selenate and -0.06 nmol cm^{-2} yr^{-1} for organic selenide. Therefore, the flux of selenite + selenate in the San Francisco Bay is different than that of Belzile et al. (2000), but the organic selenide fluxes are similar.

2.4.3. Solid Phase Internal Cycling

In order for selenium to accumulate in the estuarine sediments it has to either have a dissolved source or a change in inputs over time. For example, in fresh water sediments Belzile et al. (2000) found an increase in total selenium with depth, but this was due *in situ* fixation of dissolved selenium to solid phase selenium. To explain, the observed selenium with depth in the estuarine sites, the first step is to quantify it and then look for matching input fluxes. The depth-integrated gain or loss of each solid-phase species was

calculated using a simple equation from Berner (1980):

$$R \text{ (nmol Se cm}^{-2} \text{ yr}^{-1}) = \Delta C \, \omega \, \rho \, (1-\phi) \qquad (2.2)$$

where R is the accumulation rate, ΔC is the change in concentration over a 5 cm interval, ω is the sedimentation rate, ρ is the dry density, and ϕ is the porosity. The average sedimentation rate, dry density, and porosity for the estuary were given above in Section 2.3.1. In the Delta, total selenium was constant with depth (Section 2.3.2), which is consistent with other marine sediments (Takayanagi and Belzile, 1988; Velinsky and Cutter, 1991), but means that R=0 for the Delta.

Equation 2.2 was applied to the estuarine sediments (Section 2.3.1. gives the density, sedimentation rates, and porosity values), and the average accumulation of selenium was 0.3 ± 0.1 nmol cm^{-2} yr^{-1} (Table 4). The sedimentary speciation data indicate that all of the gains in total selenium in the estuarine sediments are in the form of elemental selenium ($+0.4 \pm 0.2$ nmol cm^{2} yr^{-1};Table 4). The dissolved selenite + selenate flux into the sediments is $+0.06 \pm 0.01$ nmol cm^{2} yr^{-1}. Therefore, for these sediments the influx can only explain $15 \pm 3\%$ of the gain in elemental selenium (Table 4). Nevertheless, the loss of sedimentary organic selenide (ΣSe - Se (O)= 0.3-0.4 = -0.1 nmol cm^{2} yr^{-1}) matches the efflux of dissolved organic selenide (0.09 nmol cm^{2} yr^{-1}, as above). Even though these estuarine sediment mass balance calculations appear to be correct, they cannot explain the observed increase in total sedimentary selenium.

Since dissolved pore water fluxes cannot account for the accumulation of sedimentary selenium in the estuary, the only other possible explanation could be a historical change in the inputs. These changes could be from a greater flux in particulate

selenium or inputs of dissolved selenium from the overlying water via pore water exchange. Suspended particulate selenium data from Cutter (1989b) and Doblin et al. (in prep.) show that in the last ten years, the concentration of particulate selenium has remained relatively constant; changes in particulate selenium inputs then seem unlikely. However, Cutter and Cutter (in prep.) show a clear decrease in estuarine dissolved selenium of 2 nmol L^{-1} over the last 10 years, suggesting that pore water fluxes in the past may have been greater.

To calculate if a historical change could explain the accumulation of selenium, it was assumed under steady state that the sedimentary selenium profile would be uniform with depth from the surface. The difference between this and the observed profiles is then selenium from any additional fluxes. Since the change in estuarine dissolved selenium has occurred over the last 10 years, cores in the upper 10 cm were used for the following calculations (i.e., sedimentation rate of 0.9 cm yr^{-1}) so that sediment records were on the same time scale as dissolved data. Average total sedimentary selenium in the estuary at the surface (0-2 cm) was 2.32 ± 0.28 nmol g^{-1} (n=2), and extending this steady state concentration to 10 cm gives an excess selenium concentration of 0.3 ± 0.2 nmol g^{-1} for the estuary. This difference was used in Equation 2.2 to get an accumulation rate of 0.2 ± 0.1 nmol cm^2 yr^{-1} for the estuary.

Cutter and Cutter (in prep.) found that the change in dissolved selenium in the estuary for 1986 to 1999 was due to a decrease in inputs of dissolved selenite + selenate from the refineries. The calculation above show dissolved selenite + selenate is currently fluxing into the sediments, and this flux would have been greater in the past when water

column selenite + selenate concentrations were higher. Assuming that the average pore water concentration in the upper 2 cm (0.5 ± 0.3 nmol L^{-1}) has not varied in the last 10 years, the concentration of selenite + selenate in the overlying water that would be needed to explain the excess accumulation of selenium was calculated using Equation 2.1, 3.0 ± 1.1 nmol L^{-1}. In comparison, dissolved selenite + selenate concentrations were as high as 2.8 nmol L^{-1} 10 years ago (Cutter, 1989b; Cutter and San Diego-McGlone, 1990). Based on these calculations, the accumulation of solid phase selenium that cannot be explained by internal cycling of selenium may actually be due to a historical change in refinery inputs of dissolved selenite + selenate in the estuary.

2.4.4. Conclusions

The primary sources of selenium to the San Francisco Bay sediments are particulate selenium from the rivers (biogenic and mineral detritus), biogenic particles produced in the water column (organic phytoplankton detritus), and diffusion of dissolved selenite + selenate from the water column followed by *in situ* reduction to insoluble elemental selenium. Unlike other marine sediments, the San Francisco Bay has sedimentary selenium concentrations that increase slightly with depth. Simple calculations indicate that this increase may be due to historical changes in overlying water concentrations of selenite + selenate (e.g., a change in the pore water flux and *in situ* fixation). However, deeper sediment cores (i.e., > 50 cm) would provide confirmation of this hypothesis by sampling sediments that predate the refineries.

Prior to this study, the speciation of solid phase selenium and the pore water flux

from the sediments in San Francisco Bay were unknown. Solid phase elemental, selenite + selenate and organic selenide concentrations that were needed to simulate particulate selenium in the estuary can now be specified (Equations 1.34, 135, and 1.40). The surface sediment concentrations of elemental selenium, selenite + selenate, and organic selenide from this Chapter will be used for the BEPS concentrations in Equations 1.34, 1.35 and 1.40).

CHAPTER III

MODEL SENSITIVY AND CALIBRATION

3.1. INTRODUCTION

A major goal in modeling is to simulate the behavior of a system, without the model being over-parameterized (Tebes-Stevens et al., 2001). A systematic and comprehensive test, known as a sensitivity analysis, is preformed to investigate how changes in a parameter affect the model output (Beres and Hawkins, 2001; Starfield and Beleloch, 1991). The model used here has many parameters that need to be specified in order to simulate dissolved and particulate selenium behavior (Chapter I). Some of these parameters can be measured in the field (e.g., river discharge), while others parameters are determined through laboratory experiments (e.g., maximum rate of photosynthesis). Laboratory experiments usually establish limits for parameter values (Motovilov et al., 1999), but there are those parameters where the limits are still under investigation (e.g., uptake of specific selenium forms by phytoplankton). The sensitivity analysis provides the modeler with a quantitative assessment of a parameters (e.g., must it be very accurately measured, or can it even be eliminated?). The quantitative results of a sensitivity analysis can also be used in interpreting the complex interactions between input variables, that would normally be hard to determine (Tebes-Stevens et al., 2001).

Once the sensitivity of the model is tested, a variety of procedures can be used to adjust the model parameters to the San Francisco Bay. These methods include model

"calibration" and "data assimilation" (McLaughlin, 1995). Data assimilation methods use models to constrain parameters and are utilized when there are limited data (McLaughlin, 1995). Parameter values are often updated whenever new data become available (Daley, 1991; McLaughlin, 1995). Calibration involves using observed data to constrain parameters in the model (McLaughlin, 1995). For example, the maximum rate of photosynthesis at optimal light intensity (P_m, Equation 1.19) has a range from 24 to 219 mg C (mg chl)$^{-1}$ d^{-1}. By doing a step-wise approach and looking at the fit between the model-derived output and the observed data, a P_m value is selected/optimized.

Extensive research has been done in the San Francisco Bay, and salinity, total suspended material, phytoplankton concentrations, and light attenuation coefficients in the water column have been measured for most months since 1969 by the United States Geological Service in California (http://sfbay.wr.usgs.gov/access/wqdata/webbib.html). Dissolved and particulate selenium sampling occurred in 1986, 1987, 1988, 1997, 1998, and 1999 (Cutter, 1989b; Cutter and San Diego-McGlone, 1990; Cutter and Cutter, in prep.; Doblin et al., in prep). Since data are available, the method of calibration was used to constrain model parameters. The most extensive data set exists for the flow year 1999 (e.g., chlorophyll-a, TSM, sedimentary selenium, dissolved selenium and its speciation, and particulate selenium and its speciation), and therefore it was used to calibrate the model. The calibrated model results are presented in this Chapter after the sensitivity analysis.

3.2. METHODS

3.2.1. Implementation

Simulations to test different time step values were run, and model simulations were solved with a time step of every 1.4 minutes (1/1000 of a day). The initial model parameter values (Table 5) were within the range of literature values cited above in Chapter I. The model was run from January 1, 1999 to December 31, 1999 for calibration and to obtain a "reference simulation". The reference simulation was then used in comparing model output data from the sensitivity analyses.

3.2.2. Analytical Sensitivity Analysis

There are four types of model uncertainties, including model structure, parameter values, ability to predict future system behavior, and experimental design and monitoring (Beck, 1987). Uncertainties in the model structure are investigated with the results from a sensitivity analysis. For this sensitivity analysis, the model output for all species of dissolved and particulate selenium were monitored. All the forms of selenium were monitored to determine if one species would be more difficult to simulate than another.

The large number of parameters in the model makes it extremely time-consuming to estimate the uncertainty of every parameter. Therefore, parameters used in the model were classified into one of the three categories (Table 6): accurately known parameters (accepted values), moderately inaccurate parameters (i.e., known, but have a large range); and very poorly known parameters (i.e., no published values). It is important to note that

Table 5
Initial parameter values for calibration of the model to dissolved and particulate selenium data from 1999

Parameter	Description	Value	Units	Reference
a	Resuspended sediment at river end member	0.00463	$g\ d^{-1}$	Harris et al. (1984)
b	Permanently suspended sediment at the riverine end	0.00029	$g\ L^{-1}$	Harris et al. (1984)
c	Scales freshwater discharge to sediment input	0.7		
d	Scaling factor for U_{beps}	0.007		
e	Scaling factor for U_{beps}	2		Schoellhamer (2001)
ε	Scaling factor K_{beps}	32	m	
ψ	Scaling factor K_{beps}	20	m	
M_2Phase	Tidal phase	125	degrees	Godin (1972)
K_1 Phase	Tidal phase	264	degrees	Godin (1972)
O_1 Phase	Tidal phase	51	degrees	Godin (1972)
M_2Frequency	Tidal frequency	695.52	degrees d^{-1}	Godin (1972)
K_1 Frequency	Tidal frequency	360.96	degrees d^{-1}	Godin (1972)
O_1 Frequency	Tidal frequency	334.56	degrees d^{-1}	Godin (1972)
M_2	Tidal amplitude	0.58	m	Uncles and Peterson (1996)
K_1	Tidal amplitude	0.37	m	Uncles and Peterson (1996)
O_1	Tidal amplitude	0.23	m	Uncles and Peterson (1996)
P_m	Maximum rate of photosynthesis	73.95	mg C mg^{-1} chl-a d^{-1}	Alpine and Cloern (1992)
W	Zooplankton weight	13	μg C $animal^{-1}$	Hutchinson (1981)
B_{sea}	Initial phytoplankton concentrations and seawater end member	2.3	μg chl-a L^{-1}	Alpine and Cloern (1992)
α	Slope of the light-saturation curve divided by P_m	0.00394	Einst. $m^2\ d^{-1}$	Peterson and Festa (1984)
k_s	Light scattering due to suspended particles	10	$L\ g^{-1}\ m^{-1}$	
k_w	Light scattering due to water	0.05	m^{-1}	Miller and Zepp (1979)
k_d	Light scattering due to dissolved mater	0.05	m^{-1}	Miller and Zepp (1979)
r	Mortality of phytoplankton through respiration	7.395	d^{-1}	Cole and Cloern (1987)
C:Chl a	Carbon to chlorophyll-a ratio	51	mg C mg^{-1} chl-a	Alpine and Cloern (1992)
k_1	Rate constant	0.05	d^{-1}	Cutter (1991)
k_2	Rate constant	0.004	d^{-1}	Cutter (1991)
k_3	Rate constant	2.4×10^{-6}	d^{-1}	Cutter and Bruland (1984)
k_4	Phytoplankton uptake constant	15.905	$L\ hr^{-1}$ chl-a^{-1}	Riedel et al. (1996)
k_5	Phytoplankton uptake constant	3.37	$L\ hr^{-1}$ chl-a^{-1}	Riedel et al. (1996)
k_6	Phytoplankton uptake constant	7.9525	$L\ hr^{-1}$ chl-a^{-1}	Riedel et al. (1996)
$Se\ O_{psp}$	Elemental sedimentary selenium in PSP	1.25	nmol g^{-1}	Chapter II

Table 5 Continued

Parameter	Description	Value	Units	Reference
$Se\ (IV+VI)_{psp}$	Se IV+VI sedimentary selenium in PSP	0.63	$nmol\ g^{-1}$	Chapter II
$Org.\ Se\ -II_{psp}$	Org. Se -II sedimentary selenium in PSP	0.63	$nmol\ g^{-1}$	Chapter II
a'	Rate of adsorption	0.13	$L\ g^{-1}\ d^{-1}$	Zhang and Sparks (1990)
$BEPS_{river}$	Riverine end member of BEPS	0.00463	$g\ d^{-1}$	Harris et al. (1984)
$BEPS_{sea}$	Sea water end member of BEPS	0	$g\ d^{-1}$	
V_s	Sinking of BEPS	86.4	$m\ d^{-1}$	McDonald and Cheng (1997)
w_s	Sinking of Phytoplankton	0.5	$m\ d^{-1}$	Cloern (1991)
$PSM_{seawater}$	Seawater end member concentration of PSM	0.1	$g\ L^{-1}$	Harris et al. (1984)
Delta removal effect	Removal of selenium as transported through the Delta to the Bay	60 %		

Table 6
Classification of parameters needed in ECoS to simulate the biogeochemical cycle of selenium in the Northern Reach.

Well-known Parameters	Moderately-known Parameters	Poorly known Parameters
River Discharge	P_m	a
Refinery inputs	α	b
M_I	W	c
K_I	r	d
O_I	k_1	e
$B_{initial}$	k_2	ε
I	k_3	ψ
A	Z	k_s
$S_{initial}$	$Se(0)_{BEPS}$	k_4
$TSM_{initial}$	$Se(IV+VI)_{BEPS}$	k_5
	Org. $Se(-II)_{BEPS}$	k_6
		P_g
		a
		Delta removal effect

even if a parameter is well known (e.g., river discharge), the model can be sensitive to it. To account for this, sensitivity analyses were done on all the poorly known parameters, and some of the moderately and well-known parameters.

The effects of parameter sensitivity can be determined by analytical methods (e.g., Fashem et al., 1993; Friedrichs and Hoffman, 2001) or by numerical estimates using Monte Carlo simulations (Annan, 2001). For the San Francisco Bay model, analytical methods were used to determine the sensitivity of various parameters using the technique of Fashem et al. (1993) and Friedrichs and Hoffman (2001). The sensitivity of the simulation to varying a given parameter was quantified by the normalized sensitivity ($S_{c,k}$), as defined by Friedrichs and Hoffman (2001)

$$S_{C,k} = \frac{\frac{C_r - C_s}{C_s}}{\frac{k_r - k_s}{k_s}} \tag{3.1}$$

where C_r is the reference simulation (Section 3.2.1), k_r is the reference parameter, k_s is the adjusted parameter, and C_s is the simulation result when k_r is changed. The model is insensitive if the $|S_{c,k}|$ is less than 0.15, and sensitive if $|S_{c,k}|$ is greater than 0.15 (Friedrichs and Hoffman, 2001). Due to the differences in flow within one year (Fig. 12), sensitivity results were divided into two periods, high flow months (December to May) and low flow months (June to November), to determine if there is a difference in sensitivity as a function of river discharge. The values reported in Section 3.3 are the estuarine averages for each flow period.

Five parameters were first tested to see if there was a difference in the normalized

sensitivity when a parameter was varied by ±25%, ±50% and ±75%. Parameters chosen for this were riverine inputs, refinery inputs, phytoplankton growth, phytoplankton uptake, and sediment inputs (Appendix A). It was found that increasing the reference parameters by +25% produced similar $S_{c,k}$'s to when the parameter was increased by 50% or 75% (Appendix B). Since some of the unknown parameters were also sensitive with a 25% increase in k_r, all other parameters were only varied by 25%. This allowed for a comparison between parameters to determine which were affecting the model output of a constituent. Furthermore, the only difference between a 25% increase in k_r and a 25% decrease in k_r was the sign of $S_{c,k}$ (the absolute value was the same, Appendix B). Therefore, the results reported here are for increasing k_r by +25%.

3.2.3. Model Calibration

Model calibration simulations for salinity, total particulate material, light attenuation, and dissolved and particulate selenium were compared to observed data. During calibration, literature values were used when possible, but there often was a large range in the reported values (e.g., k_l, Table 3). For these parameters, a step-wise approach was used to determine which value produced the best fit between the model output and the observed data. A step-wise approach involves increasing/decreasing the parameter by 10% and finding the value that produces the best fit (i.e., correlation coefficient) between the model output and observed data. When literature ranges were available, they were used to constrain this parameter optimization. If literature values were not available, parameter values were first set to zero then a step-wise approach was

used. As discussed earlier, 1999 data were used to calibrate the model. There were reliable salinity, TSM, light attenuation coefficients, and phytoplankton concentrations for 9 of the 12 months of this year. Therefore, model calibration was done on these 9 months for the above constituents. For dissolved and particulate selenium (and its speciation) data were only collected in April and November 1999, and the model could only be calibrated to these months.

Criterion for determining the best fit of a model to actual data often involves using two or more statistical measurements (Weglarczyk, 1998). For this model, three statistical analyses were used to determine the ability of the model to reproduce the observed behavior of salinity, total particulate material (TSM), the attenuation of light (k), and the speciation of dissolved and particulate selenium. The linear correlation coefficient, r, between the simulated values and the observed data was reported as one statistical parameter. The correlation coefficient does not indicate the bias of the model (Weglarczyk, 1998), but is used mainly for model optimization (Alewell and Manderscheid, 1998). Outliers in the observed data, and invariance of the data affect the correlation coefficient, which is why it is usually used mainly for model optimization. The criterion for determining if a correlation coefficient is significant depends on the degrees of freedom (Zuwaylif, 1979). The statistical significance of the correlation coefficient as a function of the degrees of freedom is determined from standard statistical tables (e.g., Zuwaylif, 1979) and for the correlation coefficient, the 95% confidence interval was used ($r_{0.05}$).

Model bias is reported as the mean cumulative error, M (Perrin et al., 2001). The

mean cumulative error is the sum of the simulated concentration minus the observed concentration divided by the number of observations. A negative sign indicates that the model is under predicting relative to the observed values, while a positive sign shows the model is over predicting. The mean cumulative error is only used as an indication of model bias, but it can also be expressed as a confidence interval. The overall ability, or confidence, of the model to reproduce the observed data can be defined by the equation from Perrin et al. (2001)

$$CI(\%) = 100 * \left[1 - \left| \sqrt{\frac{\sum x_{cal}}{\sum x_{obs}}} - \sqrt{\frac{\sum x_{obs}}{\sum x_{cal}}} \right| \right] \qquad (3.2)$$

where CI is the confidence interval, x_{cal} is the model simulation concentration and x_{obs} is the observed concentration. A perfect agreement between the two occurs when CI is 100%. A confidence interval of 50% indicates that the model is able to simulate the observed concentration 50% of the time. Unlike the correlation coefficient, the confidence interval is not affected by outliers or data variation, and therefore it is often a better indicator of model fit (Perrin et al., 2001). Finally, mean selenium concentrations in the estuary (sum of the concentrations divided by the number of observations) for model simulations and the observed field data were also used in comparing overall model fit to the data.

The best fit is when the significance of the linear correlation coefficient is greater than the critical $r_{0.05}$, the overall model confidence interval is greater than 75%, and model-derived averages for the estuary are within the errors of the observed estuarine

averages (Perrin et al., 2001). A correlation coefficient that is less than $r_{0.05}$ does not necessarily indicate that the model is not working, but could be a reflection of outliers (noise) in the data and/or invariance of the data (i.e., the concentration of some parameter is relatively constant across the salinity gradient). Therefore, a reasonable fit between the simulated concentrations and the observed concentrations still exits if the confidence interval is greater than 75% and the estuarine averages agree.

3.3. SENSITIVITY ANALYSIS

3.3.1. High Flow Sensitivity Analyses

As noted above, the model was considered sensitive to a parameter when the absolute $S_{c,k}$ was 0.15 or greater, and can be used to indicate which parameters are controlling the model output. Therefore, the values reported in the following discussion are the absolute values unless otherwise indicated. Modeled total dissolved selenium concentrations during the high flow months (December to May) were only sensitive to riverine discharge ($S_{c,k}$ = 1.00) and the "Delta removal effect" (refer to Section 1.4.8. for a detailed explanation) applied to the San Joaquin River ($S_{c,k}$ = 0.44). Absolute $S_{c,k}$'s indicate that during high flow, river discharge was more important in model output of total dissolved selenium than the "Delta removal effect" (Table 7).

Varying river discharge had the greatest effect on selenate concentrations relative to the reference simulation ($S_{c,k}$ =2.68), but the $S_{c,k}$ of selenite and organic selenide indicated that they were also sensitive to river discharge (Table 7). However, $S_{c,k}$ shows that selenite was affected more by the "Delta removal effect" (0.34) than by the increase

Table 7
Sensitivity analyses for changing parameters by 25 % during high flow months (December to May). Dash lines indicate that the model is insensitive to varying that parameter ($|S_{c,k}| < 0.15$)

Parameter	D ∑Se	D Se IV	D Se VI	D Org. Se –II	Part. ∑Se	Part. Se IV+VI	Part Se O	Part. Org Se-II
a	-	-	-	-	-	-	-	-
b	-	-	-	-	0.24	0.24	0.26	0.25
c	-	-	-	-	1.07	1.13	1.22	0.81
d	-	-	-	-	0.18	0.17	0.19	0.18
e	-	-	-	-	-	0.17	-	-
ε	-	-	-	-	-	-	-	-
ψ	-	-	-	-	-0.20	-0.22	-0.22	-0.16
P_m	-	-	-	-	-	-	-	0.36
α	-	-	-	-	-	-	-	0.35
W	-	-	-	-	-	-	-	-
k_s	-	-	-	-	-	-	-	-
k_1	-	-	-	-	-	-	-	-
k_2	-	-	-	-	-	-	-	-
k_4	-	-	-	-	-	-	-	-
k_5	-	-	-	-	-	-	-	-
k_6	-	-	-	-	-	-	-	-
River Discharge	1.00	0.17	2.68	0.15	0.45	0.54	0.33	0.49
Refinery	-	-	-	-	-	-	-	-
I_λ	-	-	-	-	-	-	-	0.35
R	-	-	-	-	-	-	-	-
A'	-	-	-	-	-	0.21	-	-
Z	-	-	-	-	-	-	-	-
P_g	-	-	-	-	-	-	-	-
Delta removal effect	-0.44	-0.34	-0.51	-0.35	-	-	-	-0.16

in river discharge (0.17). This was also observed for organic selenide (Table 7), but for selenate a change in river discharge resulted in a higher $S_{c,k}$ (2.68) than the "Delta removal effect" (0.51). It was surprising that during high flow months an increase in the parameters that define oxidation of selenium (k_1 to k_3) and selenium uptake (k_4 to k_6) had no effect on total dissolved selenium and its speciation ($S_{c,k}$'s less than 0.15). This may be due to relative short residence time of the water (e.g., 14 days).

Particulate selenium concentrations during high flow were dependent on a number of variables, including river discharge, parameters that define PSM inputs, and the velocity and movement of BEPS (Table 7). Varying the parameter that scales river discharge to sediment inputs of PSM (c in Equation 1.13), resulted in the highest change in particulate selenium concentrations ($S_{c,k}$ = 1.07), followed by varying the riverine input ($S_{c,k}$ = 0.45). Modifying the concentration of suspended sediment at the riverine end member (b in Equation 1.13) had a modest effect and resulted in a $S_{c,k}$ of 0.24 for total particulate selenium. The absolute values of $S_{c,k}$ show that total particulate selenium is largely defined by parameter c (1.07), followed by river discharge (0.45).

Like total particulate selenium, particulate selenite + selenate was sensitive to parameter c ($S_{c,k}$ = 1.13) and river discharge ($S_{c,k}$ = 0.54). Varying b (Equation 1.13), the constants in the velocity of BEPS (d and e Equation 1.15), the rate of adsorption (a' in Equation 1.36, 1.38, 1.39), and ψ constant in the dispersion of BEPS (Equation 1.16) resulted in similar absolute values of $S_{c,k}$ (range from 0.17 to 0.24) for particulate selenite + selenate (Table 7), As with total selenium, the absolute value of $S_{c,k}$ model output is largely controlled by parameter c.

Elemental selenium was sensitive to b and c (Equation 1.13), the parameter constants used to define the velocity of BEPS (d and e in Equation 1.15), the constant in the dispersion of BEPS (ψ in Equation 1.16) and riverine discharge. A change in parameter c resulted in the highest change in elemental selenium ($S_{c,k}$ = 1.22). River discharge, b (Equation 1.13), d and e (Equation 1.15), and ψ (Equation 1.16) resulted in similar $S_{c,k}$ (range 0.19 to 0.33). As with particulate selenite + selenate, elemental selenium is largely a function or parameter c (Equation 1.13, absolute $S_{c,k}$=1.22).

Unlike inorganic particulate selenium, particulate organic selenide was sensitive to more of the parameters in the model. In addition to those for elemental selenium, particulate organic selenide was also sensitive to the maximum rate of photosynthesis at optimal light intensity (P_m in Equation 1.19, $S_{c,k}$ =0.36), the initial slope of the light-saturated curve (α in Equation 1.19, $S_{c,k}$ =0.35), the daily surface photosynthetically active radiation (I_λ in Equation 1.21, $S_{c,k}$ =0.35), and the "Delta removal effect" of selenium from the San Joaquin River ($S_{c,k}$ =0.16, Table 7). Particulate organic selenide $S_{c,k}$'s also indicate that parameters affecting phytoplankton growth (P_m, α, and I_λ) produced higher $S_{c,k}$ (0.35) than varying d or e (0.16 to 0.25), suggesting that phytoplankton growth has more of a control than sediment resuspension over model-derived particulate organic selenide concentrations. However, parameter c is still the dominant parameter in defining the model-derived particulate organic selenide concentrations.

In summary, the absolute values of $S_{c,k}$ indicate that during high flow for total dissolved selenium, the model output is sensitive to river discharge and "Delta removal

effect" of the San Joaquin input. Model-derived particulate selenium was controlled by the riverine input of PSM (c in Table 7), followed by riverine discharge rates (Table 7). The sensitivity results indicate that for high flow months the speciation of dissolved selenium was affected by 2 of the 24 parameters tested, while total particulate selenium output was affected by 5 of the 24 parameters tested. Particulate organic selenide was affected by the most number of parameters (9 of the 24 tested).

3.3.2. Low Flow Sensitivity Analyses

As with the high flow months, only the absolute values will be discussed since they can be used to indicate which parameters are largely defining the model output. For low flow months (June to November), total dissolved selenium concentrations were affected by varying river discharge and the refinery effluent discharge rates (Table 8). Increasing refinery discharge rates resulted in a $S_{c,k}$ of 0.33 for total dissolved selenium, while the $S_{c,k}$ was 0.25 when riverine discharge was varied. Not surprisingly, the model is more sensitive to refinery discharge during low flow than during high flow (Table 7, $S_{c,k}$ less than 0.15). All of the species of dissolved selenium were affected when river discharge and refinery inputs were varied, but selenate was affected the most ($S_{c,k}$ of 0.39 for river discharge and 0.36 for refinery inputs). A $S_{c,k}$ of 0.40 resulted when the uptake of selenate by phytoplankton (k_5 in Equation 1.30) was varied. This is greater than the $S_{c,k}$ for an increase in river discharge (0.39) and refinery inputs (0.36), suggesting that phytoplankton uptake is important in predicting selenate concentrations in the estuary during low flow months. It was surprising that the model was not sensitive to

Table 8
Sensitivity analyses for changing parameters by 25 % during low flow months (June to November). Dash lines indicate that the model is insensitive to varying that parameter ($|S_{c,k}| < 0.15$)

Parameter	D ∑Se	D Se IV	D Se VI	D Org. Se –II	Part. ∑Se	Part. Se IV+VI	Part Se O	Part. Org Se-II
a	-	-	-	-	-	-	-	-
b	-	-	-	-	0.16	0.28	0.30	-
c	-	-	-	-	0.84	1.41	1.32	0.18
d	-	-	-	-	-0.37	-0.37	-0.61	-0.21
e	-	-	-	-	0.39	0.45	0.59	0.21
ε	-	-	-	-	-	-	-	-
ψ	-	-	-	-	-	-0.18	-	-
P_m	-	-	-	-	0.97	-	-	1.58
α	-	-	-	-	0.95	-	-	1.56
W	-	-	-	-	-0.20	-	-	-0.40
k_s	-	-	-	-	-	-	-	-0.23
k_1	-	-	-	-	-	-	-	-0.15
k_2	-	0.18	-	-	-	-	-	-
k_4	-	-	-	-	-	-	-	0.15
k_5	-	-	0.40	-	0.21	-	-	0.40
k_6	-	-	-	-	-	-	-	0.24
River discharge	0.25	0.34	0.39	0.15	0.96	1.45	1.39	0.22
Refinery	0.33	0.33	0.36	0.28	0.23	-	-	0.36
I_λ	-	-	-	-	0.95	-	-	1.56
R	-	-	-	-	-0.44	-	-	-0.94
a'	-	-	-	-	0.15	0.50	-	-
Z	-	-	-	-	-	-	-	-0.15
P_g	-	-	-	-	-	-	-	-0.70
Delta removal effect	-	-	-	-	-	-	-	-

the uptake of selenite (k_4 in Equation 1.31) and organic selenide (k_6 in Equation 1.32). This was probably due to the uptake being a function of concentration (Equation 1.30 to 1.32); even though the uptake rate was increased, the low selenite and organic selenide concentrations in the estuary controlled the overall rate. When k_2, the oxidation of dissolved organic selenide to selenite (Equation 1.31), was varied the $S_{c,k}$ was 0.18 (Table 8). Increasing the "Delta removal effect" of the San Joaquin River had no effect (Table 8) due to the small discharge from the San Joaquin (usually less than 10 $m^3 s^{-1}$) during these low flow periods. Overall, model output for total dissolved selenium was largely controlled by refinery inputs followed by riverine inputs.

Total particulate selenium was sensitive ($|S_{c,k}|$ greater than 0.15) to the same parameters at low flow as those at high flow (Table 8). In addition, model output of total particulate selenium was also sensitive to the refinery inputs ($S_{c,k} = 0.23$), P_m and α (Equation 1.19; $S_{c,k}$ range 0.95 to 0.97), I_k (Equation 1.21 $S_{c,k} = 0.95$), the rate of adsorption (a' in Equation 1.36, 1.38, 1.39, $S_{c,k} = 0.15$), and mortality due to respiration (R in Equation 1.17, $S_{c,k}$=0.44). Contrary to what was observed during the high flow months (Table 7), the absolute $S_{c,k}$ value for total particulate selenium was the highest when P_m was varied ($|S_{c,k}| = 0.97$; Table 8). Therefore, phytoplankton productivity is as important as other parameters like river discharge for the low flow months. Overall, total particulate selenium was sensitive to 13 of the 24 parameters (Table 8) varied.

Particulate selenite + selenate had a $S_{c,k}$ of 1.45 when river discharge was varied, and 1.41 when the riverine input of PSM was increased (c in Table 8). During low flow, the model was sensitive to the same parameters as described in Section 3.3.1, but the

magnitude of each increased. For example, increasing adsorption during high flow resulted in a $S_{c,k}$ of 0.21 (Table 7), but the same increase during low flow resulted in a $S_{c,k}$ of 0.50 (Table 8). This increase is likely due to the longer residence time of the water during low flow periods (i.e., 30 days). As with particulate selenite + selenate, elemental selenium was sensitive to the same parameters identified during high flow conditions (Section 3.3.1), with the highest $S_{c,k}$ value of 1.39 when river discharge was increased. Overall, for both particulate selenite + selenate and particulate elemental selenium river discharge had the greatest effect on model output ($|S_{c,k}|$ values of 1.45 and 1.39,respectively, Table 8).

Sensitivity results for particulate organic selenide during low flow were different than those during high flow months. In addition to being sensitive to the parameters discussed during high flow months, the model output was also sensitive to k_s (light attenuation due to particles, Equation 1.23, $S_{c,k} = 0.23$), the conversion of particulate organic selenide to dissolved organic selenide (k_1 in Equation 1.32, $S_{c,k} = 0.15$), the uptake of selenite, selenate, and organic selenide (Equation 1.30 through 1.32; $S_{c,k}$ range 0.15 to 0.40), zooplankton biomass (Z in Equation 1.25, $S_{c,k} = 0.15$), and the morality rates of phytoplankton (R and P_g in Equation 1.17, $S_{c,k}$ range of 0.74 to 0.90). For particulate organic selenide, the model output was greatly affected by P_m (1.58), α (1.56), and I_λ (1.56). In comparison, riverine discharge resulted in a $|S_{c,k}|$ of 0.22, which was seven times lower than the absolute $S_{c,k}$ of the aforementioned parameters. For particulate organic selenide, the model outputs for 17 of the 24 parameters tested were sensitive to a 25% variation.

In summary, total dissolved selenium during low flow is a function of river discharge rates and refinery inputs, while total particulate selenium is sensitive to parameter c, phytoplankton growth parameters, and river discharge. The most difficult species to simulate is particulate organic selenide for both low flow and high flow months (Table 7 and 8).

3.3.3. Conclusions Based on Sensitivity Analyses

As discussed earlier, sensitivity analysis can be used for model simplification and for understanding which parameters are responsible for observed particulate and dissolved selenium concentrations in an estuary for each flow period. The sensitivity analyses indicate that the modeled dissolved selenium is mostly defined by the variability in river discharge and refinery inputs. Particulate selenium concentrations, however, are dependent on a large number of parameters ranging from riverine inputs to biological uptake. In some estuaries, river flow dominates the estuarine profile of a nutrient throughout the year (e.g., Apalachicola Bay Estuary, Florida; Chanton and Lewis, 1999), while other estuaries (e.g., Chesapeake Bay) are dominated by phytoplankton changes (McCarthy et al., 1975). The sensitivity analyses show that the dissolved selenium concentration is river flow dominated for both high flow and low flow periods. However, particulate selenium in the San Francisco Bay is between these two extremes, with river dominance during high flow periods and biological productivity dominating during low flow periods (i.e., $|S_{c,k}|$ was greater for increasing optimal phytoplankton growth, P_m, than for increasing river discharge). This behavior has been observed by Peterson et al. (1985)

for nutrients in the San Francisco Bay where, depending on the river flow, the estuary can be river-dominated or phytoplankton-dominated.

Sensitivity analyses further indicate that the only parameter that had an absolute $S_{c,k}$ value less than 0.15 was parameter a (concentration of bed-exchangeable sediment at the river end member, Equation 1.13). For some of the parameters tested (e.g., k_1), the effect on total dissolved selenium and its speciation was minor, but the $S_{c,k}$ of particulate organic selenide was greater than 0.15. Therefore, dissolved selenium uptake is important for predicting particulate selenium and these parameters needs to remain in the model. Based on the above findings from the sensitivity analyses, the only simplification to the model before calibration can be the removal of a in Equation 1.13 because varying it has no effect on the model derived concentrations. With this removal, the model can now be calibrated to the observed data from 1999.

3.4. MODEL CALIBRATION

3.4.1. Conservative Solute

The transport of a solute in the estuary is a function of the water velocity and the dispersion coefficient (Equation 1.9). Both of these variables are a function of the cross-sectional area of the estuary (Section 1.4.5.). The model-simulated area (Fig. 24) indicated excellent agreement ($r = 0.999$, CI = 100%) between the simulated area and that of Uncles and Peterson (1996), suggesting that the estuarine shape is correctly defined.

Actual observed dispersion coefficients for the time period of interest were not available, but past research by Selleck (1968), Gleene and Selleck (1969), and Cifuentes

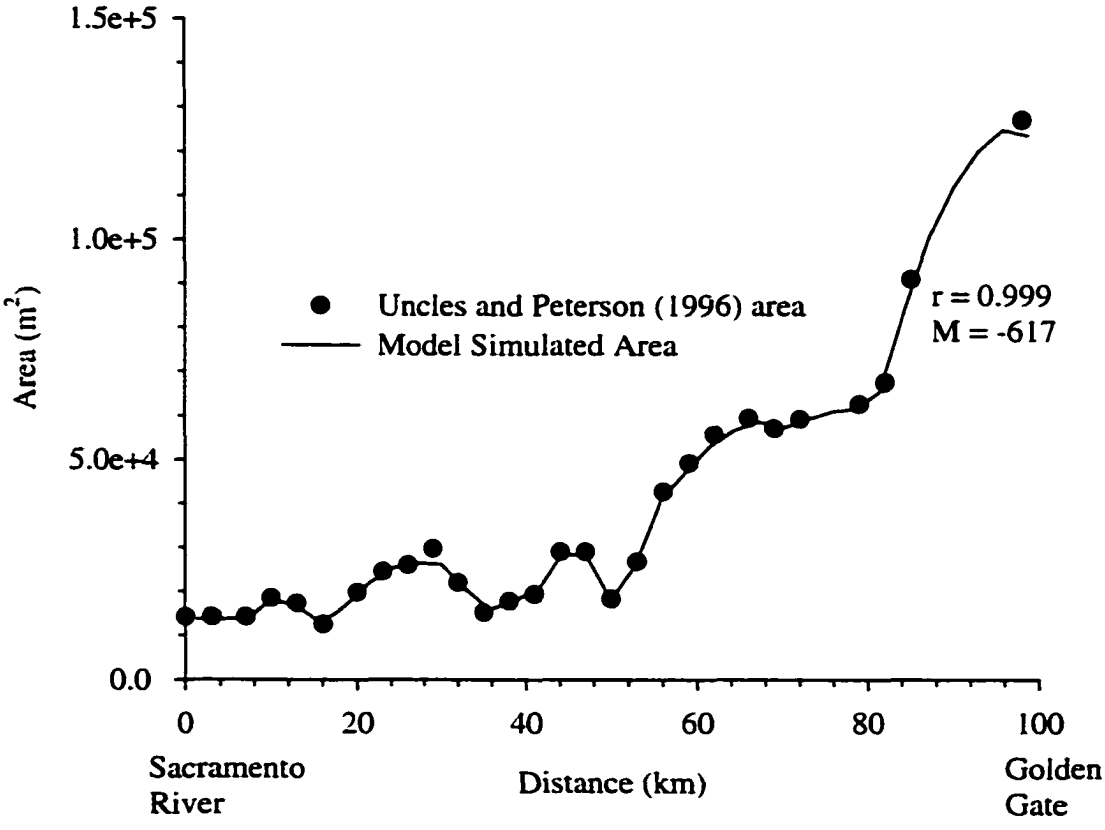

Fig. 24. Model simulated area compared to measured area.

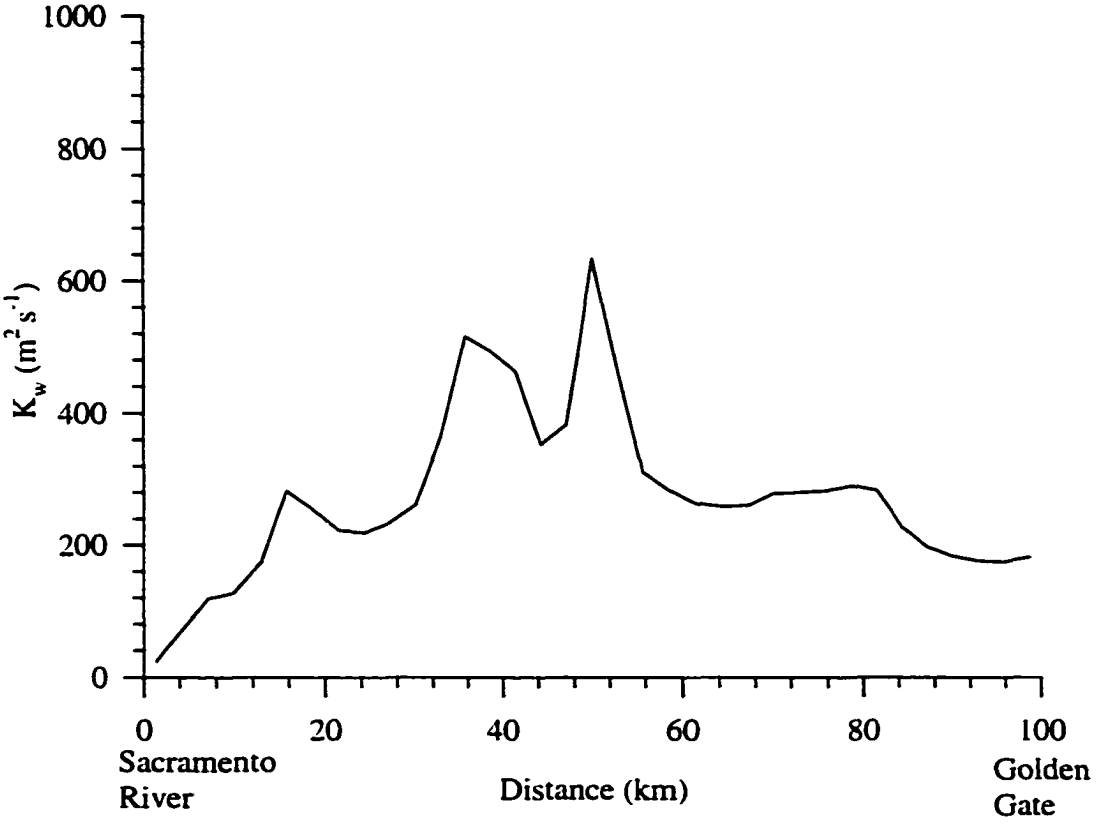

Fig. 25. Model simulated K_W for the Northern Reach of the San Francisco Bay.

et al. (1990) found that the dispersion coefficient in the Northern Reach of the Bay varied between 16 to 812 $m^2 s^{-1}$, with the highest values in Carquinez Strait. The model simulated dispersion coefficient (Equation 1.10) was between 24 to 650 $m^2 s^{-1}$ in April of 1999 (Fig. 25), with the lowest dispersion coefficient at the riverine end member and it increased to its maximum value in Carquinez Strait. This trend is consistent with past results (Selleck, 1968; Gleene and Selleck, 1969; Cifuentes et al., 1990), indicating that the dispersion of water within the model was correctly defined by Equation 1.10.

Salinity is a conservative tracer and the comparison of model simulated versus actual salinity can be used to determine if the hydrological parameters (e.g., tides, river flow) in the model are correctly assigned. Salinity data for 1999 was obtained from the United States Geological Service (USGS) continual monitoring program in the Northern Reach (http://sfbay.wr.usgs.gov/access/wqdata/webbib.html), and Cutter and Cutter (in prep.). During the spring, high river discharge resulted in fresh water intrusion into Suisun Bay (December through June, Fig. 26), while in the fall, low river discharge allowed salt water intrusion into the fresh water end member (August to November, Fig 3.3). Salinity at the Golden Gate varied from 25 in the spring to 32.5 in the fall (Fig 26). Model computations reproduced the observed salinity variability within the estuarine for the entire year (Fig. 26). The model-simulated salinities relative to the measured data have linear correlation coefficients greater than 0.95 for all months simulated and the correlation coefficients are significant at the $r_{0.01}$ level. The mean cumulative error varied from -3.16 to a +2.82 and the confidence interval was greater than 75% for all months (Fig. 26). Due to the large range of observed salinities within the estuary, using the

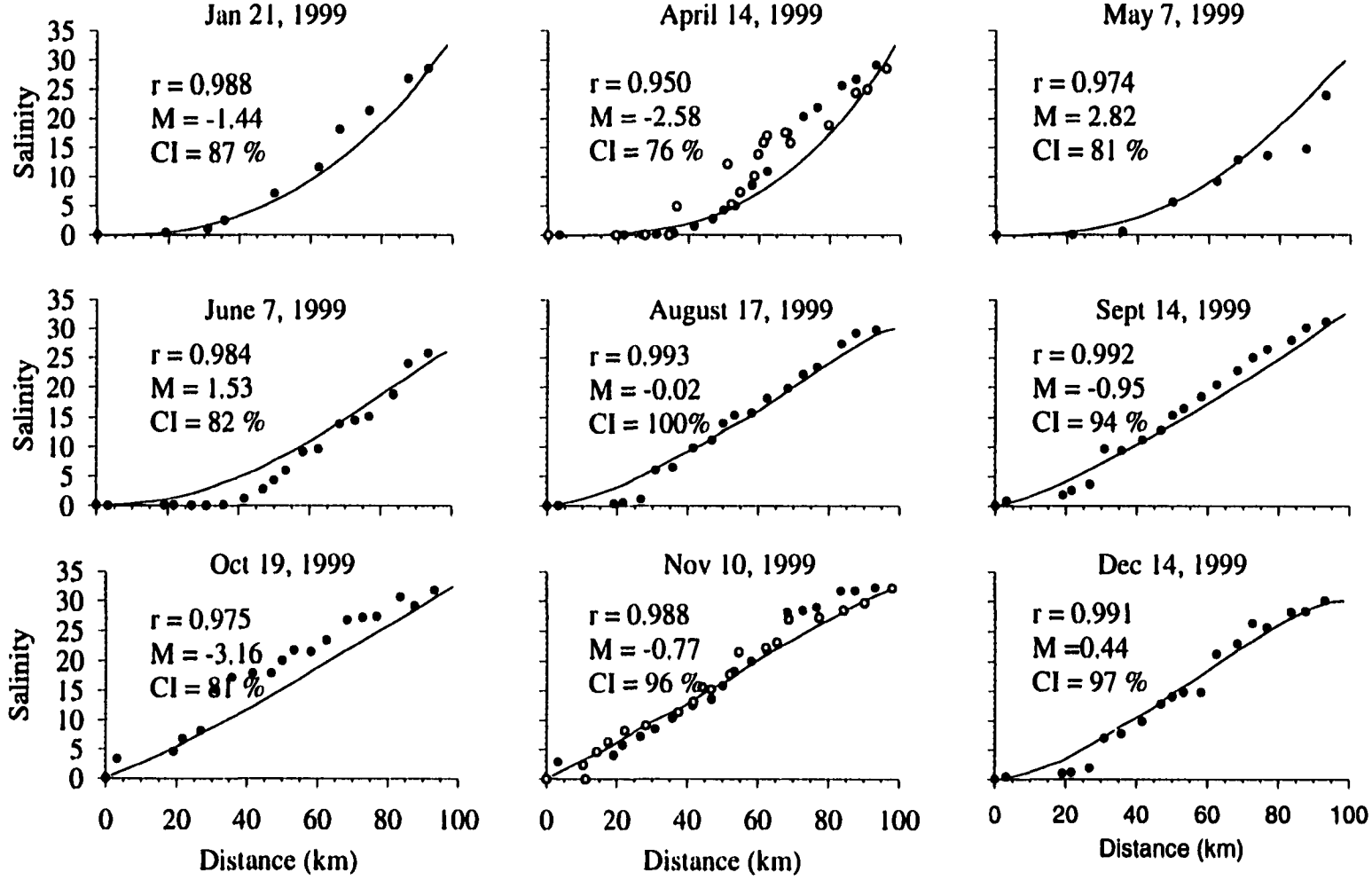

Fig. 26. Yearly salinity profiles for the Northern Reach from 1999. The observed data from the continual monitoring program of the USGS are filled circles and Cutter and Cutter (in prep.) are the open circles.

Table 9
Final parameter values for calibration of the model to dissolved and particulate selenium data from 1999

Parameter	Description	Value	Units	Reference
b	Permanently suspended sediment at the riverine end	0.00029	$g\ L^{-1}$	Harris et al. (1984)
c	Scales freshwater discharge to sediment input	0.7		
d	Scaling factor for U_{beps}	0.007		
e	Scaling factor for U_{beps}	2		Schoellhamer (2001)
ε	Scaling factor K_{beps}	32	m	
ψ	Scaling factor K_{beps}	20	m	
M_2Phase	Tidal phase	125	degrees	Godin (1972)
K_1 Phase	Tidal phase	264	degrees	Godin (1972)
O_1 Phase	Tidal phase	51	degrees	Godin (1972)
M_2Frequency	Tidal frequency	695.52	degrees d^{-1}	Godin (1972)
K_1 Frequency	Tidal frequency	360.96	degrees d^{-1}	Godin (1972)
O_1 Frequency	Tidal frequency	334.56	degrees d^{-1}	Godin (1972)
M_2	Tidal amplitude	0.58	m	Uncles and Peterson (1996)
K_1	Tidal amplitude	0.37	m	Uncles and Peterson (1996)
O_1	Tidal amplitude	0.23	m	Uncles and Peterson (1996)
P_m	Maximum rate of photosynthesis	73.95	mg C mg^{-1} chl-a d^{-1}	Alpine and Cloern (1992)
W	Zooplankton weight	13	μg C $animal^{-1}$	Hutchinson (1981)
B_{sea}	Initial phytoplankton concentrations and seawater end member	2.3	μg chl-a L^{-1}	Alpine and Cloern (1992)
α	Slope of the light-saturation curve divided by P_m	0.00394	Einst. $m^2\ d^{-1}$	Peterson and Festa (1984)
k_s	Light scattering due to suspended particles	10	$L\ g^{-1}\ m^{-1}$	
k_w	Light scattering due to water	0.05	m^{-1}	Miller and Zepp (1979)
k_d	Light scattering due to dissolved mater	0.05	m^{-1}	Miller and Zepp (1979)
r	Mortality of phytoplankton through respiration	7.395	d^{-1}	Cole and Cloern (1987)
C:Chl a	Carbon to chlorophyll-a ratio	51	mg C mg^{-1} chl-a	Alpine and Cloern (1992)
k_1	Rate constant	0.05	d^{-1}	Cutter (1991)
k_2	Rate constant	0.004	d^{-1}	Cutter (1991)
k_3	Rate constant	2.4×10^{-6}	d^{-1}	Cutter and Bruland (1984)
k_4	Phytoplankton uptake constant	15.905	L hr^{-1} chl-a^{-1}	Riedel et al. (1996)
k_5	Phytoplankton uptake constant	3.37	L hr^{-1} chl-a^{-1}	Riedel et al. (1996)
k_6	Phytoplankton uptake constant	7.9525	L hr^{-1} chl-a^{-1}	Riedel et al. (1996)
Se O_{psp}	Elemental sedimentary selenium in PSP	1.25	nmol g^{-1}	Chapter II
Se $(IV+VI)_{psp}$	Se IV+VI sedimentary selenium in PSP	0.63	nmol g^{-1}	Chapter II

Table 9 Continued

Parameter	Description	Value	Units	Reference
$BEPS_{river}$	Riverine end member of BEPS	0.00463	$g\ d^{-1}$	Harris et al. (1984)
$BEPS_{sea}$	Sea water end member of BEPS	0	$g\ d^{-1}$	
V_s	Sinking of BEPS	86.4	$m\ d^{-1}$	McDonald and Cheng (1997)
w_s	Sinking of Phytoplankton	0.5	$m\ d^{-1}$	Cloern (1991)
$PSM_{seawater}$	Seawater end member concentration of PSM	0.1	$g\ L^{-1}$	Harris et al. (1984)
Delta Removal effect	Removal of selenium as transported through the Delta to the Bay	60 %		

estuarine average criteria (Section 3.2.3) is not appropriate (i.e., the simulated average will always fall within the error bars of the observed mean). Thus, the physical dynamics that control the behavior of a conservative solute (salinity) appear to be functioning correctly. Since the model was able to accurately simulate salinity, all subsequent plots will be versus salinity instead of distance so that non-conservative and conservative behavior in the estuary can be easily identified (Loder and Reichard, 1981).

3.4.2. Total Suspended Material

Equations 1.11 through 1.16 were used to simulate total suspended particles within the estuary. Model parameters used to define TSM are given in Table 9. Observed TSM data were obtained from the USGS continual monitoring program in the Northern Reach (http://sfbay.wr.usgs.gov/access/wqdata/webbib.html) and Doblin et al. (in prep.).

TSM maxima between a salinity of 1 to 6 have been observed in the Northern Reach from 1974 to 1977 (Arthur and Ball, 1979). Recent data analysis by Shoellhamer (2001) from 1993 to 1997, reported similar findings, with the highest TSM values in August. In 1999, the observed TSM values ranged from 10 mg L^{-1} in the winter to 170 mg L^{-1} in the late summer (Fig. 27). The model was able to reproduce the annual variability in TSM concentrations and the estuarine profiles of TSM with a maximum located between salinity of 1 to 6 (Fig. 27). As with the observed data, the model produced a maximum TSM concentration in August, with the minimum occurring in November. However, the simulated TSM maximum tends to decrease at a greater rate

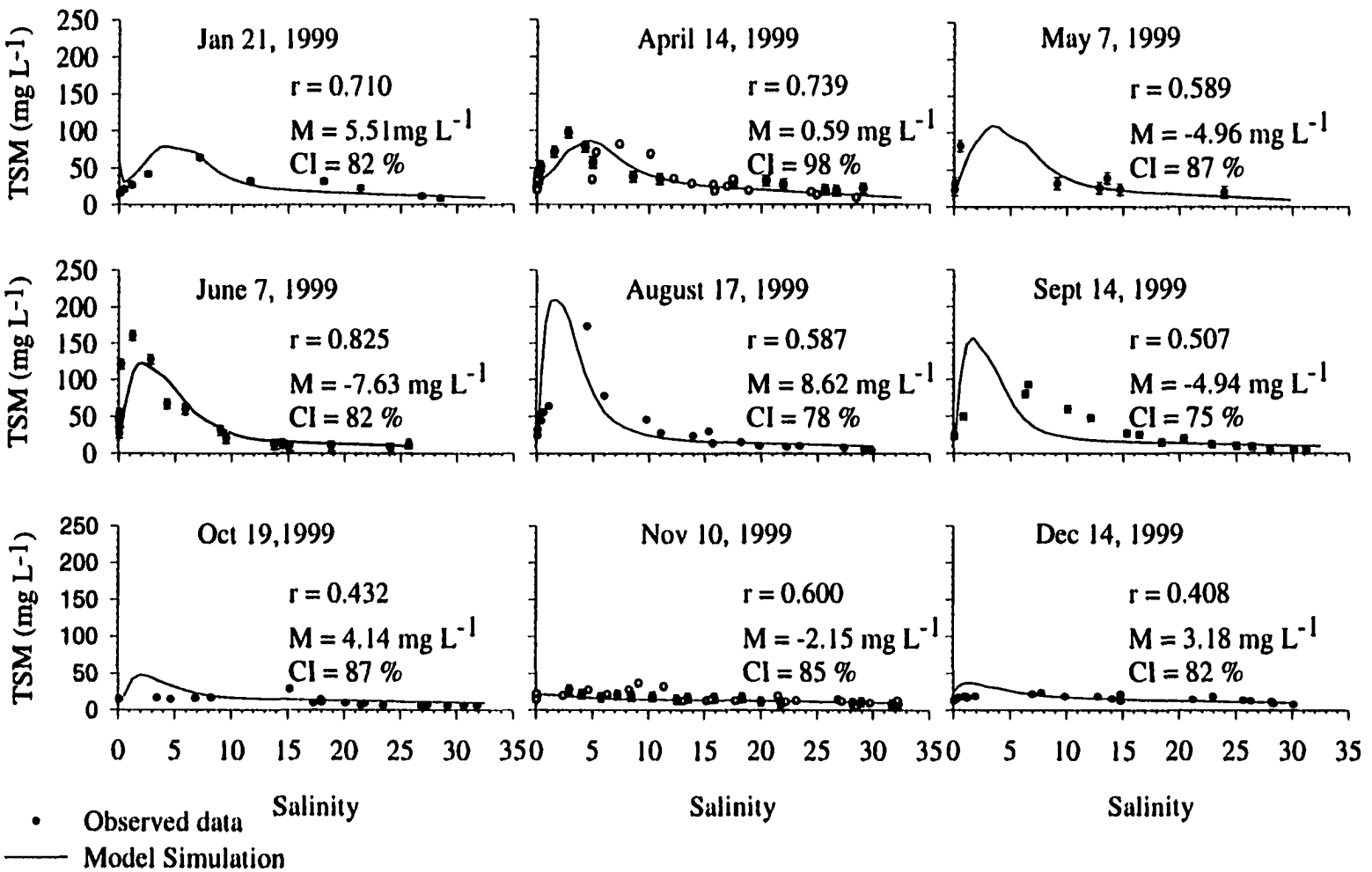

Fig. 27. TSM versus salinity for the Northern Reach from 1999. The observed data from the continual monitoring program of USGS are filled circles and from Doblin et al. (in prep.) are open circles.

than the observed TSM for some months (e.g., September 14, 1999, Fig. 27). This may be due to localized events (e.g., wind mixing) that keep sediment in suspension (Krone, 1962).

For January, April, August, October, and December the mean cumulative error indicates that the model was over predicting TSM (ranged from 0.59 to 8.62 mg L^{-1}; Fig. 27). The model was under predicting TSM for the remaining months (ranged from -7.63 to -2.15 mg L^{-1}). Even though these cumulative errors may appear to be high, the overall ability of the model to reproduce the observed estuarine concentrations ranged from 75% to 98% (Fig. 27), showing that these cumulative errors were low. The correlation coefficient ranged from 0.408 to 0.825, but based on the $r_{0.05}$, the model fit to the observed data was significant for all the months simulated except for May and December (Fig. 27). Even though the correlation coefficients were low for these months, the confidence interval was 87% for May, 87% for October, and 82% for December and the observed estuarine average (35 ± 21 mg L^{-1} for May, 11 ± 6 mg L^{-1} for October, and 16 ± 5 mg L^{-1} for December) and simulated averages agreed (39 ± 32 mg L^{-1} for May, 19 ± 11 mg L^{-1} for October, and 19 ± 9 mg L^{-1} for December; Table 10). For all months simulated estuarine observed averages agreed with the simulated averages (Table 10), with an observed yearly TSM of 29 ± 20 mg L^{-1} and a model-simulated yearly TSM of 33 ± 18 mg L^{-1}. Based on the above statistical analysis, the model is able to simulate TSM reasonably well.

Table 10
Observed average estuarine total suspended material and chlorophyll-a concentrations, and attenuation coefficient values for the Northern Reach of the San Francisco Bay compared to simulated averages for the year 1999

Month	TSM Observed ($mg\ L^{-1}$)	TSM Simulated ($mg\ L^{-1}$)	k Observed (m^{-1})	k Simulated (m^{-1})	Chl-a Observed ($\mu g\ L^{-1}$)	Chl-a Simulated ($\mu g\ L^{-1}$)
January	28 ± 17	29 ± 20	2.4 ± 1.1	2.9 ± 1.1	1.9 ± 0.6	1.2 ± 0.5
April	38 ± 22	42 ± 21	2.9 ± 1.6	3.2 ± 1.3	3.7 ± 1.4	2.9± 0.4
May	35 ± 21	39 ± 32	2.7 ± 1.9	3.2 ± 1.7	6.0 ± 2.0	4.7 ± 1.1
June	48 ± 45	49 ± 40	3.5 ± 2.3	3.4 ± 2.0	2.9 ± 1.0	2.6 ± 0.4
August	36 ± 40	46 ± 40	2.3 ± 1.9	3.5 ± 3.0	2.6 ± 0.9	2.3 ± 0.6
September	32 ± 28	40 ± 36	2.5 ± 1.2	2.8 ± 2.3	3.7 ± 2.6	3.3 ± 0.8
October	11 ± 6	19 ± 11	1.4 ± 0.5	1.7 ± 0.5	3.2 ± 1.5	1.9 ± 0.5
November	16 ± 10	15 ± 13	1.3 ± 0.4	1.5 ± 0.2	1.5 ± 0.5	1.2 ± 0.4
December	16 ± 5	19 ± 9	1.6 ± 0.5	1.7 ± 0.5	1.4 ± 0.6	1.2 ± 0.5

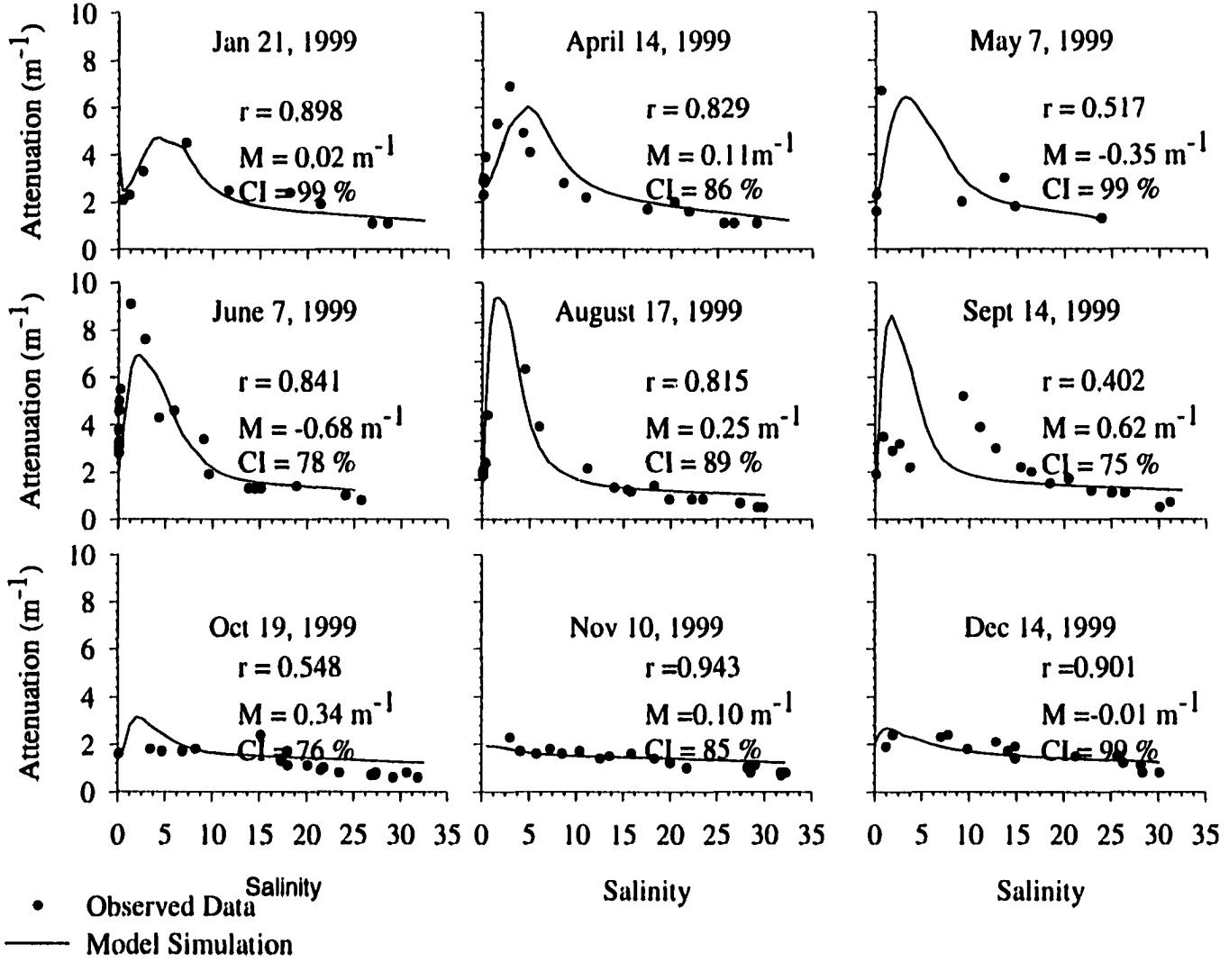

Fig. 28. Attenuation coefficient of light in the water column of the Northern Reach from 1999. The observed data was obtained from the continual monitoring program of USGS.

3.4.3. Phytoplankton Concentrations

The absorption and scattering of light due to particles within the water column, decreases the amount of light available for phytoplankton growth (Miller and Zepp, 1979). Light availability is important in the San Francisco Bay because it is a light limited estuary (Cloern, 1991; Peterson et al., 1987) and light attenuation in the water column was simulated using Equation 1.23 (final parameters values for the model in Table 9). Light attenuation in the water column is monitored by the USGS (Fig. 28; http://sfbay.wr.usgs.gov/access/wqdata/webbib.html). An observed maximum light attenuation of 9 m^{-1} occurs in June (Fig. 28). The observed estuarine profile of light attenuation was similar to the TSM profiles, with high light attenuation occurring at the TSM maxima.

The observed yearly variability in light attenuation was reproduced during model simulations (Fig. 28). Correlation coefficients ranged from a low of 0.402 for September to a high of 0.943 for November (Fig. 28). Except for May and September, the correlation coefficients were significant at the $r_{0.05}$ level (Fig. 28). Although, these months may have had lower correlation coefficient, the ability of the model to produce the overall observed behavior (confidence interval) was 99% (May) and 75% (September; Fig. 28). Confidence intervals ranged from the lowest in September and up to 99% in January, May and December (Fig. 28). Model-derived light attenuation coefficients were slightly higher than the observed data for 6 of the 9 months (highest mean cumulative error ranged from +0.02 to +0.62 m^{-1}). Simulated estuarine averages agreed with the observed data (Table 10). Therefore, the correlation coefficient, the confidence interval,

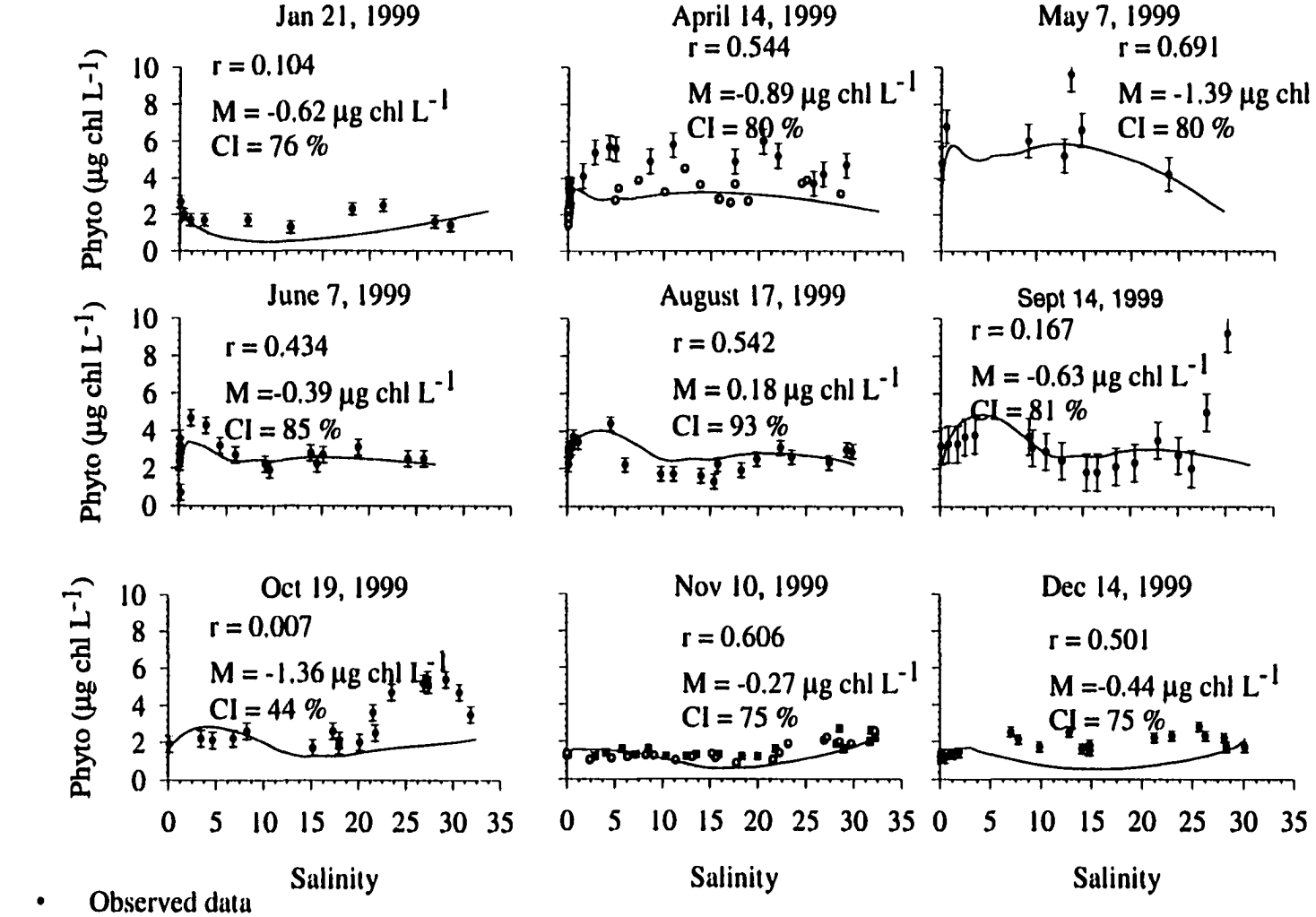

Fig. 29. Phytoplankton chlorophyll-a concentrations in the Northern Reach from 1999. The observed data from the continual monitoring program of USGS are filled circles and Doblin et al. (in prep.) are open circles.

and the estuarine averages all indicate that the model was able to reasonably reproduce the field data.

Chlorophyll-a concentrations were used as a measure of phytoplankton biomass in the estuary (Equation 1.17). Observed chlorophyll-a concentrations were obtained from the USGS continual monitoring program (http://sfbay.wr.usgs.gov/access/wqdata/webbib.html) and Doblin et al. (in prep.). Observed chlorophyll-a concentrations ranged from 1 μg chl L^{-1} to 10 μg chl L^{-1}, with a spring bloom occurring in April/May (Fig. 29). The yearly estuarine average phytoplankton concentration was 2.7 ±1.6 μg chl L^{-1}. Discrepancies between field data from the USGS data and Doblin et al. (in prep.) were observed in April (Fig. 29), but there was no indication why this difference existed, so both values were plotted.

Model simulations resulted in a spring bloom in May and low chlorophyll-a concentrations in December/January (Fig. 29). Model-simulated estuarine profiles generally agree with the observed field data (Fig. 29). The linear correlation coefficient ranged from 0.007 to 0.691. The correlation coefficient was significant at the $r_{0.05}$ level for April, August, November, and December. However, it should be noted that for some months the linear correlation coefficients did not meet the correlation coefficients 95% confidence interval, which may be due to data outliers. For example, in September there is a chlorophyll-a concentration of 10 μg chl L^{-1} which appears to be an outlier compared to the other data. If this point is removed, the correlation coefficient increases to 0.653, which then meets the $r_{0.05}$ for a linear correlation. Even though the correlation coefficient was less than the $r_{0.05}$ for January, May, and June, the simulated estuarine profiles are

within associated error bars of the data (Fig. 29). In addition, for January, May, and June the models confidence intervals were 76%, 80%, and 85%, respectively. Further confirming that although the $r_{0.05}$ for the correlation coefficient was not significant for January, May, and June, the model was able to simulate the observed phytoplankton concentrations for these months.

Model-simulated averages of chlorophyll-a were within the errors of the observed averages (Table 10), with the model under predicting for most of the months simulated (Fig. 29). For both the observed data and model simulations, the highest chlorophyll-a concentration occurred in May (6.0 ± 2.0 μg chl L^{-1} and 4.7 ± 1.1 μg chl L^{-1}, respectively). The yearly model simulated chlorophyll-a concentration was 2.4 ± 1.2 μg chl L^{-1}, which agrees with the observed data (2.7 ±1.6 μg chl L^{-1}). Model-derived chlorophyll-a concentrations were under predicting relative to the field data for eight of the nine months simulated (ranged from -0.27 to -1.39 μg chl L^{-1}; Fig. 29), but as indicated by the confidence interval these are low errors (Fig. 29). Excluding the month of October, the confidence interval ranged from 75% (November and December) to 93% in August (Fig. 29), further showing that the model did simulate chlorophyll-a concentrations correctly.

Using the carbon to chlorophyll-a ratio of 51 mg C (mg chl)$^{-1}$ (Cloern and Alpine, 1991), the observed phytoplankton biomass in units of carbon in 1999 from the observed data was 138 ± 81mg C m^{-3} (Table 10). The simulated phytoplankton biomass in units of carbon was 125 ± 61 mg C m^{-3}, which is essentially identical to the observed phytoplankton biomass (units of carbon). These combined statistical analyses indicate that the model was able to predict the yearly variability of chlorophyll-a in the estuary.

With respect to October, model generated phytoplankton concentrations in the Northern Reach deviated from the observed data at a salinity of 22 and greater. This corresponds to the mid-reach of San Pablo Bay and Central Bay (Fig. 5). A possible explanation for this deviation is that localized events (e.g., phytoplankton coming in from adjacent marshes) are causing the maximum or there are inputs from the South Bay (a third end member). If there was another end member, its effects should also be seen in the salinity, TSM and light attenuation profiles. As those figures showed the model had no problem predicting these profiles, the South Bay is probably not a source for these higher concentrations. Therefore, the only other possible explanation is a localized input. By examining the continual monitoring data from the USGS (http://sfbay.wr.usgs.gov/access/wqdata/webbib.html), the presence of higher chlorophyll-a concentrations like these observed in October are rare and the last time it was found was in 1994, and prior to that in 1991. The increase in chlorophyll-a could be due to a number of reasons including decreased grazing, phytoplankton inputs from adjacent marshes, and presence of atypical phytoplankton species (i.e., that have a higher optimal growth rate). Based on these results the deviation of the model from the observed phytoplankton biomass is probably due to localized events that cannot be easily simulated .

3.4.4. Dissolved Selenium

As discussed in Chapter I, dissolved selenium is introduced to the estuary via river water, refinery effluents, and oceanic exchange. The removal/production of selenium

Table 11
Observed estuarine average dissolved selenium and particulate selenium concentrations for the Northern Reach of the San Francisco Bay compared to simulated averages for the year 1999

Year	∑ Se (nmol L^{-1})	Se IV (nmol L^{-1})	Se VI (nmol L^{-1})	Org. Se -II (nmol L^{-1})	Part. ∑ Se (nmol L^{-1})	Se IV+VI (nmol L^{-1})	Se O (nmol L^{-1})	Org. Se -II (nmol L^{-1})
April 1999								
Model	1.73 ± 0.41	0.18 ± 0.02	0.90 ± 0.30	0.54 ± 0.09	0.16 ± 0.06	0.05 ± 0.02	0.05 ± 0.02	0.04 ± 0.02
Observed	1.49 ± 0.31	0.19 ± 0.02	0.69 ± 0.26	0.60 ± 0.37	0.20 ± 0.09	0.04 ± 0.03	0.06 ± 0.03	0.10 ± 0.10
Nov 1999								
Model	1.49 ± 0.32	0.19 ± 0.04	0.82 ± 0.23	0.49 ± 0.08	0.13 ± 0.04	0.02 ± 0.01	0.05 ± 0.02	0.04 ± 0.02
Observed	1.30 ± 0.26	0.20 ± 0.04	0.84 ± 0.16	0.30 ± 0.16	0.15 ± 0.08	0.05 ± 0.03	0.04 ± 0.02	0.07 ± 0.09

species is described in Chapter I with Equations 1.30 to 1.33. Average refinery input values are found in Appendix A, while the final parameter values needed in Equations 1.30 to 1.32 are found in Table 9. Fitting could only be done for dissolved selenium in April and November 1999 (Cutter and Cutter, in prep.), when data were available.

Observed total dissolved selenium concentrations ranged from 1.0 nmol L^{-1} to 2.2 nmol L^{-1}. In April, total dissolved selenium was conservative in the estuary, with higher concentrations in the riverine end member (Fig 30A). In November 1999, there was non-conservative production of total dissolved selenium in the mid-estuary (Fig. 31A). Model-generated total dissolved selenium profiles reproduced the conservative behavior in April and the non-conservative behavior in November (Fig. 30A and Fig. 31A, respectively). The correlation coefficient in April was 0.497, while in November it was 0.814. These correlations are significant since they are greater than the $r_{0.05}$ critical level. The mean cumulative error in April was 0.00 nmol L^{-1}, while in November the model over predicted total dissolved selenium by +0.19 nmol L^{-1}. As a overall indication of how well the model fit was, the confidence interval was 99% of the observed concentrations in April and 86% in November (Fig. 30A and 31A). The simulated estuarine average was 1.73 ± 0.41 nmol L^{-1} for April and 1.49 ± 0.32 nmol L^{-1} for November which was within the errors of the observed estuarine field data (1.49 ± 0.31 nmol L^{-1} for April and $1.30 \pm$ 0.26 for November; Table 11). Agreement between the observed and simulated estuarine averages and the high confidence interval demonstrates that model calibration of total dissolved selenium was good.

Selenite concentrations in April 1999 and November were low (range of 0.11 to

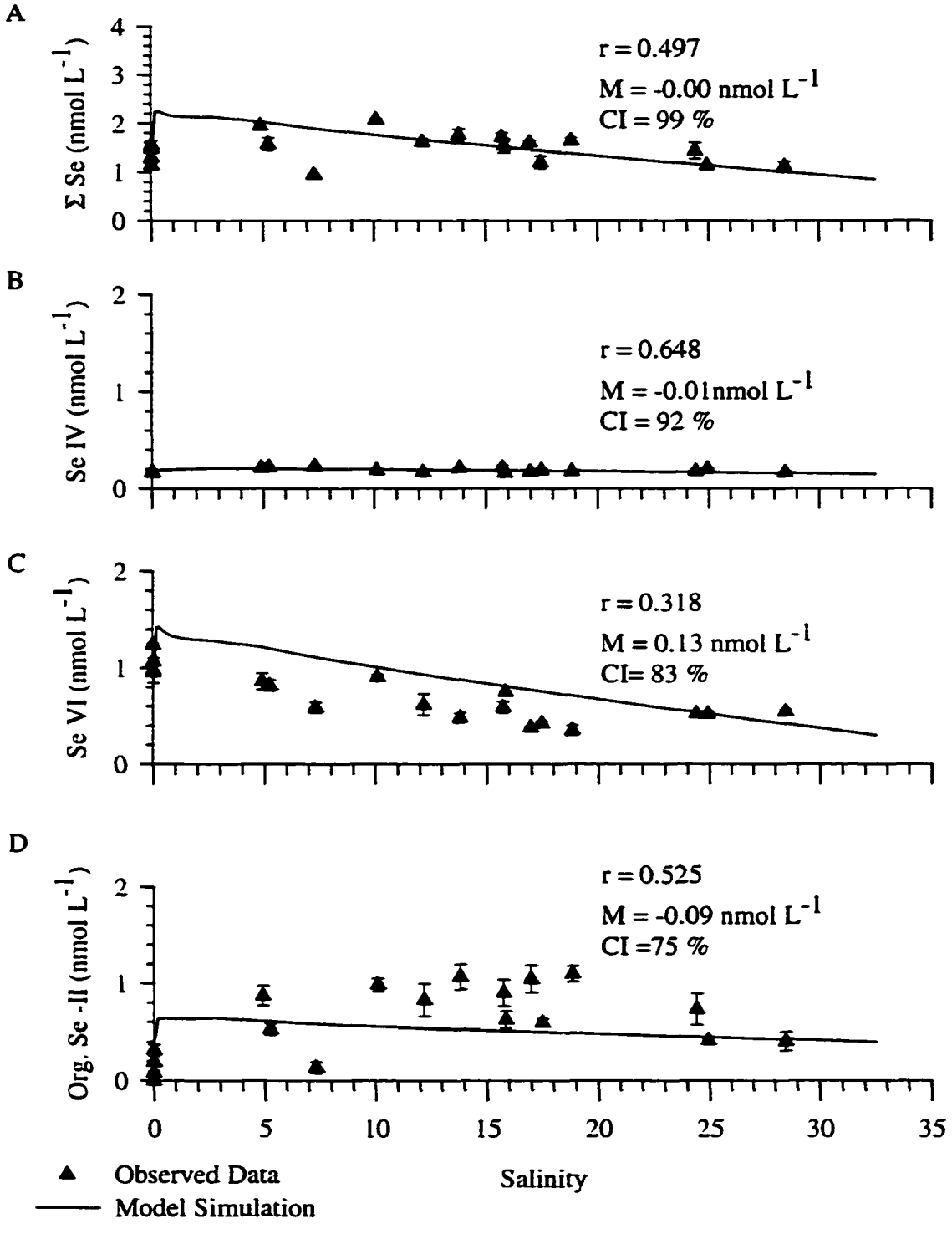

Fig. 30. Dissolved selenium in the Northern Reach April 14, 1999. The observed data are from Cutter and Cutter (in prep.).

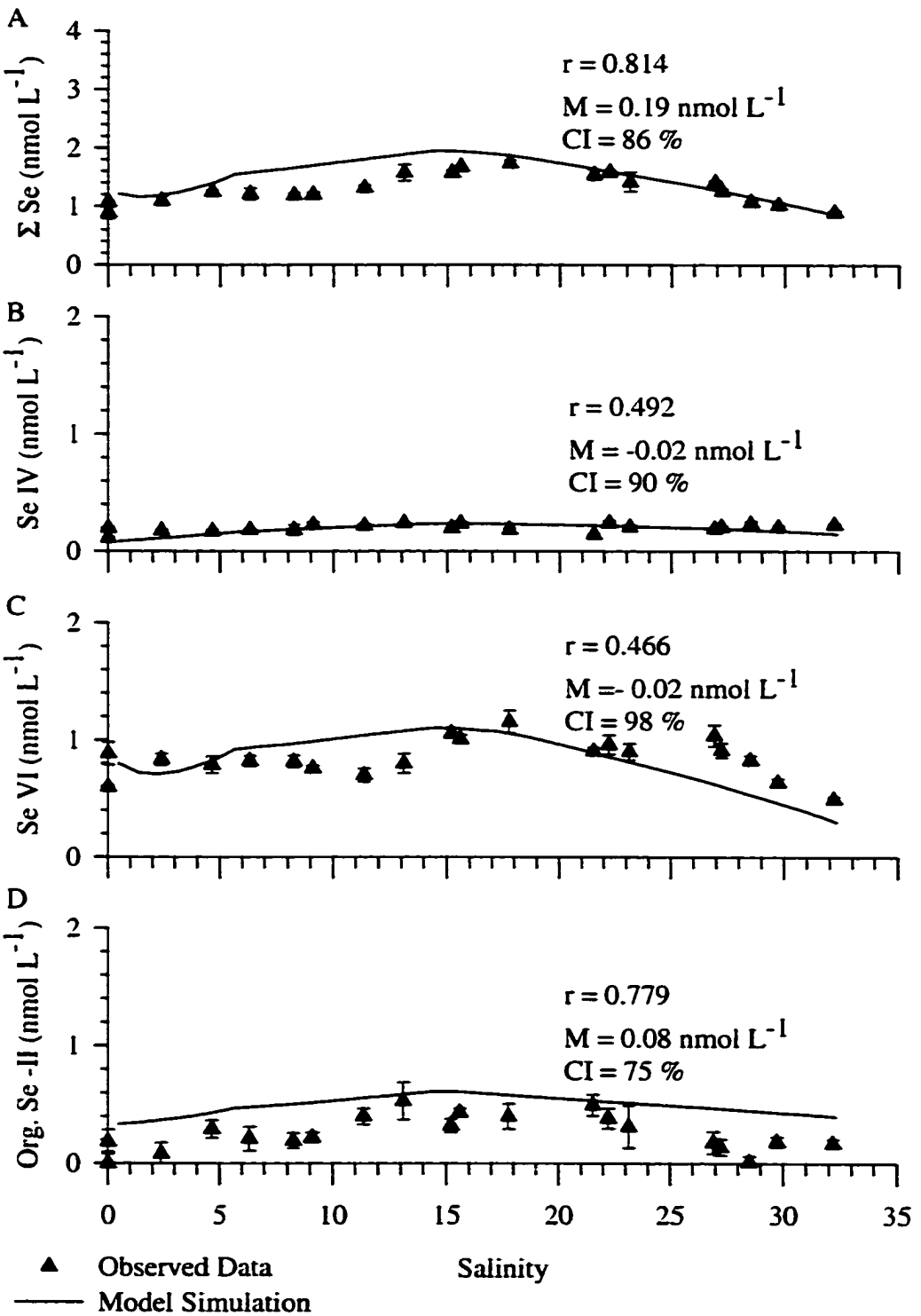

Fig. 31. Dissolved selenium in the Northern Reach on November 10, 1999. Observed data are from Cutter and Cutter (in prep.).

0.24 nmol L^{-1}) and non-conservative (Fig. 30B and Fig 31B). Simulated selenite estuarine profiles show non-conservative behavior for the estuary (Fig. 30B and Fig. 31B). The correlation coefficient was 0.648 for April and 0.492 for November, and both were above the $r_{0.05}$ level of significance. Added confirmation that the model is predicting selenite concentrations accurately are the confidence intervals, which were 92% for April and 90% for November. Observed estuarine average selenite concentrations were 0.19 ± 0.02 nmol L^{-1} (April) and 0.20 ± 0.04 nmol L^{-1} (November). Model-derived estuarine averages were 0.18 ± 0.02 nmol L^{-1} for April and 0.19 ± 0.04 nmol L^{-1} for November indicating perfect agreement with the field data (Table 11). The model was under predicting selenite for both months, (M = -0.01 nmol L^{-1} in April and -0.02 nmol L^{-1} in November), but these are within 10% of the observed estuarine average. Therefore, calibration of model for selenite was successful.

Observed selenate concentrations were 3 times greater than selenite concentrations (Fig. 30C and Fig. 31C). In April, the selenate maximum was located where the San Joaquin River joins the Sacramento River (Fig. 30C), while in November the selenate maximum was located mid-estuary (Fig. 31C). Selenate was predominately conservative in the estuary for April, while it was non-conservative in November (Fig. 30C and Fig. 31C, respectively). As with the selenite data, the correlation coefficient in April ($r = 0.381$) was lower than the $r_{0.05}$ (0.482), but the model was only slightly over predicting selenate (+0.13 nmol L^{-1}; 13% off, Fig. 30C) with a confidence interval of 83%. Furthermore, the observed estuarine averages were 0.69 ± 0.26 nmol L^{-1}, while model-simulated averages were 0.90 ± 0.30 nmol L^{-1} (Table 11). In November, the

correlation coefficient was 0.466 and is significant at the $r_{0.05}$ level. The model under predicts selenate (-0.02 nmol L^{-1}; Fig. 31C), with a confidence interval of 98%. The observed selenate estuarine average was 0.84 ± 0.16 nmol L^{-1} for November and the model-derived average was 0.82 ± 0.23 nmol L^{-1} (Table 11). Therefore, the above statistical parameters indicate that the model was able to accurately simulate selenate for the estuary.

Field data show that production of organic selenide was occurring in the estuary in April (Fig. 30D) and November (Fig. 31D). Elevated concentrations were located mid-estuary, with concentrations as high as 1.1 nmol L^{-1}. Model simulations were able to reproduce this non-conservative production behavior of organic selenide in the estuary (Fig. 30D and Fig. 31D). In April, the simulated organic selenide concentration was lower than the observed mid-estuary maximum (M = -0.09 nmol L^{-1}; 75% confidence interval), while in November the model was overestimating the organic selenide maximum (M = +0.08 nmol L^{-1}, 75% confidence interval). The correlation coefficient between the observed and the simulated data was significant at the $r_{0.05}$ for November (r = 0.779) and April (r=0.525). The model-derived averages of 0.54 ± 0.09 nmol L^{-1} (April) and 0.49 ± 0.08 nmol L^{-1} (November) were similar to the observed field data (0.60 ± 0.37 nmol L^{-1} for April and 0.30 ± 0.16 nmol L^{-1}; Table 11). For both November and April, statistical tests indicate that the fits between model-derived organic selenide concentrations and observed concentrations were good. Overall model calibrations for dissolved selenium and its speciation appear to be effective in simulating their behavior.

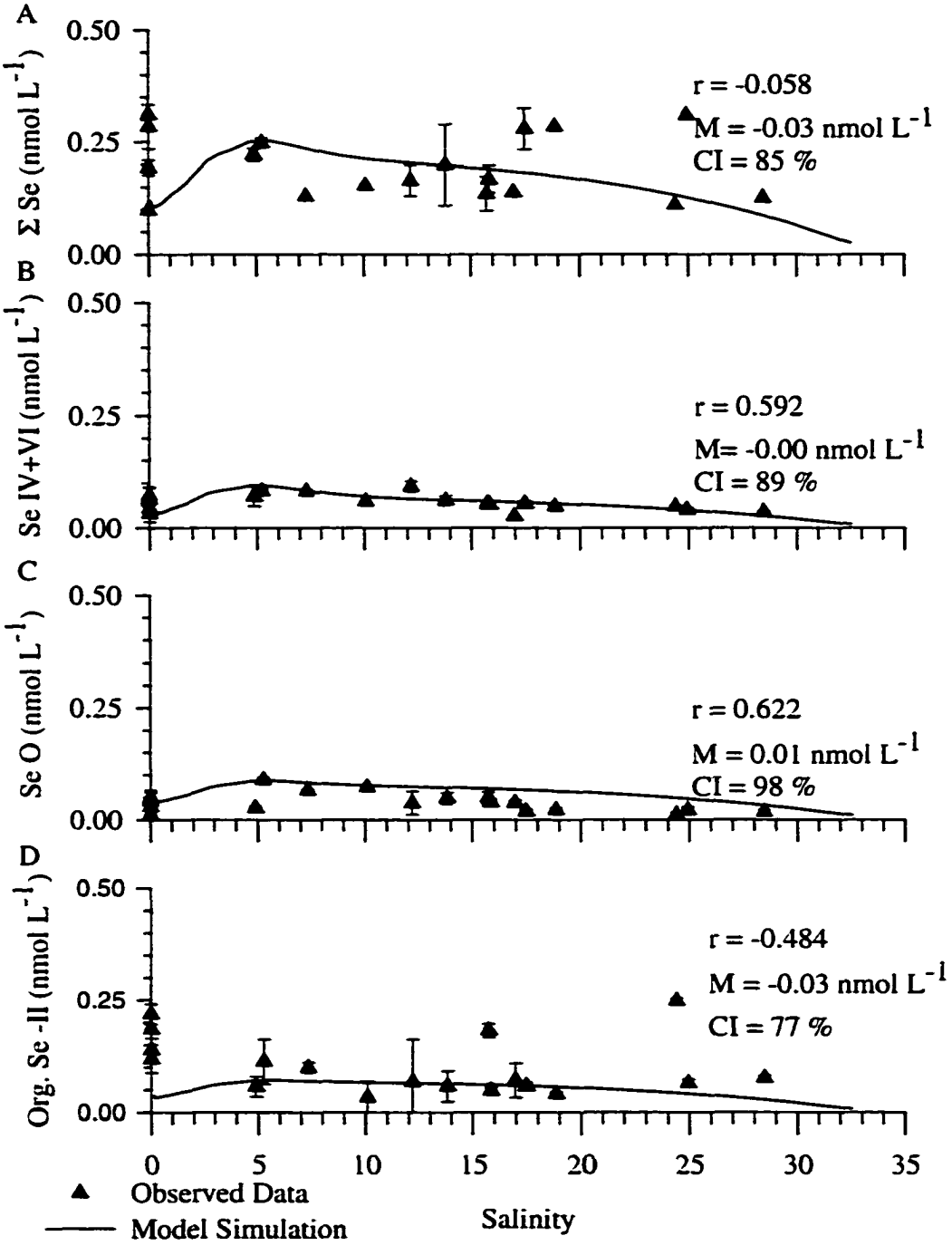

Fig. 32. Particulate selenium in the Northern Reach April 14, 1999. Observed data are from Doblin et al. (in prep.).

3.4.5. Suspended Particulate Selenium

Particulate selenium in the water column is due to sediment resuspension, riverine inputs, and *in situ* production (see Chapter I). The sensitivity analysis (Section 3.3) found that it is the most difficult constituent to simulate due to the large number of variables that can affect the model output. Particulate selenium was simulated in the model with Equations 1.34 through 1.41, and parameter values are found in Table 9. During calibration, an estuarine profile of sedimentary selenium concentrations was defined for each selenium species based on the findings from Section 2.3 (Appendix A) and used in Equation 1.34 to 1.41 for BEPS.

Observed total particulate selenium concentrations in April and November were similar (Fig. 32A and Fig. 33A respectively), and ranged from 0.09 nmol L^{-1} to 0.31 nmol L^{-1}. The particulate selenium maximum was located in the same region as the TSM maximum. Model-generated estuarine profiles of particulate selenium were consistent with the observed data in April (Fig. 32A) and November (Fig. 33A). The correlation coefficients for both April and November were low ($r = -0.058$ in April and $r = 0.375$ in November) and below $r_{0.05}$ level. As noted above, low correlation coefficients can be due to outliers and invariance in the data. In these cases, other statistical criteria are more appropriate for determining how well the model fits the data. In April, the simulated total particulate selenium concentrations have an 85% confidence interval, while in November it was 82 %. The model was under predicting total particulate selenium ($M = -0.03$ nmol L^{-1} in April and -0.02 nmol L^{-1} in November), and these are only 15 and 13% off the

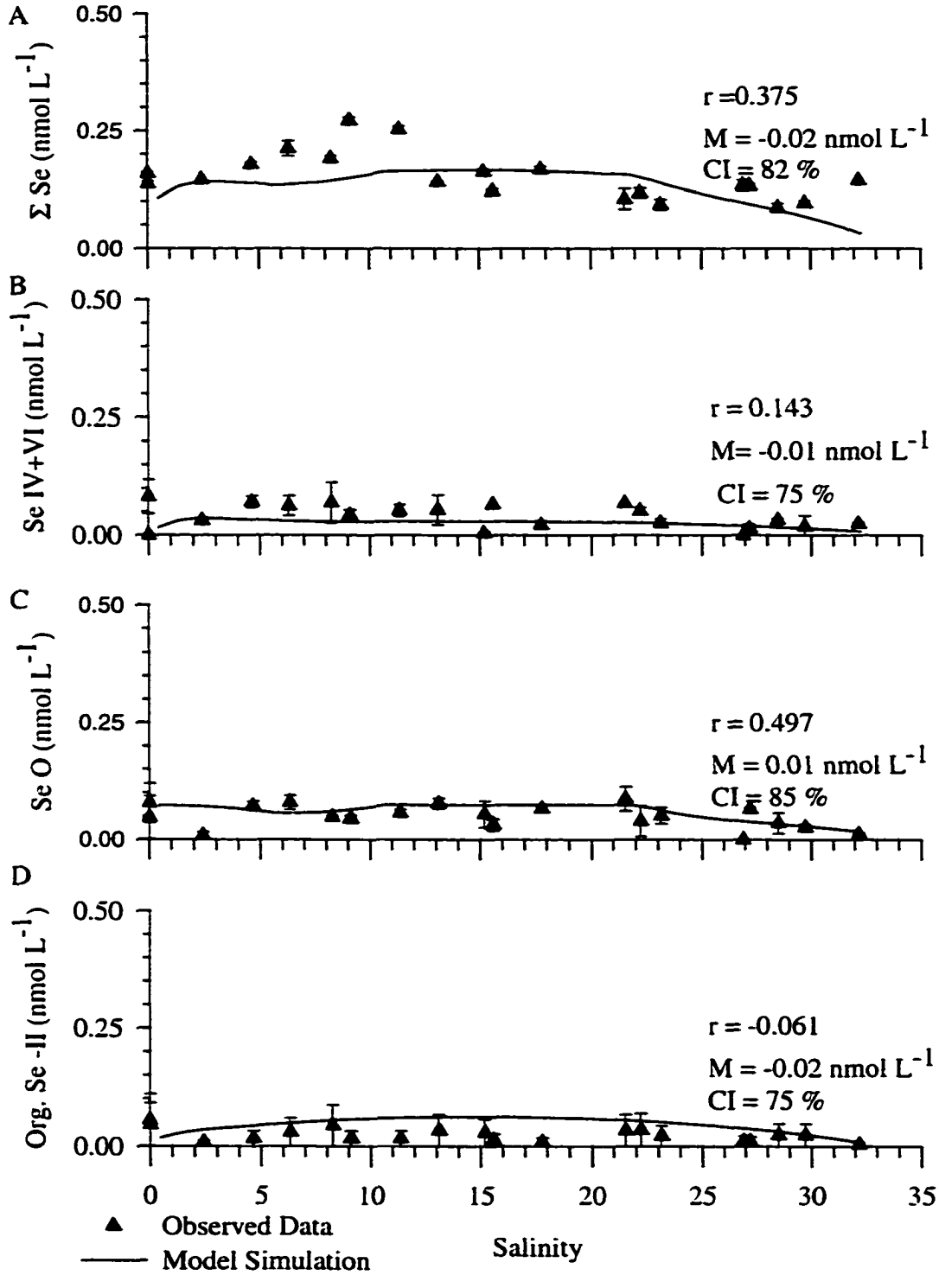

Fig. 33. Particulate selenium in the Northern Reach November 10, 1999. Observed data are from Doblin et al. (in prep.).

observed, respectively. Model-derived estuarine averages were 0.16 ± 0.06 nmol L^{-1} in April and 0.13 ± 0.04 nmol L^{-1} in November, which were within the errors of the observed data (0.20 ± 0.09 nmol L^{-1} for April and 0.15 ± 0.08 nmol L^{-1} for November; Table 11). Therefore, these combined statistical measurements indicate that the model was accurately able to simulate total particulate selenium.

Observed particulate selenite + selenate concentrations were very low in April (Fig. 32B) and November 1999 (Fig. 33B), with an estuarine average concentration of 0.04 ± 0.02 nmol L^{-1} and 0.05 ± 0.03 nmol L^{-1}, respectively. The field data show higher concentration in the upper estuary that corresponds to the location of the TSM maxima. Simulated particulate selenite + selenate profiles were within the errors of the observed data (Fig. 32B and Fig. 33B), and the reported correlation coefficient for April (r = 0.592) was above the $r_{0.05}$. The confidence interval was 89% and the observed estuarine average (0.04 ± 0.03 nmol L^{-1}) and the model-generated estuarine average (0.05 ± 0.02 nmol L^{-1}; Table 11) agreed. However, for November the correlation coefficient was 0.143 and below $r_{0.05}$ confidence. Even though the correlation coefficient appears to be insignificant, the confidence interval in November was 75%, the mean cumulative error was low (M = -0.01 nmol L^{-1}, Fig. 33B), and model-derived selenite + selenate averages (0.02 ± 0.01 nmol L^{-1}) was similar to the observed average (0.05 ± 0.01 nmol L^{-1}). Based on these analyses and considering the sensitivity analyses showed this to be difficult to parameterize, the model appears to generate accurate particulate selenite + selenate estuarine profiles.

According to Equation 1.34, elemental selenium can only be generated by

sediment resuspension (BEPS) and riverine inputs (PSM). Observed elemental selenium concentrations were observed to be higher in April than in November (Fig. 32C and Fig. 33C, respectively), which was expected because the TSM in April was higher. Estuarine averages for elemental selenium in the water column were 0.06 ± 0.03 nmol L^{-1} for April and 0.04 ± 0.02 nmol L^{-1} in November (Table 11). Model-derived elemental selenium concentrations for both months were within the errors of the observed data (0.05 ± 0.02 nmol L^{-1} for April and 0.05 ± 0.02 nmol L^{-1} for November; Table 11). The model derived salinity plots of elemental selenium were similar to the field data, and the correlation coefficients were 0.622 for April and 0.497 in November. Both of these correlation coefficients are significant at the 95 % confidence ($r_{0.05}$). In April, the model was able to predict 98% of the elemental selenium concentrations (Fig. 32C), while in November it is able to predict 85% of the observed variability (Fig. 33C). For both months, the model was over predicting elemental selenium concentrations (M = +0.01 nmol L^{-1}, Fig. 32C and Fig. 33C). Thus, the combined statistical analyses found that parameter calibration of the model was successful for elemental selenium.

Particulate organic selenide concentrations varied significantly between April and November (Fig. 32D and Fig. 33D). Simulated particulate organic selenide concentrations were able to reproduce the observed estuarine profile (Fig. 32D and Fig. 33D). The correlation coefficient for April (r = -0.484) was significant at the $r_{0.05}$ confidence level, while the correlation coefficient in November was not significant (r = -0.061). However, the confidence interval in November was 75% and the observed estuarine average of 0.07 ± 0.10 nmol L^{-1} agreed with the model-generated average (0.04

$\pm$ 0.02 nmol L^{-1}; Table 11). Mean cumulative errors were low compared to the errors on the observed data and showed that model simulations were under predicting particulate organic selenide for both months (M = -0.03 nmol L^{-1} in April and M = -0.02 nmol L^{-1} in November). The observed estuarine average in April was 0.10 $\pm$ 0.10 nmol L^{-1}, similar to the model-generated estuarine averages (0.04 $\pm$ 0.02 nmol L^{-1};Table 11). Based on the above statistical analysis model parameterization for particulate organic selenide concentrations were successful.

As an additional check of the model performance, the model-generated uptake of selenium by phytoplankton can be compared to observed selenium concentrations in phytoplankton. Doblin et al. (in prep.) found that for cultures of phytoplankton native to the San Francisco Bay, the atomic ratio of selenium to carbon ranged from 0.7 to 4.4 x 10^{-6}, with an average of 3.2 $\pm$ 6.2 x 10^{-6}. The model-derived phytoplankton selenium to carbon atomic ratios ranged from 0.9 to 12 x 10^{-6} for both April and November (combined average 5.6 $\pm$ 2.3 x 10^{-6}), which agrees with those observed by Doblin et al. (in prep.). Therefore, the uptake of dissolved selenium using the rate constants of Riedel et al. (1996) appears to generate similar selenium to carbon ratios found in phytoplankton from the San Francisco Bay.

To evaluate whether the modeled selenium concentrations on the particles themselves ($\mu g\ g^{-1}$) are comparable to observed values, the modeled particle selenium concentration (nmol L^{-1}) was divided by the total suspended material concentration (mg L^{-1}). Doblin et al. (in prep.) reported that in April and November, particle associated selenium ranged from 0.2 $\mu g\ g^{-1}$ to 1.6 $\mu g\ g^{-1}$, with an average of 0.63 $\pm$ 0.40 $\mu g\ g^{-1}$ in

April and 0.74 ± 0.27 μg g^{-1} in November. The selenium concentration associated with particles for the model were 0.35 ± 0.16 μg g^{-1} in April and 0.64 ± 0.19 μg g^{-1} in November, which both fall within the errors of the observed values. Model-generated particle associated selenium may be lower in April than the observed data since the model was over predicting TSM.

3.5. CONCLUSIONS

The equations used in Chapter I were able to simulate the variability of salinity, TSM, and phytoplankton biomass within the estuary. Furthermore, the calibration of the model to the dissolved and particulate selenium concentrations under high (April) and low (November) flow conditions was successful; the full set of optimized parameters are in Table 9. Some of the discrepancies that were found between the simulation and the observed data can be explained by: (1) simulations were run for the day of interest at midnight, while it takes 2 days to collect samples (averaging problem); (2) localized effects were not included (e.g., wind forcing); (3) negative discharge flows for the San Joaquin (i.e., Delta withdrawals greater than actual flow rates) were ignored; (5) large errors in the observed data; and (6) data missing along the salinity gradient (e.g., the month of May where there were only 7 stations for salinity, TSM, and phytoplankton concentrations). With successful calibration, the model can be validated to other environmental conditions (Chapter IV).

CHAPTER IV

MODEL VALIDATION AND PREDICTIVE MODELING

4.1. INTRODUCTION

The underlying principle in validating, or verifying, a model is to test if the calibrated model can simulate the observed behavior of a constituent for years other than that used for calibration (Schlesinger et al., 1979; Klemes, 1986). Model validation involves keeping the parameters used to calibrate the model unchanged, while applying the model to different sets of environmental conditions to determine its accuracy (Canale et al., 1995). A model is "truly" validated when model simulations match the observations (Canale et al., 1995). Often model validation is impossible to accomplish because independent sets of data are not available (Canale et al., 1995). When a sufficient set of data is available, the data can be split and a subset used to validate the model (Omlin et al., 2001). Splitting the observed data is known as predictive validation (Power, 1993) and is useful when the objective of the model is to be able to predict future scenarios. In the San Francisco Bay, dissolved and particulate selenium samples have been measured in 1986, 1987, 1988, 1997, 1998, and 1999. The dissolved and particulate data were split so that calibration of the model was done on data from 1999 (Chapter III), and validation of the model was done using the other data.

Not only are more field data needed in order to validate a model, but the field data must also represent a variety of environmental conditions (Canale et al., 1995). Based on river discharge from the Delta into the Bay, 1986, 1997, and 1998 were wet years

(summer discharge was greater than 400 $m^3 s^{-1}$), 1987 was dry (summer discharge was greater than 120 $m^3 s^{-1}$ but less than 200 $m^3 s^{-1}$), and 1988 was a drought year (summer discharge was less than 120 $m^3 s^{-1}$). Thus, a variety of discharge conditions are available for proper validation. Furthermore, from 1986 to 1998 there have been a change in the selenium speciation and discharge rate from the refineries (predominately selenite in 1986 and selenate in 1998, 1999; Appendix A). Changes in the biological structure of the system have also occurred due to the introduction of the filter-feeding bivalve *Potomocorbula amurensis* (Cloern and Alpine, 1991). Prior to 1986, the main control on phytoplankton populations was zooplankton grazing (Cloern et al., 1985). Cloern and Alpine (1991) proposed that prior to 1987, even with the presence of the native clam *Mya arenaria*, the benthic grazing had little effect on the phytoplankton biomass. Because the observed data were collected under a variety of environmental conditions, predictive validation of the model can be done. Once the model is validated, it can be used to make predictions about the future state of selenium in the Northern Reach of the San Francisco Bay.

4.2. METHODS

For validating the model, river discharge for each simulation was obtained from the Interagency Ecological Program (www.iep.ca.gov), as discussed in Chapter I. Refinery discharge rates were obtained from the San Francisco Bay Regional Water Quality Control Board (personal communication), while the speciation data were obtained from Cutter (1989b) and Cutter and Cutter (in prep.; see Appendix A for the daily

refinery fluxes into the Bay). For the simulation in 1986, the benthic grazing term was negligible based on observations by Cloern and Alpine (1991). Other than these changes, the rest of the parameters defined in Table 9 were used.

In model calibration discussion (Chapter III), the linear correlation coefficient, mean cumulative error, observed and simulated estuarine mean, and the confidence interval were computed (see Section 3.2.3 for background information). In brief, the best fit is when the linear correlation coefficient is significant at the $r_{0.05}$ level (95 % confidence), the mean cumulative error is low and the confidence interval is 75% or greater, and the estuarine averages agree. However, if the correlation coefficient is insignificant at the $r_{0.05}$, a reasonable fit can still exist if the other conditions are met. When the statistical parameters demonstrate that the model was able to reproduce the observed data for a majority of the years simulated, then model validation was considered successful.

4.3. VALIDATION RESULTS AND DISCUSSION

The observed data for dissolved selenium were collected using two different sampling techniques. Data collected in 1986, 1997, 1998 followed the salinity gradient so that integrated biogeochemical processes could be observed. For these samples, salinity, TSM, chlorophyll-a, and dissolved and particulate selenium samples were taken. However, in 1987 and 1988 samples were obtained using an Eulerian approach and stations were at fixed locations in the San Pablo to Suisun Bays (Cutter and San Diego-McGlone, 1990). These stations were specifically sited to maximize selenium "signals"

from refinery inputs to the Bay (Cutter and San Diego-McGlone, 1990). Furthermore, there were no TSM, chlorophyll-a concentrations, or particulate selenium samples taken. Another potential problem with the 1987-1988 data is that there were no end member samples (both river and seaward). Even though these problems in the 1987-1988 data exist, model simulations were run for all years data were collected.

In order to present an in-depth discussion on model-derived selenium concentrations, the selenium results will be split according to the sampling strategy used. The first discussion will focus on data from the salinity gradient sampling. To simplify the presentation of results, only 1998 simulations will be shown: the remaining validation data are in Appendix C. This year was chosen because dissolved and particulate selenium speciation data were available for high flow and low flow months. The second discussion will focus on model-simulated dissolved selenium concentrations for May 1988 when samples were taken using the Eulerian approach. This month was chosen over those in 1987 because it represents an extreme flow condition (a drought year). Model-derived simulations for all of the Eulerian samplings are located in Appendix C.

4.3.1. Salinity, TSM and Phytoplankton Validations

The salinity, phytoplankton, and TSM data for 1998 were obtained from Cutter and Cutter (in prep.) and Doblin et al. (in prep.). The observed salinity varied from zero at the riverine end member to 33 at the Golden Gate (Fig. 34). Model-derived salinity profiles were able to accurately reproduce the estuarine salinity distributions (Fig. 34). The correlation coefficient in June 1998 was 0.974 and 0.960 in October 1998, which are

significant at the $r_{0.01}$ confidence level. For both months, the mean cumulative errors indicate that the model is over predicting salinity (M = +0.13 nmol L^{-1} June and M = +0.08 nmol L^{-1} October), however the confidence interval is 80% (June) and 86% (October). The estuarine average salinity was not used in determining the fit of the model because it has large errors. Table 12 shows that the model was valid for salinity in all years simulated. As a result, all remaining figures will be plotted against salinity so that removal/production processes can be seen.

Table 12
Summary of validation results for all years for salinity simulations

Year	Correlation Coefficient	$r_{0.01}$	M*	Confidence Interval (%)
April 23, 1986	0.966	0.623	-0.07	92
September 23, 1986	0.995	0.561	+0.06	95
October 8, 1987	0.979	0.661	-0.08	96
December 7, 1987	0.894	0.623	-2.77	79
March 15, 1998	0.952	0.606	-0.27	80
May 11, 1998	0.979	0.590	+0.35	97
November 6, 1997	0.984	0.449	-0.83	86
June 12, 1998	0.974	0.590	+0.13	80
October 12, 1998	0.960	0.537	+0.08	86

* a (-) sign indicates model was under predicting relative to the observed, while a "+" sign indicates model was over predicting

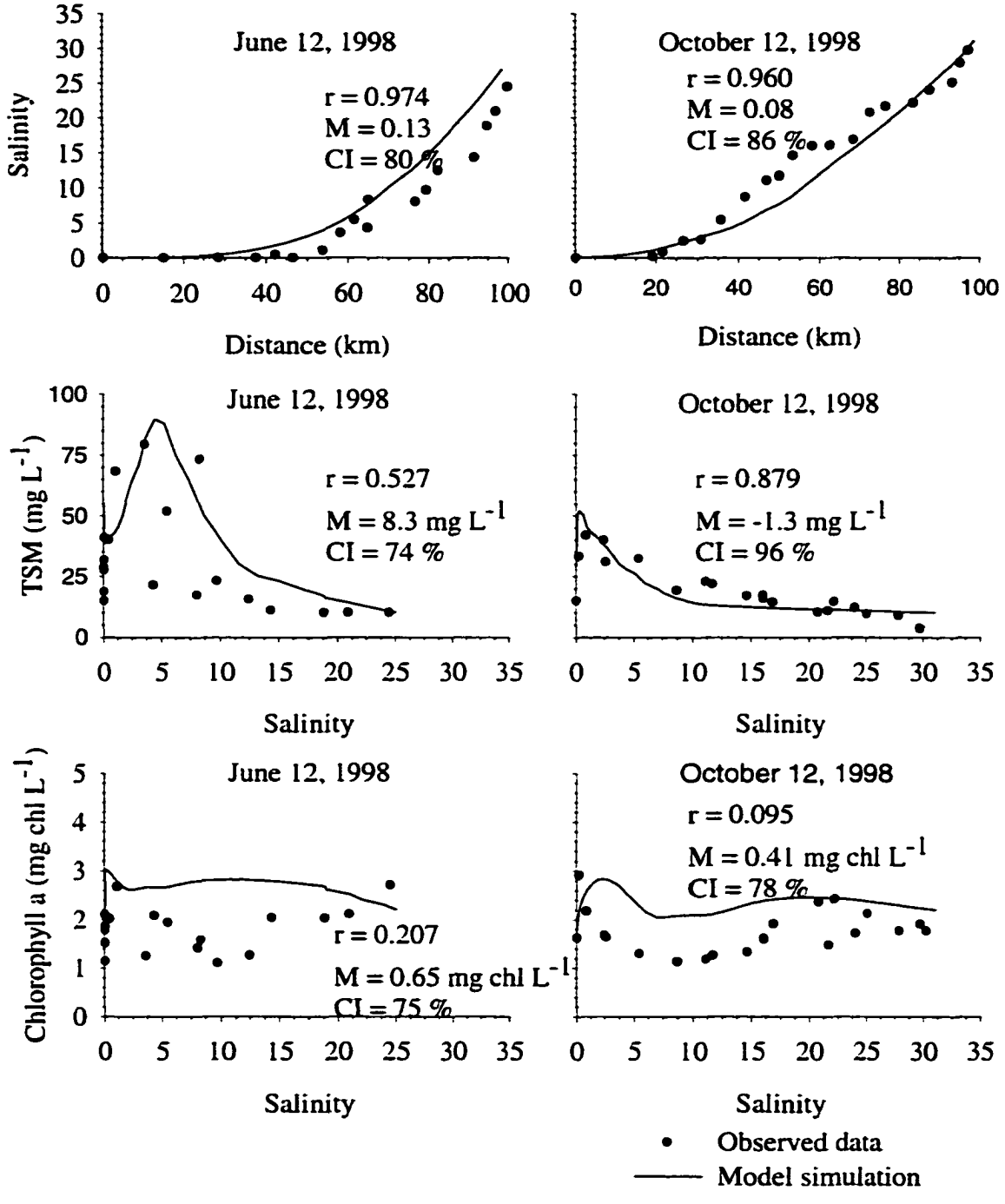

Fig. 34. Salinity, TSM, and phytoplankton biomass in the Northern Reach for June 14, 1998 and October 12, 1998. Observed data for salinity are from Cutter and Cutter (in prep.), with observed TSM and chlorophyll-a concentrations from Doblin et al. (in prep.).

The observed TSM showed a maxima in the upper reaches of the estuary, and model simulations reproduced these maxima (Fig. 34). The correlation coefficient in June was 0.527 while in October it was 0.879, which are significant at the $r_{0.05}$ level. Model-generated estuarine average TSM's were 47 ± 21 mg L^{-1} in April and 20 ± 14 mg L^{-1} in October and agree with observed estuarine averages (32 ± 20 mg L^{-1} in April and 19 ± 11 mg L^{-1} in October; Table 13).

Table 13
Summary of validation results for all years of TSM simulations

	Correlation coefficient	$r_{0.05}$	M* (mg L^{-1})	CI (%)	Observed Average (mg L^{-1})	Model Average (mg L^{-1})
April 23, 1986	0.678	0.497	+2.8	93	40 ±14	43 ±25
September 23, 1986	0.626	0.456	-3.5	86	29 ± 16	32 ±13
November 6, 1997	0.589	0.433	+1.1	96	13 ± 6	14 ± 2
June 12, 1998	0.527	0.468	+8.3	74	32 ± 20	47 ± 21
October 12, 1998	0.879	0.788	-1.3	96	19± 11	20 ±14

* a (-) sign indicates model was under predicting relative to the observed, while a "+" sign indicates model was over predicting

The model under predicted in October by -1.3 mg L^{-1}, which results in a confidence interval of 96%, while in June it over predicts by +8.3 mg L^{-1} and the confidence interval in June of 1998 was 74%. Even though the confidence interval in June was lower than 75%, since the estuarine averages agree and the correlation coefficient is significant, the ability of the model to accurately predict TSM for this month is considered reasonable.

Model-derived TSM were similar to the observed TSM for all the years that data were collected (Table 13), and model validation for TSM is complete.

Phytoplankton chlorophyll-a concentrations in 1998 showed higher concentrations in the upper estuary (Fig. 34). The correlation coefficient was low for both June (r=0.207) and October (r =0.095) and were not significant. However, the mean cumulative errors were low (+0.65 μg chl L^{-1} in June and +0.41 μg chl L^{-1} in October) and the resulting confidence intervals were 75% (June) and 78% (October). Furthermore, model-derived estuarine averages (3.2 ± 0.3 μg chl L^{-1} for June and 2.8 ± 0.3 μg chl L^{-1} for October) were similar to observed averages in both June and October (2.6 ± 0.8 μg chl L^{-1} for June and 2.4 ± 0.3 μg chl L^{-1}, respectively; Table 14).

Table 14
Summary of validation results for all years of phytoplankton simulations

	Correlation coefficient	$r_{0.05}$	M* (μg chl L^{-1})	CI (%)	Observed Average (μg chl L^{-1})	Model Average (μg chl L^{-1})
April 23, 1986	0.789	0.497	+0.97	84	7.3 ±1.4	8.0 ± 2.7
September 23, 1986	0.635	0.456	+0.71	79	3.9 ± 1.7	4.3 ±1.3
November 6, 1997	0.469	0.433	-0.24	81	1.4 ± 0.5	1.3 ± 0.4
June 12, 1998	0.207	0.468	+0.65	75	2.6 ± 0.8	3.2 ± 0.3
October 12, 1998	0.095	0.788	+0.41	78	2.4 ± 0.3	2.8 ± 0.3

*a (-) sign indicates model was under predicting relative to the observed, while a "+" sign indicates model was over predicting

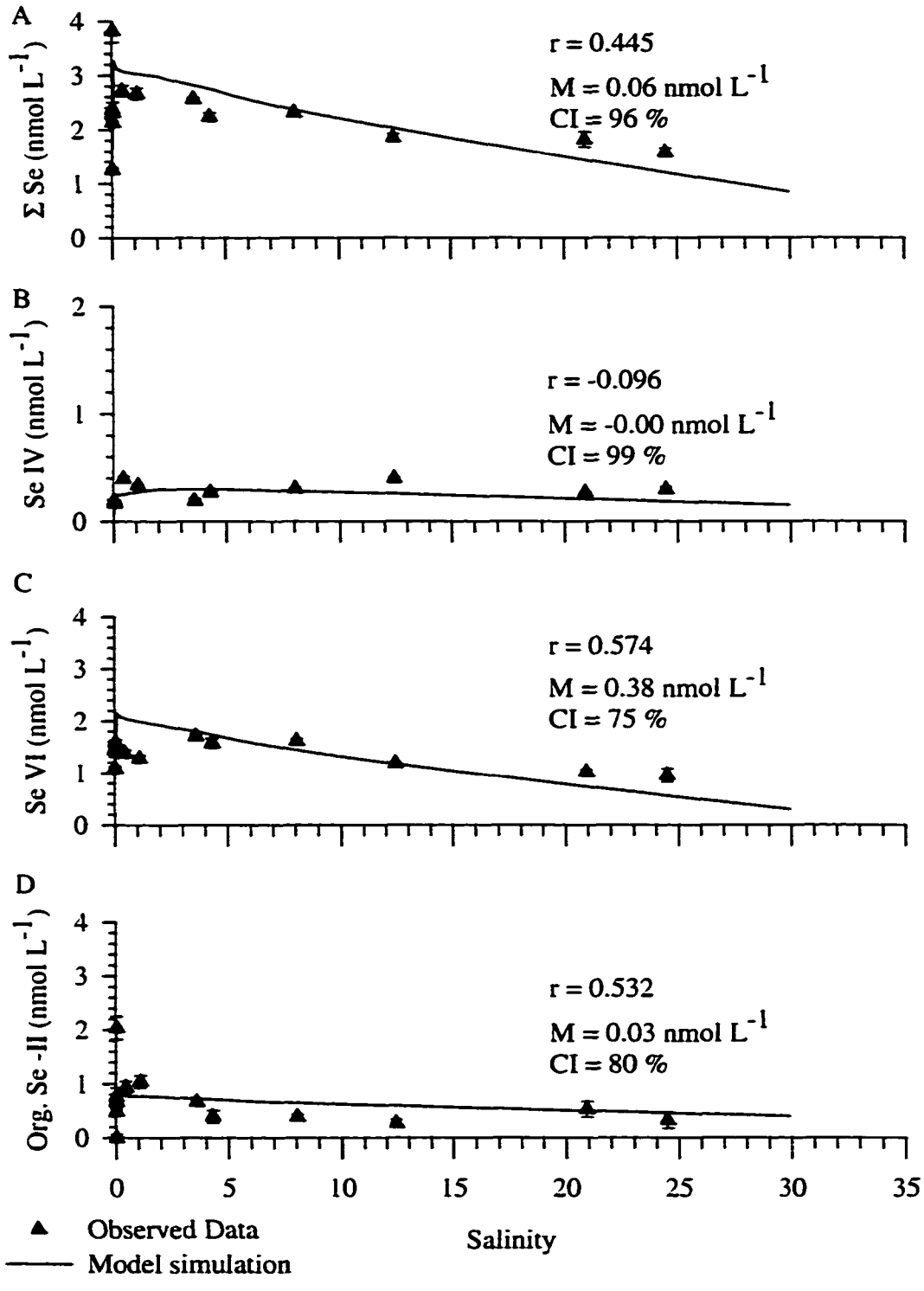

Fig. 35. Dissolved selenium for the Northern Reach on June 14, 1998. Observed data were obstained from Cutter and Cutter (in prep.).

Model-generated phytoplankton concentrations were similar to the observed data for all years simulated (Table 14), and thus the calibrated model was able to simulate chlorophyll-a concentrations for different environmental conditions.

4.3.2. Dissolved Selenium Validations: Salinity Gradient Sampling

Total dissolved selenium in the estuary during 1998 was conservative in June (Fig. 35A) and non-conservative in October (Fig. 36A). Model simulations were able to reproduce the conservative and non-conservative behavior of total selenium for both months (Fig. 35A and Fig. 36A). In June the correlation coefficient was 0.445, while in October it was 0.613. The correlation coefficient was not significant for June, but it may be due to an outlier (e.g. 3.9 nmol L^{-1} at the fresh water end member; Fig. 36A). Model-generated total selenium concentrations plotted against observed concentrations (Fig. 37) supports the interpretation that the observed value of 3.9 nmol L^{-1} may be an outlier. If this data point is then omitted, the correlation coefficient increases to 0.788, which is significant at the $r_{0.05}$ level. The confidence interval for June was 96% (M was over predicting by +0.06 nmol L^{-1}) and the model-simulated estuarine average (2.29 ± 0.74 nmol L^{-1}) agreed with observed averages (2.28 ± 0.64 nmol L^{-1}), showing that the model was able to simulate total dissolved selenium in June. The correlation coefficient for October (0.613) was above the $r_{0.05}$ significance level, and while model-generated total dissolved selenium concentrations were lower than the observed concentrations (M = -0.11 nmol L^{-1}), the confidence interval was 93%. Observed estuarine averages (1.50 ± 0.30 nmol L^{-1}) are

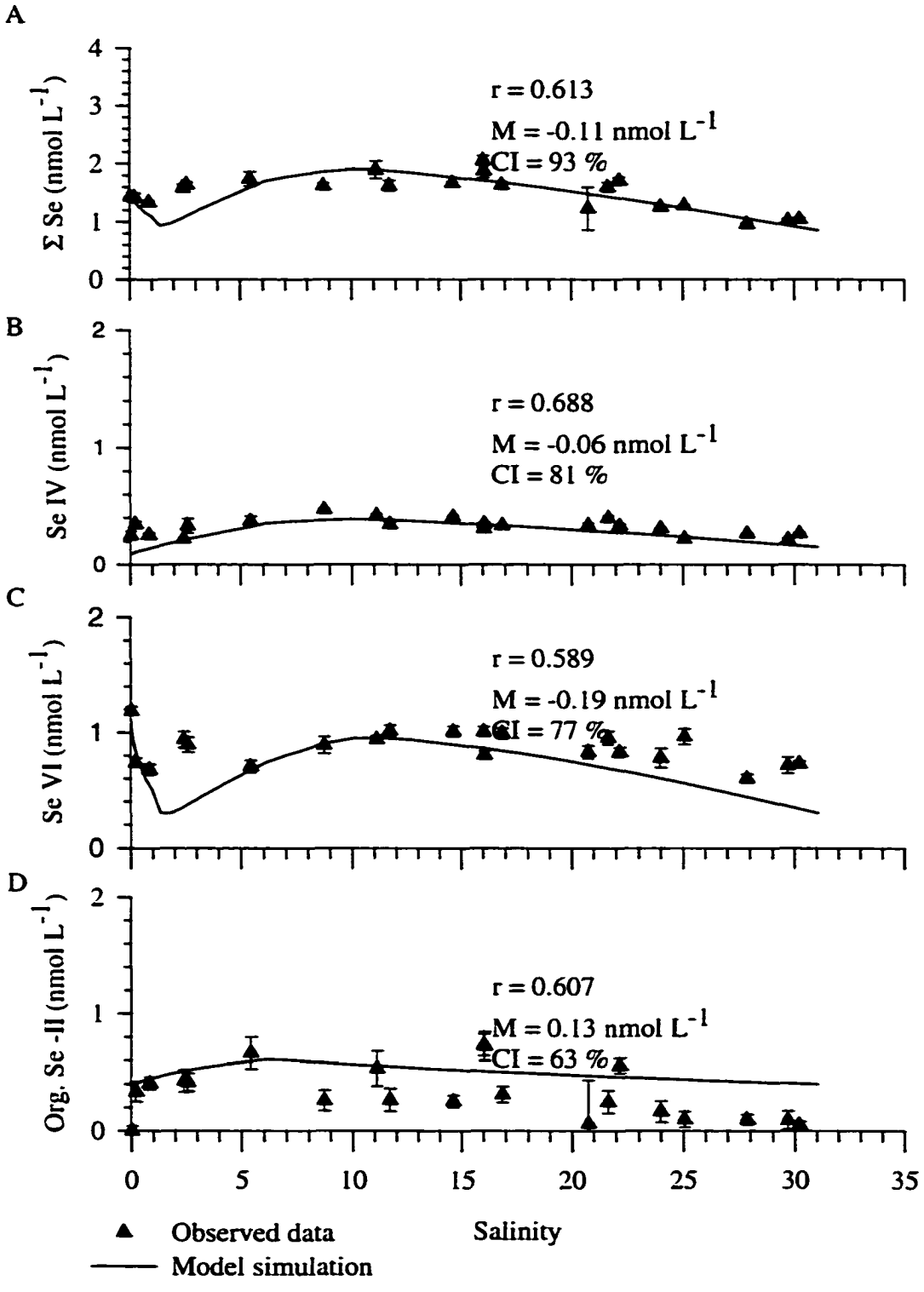

Fig. 36. Dissolved selenium in the Northern Reach on October 12, 1998. Observed data were obtained from Cutter and Cutter (in prep.).

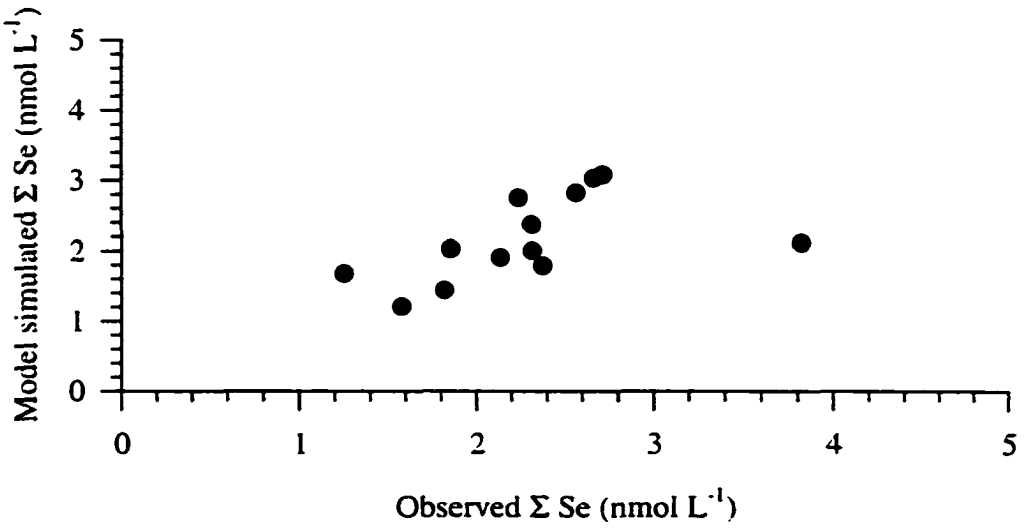

Fig. 37. Plot of model-derived total selenium and observed total selenium. The possibility of an outlier can be seen at an observed total selenium concentration of 3.9 nmol L^{-1}.

similar to the model-derived average (1.33 ± 0.48 nmol L^{-1}). Therefore, for 1998 model validation for total dissolved selenium was accomplished. Table 15 shows that the model was able to accurately predict total dissolved selenium in the estuary for all cruises that followed the salinity gradient, and thus the model is valid for total dissolved selenium.

Table 15
Model validation of dissolved selenium and its speciation for samples that were taken following a salinity gradient

	Correlation coefficient	$r_{0.05}$	M* (nmol L^{-1})	CI (%)	Observed Average (nmol L^{-1})	Model Average (nmol L^{-1})
April 23, 1986						
Total selenium	0.791	0.497	-0.18	91	2.17 ± 0.61	2.05 ± 0.60
Selenite	0.902	0.497	-0.02	95	0.40 ± 0.13	0.36 ± 0.15
Selenate	0.832	0.497	-0.25	76	1.18 ± 0.60	1.16 ± 0.48
Organic selenide	0.319	0.553	-0.05	92	0.59 ± 0.33	0.55 ± 0.10
September 23, 1986	0.882	0.444	-0.16	92	2.17 ± 0.52	1.98 ± 0.53
Total selenium	0.946	0.444	-0.13	85	0.78 ± 0.40	0.69 ± 0.35
Selenite	0.296	0.444	-0.06	91	0.77 ± 0.23	0.75 ± 0.23
Selenate	0.576	0.456	-0.02	96	0.62 ± 0.13	0.54 ± 0.10
Organic selenide						
November 6, 1997						
Total selenium	0.550	0.482	-0.22	91	2.43 ± 0.63	2.13 ± 0.66
Selenite	0.551	0.468	-0.08	87	0.54 ± 0.24	0.45 ± 0.22
Selenate	0.622	0.456	-0.48	63	1.28 ± 0.44	0.79 ± 0.25
Organic selenide	0.525	0.468	+0.25	60	0.63 ± 0.47	0.89 ± 0.39
June 12, 1998						
Total selenium	0.445	0.553	+0.06	96	2.28 ± 0.64	2.29 ± 0.74
Selenite	-0.096	0.553	-0.00	99	0.26 ± 0.08	0.23 ± 0.07
Selenate	0.574	0.553	+0.38	75	1.36 ± 0.24	1.44 ± 0.55
Organic selenide	0.532	0.576	+0.03	80	0.65 ± 0.50	0.63 ± 0.15
October 12, 1998						
Total selenium	0.613	0.433	-0.11	93	1.50 ± 0.30	1.33 ± 0.48
Selenite	0.688	0.433	-0.06	81	0.32 ± 0.07	0.25 ± 0.09
Selenate	0.589	0.433	-0.19	77	0.87 ± 0.14	0.56 ± 0.27
Organic selenide	0.607	0.433	+0.13	63	0.34 ± 0.26	0.51 ± 0.12

* a (-) sign indicates model was under predicting relative to the observed, while a "+" sign indicates model was over predicting

Selenite concentrations in the estuarine ranged from 0.2 nmol L^{-1} to 0.5 nmol L^{-1} and were non-conservative (Fig. 35B and Fig. 36B). The model was able to predict the non-conservative behavior of selenite (Fig. 35B to Fig. 36B). As indicated earlier, the correlation coefficient sometimes is not a good indicator of fit due to little variation in the observed data or the presence of outliers. In June 1998, the correlation coefficient was -0.096 (Fig. 35B), which is not significant. Nevertheless, the mean cumulative error was 0.00 nmol L^{-1} and the confidence interval was 99%, indicating a fit between the model and field data. Furthermore, the model-generated estuarine average (0.23 ± 0.07 nmol L^{-1}) is very similar to the observed estuarine average (0.26 ± 0.08 nmol L^{-1}), thus confirming that the model was able to simulate selenite for June. The correlation coefficient (0.688) in October was significant at the $r_{0.05}$ level. The model under predicted selenite by -0.06 nmol L^{-1}, but the model could predict 81% of the observed selenite. Observed estuarine means (0.32 ± 0.07 nmol L^{-1}) and simulated means (0.25 ± 0.09 nmol L^{-1}) agreed with each other as more evidence that the model was able to predict selenite concentrations. Additionally model-derived selenite concentrations agreed with the observed data for 1986, 1997, and 1998 (Table 15) further showing that the model could simulate selenite estuarine profiles for other years, confirming model validation for selenite.

Observed selenate concentration varied from 1.0 nmol L^{-1} to a maximum of 2.0 nmol L^{-1} (Fig. 35C and Fig. 36C). Selenate was conservative in June 1998 (Fig. 35C) and non-conservative in October 1998 (Fig. 36C). Estuarine simulated profiles produced the observed conservative (June, Fig. 35C) and non-conservative behavior (October, Fig.

36C). The correlation coefficient in June was 0.574, while in October it was 0.589 (Fig. 35C and Fig. 36C) and both are significant at the $r_{0.05}$ level. Model-predicted selenate concentrations may appear high in June (M =+0.38 nmol L^{-1}), but normalized to the mean the model predicts 75% of the observed data. Selenate concentrations were lower than the observed values (M =-0.19 nmol L^{-1}) for October, but the confidence interval was 77%. To further support validation of selenate, the observed estuarine averages (1.36 ± 0.24 nmol L^{-1} for June and 0.87 ± 0.14 nmol L^{-1} for October) agree with the model-derived averages (1.44 ± 0.55 nmol L^{-1} in June and 0.56 ± 0.27 nmol L^{-1} in October; Table 15). The statistical analysis of model-derived concentrations versus observed concentrations, show that the model can predict the observed selenate behavior for all periods (Table 15). Therefore, the model was able to predict the observed behavior of selenate under a variety of environmental conditions.

The dissolved organic selenide estuarine average was greater in June (0.65 ± 0.50 nmol L^{-1}) than that in October (0.34 ± 0.26 nmol L^{-1}). Dissolved organic selenide concentrations varied from non-detectable to approximately 2.0 nmol L^{-1} and displayed non-conservative behavior in the estuary, which the model was able to simulate (Fig. 35D through Fig. 36D). Simulated estuarine averages were 0.63 ± 0.15 nmol L^{-1} (June) and 0.51 ± 0.12 nmol L^{-1} (October), which are within the errors of the observed means. For both months, the model was over predicting organic selenide (M = +0.03 nmol L^{-1} for June and M = +0.13 nmol L^{-1} for October), but had confidence intervals of 80% (June) and 63% (October). Even though the confidence interval in October is slightly lower than normally observed, the correlation coefficient is high (0.607) and is significant at the $r_{0.05}$

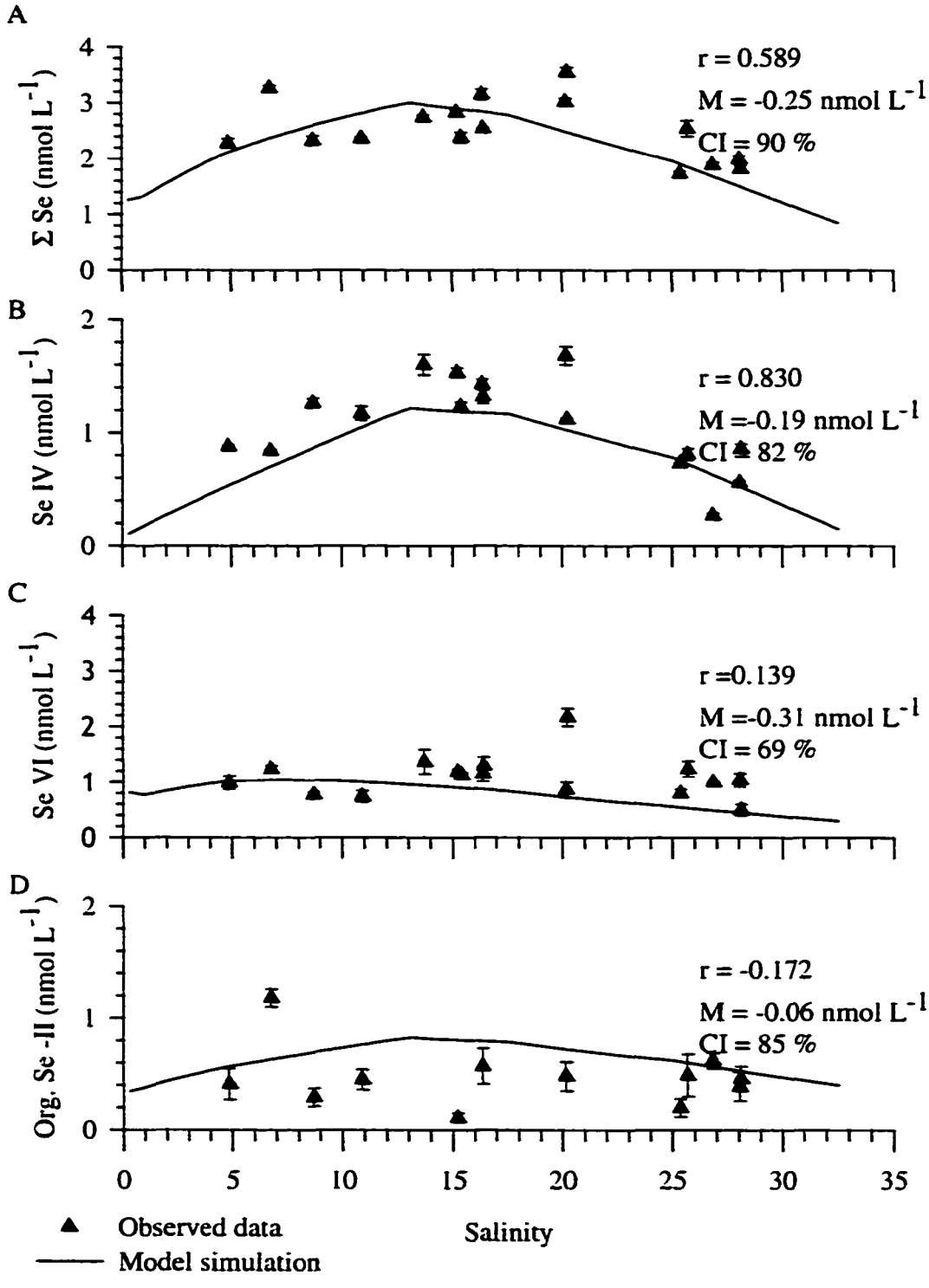

Fig. 38. Dissolved selenium in the Northern Reach on May 11, 1998. The observed data were from Cutter and San Diego-McGlone (1990).

level. For June, the correlation coefficient was 0.532, which is slightly lower than the $r_{0.05}$ criteria needed to state that the correlation is significant. However, the other statistical parameters indicate that the model-predicted concentrations were similar to the observed data. Not only was the model able to predict dissolved organic selenide for 1998, but it was also able to predict it for 1986 and 1997 (Table 15 and Appendix C). Therefore, the model was also able to simulate the observed organic selenide concentrations under a variety of environmental conditions.

4.3.3. Eulerian Validations

As discussed above, the samples from 1987 and 1988 were Eulerian measurements. Table 12 shows that the model was able to simulate the salinity for these years (also see Appendix C). Even though the model could accurately simulate salinity for this time period, it may be more difficult to simulate dissolved selenium since the stations were positioned to highlight the effects of refinery outputs (Cutter and San-Diego McGlone, 1990). May 11, 1998 will be used to compare model output to the observed data for Eulerian selenium samples, with the other simulations found in Appendix C and a summary of their results in Table 16.

The input from the refineries was the mean concentration as determined by Cutter (1989b) and Cutter and Cutter (in prep.). The variability of selenium discharge from the refineries was quite large. For example, in 1988 the total dissolved selenium discharged from Shell was 972 ± 557 nmol L^{-1} (Cutter, 1989b). For the May 1988 validation (Fig. 38), the mean concentrations for each species in refinery discharge were used, but the

Table 16
Model validation of dissolved selenium and its speciation for Eularian samples

	Correlation coefficient	$r_{0.05}$	M^* (nmol L^{-1})	CI (%)	Observed Average (nmol L^{-1})	Model Average (nmol L^{-1})
October 8, 1987						
Total selenium	0.568	0.514	-0.12	96	2.76 ± 0.60	2.40 ± 0.66
Selenite	0.543	0.514	+0.06	95	1.16 ± 0.41	0.83 ± 0.33
Selenate	0.561	0.532	-0.35	72	1.25 ± 0.80	0.93 ± 0.23
Organic selenide	0.111	0.707	+0.01	98	0.67 ± 0.35	0.64 ± 0.16
December 17, 1987						
Total selenium	0.194	0.532	+0.22	90	2.24 ± 0.46	2.37 ± 0.63
Selenite	0.555	0.553	+0.03	94	0.98 ± 0.29	1.02 ± 0.40
Selenate	-0.078	0.532	-0.17	80	0.81 ± 0.34	0.73 ± 0.23
Organic Selenide	-0.066	0.632	+0.10	70	0.45 ± 0.23	0.62 ± 0.15
March 15, 1998						
Total selenium	0.991	0.497	+0.03	99	2.43 ± 0.57	2.24 ± 0.83
Selenite	0.890	0.497	+0.01	98	0.90 ± 0.34	0.78 ± 0.37
Selenate	0.497	0.497	-0.10	90	1.03 ± 0.36	0.93 ± 0.32
Organic Selenide	0.625	0.707	+0.09	80	0.50 ± 0.14	0.54 ± 0.16
May 11, 1998						
Total selenium	0.589	0.497	+0.06	97	2.64 ± 0.54	2.66 ± 0.64
Selenite	0.807	0.497	-0.11	89	1.08 ± 0.40	1.03 ± 0.35
Selenate	0.197	0.497	-0.13	87	1.09 ± 0.37	1.01 ± 0.24
Organic Selenide	0.110	0.707	+0.11	76	0.47 ± 0.27	0.61 ± 0.14

* a (-) sign indicates model was under predicting relative to the observed, while a "+" sign indicates model was over predicting

model could not successfully predict total dissolved selenium and its speciation (low correlation coefficient, low confidence interval). Specifically, the mean cumulative errors indicated that the model was under predicting the concentrations relative to the observed data (Fig. 38). According to the sensitivity results, river discharge and refinery inputs largely control the model output of dissolved selenium (Section 3.3). During this sampling period, the water input from the Sacramento River was low due to drought conditions (average discharge was 174 $m^3 s^{-1}$ in May) and thus the riverine inputs would be minor compared to the refinery inputs. Because the field sampling was designed to highlight/maximize the effects of refinery outputs, model simulations were run to examine what the predicted estuarine concentrations would be if the refinery concentrations of selenium were increased by 10% from the mean; this is well within the observed variability (Appendix A).

Increasing the concentration of selenium in the refinery effluent by only 10% resulted in a more accurate model simulations relative to the observed data. In May 1998 total dissolved selenium was non-conservative (Fig. 39A) and the model was able to simulate this behavior (Fig. 39A). The correlation coefficient was 0.589 for total dissolved selenium and it was significant at the $r_{0.05}$ level. The model over predicted total selenium (+0.06 nmol L^{-1}), which was low relative to the mean and thus the confidence interval was 97%. The observed estuarine average of total selenium in May was 2.64 ± 0.54 nmol L^{-1}, while the simulated estuarine average was well within the errors of the observed data (2.66 ± 0.64 nmol L^{-1}). Model-derived total dissolved selenium for the other Eulerian samples suggests that when the refinery fluxes were increased 10% above

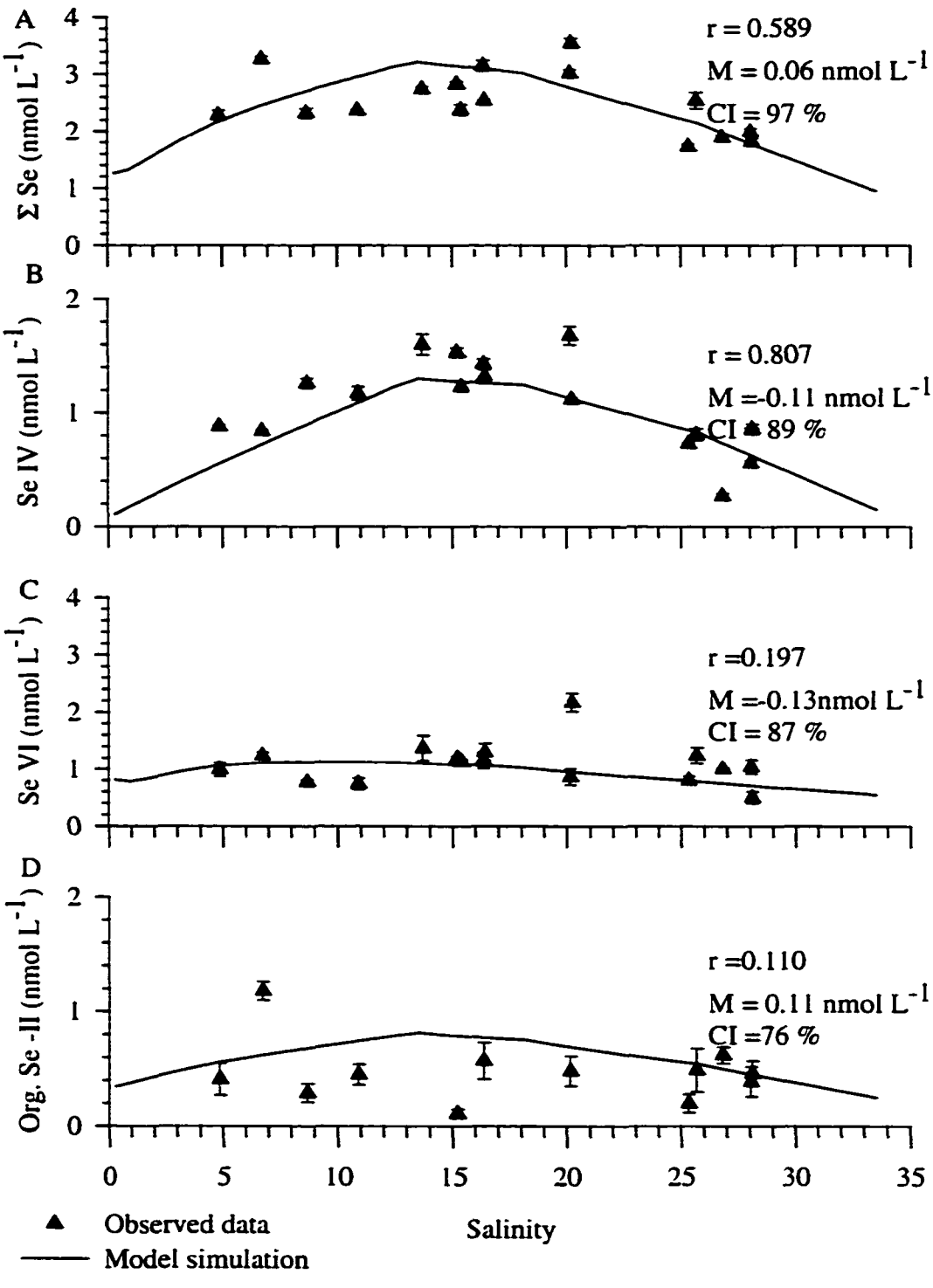

Fig. 39. Dissolved selenium in the Northern Reach on May 11, 1988 by increasing refinery input by 10%. Observed data were obtained from Cutter and San Diego-McGlone (1990).

their means the model could predict the observed behavior (Table 16).

Selenite was the dominant species in 1988 with a mid-estuary maximum (Fig. 39B). Again using the 10% increased refinery flux, model-generated selenite concentrations produced the non-conservative behavior of selenite (Fig. 39B). The correlation coefficient was 0.807, which was significant at the $r_{0.05}$ level. Furthermore, the mean cumulative error was -0.11 nmol L^{-1}, which results in a confidence interval of 89%. The simulated average selenite concentration in the estuary was 1.03 ± 0.35 nmol L^{-1}, and is similar to the observed mean (1.08 ± 0.40 nmol L^{-1}). Based on these statistical analyses the model was able to predict selenite in 1988. Table 16 shows that the model was also able to generate selenite concentrations that agreed with the observed data for the remaining 1987-1988 samplings.

The estuarine average selenate concentration was 1.09 ± 0.37 nmol L^{-1} and was non-conservative in the estuary (Fig. 39C). The linear correlation coefficient was low (0.197) and not significant at the $r_{0.05}$ level. This could be due to little variation in the observed data, and thus when the model-derived concentration is plotted against the observed data (Fig. 40) it was found that the model was not able to reproduce the variability observed in the real data. However, the confidence interval was 87% (M= -0.13 nmol L^{-1}) and the model-derived mean (1.01 ± 0.24 nmol L^{-1}) was similar to above average. The high confidence interval and agreement between the observed and simulated averages show that the model is able to simulate similar selenate concentrations observed in the estuarine when samples were collected using Eulerian methods s.

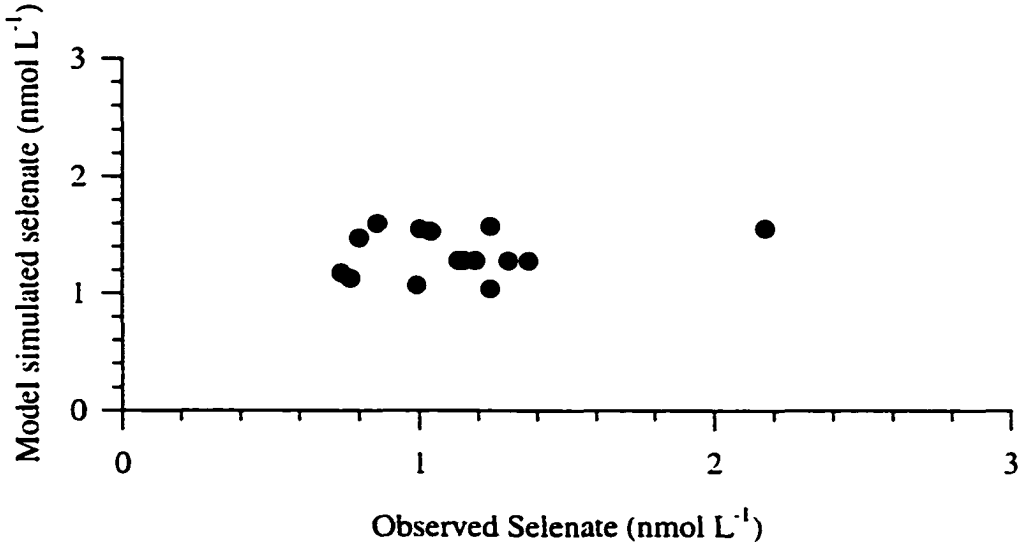

Fig. 40. Plot of model-derived selenate and observed selenate. The possibility of non-linear behavior could be due to little variation in the data.

Like inorganic selenium, dissolved organic selenide was non-conservative in the estuary in May 1988 (Fig. 39D). The observed estuarine average was 0.47 ± 0.27 nmol L^{-1}. Model-derived organic selenide concentrations had an estuarine average of 0.61 ± 0.14 nmol L^{-1}, which was similar to the observed average. The model was also able to simulate the non-conservative behavior of organic selenide (Fig. 39D), but the linear correlation was low (0.110) and non-significant. Due to the low mean cumulative error (+0.11nmol L^{-1}), which results in a 76% confidence interval, and the agreement between the means, a reasonable fit between model simulations and observed concentrations was found. For the other simulations (Table 16), the model was able to predict the observed organic selenide concentrations. In summary, the calibrated model was able to simulate concentrations similar to the observed data collected using an Eulerian approach, as well as for those samples taken following the salinity gradient.

4.3.4. Particulate Selenium Validations

Cutter (1989b) measured total particulate selenium concentrations in April and September of 1986, and Doblin et al. (in prep.) sampled in November 1997, June 1998, and October 1998. Doblin et al. (in prep.) also determined the speciation of particulate selenium in the water column. As with dissolved selenium, the discussion will focus only on the 1998 data since they represent both flow periods, and the model simulations for the other years can be found in Appendix C.

Total particulate selenium concentrations ranged from 0.1 nmol L^{-1} to 0.3 nmol

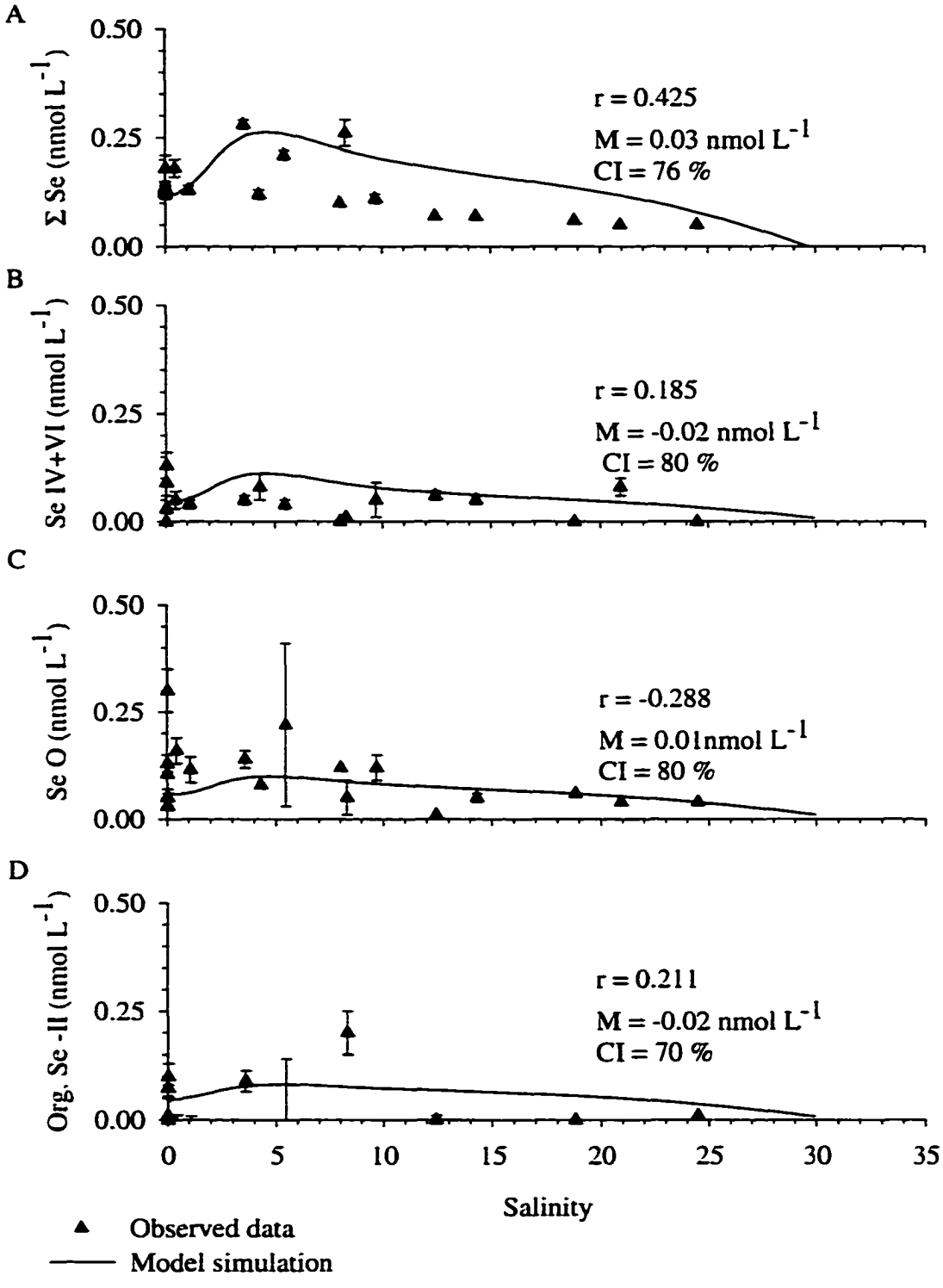

Fig. 41. Particulate selenium in the Northern Reach on June 14, 1998. Observed data were from Doblin et al., (in prep.).

L^{-1} (Fig. 41A and Fig. 42A). Total particulate selenium maxima were located in the upper estuary, corresponding to where the TSM maxima were located (Fig. 34). Model-derived total particulate selenium concentrations were able to reproduce the upper estuarine maxima (Fig. 41A through 42A). The linear correlation for October was significant (0.623) at the $r_{0.05}$ level, while the one in June was not (0.425). However, even though the correlation was low, the model was only slightly over predicting total particulate selenium (M =+ 0.03 nmol L^{-1}), the confidence interval was 76%, and the derived estuarine average of 0.19 ± 0.01 nmol L^{-1} was very similar to the observed average (0.13 ± 0.07 nmol L^{-1}). These statistical analyses show that the model was able to predict total dissolved selenium in June even though the correlation coefficient was low. For October, the model under predicted by -0.03 nmol L^{-1}, which results in a 78% confidence interval. The observed estuarine average concentration (0.13 ± 0.03 nmol L^{-1}) and the model-generated average (0.14 ± 0.06 nmol L^{-1}) were within errors of each other. Overall, the model was able to simulate total particulate selenium concentrations for this year and the other years (Table 17), and since the statistical requirements were met, the model was validated for total particulate selenium.

There was little variation in the estuarine profiles of particulate selenite + selenate (Fig. 41B through Fig. 42B) and concentrations ranged from non-detectable to 0.15 nmol L^{-1}. Observed estuarine averages were 0.08 ± 0.07 nmol L^{-1} in June and 0.04 ± 0.03 nmol L^{-1} in October. Simulated selenite + selenate concentrations profiles appear to be within the errors of the observed data (Fig. 40B to Fig. 41B). The linear correlation coefficients were 0.185 in June 1998 (Fig. 41B) and 0.152 in October 1998 (Fig. 42B).

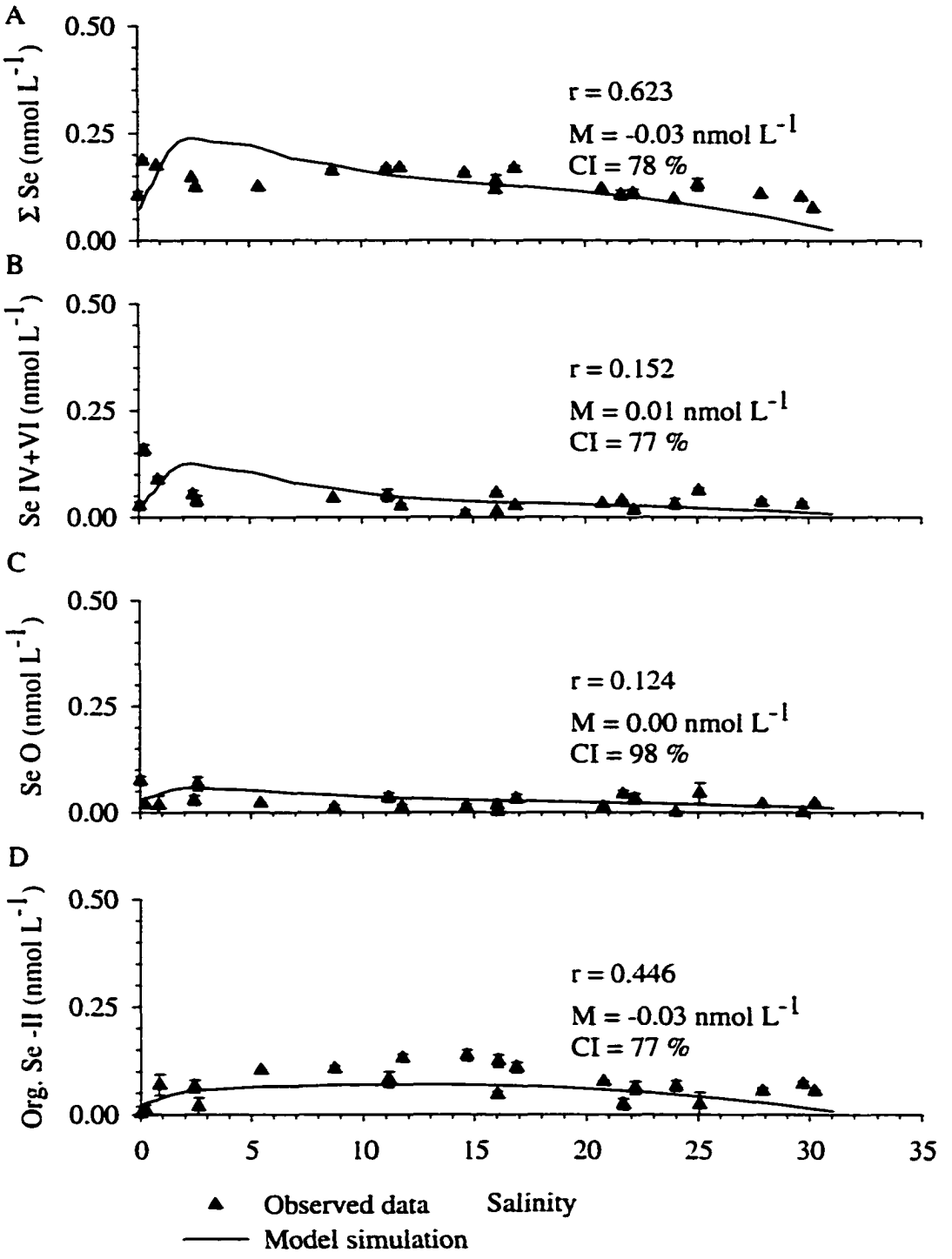

Fig. 42. Particulate selenium in the Northern Reach on October 12, 1998. Observed data were obtained from Doblin et al. (in prep.).

Table 17
Model validation of particulate selenium and its speciation for all sample periods

	Correlation coefficient	$r_{0.05}$	M* (nmol L^{-1})	CI (%)	Observed Average (nmol L^{-1})	Model Average (nmol L^{-1})
April 23, 1986						
Total selenium	0.742	0.514	+0.01	93	0.14 ± 0.06	0.19 ± 0.08
September 23, 1986	0.778	0.482	+0.03	84	0.24 ± 0.09	0.32 ± 0.13
Total selenium						
November 6, 1997						
Total selenium	0.439	0.433	+0.02	85	0.15 ± 0.04	0.16 ± 0.06
Selenite +	0.683	0.444	-0.01	82	0.05 ± 0.04	0.03 ± 0.01
Selenate	-0.261	0.433	-0.01	87	0.07 ± 0.11	0.07 ± 0.04
Elemental	-0.115	0.497	-0.01	83	0.04± 0.04	0.06 ± 0.02
Organic selenide						
June 12, 1998						
Total selenium	0.425	0.468	+0.03	76	0.13 ± 0.07	0.19 ± 0.01
Selenite +	0.185	0.482	-0.02	80	0.08 ± 0.07	0.07 ± 0.01
Selenate	-0.288	0.468	+0.01	80	0.04 ± 0.04	0.06 ± 0.01
Elemental	0.211	0.707	-0.02	70	0.02 ± 0.07	0.06 ± 0.01
Organic selenide						
October 12, 1998						
Total selenium	0.623	0.433	-0.03	78	0.13 ± 0.03	0.14 ± 0.06
Selenite +	0.152	0.456	+0.01	77	0.04 ± 0.03	0.04± 0.01
Selenate	0.124	0.433	+0.00	98	0.02 ± 0.02	0.06 ± 0.01
Elemental	0.446	0.444	-0.01	77	0.06 ± 0.04	0.05 ± 0.01
Organic selenide						

* a (-) sign indicates model was under predicting relative to the observed, while a "+" sign indicates model was over predicting

The low correlation coefficient could be due to invariance of the data. Model-derived concentrations of particulate selenite+selenate were plotted against observed concentrations for October. As Fig. 43 shows the observed data clustered around

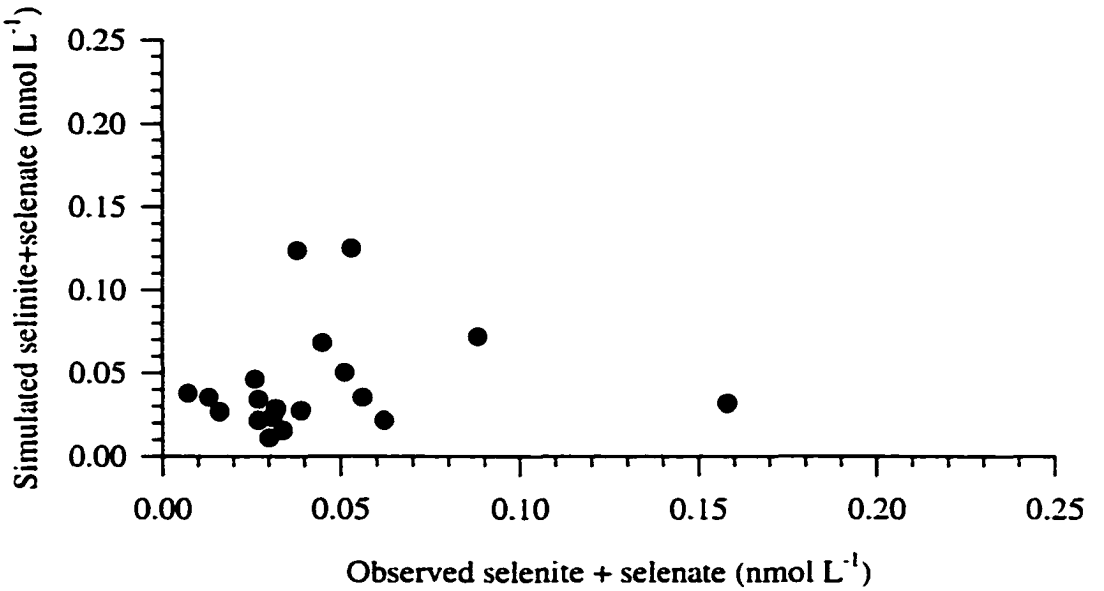

Fig. 43. Plot of model-derived particulate selenite + selenate and observed particulate selenite+selenate. The possibility of non-linearity could be due to little variation in the data.

0.04 nmol L^{-1} and there appears to be outliers in the data (e.g., 15 nmol L^{-1}). Therefore, the low correlation coefficient is probably due to invariance of particulate selenite+selenate and outliers. Even though the correlation coefficients were low, the model was only slightly under predicting in June (-0.02 nmol L^{-1}) and over predicting in October (+0.01 nmol L^{-1}). These result in a confidence interval of 80% (June; Fig. 41B) and 77% (November; Fig. 42B). The June model-simulated average was 0.07 ± 0.01

nmol L^{-1}, while the October simulated average was 0.04 ± 0.01 nmol L^{-1}. Therefore, the statistical parameters confirm the visual observation that the model was able to simulate particulate selenite + selenate. The model was also able to simulate the observed behavior for the other years (Table 17 and Appendix C) and can be used to predict particulate selenite + selenate.

Observed particulate elemental selenium concentrations were low in the San Francisco Bay and ranged from non-detectable to 0.25 nmol L^{-1} (Fig. 41B through Fig 42B), with higher concentrations located in the upper estuary. Model-derived concentrations of elemental selenium had an estuarine distribution similar to the observed data for June 1998 (Fig. 41C), and October 1998 (Fig. 42C). The linear correlation coefficient was low for both months (-0.288 in June and 0.124 in October). However, the confidence interval 80% in June and 98% for October 1998 (Fig. 41C and Fig. 42C) demonstrates that the model was able to predict elemental selenium for these months. The mean cumulative error was +0.01 nmol L^{-1} for June and 0.00 nmol L^{-1} for October. The observed estuarine average was 0.04 ± 0.04 nmol L^{-1} (June) and 0.02 ± 0.02 nmol L^{-1} (October) and the model-generated means agreed at 0.06 ± 0.01 nmol L^{-1} for June and 0.06 ± 0.01 nmol L^{-1} for October. The model was able to predict elemental selenium for all of the simulated runs (Table 17) and was valid under different environmental conditions.

An observed mid-estuary maximum of particulate organic selenide was detected in samples taken in October 1998 (Fig. 42D). Organic selenide concentrations ranged from non-detectable to 0.2 nmol L^{-1} (Fig. 41D through Fig. 42D) with an average

estuarine concentration of 0.06 ± 0.04 nmol L^{-1} for October and 0.02 ± 0.07 nmol L^{-1} for June (Table 17). The correlation coefficient in June was low (r = 0.211). Model-generated organic selenide concentrations were lower than observed concentrations (M =- 0.02 nmol L^{-1}), which resulted in a confidence interval of 70%. The simulated mean (0.06 ± 0.01 nmol L^{-1}) was similar to the observed mean. It may appear that the model was not able to simulate organic selenide well for June, but since only five of the eighteen samples in June 1998 had any detectable particulate organic selenide, the fit is reasonable. The correlation coefficient in October was 0.446 and significant at the $r_{0.05}$ level. Furthermore, the model-computed estuarine average was 0.05 ± 0.01 nmol L^{-1} (Table 17) and is essentially identical to the observed estuarine average (0.06 ± 0.04 nmol L^{-1}). The mean cumulative error indicates that the model was under predicting particulate organic selenide (M = -0.01 nmol L^{-1} in October 1998), which results in a confidence interval of 77%. Thus, the model was able to predict particulate organic selenide for these two months and other simulations successfully (Table 17), showing that the calibrated model can be used to predict particulate organic selenide.

As discussed in Section 3.4.5, the concentration of selenium associated with particles is a better indicator of the availability of particulate selenium to higher trophic levels (Luoma and Presser, 2000). Using the model-derived TSM and the total particulate selenium concentrations, the amount of selenium associated with particles in the water column was calculated (see Section 3.4.5). The model-derived concentration of selenium associated with particles was 0.30 μg g^{-1} ± 0.15 μg g^{-1} (June) and 0.55 ± 0.18 μg g^{-1} (October, Table 18). In comparison, observed particle-associated selenium were 0.49 ±

0.32 μg g^{-1} for June and 0.63 ± 0.24 μg g^{-1} for October (Table 18).

Table 18
Total selenium associated with particles in the water column

Year	Part. Σ Se (μg g^{-1})
April 1986	
Model	0.35 ± 0.18
Observed	0.41± 0.17
Sept 1986	
Model	0.79± 0.17
Observed	0.74 ± 0.24
Nov 1997	
Model	0.90 ± 0.10
Observed	0.85 ± 0.29
June 1998	
Model	0.30 ± 0.15
Observed	0.49 ± 0.32
Oct 1998	
Model	0.55 ± 0.18
Observed	0.63 ± 0.24

For all sampling periods, the model-derived particulate selenium concentrations were similar to the observed values (Table 18). Higher values were observed in the fall than the spring, but none of the estuarine averages were greater than 1 μg g^{-1}, which has been known to cause elevated selenium concentrations in clams (Luoma et al., 1992).

4.4. PREDICTIVE MODELING

4.4.1. Future Scenarios

Having validated the complete model under a variety of environment conditions, it now can be used for predictive purposes. Predictive simulations, or forecasting, can be

useful in understanding how a system will respond to specific changes. As examples, models are currently being used to predict the growth of fish populations in streams (Bell et al., 2000), past and future conditions of aquatic systems (Menshutkin et al., 1998), and the effects of global warming (Monirul Qader Mirza, 2002; Gu et al., in press; Eide and Heen, 2002).

In the San Francisco Bay, it is the goal of the State of California to "reduce the impacts of water diversion on the Bay-Delta system" (http://www.baydeltawatershed.org/pdf/prog_plan.pdf). This goal includes restoring some of the flow from the San Joaquin River, which for most of the year has little or no water entering the estuary (Arthur and Ball, 1979). Presser and Piper (1998) found that 98% of the flow from the San Joaquin River was being diverted for irrigation practices. Increasing the flow from the San Joaquin River could alter the total dissolved and particulate selenium concentrations in the estuary and the model was therefore used to examine this scenario.

Sensitivity results from Section 3.3 as well as previous field studies (Cutter, 1989b; Cutter and San Diego McGlone, 1990), show that total dissolved selenium in the estuary are strongly influenced by selenium discharges from refineries. Using the validated model, the effects of increased and decreased refinery discharges have on the biogeochemical cycle of selenium in the Northern Reach of the San Francisco Bay were examined.

For all predictive simulations, only the total dissolved and particulate selenium data will be shown to shorten the discussion, but the complete set of future simulations

are given in Appendix D.

4.4.2. Variable San Joaquin River Flow

For simulations on increasing the discharge from the San Joaquin River, the discharge rate from Vernalis (San Joaquin freshwater end member) was used as the San Joaquin discharge rate into the Delta (www.iep.ca.gov). The flow at Vernalis is greater than what is currently discharged into the San Francisco Bay from the San Joaquin River and is representative of what the flow might be if there was no water removal for irrigation practices. It should also be remembered that an empirical relationship was established to account for removal of selenium during its transport through the Delta, the interface between the San Joaquin River at Vernalis and the Bay. It is hypothesized that if the water flow is increased, the net removal may not be as large due to a shorter residence time. Therefore, a model simulation was also done to examine how removing the "Delta removal effect" (described in Section 1.4), would affect the biogeochemical cycle of selenium. For this no "Delta removal effect" simulation, the flow from Vernalis was also used. Both of these results were then compared to estuarine profiles during a normal flow year for the San Joaquin River (2000; www.iep.ca.gov; labeled "normal year" in all figures and tables). The discharge from the Sacramento River was not altered and was also from the flow year 2000 (www.iep.ca.gov). The simulations were run for a high flow month (April) and a low flow month (November).

Predicted total dissolved selenium in the estuary during a high flow month was

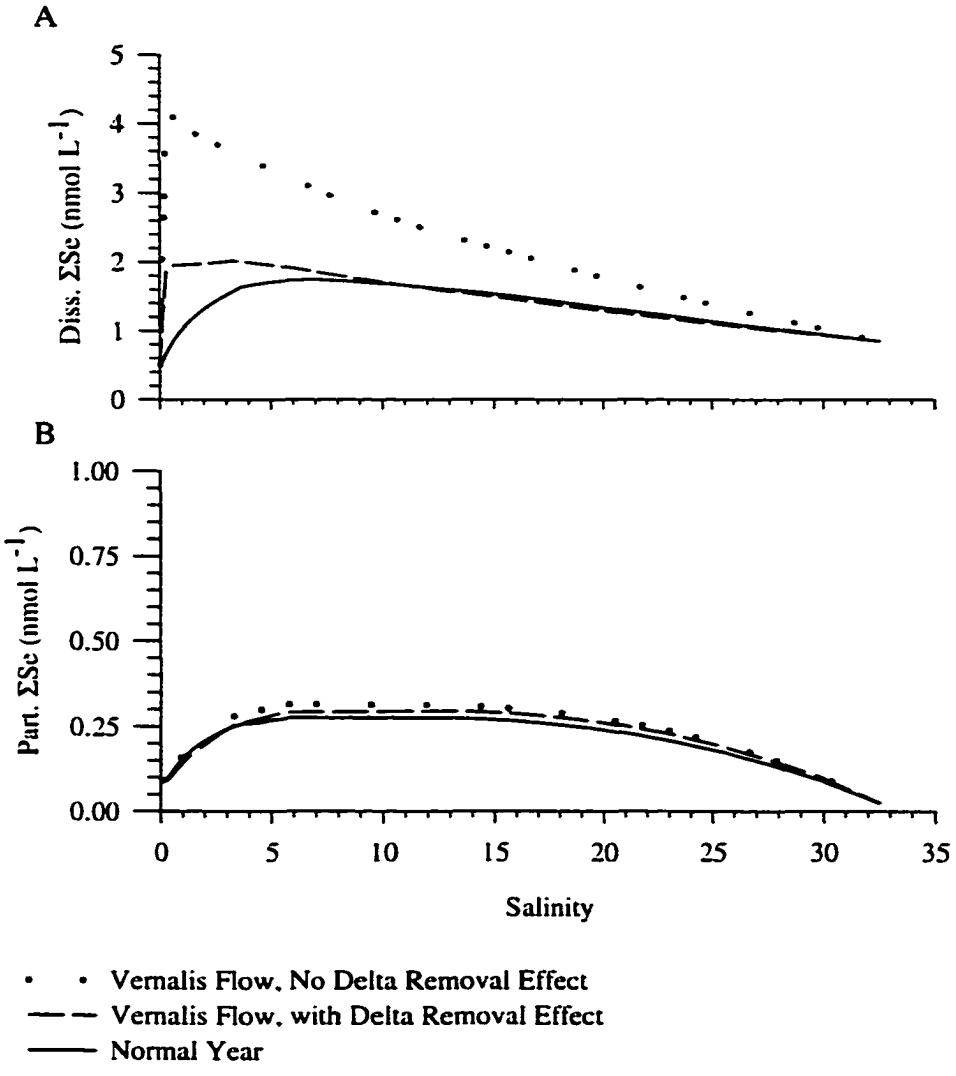

Fig. 44. Predictive simulations of total dissolved (A) and particulate selenium (B) for different discharges from the San Joaquin River during a high flow month (April).

non-conservative (Fig. 44A) for the normal flow conditions. Using the discharge rate from Vernalis and removing the "Delta removal effect" of selenium did not change the non-conservative behavior (Fig. 44A). Under currently observed flow conditions in April, the model predicts an average estuarine concentration of 1.22 ± 0.42 nmol L^{-1}, while using the higher flow from Vernalis resulted in an increase to 1.43 ± 0.44 nmol L^{-1} (Table 19). Removing the "Delta removal effect" resulted in a predicted estuarine average concentration of 2.33 ± 0.92 nmol L^{-1} (Table 19), which is 1.11 nmol L^{-1} higher than what would be observed under the current discharge rates from the San Joaquin River (Table 19).

Low flow predictions (November) show that total dissolved selenium was non-conservative in the estuary (Fig. 45A). Under normal flow conditions from the San Joaquin River, a mid-estuary peak of total dissolved selenium was predicted (Fig. 45A). Using the higher discharge from Vernalis, a broader total dissolved selenium peak is created and shifted toward the riverine end members. Combining the increased flow for the San Joaquin River with no "Delta removal effect" increased the lower salinity maxima to 5 nmol L^{-1}, which is greater than any observed in the past (Cutter, 1989b; Cutter and San-Diego 1990; Cutter and Cutter, in prep.). The predicted estuarine average total dissolved selenium concentration was 1.58 ± 0.33 nmol L^{-1} during normal low discharge from the San Joaquin, 2.06 ± 0.59 nmol L^{-1} with the higher discharge from Vernalis, and 3.14 ± 1.23 nmol L^{-1} when the combined effects of discharge from Vernalis and no "Delta removal effect" were run (Table 19). The higher concentrations during low flow are consistent with a longer water residence time (Cutter, 1989b; Cutter and San

Table 19
Predicted dissolved selenium and particulate selenium concentrations during a typical high flow month (April) and low flow month (November) for increased flow from the San Joaquin River and different refinery discharge rates

	Diss. $\sum$ Se (nmol L^{-1})	Part. $\sum$ Se (nmol L^{-1})	Part. Σ Se ($\mu g\ g^{-1}$)
April			
Vernalis Flow, no "Delta removal effect"	2.33 ± 0.92	0.21 ± 0.09	0.44 ± 0.28
Vernalis Flow, with "Delta removal effect"	1.43 ± 0.44	0.19 ± 0.07	0.44 ± 0.26
Normal San Joaquin flow	1.22 ± 0.42	0.19 ± 0.07	0.43 ± 0.26
November			
Vernalis Flow, no "Delta removal effect" "	3.14 ± 1.23	0.24 ± 0.13	1.00 ± 0.32
Vernalis Flow, with "Delta removal effect"	2.06 ± 0.59	0.16 ± 0.10	0.64 ± 0.16
Normal San Joaquin Flow	1.58 ± 0.33	0.12 ± 0.06	0.51 ± 0.11
April			
99mol d^{-1} total selenium	1.40 ± 0.55	0.19 ± 0.07	0.43 ± 0.26
38 mol d^{-1} total selenium	1.22 ± 0.42	0.19 ± 0.07	0.43 ± 0.26
No refinery inputs	1.05 ± 0.30	0.19 ± 0.07	0.43 ± 0.26
November			
99 mol d^{-1} total selenium	1.98 ± 0.52	0.14 ± 0.06	0.62 ± 0.14
38 mol d^{-1} total selenium	1.58 ± 0.33	0.12 ± 0.06	0.51 ± 0.11
No refinery inputs	1.18 ± 0.20	0.09 ± 0.06	0.43 ± 0.09

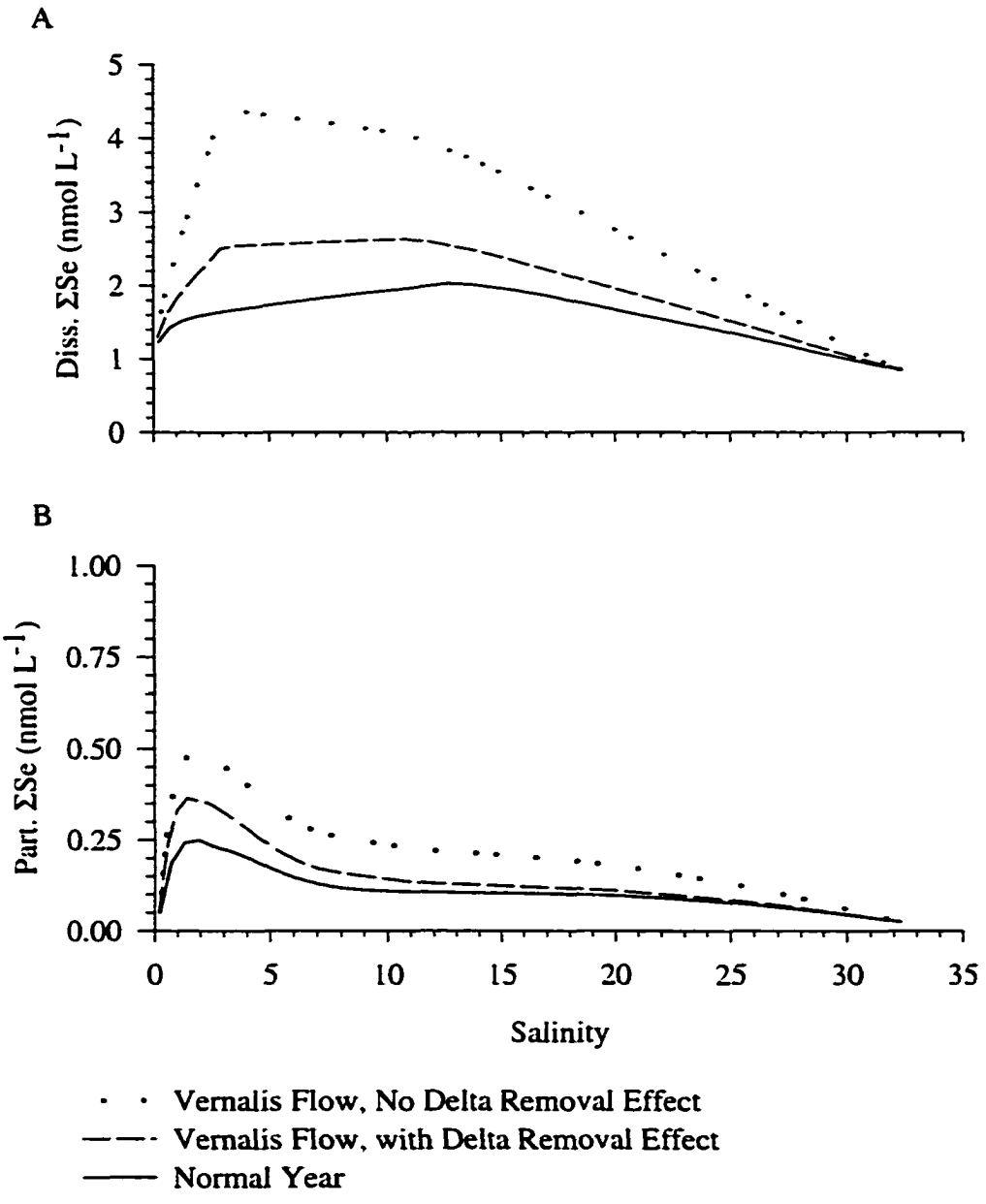

Fig. 45. Predictive simulations of total dissolved (A) and particulate selenium (B) for different discharges from the San Joaquin River during a low flow month (November).

Diego-McGlone, 1990).

Total particulate selenium profiles in April (high flow) show production of particulate material within the estuary (Fig. 44B). Nevertheless, the net effect of increasing the discharge rate from the San Joaquin River (Vernalis flow and no Delta reduction) had a negligible effect on the concentrations of total particulate selenium (Fig. 44B); the estuarine averages of total particulate selenium were similar to each other (Table 19). However, increasing the flow in the San Joaquin River for a low flow month resulted in an increase in total particulate selenium in the estuary (Fig. 45B). Under normal flow conditions from the San Joaquin River, the average estuarine total particulate selenium concentration was 0.12 $\pm$ 0.06 nmol L^{-1} (Table 19), while it increased to 0.16 $\pm$ 0.06 nmol L^{-1} under higher Vernalis flow, and to 0.24 $\pm$ 0.13 nmol L^{-1} when the discharge was increased with no "Delta removal effect" factor applied.

The increase of total particulate could be due to either an increase in sediment resuspension or *in situ* production of particles (Section 1.4.9, Equations 1.34 to 1.41). Determining the particle associated selenium can be used as an indication of whether *in situ* production might be responsible for the predicted increase. In particular, if the increase is only due to an increase in sediment resuspension, the particle-associated selenium ($\mu g\ g^{-1}$) should be similar for each simulation. A change in particulate selenium (nmol L^{-1}) was observed during a low flow month (Fig. 45B) and the resulting particle-associated selenium indicates that with increased flow and no "Delta removal effect" the particulate associated selenium could be greater than $1 \mu g\ g^{-1}$ (Fig. 46). This concentration is enough to cause elevated concentration of selenium in tissues of benthic consumers

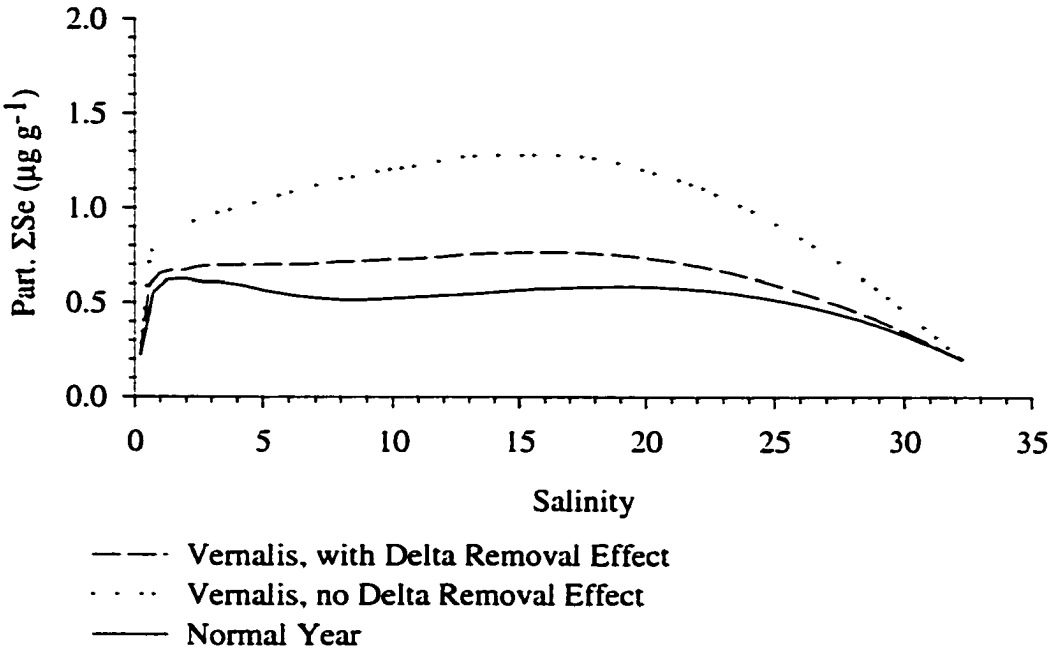

Fig. 46. Particle-associated selenium for the San Francisco Bay when the discharge from the San Joaquin River is increased for a low flow month (November).

like *M. balthica* (Luoma et al., 1992) and therefore may have effects on the rest of the estuarine food web. The estuarine averaged selenium associated with particles did not vary in April when the flow from the San Joaquin was altered (0.44 ± 0.26 μg g^{-1}; Table 19). However, in November the particle-associated selenium during normal river discharge was predicted to be 0.51 ± 0.11 μg g^{-1}, and increasing to 0.64 ± 0.16 μg g^{-1} when the discharge from Vernalis was used. Under the no "Delta removal effect" scenario, estuarine averaged particle-associated selenium concentrations increased to 1.00 ± 0.32 μg g^{-1} (Table 19).

4.4.3. Altered Refinery Inputs

Simulations were run to determine how changes in the refinery discharge flux would affect total dissolved and particulate selenium concentrations within the estuary. In 1986, the refineries were discharging 99 mol d^{-1} of total selenium with 64% of the total as selenite (Cutter, 1989b). It can be hypothesized that if the refineries are discharging selenate instead of selenite, this would have a minimal effect on biotic processes (via uptake of particulate selenium) since the phytoplankton uptake rate for selenate is 4.5 times lower than that for selenite. Therefore, three different fluxes were used to simulate how refinery inputs affects total dissolved and particulate selenium in the estuary. The discharge fluxes used were: 38 mol d^{-1} as a reference (current conditions), 99 mol d^{-1}, and finally no flux. For these simulations, the speciation of selenium from the refineries was held at 13% of the total as selenite, 57% as selenate, and 30% as organic selenide. Thus, the selenate fluxes from the refineries for each simulation were either 0 mol d^{-1}, 22 mol

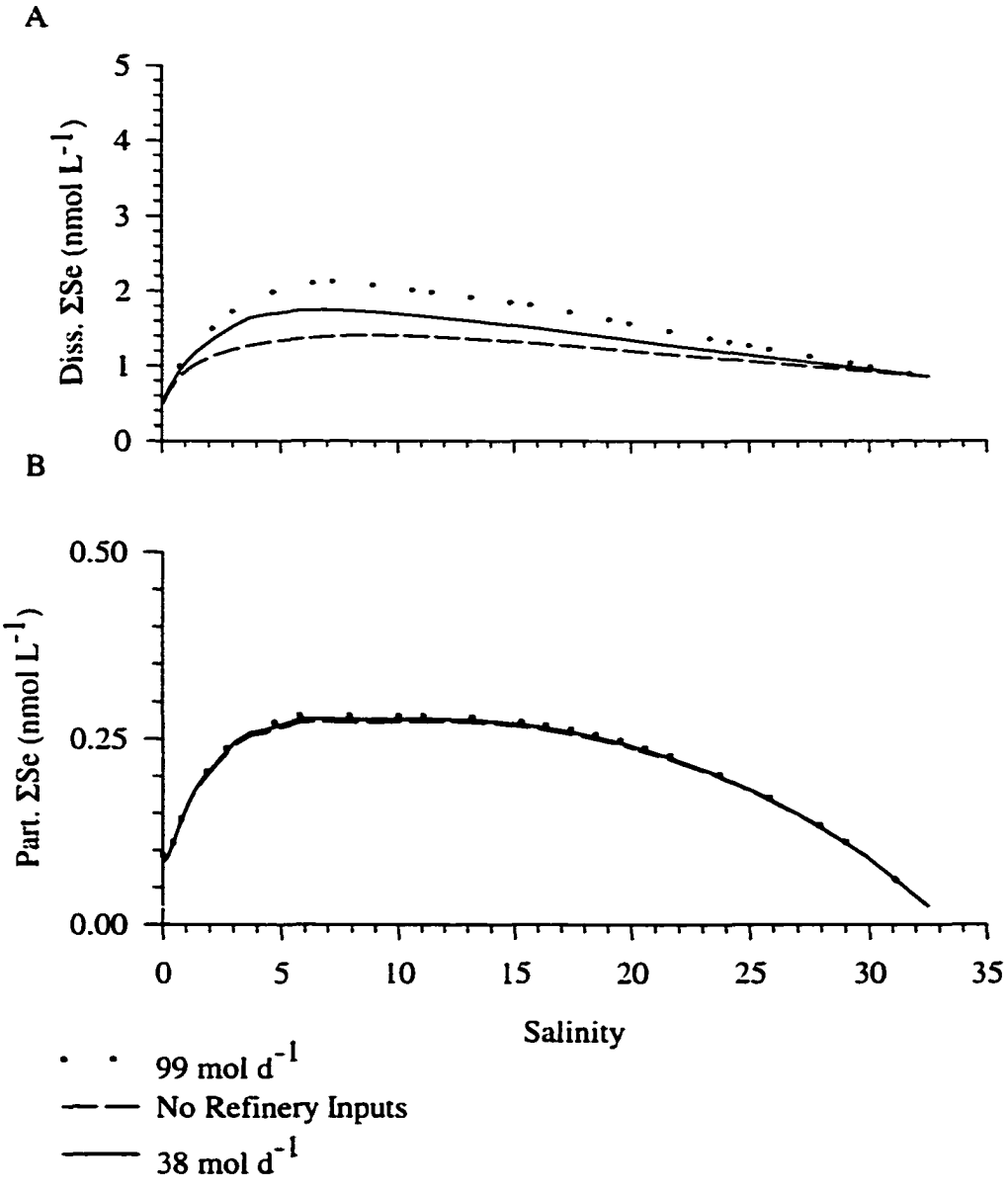

Fig. 47. Predictive simulations of total dissolved (A) and particulate selenium (B) for different refinery discharges during a high flow month (April).

d^{-1}, or 56 mol d^{-1}. The discharge rate for the Sacramento and San Joaquin Rivers were from a normal year (2000, www.iep.ca.gov). The model was run for a high flow month (April) and a low flow month (November).

The predicted estuarine profile was non-conservative for all simulations (Fig. 47A). In April (high flow), without any refinery inputs the predicted estuarine average total dissolved selenium concentration was 1.05 ± 0.30 nmol L^{-1} (Table 19). The predicted estuarine average with a discharge rate of 99 mol d^{-1} resulted in an estuarine average of 1.40 ± 0.55 nmol L^{-1} (Table 19), which was 33% higher than what would be observed if there were no refinery inputs. The intermediate refinery flow gave an estuarine average of 1.22 ± 0.42 nmol L^{-1}. Total particulate selenium (Fig. 47B) showed no change within the estuary due to an increase/decrease in refinery inputs, with an estuarine average total particulate concentration of 0.19 ± 0.07 nmol L^{-1}.

For a low flow month without any refinery inputs, total dissolved selenium was non-conservative (Fig. 48A) and had an estuarine average of 1.18 ± 0.20 nmol L^{-1}. The discharge of selenium into the estuary from the refineries resulted in non-conservative estuarine profiles, with a mid-estuary maximum (Fig. 48A) and estuarine averages of 1.58 ± 0.33 nmol L^{-1} when the total discharge was 38 mol d^{-1}, and 1.98 ± 0.52 nmol L^{-1} when the total discharge was 99 mol d^{-1} (Table 19). Under current refinery discharge rates (38 mol d^{-1}) the total dissolved selenium concentration is 34% higher than what would be observed with out any refinery inputs, and using a discharge rate of 99 mol d^{-1}, it is 70% higher (Table 19). There is a slight change in total particulate selenium in the estuary as the refinery inputs increase (Fig. 48B).

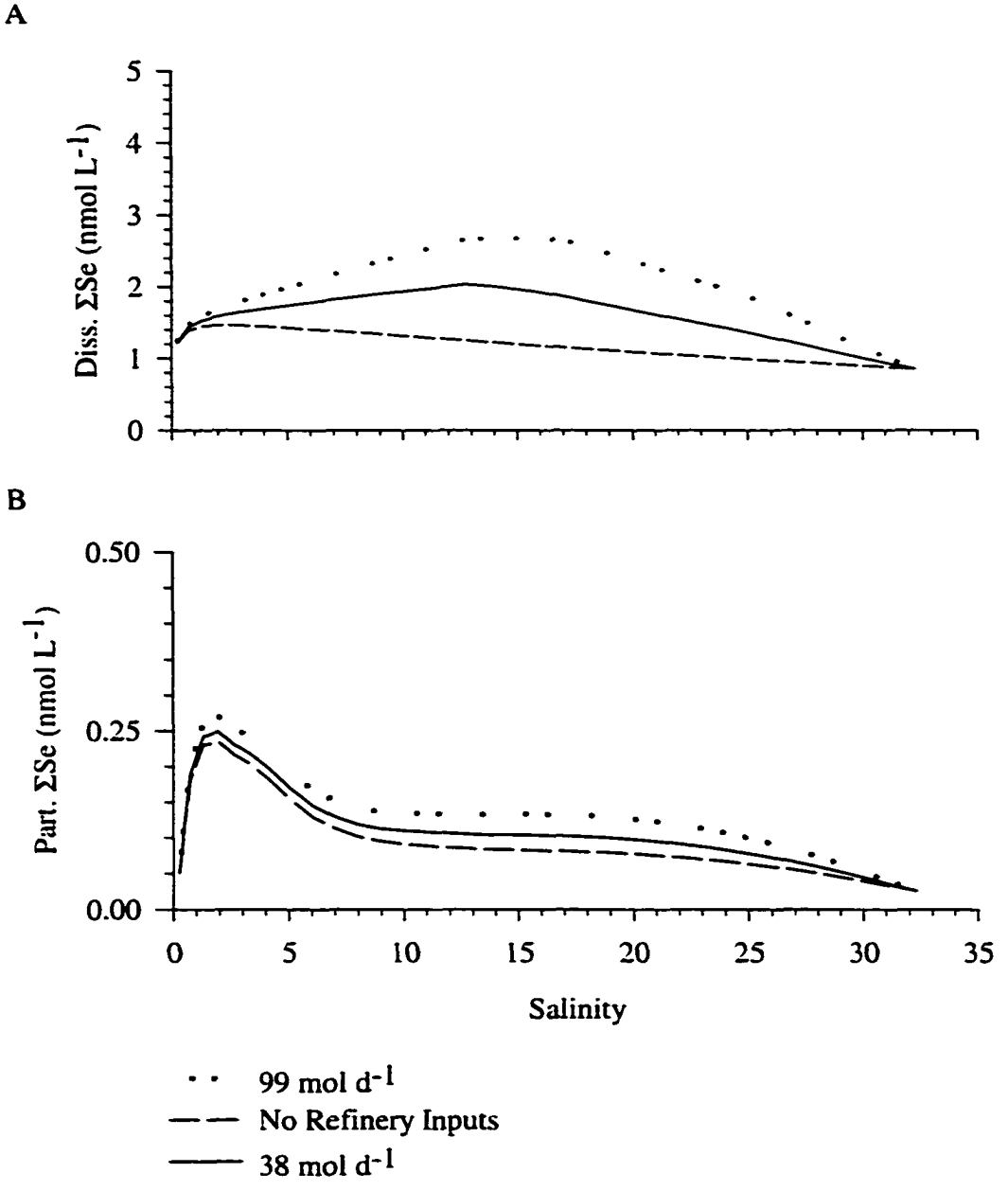

Fig. 48. Predictive simulations of total dissolved (A) and particulate selenium (B) for different discharge rates from the refineries during a low flow month (November).

In November (low flow), the total particulate selenium concentration was 0.09 ± 0.07 nmol L^{-1} with no refinery inputs, and it increased to 0.14 ± 0.06 nmol L^{-1} when the refinery input was 99 mol d^{-1} of total selenium (Table 19). Any increase in total particulate selenium, must be due to *in situ* production since the flow from the refineries had no effect on the amount of sediment suspended or discharged into the Bay (Section 1.4.6 and Section 1.4.9). The particle associated selenium increased from 0.43 ± 0.09 μg g^{-1} without any refinery inputs to 0.62 ± 0.14 μg g^{-1} when 99 mol d^{-1} of total dissolved selenium was discharged (Table 19). Under current refinery discharge rates (38 mol d^{-1}) the particle-associated selenium was 0.51 ± 0.11 μg g^{-1}. Thus, there is little net difference between particle-associated selenium within the estuary when the discharge rate from the refineries was increased. However, the change in particle-associated selenium for a low flow months indicates that a maximum particle-associated selenium concentration (Fig. 49) occurs where the refineries are located. Therefore, although increasing the discharge from the refineries (predominately selenate) increases total dissolved selenium, it has very little effect on particle-associated selenium on a normal flow year. However, if the simulation is run using observed river flow under dry conditions (river discharge from 1977) with the higher refinery inputs (99 mol d^{-1}) which 57% of the total is selenate, the particle-associated selenium increases to a maximum of 2.1 μg g^{-1} (Fig. 50). This is greater than what would occur if the flow from the San Joaquin River was increased, suggesting that the affects from the refineries can be magnified depending on the residence time of the water. Therefore, the refineries should not increase there discharge rate in the form of selenate since it can results in an estuarine average particulate

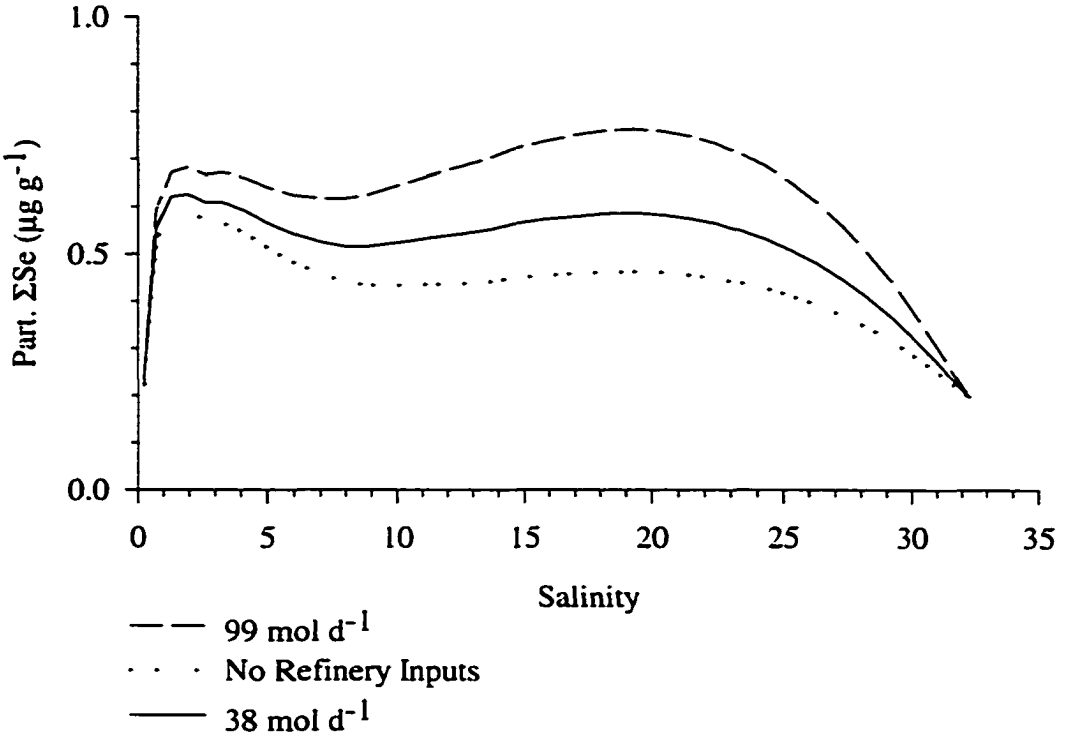

Fig. 49. Predictive simulations of particle-associated selenium for a low flow month (November).

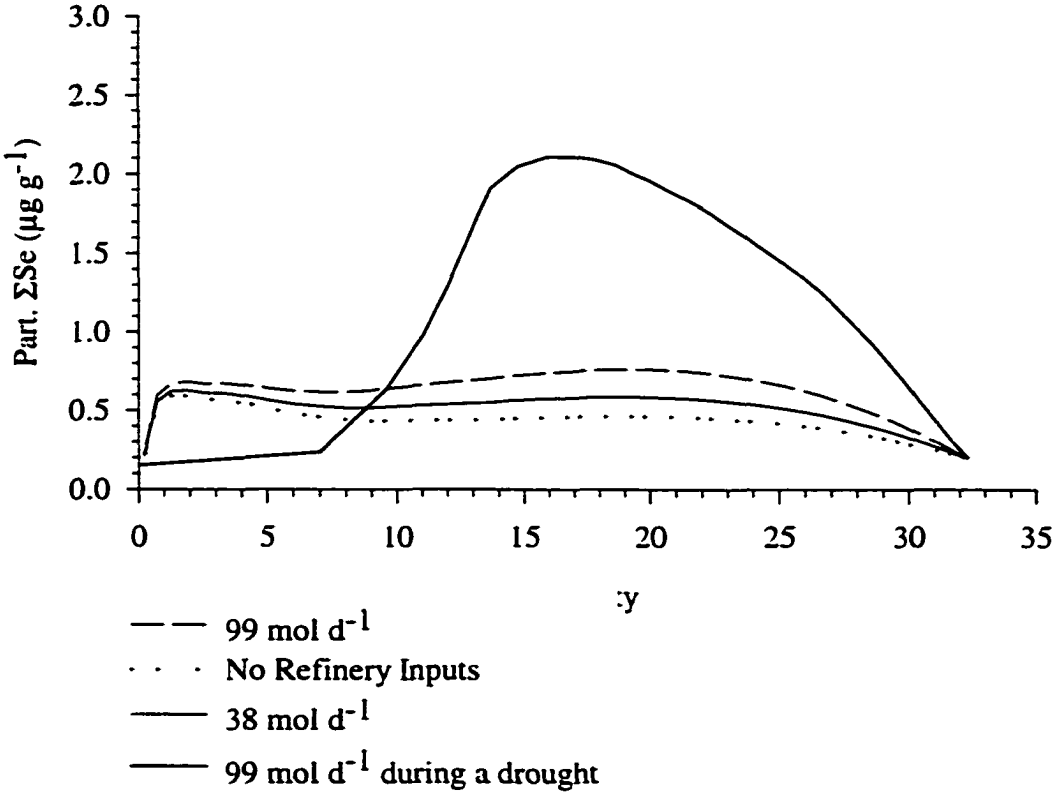

Fig. 50. Predictive simulations of particle-associated selenium for a low flow month (November), with increase refinery inputs during a drought.

selenium concentration of 1.27 ± 0.64 μg g^{-1} during a dry year.

selenium concentration of 1.27 ± 0.64 μg g^{-1} during a dry year.

4.5. CONCLUSIONS

The confidence associated with the model's ability to predict future scenarios is dependent on the number of validation runs that can be done. If the model was validated under extreme conditions (as observed for dissolved selenium), the confidence in the model ability to predict future scenarios is greater. For total particulate selenium, the model was also able to simulate observed concentrations. However, the speciation data for selenium were only from 1 high flow and 2 low flow months. The validation results proved that the model was able to successfully simulate the observed behavior for these time periods, but more confidence in predicted speciation data would occur if there were more data available for validation tests. Once more data become available, the model can be further validated to ensure that it can simulate the extreme conditions that were observed in the dissolved selenium data (e.g., drought conditions).

When validation of a model is successful as it was above, the model can be used to predict how a slight change in the estuary can effect the biogeochemical cycle of selenium. As the above future scenarios demonstrated, a minor change in the inputs to the estuary can have a dramatic affect (increased San Joaquin River flow) or no effect at all (increased refinery inputs). In combination with food web models, the results generated with this model can be used to investigate higher food-web interactions and how policy-making decisions, like restoring the San Joaquin River flow, can affect organisms in the Bay.

CHAPTER V

CONCLUSIONS

5.1. MODEL PERFORMANCE

Models are used to synthesize existing information about systems and their output can provide additional information about the direction of future work (Costanza and Voinov, 2001). The discrepancies between model-derived concentrations and the observed data can be used to determine if there are missing sources/sinks or processes in the biogeochemical cycle of selenium (Fig. 10). Differences between model-generated particulate and dissolved selenium at the riverine end member (Chapter IV and Appendix C and D) suggest that the current model input of riverine selenium may not be accurate. In the model, the Sacramento and San Joaquin Rivers were treated as separate inputs that had no exchange until the San Joaquin entered the Bay at Antioch. However, Monson (2001) suggested that the exchange of water between the Sacramento River and the San Joaquin River, via Threemile Slough (Fig. 51), might be significant. In total, there are four connectors (Fig. 51) between the Sacramento River and the San Joaquin River that could account for water exchange between the two rivers. If this exchange is significant, it could explain why the model sometimes underestimates the riverine end member of constituents in the model (e.g., TSM, phytoplankton, dissolved and particulate selenium). Current studies by the USGS are examining the exchange of water between the two rivers. If the exchange is significant, it may be necessary to re-define the riverine

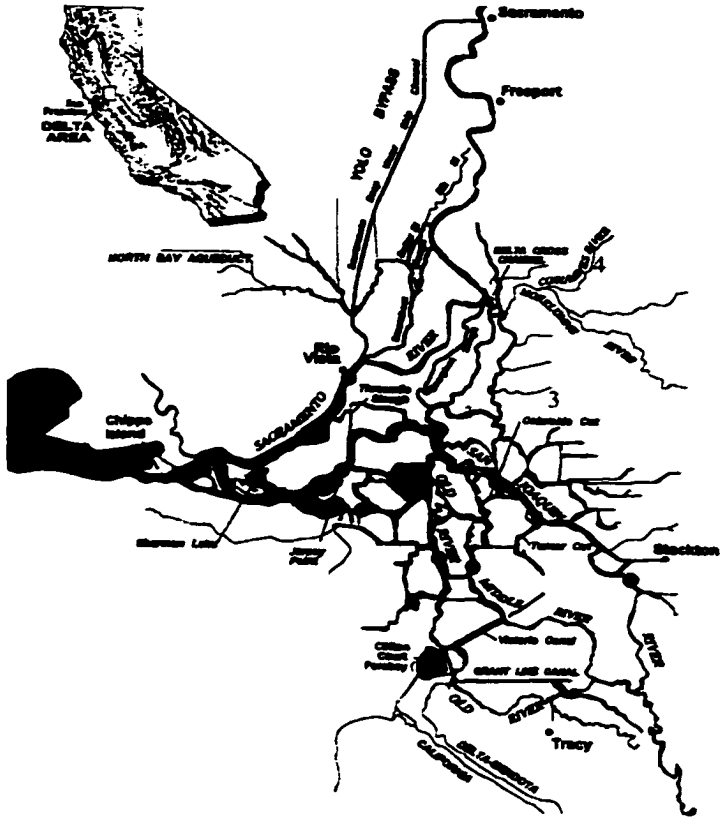

Fig 51. The Sacramento-San Joaquin River with possible exchange pathways between the two rivers. They are (1) Sherman Lake, (2) Threemile Slough, (3) Georginna Slough, and (4) the Delta Cross Channel.

inputs of selenium so that the Sacramento River and San Joaquin River are not treated as separate freshwater inputs.

With respect to the San Joaquin River, an empirical relationship was established to account for any removal/production of dissolved selenium between Vernalis and the Bay during its transport through the Delta. There are very little data available on this "Delta Removal Effect" of selenium, but the existing results suggest that this reduction could be significant (up to 80%; Cutter, unpublished data). It was assumed that the "Delta Removal Effect" was due to biogeochemical processes, but it could also be due to physical processes (e.g., different water masses mixing). As discussed above, there are studies being done to determine how much water exchange is occurring between the Sacramento and San Joaquin River. If this relationship is due to different water masses mixing, adjustments to account for river mixing may allow the Delta Reduction Effect to be eliminated from the model.

Model calibration also indicated that the understanding of *in situ* production of particulate selenite+selenate is not fully quantified. In the model, the concentration of particulate selenite+selenate in the estuary was a function of riverine inputs, sediment resuspension, and adsorption. Research on adsorption of selenite and selenate in estuarine environments is limited. Most of the current studies (Section 1.4.9) have been in low ionic strength soils, which makes their results difficult to apply for an estuary. Further studies need to be done to investigate the affects of adsorption of selenite in estuarine waters.

The sensitivity analyses indicated that particulate selenium is the most difficult

species to simulate (it was sensitive to 17 of the 24 parameters tested). Phytoplankton production and uptake during low flow periods resulted in the greatest change in model output (Section 3.3.2). The model needs to be adjusted to simulate phytoplankton growth rates for different phytoplankton species and the uptake rates using Michaelis-Menton for species in the San Francisco Bay. *In situ* experiments within the Delta suggest that the uptake of selenium by phytoplankton may be on a diurnal time scale and with a high organic selenide uptake rate (Cutter, unpublished data). It is recommended that further research is done to investigate the uptake of selenium through *in situ* experiments (as with the Delta data) for phytoplankton species in the San Francisco Bay. With a better understanding on phytoplankton growth rates and uptake rates of selenium, the models ability to predict particulate organic selenide may be improved.

Even with these limitations and the need for added research, the model could predict with a confidence of 75% or greater the observed data in the estuary. Managers could use this model to help in determining the effects of added riverine inputs, refinery inputs, or an increase in phytoplankton productivity for the entire Northern Reach. However, the model is not designed for a specific area (e.g., Grizzley Bay) and the resolution of the model (3 km) is greater than the length of some of the Bays within the Northern Reach (Grizzly Bay is 6 km long). Models would need to be developed for each Bay to obtain finer resolution if management efforts were on a specific area of the Bay instead of the entire Northern Reach.

There are limitations of the model. For example, over time scales of decades, the bathymetry of an estuary changes. The model currently does not account for changes in

the area or depth of the estuary. These changes would affect the dispersion of a constituent in the estuary (Equation 1.10). Therefore, the model can not be used if bathymetry changes are significant. But the model could be linked to model that predict changes in the bathymetry of the estuary to determine the effects on the biogeochemical cycle of selenium in the Northern Reach.

The June 1998 simulation indicates that during intense El Niño years, even though the model was able to simulate 75% of the observed behavior of total dissolved and particulate, the errors between the observed and predicted concentrations were greater than other simulations. This may be due to water column stratification in the estuary. Recent research suggests that El Niño events are becoming more frequent and intense (Chen et al., 2002). Based on the possibility of more El Niño events, the model may need to be adjusted to simulate a partially-mixed estuary.

5.1.1. Model Applications to Other Estuaries

The conservative and non-conservative behavior of dissolved selenium has been observed in other estuaries (Takayanagi and Wong, 1984; Takayanagi and Cossa, 1985; van der Sloot et al., 1985). ECoS 3 was adapted to simulate the biogeochemical cycle of selenium in the Northern Reach of the San Francisco Bay. Often the development of models can result in it only being applicable to the system of interests. However, research indicates that the processes in Fig. 10 should occur in all aquatic systems. Since Fig. 10 is applicable to other estuaries, this model could be used to predict the biogeochemical cycle of selenium in other well-mixed estuaries. Obviously some of the

inputs (e.g., refinery inputs) may need to be removed from the model and the productivity of phytoplankton may need to be adjusted. For example, in the San Francisco Bay phytoplankton growth is light limited, while in other estuaries growth could be limited by nutrients and the benthic grazing terms might not be as high as in the San Francisco Bay. These minor modifications may need to be done to the model to account for differences between estuaries. In addition, model parameters such as sediment resuspension would need to be calibrated for other estuaries before this model could predict dissolved and particulate selenium for other well-mixed estuaries.

5.2. SUMMARY OF MODEL RESULTS

Recent advances in modeling the physical, chemical, and biological interactions in an estuary, allowed the development of a model that simulates the biogeochemical cycle of selenium in the San Francisco Bay. Findings from this model show that:

(1) Dissolved selenium concentrations and speciation are controlled by the inputs from the Sacramento-San Joaquin Delta and oil refineries for both high flow and low flow conditions;

(2) Particulate selenium concentrations are controlled by sediment resuspension, riverine inputs, and *in situ* production.

(3) Sensitivity analyses found that particulate organic selenide was the most difficult species to simulate due to the large number of variables on which it is dependent. Some of the parameters needed in simulating particulate organic selenide (e.g., rates of dissolved selenium uptake by phytoplankton) are still

under investigation. Once these parameters are better quantified, model simulations of organic selenide should improve;

(4) The Northern Reach of the San Francisco Bay is river- and refinery-dominated for total dissolved selenium, while for particulate selenium, it is river-dominated in the high flow periods and phytoplankton-dominated in low flow times;

(5) Future simulations suggest that an increase in the San Joaquin River flow to the estuary could result in particle-associated selenium concentrations that are higher than what is currently observed. The particle-associated selenium could potentially be as high as 1 $\mu g\ g^{-1}$, which could cause elevated concentrations in filter feeding clams;

(6) Increasing the input of selenium from oil refineries, in the form of selenate, would have little net affect on the currently observed particle-associated selenium. However, during dry conditions an increase in refinery inputs would result in particle-associated concentrations greater than 1 $\mu g\ g^{-1}$.

5.3. CONCLUSIONS

In conclusion, models like that used here are useful for predicting the behavior of trace metals in an estuary. Modeling results from this study can be used in other models that examine the bioaccumulation of selenium in higher trophic levels in the estuary. For example, in the San Francisco Bay the bioaccumulation of selenium is dependent on the concentration and distribution of particulate selenium in the Bay that this model could

provide. Furthermore, the model can be used as a template to study the biogeochemical cycle of other elements, which could be useful in restoration projects, pollution control, and other trophic transfer scenarios.

REFERENCES

Ahlrichs, J.S., Hossner, L.R., 1987. Selenate and selenite mobility in overburden by saturated flow. J. Environ. Qual. 16, 95-98.

Alewell, C., Manderscheid, B., 1998. Use of objective criteria for the assessment of biogeochemical ecosystem models. Ecol. Model. 107, 213-224.

Alpine, A.A., Cloern, J.E., 1988. Phytoplankton growth rates in a light-limited environment, San Francisco Bay. Mar. Ecol. Prog. Ser. 44, 167-173.

Alpine, A.A., Cloern, J.E., 1992. Seasonal changes in the spatial distribution of phytoplankton in small, temperate-zone lakes. J. Plankton Res. 14, 1017-1024.

Ambler, J.W., Cloern, J.E., Hutchinson, A., 1985. Seasonal cycles of zooplankton from San Francisco Bay. Hydrobiologia 129, 177-197.

Amourous, D. , Liss, P., Tessier, E. Hamren-Larsson, M. , Donard, O., 2001. Role of oceans as biogenic sources of selenium. Earth Planet. Sci. Lett. 189, 277-283.

Annan, J.D., 2001. Modelling under uncertainty: Monte Carlo methods for temporally varying parameters. Ecol. Model. 136, 297-302.

Apte, S.C., Howard, A.G, Morries, R.J., McCartney, M.J., 1986. Arsenic, antimony and selenium speciation during a spring phytoplankton bloom in a closed experimental ecosystem. Mar. Chem. 20, 119-130.

Arthur, J.F., Ball, M.D., 1979. Factors influencing the entrapment of suspended material in the San Francisco Bay-Delta Estuary. In: Conomos, T.J. (Ed), San Francisco Bay: The Urbanized Estuary. Association for the Advancement of Science, Washington, D.C., pp. 143-174.

Baeyens, W., Monteny, F., Van Ryssen, R., Leermakers, M., 1998. A box-model of metal flows through the Scheldt estuary (1981-1983 and 1992-1995). Hydrobiologia 366, 109-128.

Baines, S.B., Fisher, N.S., 2001. Interspecific differences in the bioconcentration of selenite by phytoplankton and their ecological implications. Mar. Ecol. Prog. Ser. 213, 1-12.

Baines, S.B., Fisher, N.S., Doblin, M.A., Cutter, G.A., 2001. Uptake of dissolved organic selenides by marine phytoplankton. Limnol. Oceanogr. 46, 1936-1944.

Bale, A.J., 1987. The characteristics, behaviour and heterogeneous chemical reactivity of estuarine suspended particles. Ph.D. Thesis, Plymouth Polytechnic. 182 pp.

Balistrieri, L.A., Chao, T.T., 1986. Selenium adsorption by geothite. Soil Sci. Soc. Am. J. 51, 1145-1151.

Bar-Yosef, B., Meek, D., 1987. Selenium sorption by kaolinite and montmorillonite. Soil Sci. 144, 11-19.

Beck, M.B., 1987. Water quality modeling: a review of the analysis of uncertainty. Water Resour. Res. 23, 1393-1442.

Bell,V., Elliot, J., Moore, R.J., 2000. Modelling the effects of drought on the population of brown trout in Black Brows Beck. Ecol. Model. 127,141-159.

Belzile, N., Lebel, J., 1988. Selenium profiles in the sediments of the Laurentian trough (Northwest North Atlantic). Chem.Geo. 68, 99-103.

Belzile, N., Yu-Wei, C., Xu, R., 2000. Early diagenetic behaviour of selenium in freshwater sediments. Appl. Geochem. 15, 1439-1454.

Bender, M., Martin, W., Hess, J., Sayles, F., Ball, L., Lamber, C., 1987. A whole core squeezer for interfacial pore-water sampling. Limnol. Oceanogr. 32, 1214-1225.

Bennett, W.N. 1988. Assessment of selenium toxicity in algae using turbidostat culture. Water Res. 22, 939-942.

Beres, D.L., Hawkins, D.M., 2001. Plackett-Burman technique for sensitivity analysis of many-paramatered models. Ecol. Model. 141, 171-183.

Berner,R.A., 1980. Early Diagenesis: A Theoretical Approach. Princeton University Press, Princeton, 237 pp.

Boisson, F., Gnassia-Barelli, M., Romeo, M. 1995. Toxicity and accumulation of selenite and selenate in the unicellular marine algae *Cricosphaera elongata*. Arch. Environ. Contam. Toxicol. 28, 487-493.

Bottino, N.R., Banks, C.H., Irgolic, K.J., Micks, P., Wheeler, A.E., Zingaro, R.A., 1984. Selenium containing amino acids and proteins in marine algae. Photochemistry 23, 2445-2452.

Boughriet, A., Ouddane, B., Fischer, J.C., Wartel, M., Leman,G., 1992. Variability of dissolved Mn and Zn in the Seine estuary and chemical speciation of these metals in suspended matter. Water Res. 26, 1359-1378.

Bruland, K.W., Donat, J.R., Hutchins, D.A., 1991. Interactive influences of bioactive trace metals on biological production in oceanic waters. Limnol. Oceanogr. 36, 1555-1577.

Canale, R.P., Owens, E.M., Auer, M.T, Effler, S.W., 1995. Validation of Water-Quality model for Seneca River, NY. J.Water Resour. Plann. Manage. 121, 241-250.

Chanton, J.P, Lewis, F.G., 1999. Plankton and Dissolved Inorganic Carbon Isotopic Composition in a River-Dominated Estuary: Apalachicola Bay, Florida. Estuaries 22, 575-583.

Chen, J.P., Lin, M., 2001. Equilibrium and kinetics of metal ion adsorption onto a commercial H-type granular activated carbon: experimental and model studies. Wat. Res. 35, 2385-2394.

Chen, J., Carlson, B.E., Del Genio, A.D., 2002. Evidence for Strengthening of the Tropical General Circulation in the 1990s. Science 295, 838-840.

Cheng, R.T., Casulli, V., Gartner, J.W., 1993. Tidal, residual, intertidal mudflat (TRIM) model and its applications to San Francisco Bay, California. Estuar. Coast. Shelf Sci. 36, 235-280.

Cifuentes, L.A., Schemel, L.E., Sharp, J.H., 1990. Qualitative and Numerical Analyses of the Effects of River Inflow Variations on Mixing Diagrams in Estuaries. Estuar. Coast. Shelf Sci. 30, 411-427.

Cloern, J.A., personal communication. Chief, Branch of Regional Research, U.S. Geological Survey MS472, 345 Middlefield Road, Menlo Park, California 94025, (415) 329-4412.

Cloern, J.E., 1982. Does the benthos control phytoplankton biomass in south San Francisco Bay? Mar. Eco. Prog. Ser. 9, 191-202.

Cloern, J.E., 1991. Tidal stirring and phytoplankton bloom dynamics in an estuary. J. Mar. Res. 49, 203-221.

Cloern, J.E., Alpine, A., 1991. *Potamocorbula amurensis* , a recently introduced Asian clam, has had dramatic effects on the phytoplankton biomass and production in northern San Francisco Bay. J. Shellfish Re. 10, 258-259.

Cloern, J.E., Cole, B.E., Raymond, L., Wong, J., Alpine, A.E., 1985. Temporal dynamics of estuarine phytoplankton: A case study of San Francisco Bay. Hydrobiologia 129, 153-176.

Cole, B.E., Cloern, J.E., 1984. Significance of biomass and light availability to phytoplankton productivity in San Francisco Bay. Mar. Ecolo. Prog. Ser. 17, 15-24.

Cole, B.E., Cloern, J.E., 1987. An empirical model for estimating phytoplankton productivity in estuaries. Mar. Ecol. Prof. Ser. 36, 299-305.

Colemon, R.G., Radojevic, M., 1957. Occurrence of selenium in sulfides from some sedimentary rocks of the western United States. Econ. Geol. 52, 499-527.

Conomos, T.J., 1979. Properties and circulation of San Francisco Bay waters. In: San Francisco Bay: The Urbanized Estuary, Association for the Advancement of Science, Pacific Division, San Francisco, pp. 47-84.

Conomos, T.J., Smith, T.E., Peterson, D.H., Hager, S.W., Schemel, L.E., 1979. Processes affecting seasonal distributions of water properties in the San Francisco Bay estuarine system. In: Conomos, T.J. (Ed), San Francisco Bay: The Urbanized Estuary. Association for the Advancement of Science, Washington, DC, pp. 115-142.

Conomos, T.J., Peterson, D.H., 1977. Suspended-Particle Transport and Circulation in San Francisco Bay: An Overview. Estuarine Processes Vol. II; Circulation, Sediments, and Transfer of Material in the Estuary, 1977. Academic Press, Inc., NY, pp. 82-97.

Comans, R.N.J., Van Dijk, C.P.J., 1988. Role of complexation processes in cadmium mobilization during estuarine mixing. Nature 336, 151-154.

Conomos, T.J., Smith, T.E., Gartner, J.W., 1985. Environmental setting of San Francisco Bay. Hydrobiologia 129, 1-12.

Conover, R. J., 1956. Oceanography of Long Island Sound, 1952-1954. VI. Biology of *Acartia clausi* and *A. tonsa*. Bull. Bingham. Oceanogr. Coll. 15, 156-233.

Cooke, T.D., Bruland, K.W., 1987. Aquatic chemistry of selenium: evidence of bimethylation. Environ. Sci. Technol. 21, 1214-1219.

Costanza, R., Voinov, A. 2001. Modeling ecological and economic systems with Stella: Part III. Ecol. Model. 143, 1-7.

Cutter, G.A., personal communication. Old Dominion University. 4400 Elkhorn Ave., Norfolk, VA 23508. (757) 683-4941.

Cutter, G. A., 1978. Species determination of selenium in natural waters. Anal. Chim. Acta 98, 59-66.

Cutter, G.A., 1982. Selenium in reducing waters. Science 217, 829-831.

Cutter, G.A., 1983. Elimination of nitrite interferences in the determination of selenium by hydride generation. Anal. Chim. Acta 149, 391-394.

Cutter, G.A., 1985. Determination of selenium speciation in biogenic particulate material and sediments. Anal. Chem. 57, 2951-2955.

Cutter, G.A., 1989a. Selenium in fresh water systems. In: Ihnat, M., (Ed), Occurrence and Distribution of Selenium. CRC Press, FL, pp. 243-262.

Cutter, G.A., 1989b. The Estuarine Behaviour of Selenium in San Francisco Bay. Estuar. Coast. Shelf Sci. 28, 13-34.

Cutter, G.A., 1992. Kinetic controls on metalloid speciation in seawater. Mar. Chem. 40, 65-80.

Cutter, G.A., Bruland, K.W., 1984. The marine biogeochemistry of selenium in a simple system. Geochim. Cosmochim. Acta 48, 1417-1433.

Cutter.G.A., Cutter, L. in prep. The biogeochemistry of selenium in the San Francisco Bay estuary: changes in water column behavior. In preparation for Estuarine and Coastal Shelf Science.

Cutter, G.A., San Diego-McGlone, M.L.C., 1990. Temporal variability of selenium fluxes in the San Francisco Bay. Sci. Total. Environ. 97, 235-250.

Cutter, G.A., Radford-Knoery, J., 1991. Determination of carbon, nitrogen, sulfur, and inorganic sulfur species in marine particles. Marine Particles: Analysis and Characterization 63, 57-63.

Dalye, R., 1991. Atmospheric Data Analysis, Cambridge University Press, NY, pp. 100.

Decho, A.W., Luoma, S.N., 1996. Flexible digestion strategies and trace metal assimilation in marine bivalves. Limnol. Oceanogr. 41, 568-572.

Dinehart, R.L., Schoellhamer, D.H., 1999, Sedimentation in the Delta of the Sacramento and San Joaquin Rivers: Proceedings of the 4th biennial State of the Estuary Conference, San Francisco, CA, p. 75.

Doblin, M.A., Blackburn, S.I., Hallegraeff, G.M., 1999. Comparative study of selenium requirements of three phytoplankton species: *Gymnodinium catenatum*, *Alexandrium minu*tum (Dinophyta) and *Chaetoceros cf. tenuissimus* (Bacillariophyta). J. Plankton Res. 21, 1153-1169.

Doblin, M.A., Baines, S., Cutter, L.S., Cutter, G.A., in prep. Biogeochemistry of Selenium in San Francisco Bay Part II: Seston and Phytoplankton. Estuar. Coast. Shelf Sci.

Dyer, K.R., 1997. Salt Balance. In: Estuaries: A Physical Introduction. John Wiley and Sons, London, UK, pp. 80.

Eide, A., Heen, K., 2002. Economic impacts of global warming; A study of the fishing industry in North Norway. Fish. Res. 56, 261-274.

Elrashidi, M.A., Adriano, D.C., Workman, S.M., Lindsay, W.L., 1987. Chemical equilibria of selenium in soils. Soil Sci. 144, 141-152.

Elrashidi, M.A., Adriano, D.C., Lindsay, W.L., 1989. Solubility, speciation, and transformations of selenium in soils. In: Selenium in Agriculture and the Environment. Soil Science Society of Agronomy, WI, pp. 51 - 63.

Emerson, S., Jahnke, R., Heggie, D., 1984. Sediment-water exchange in shallow water estuarine sediments. J. Mar. Res. 42, 709-730.

Fashem, M.J.R., Sarmiento, J.L., Slater, R.D., Ducklow, H.W.,Williams, R., 1993. Ecosystem behavior at Bermuda Station "S" and Ocean Weather Station "India": A general circulation model and observational analysis. Glob. Biogeochem. Cycles 7, 379-415.

Fischer, H.B., 1972. Mass transport mechanism in partially stratified estuaries. J. Fluid Mech. 5, 59-78.

Fisher, J.S., Reinfelder, J.R., 1991. Assimilation of selenium in the marine copepod *Acartia tonsa* studied with a radio tracer ratio method. Mar. Ecol. Prog. Ser. 70, 157-164.

Fowler, S.W., Benayoun, G., 1976. Accumulation and distribution of selenium in mussel and shrimp tissues. Bull. Environ. Contam. Toxicol. 16, 339-346.

Frechette, M., Bourget, E., 1985a. Food-liminted growth of *Mytilus edulis L.* in relation to the benthic boundary layer. Can. J. Fish. Aquat. Sci. 42, 1166-1170.

Frechette, M., Bourget, E., 1985b. Energy flow between the pelagic and benthic zones: Factors controlling particulate organic matter available to an intertidal mussel bed. Can. J. Fish. Aquat. Sci. 42, 1158-1165.

Frechette, M., Butman, C.A., Geyer, W.R., 1989. The importance of boundary-layer flows in supplying phytoplankton to the benthic suspension feeder, *Mytilus edulis*.

Limnol. Oceanogr. 34, 19-36.

Friedrichs, M., and Hofmann, E., 2001. Physical control of biological processes in the central equatorial Pacific Ocean. Deep Sea Res. I 48, 1023-1069.

Fuller, C.C., van Geen, A., Baskaran, M., Anima, R., 1999. Sediment chronology in San Francisco Bay, California defined by ^{210}Pb, ^{234}Th, ^{137}Cs, and $^{239,240}Pu$. Mar. Chem. 64, 7-27.

Geering, H.R., Cary, E.E., Jones, L.H.P., Allaway, W.H., 1968. Solubility and redox criteria for the possible forms of selenium in soils. Soil Sci. Amer. Proc. 32, 35-40.

Glenne, B., Selleck, R.E., 1969. Longitudinal estuarine diffusion in San Francisco Bay, California. Water Res. 3, 1-20.

Gobler, C.J., Donat, J.R., Consolvo, J.A., Sanudo-Wilhelmy, S.A., 2002. Physicochemical speciation of iron during coastal algal blooms. Mar. Chem. 77, 71-89.

Guentzel, J.L., Powell, R.T., Landing, W.M., Mason, R.P., 1996. Mercury associated with colloidal material in an estuarine and an open-ocean environment. Mar. Chem. 55, 177-188.

Guo,S., Wang, J., Xiong, L., Aiwen, Y., Li, D., 2002. A macro-scale and semi-distributed monthly water balance model to predict climate change impacts in China. J. Hydrol. in press.

Hammond, D.E., Fuller, C., Harmon, D., Hartman, B, Korosec, M., Miller, L.G., Rea, R., Warren, S., Berelson, W., Hager, S.W., 1985. Benthic fluxes in San Francisco Bay. Hydrobiologia 129, 69-90.

Hansen, D.V., Rattray, M. Jr., 1966. New dimensions in estuary classification. Limnol. Oceanogr. 11, 319-326.

Harris, J.R.W., Bale, A.J., Bayne, B.L., Mantoura, R.F.C, Morris, A.W., Nelson, L.A., Radford, P.J., Uncles, R.J., Weston, S.A., Widdow, J., 1984. A preliminary model of the dispersal and biological effect of toxins in the Tamar Estuary, England. Ecol. Model. 22, 253-284.

Harris, J.R.W., Gorley, R.N., 1998. An introduction to modeling estuaries with ECoS3. Available from Plymouth Marine laboratory, Prospect Place, Plymouth PL1 3DH, UK.

Howard, J.H., III, 1977. Geochemistry of selenium: formation of ferroselite and selenium behavior in the vicinity of oxidizing sulfide and uranium deposits. Geochim. Cosmochim. Acta 41, 1665-1678.

Hu, M., Yang, Y., Martin, J.M., Yin, K., Harrison, P.J., 1996. Preferential uptake of Se(IV) over Se (VI) and the production of dissolved organic Se by marine phytoplankton. Mar. Environ. Res. 44, 225-231.

Hutchinson, A., 1981. Plankton studies in San Francisco Bay. 5. Zooplankton species composition and abundance in the South Bay, 1980-1981. U.S. Geological Survey, Open-File Report 81-132.

Ikeda, T., 1974. Nutritional ecology of marine zooplankton. Mem. Fac. Fish., Hokkaido Univ. 22, 1-97.

Ippen, A.T., Harleman, D.R.F., 1961. One-dimensional analysis of salinity intrusion in estuaries. Tech. Bull. 5, Comm. Tidal Hydraul. Corps. Eng. US ARMY.

Ishimaru, T., Takeguchi, T., Fukuyo, Y., Kodama, M., 1989. The selenium requirement of *Gymnodinium nagasakiense*. In: Okaichi,T., Anderson, D.M., Nemoto, T. (Eds.), Red Tides: Biology, Environmental Science and Toxicology. Elsevier Science, NY, pp. 357-360.

Jay, D.A., Musiak, J.D., 1994. Particle trapping in estuarine tidal flows. J. Geophys. Res. C. Oceans 99, 445-460.

Jay, D.A., Smith, J.D., 1988. Residual circulation in and classification of shallow, stratified estuaries. In: Dronkers, J., van Leussen, W. (Eds.), Physical Processes in Estuaries. Springer-Verlag, Berlin, pp. 21-41.

Johns, C., Luoma, S.N., Elrod, V., 1988. Selenium accumulation in benthic bivalves and fine sediments of San Francisco Bay, the Sacramento-San Joaquin Delta, and selected tributaries. Estuar. Coast. Shelf Sci. 27, 381-396.

Jones, B., Turki, A., 1997. Distribution and speciation of heavy metals in surficial sediments from the Tees Estuary, northeast England. Mar. Pollut. Bull. 34, 768-779.

Kennish, M.J., 1990. Ecology of estuaries. Volume II. Biological Aspects, CRC PRESS, Boston, MA, pp. 391.

Klemes, V., 1986. Operational testing of hydrological simulation models. Hydrol. Sci. J. 131, 13-24.

Kolbl, G., 1995. Concepts for the identification and determination of selenium compounds in the aquatic environment. Mar. Chem. 48, 185-197.

Koseff, J.R., Holen, J.K., Monismith, S.G., Cloern, J.E., 1993. Coupled effects of

vertical mixing and benthic grazing on phytoplankton populations in shallow, turbid estuaries. J. Mar. Res. 51, 843-868.

Kozelka, P.B., Bruland, K.W., 1998. Chemical speciation of dissolved Cu, Zn, Cd, Pb in Narragansett Bay, Rhode Island. Mar. Chem. 60, 267-282.

Krone, R.B., 1962. Flume studies of transport of sediment in estuarial shoaling processes, Final Report, Hydraulics Engineering Research Laboratory, University of California, Berkely CA.

Kumar, H.D., Prakash,G., 1971. Toxicity of selenium to the Blue-green algae, *Anacystis Nidulans* and *Anabaena Variabilis*. Ann. Bot. 35, 697-705.

Lakin, H.W., 1973. Selenium in our environment. In: Kothny, E. (Ed.), Trace Elements in the Environment Amer. Chem. Soc., Washington, DC, pp. 123.

Lehman, P.W., 2000. The influence of climate on phytoplankton community biomass in San Francisco Bay Estuary. Limnol. Oceanogr. 45, 580-590.

Lemly, A.D., 1985. Toxicology of selenium in a freshwater reservoir: Implications for environmental hazard evaluation and safety. Ecotoxicol. Environ. Saf. 10, 314-338.

Li, Y.H., Gregory, S., 1974. Diffusion of ions in sea water and in deep sea sediments. Geochim. Cosmochim. Acta 38, 703-714.

Lindstrom, K., 1980. *Peridinium cinctum* bioassays of Se in Lake Arken. Arch. Hydrobiol. 82, 110.

Lindstrom, K., Rodhe,W., 1978. Selenium as a Micronutrient for the Dinoflagellate *Peridinium Cinctum Fa.* Westii. Mitt. Int. Ver. Theor. Angew. Limnol. 21, 1968.

Liu, Y.P., Millward, G.E., Harris, J.R.W., 1998. Modelling the distributions of dissolved Zn and Ni in the Tamar estuary using hydrodynamics coupled with chemical kinetics. Estuar. Coast. Shelf Sci. 47, 535-546.

Loder, T.C., Reichard, R.P., 1981. The dynamics of conservative mixing in estuaries. Estuaries 4 , 64-69.

Lucas, L.V., Cloern, J.E., Koseff, J.R., Monismith, S.G., Thompson, K.J., 1998. Does the Sverdrup critical depth model explain bloom dynamics in estuaries? J. Mar. Res. 56, 375-415.

Luoma, S.N., Presser, T., 2000. Forecasting selenium discharges to the San Francisco Bay-Delta Estuary. Ecological effects of a proposed San Luis Drain extension. USGS

Open File report 00-416, 340 pp.

Luoma, S. N., Johns, C., Fisher, N.S., Steinberg, N.A., Oremland, R.S., Reinfelder, J.R., 1992. Determination of selenium bioavailability to a benthic bivalve from particulate and dissolved pathways. Environ. Sci. Technol. 26, 485-491.

Mason, R.P., Lawson, N.M., Lawrence, A.L., Leaner, J.J., Lee, J.G., Sheu, G.R. 1999. Mercury in the Chesapeake Bay. Mar. Chem. 65, 77-96.

McCarthy, J.C., Taylor, W.R., Taft, J.L.. 1975. The dynamics of nitrogen and phosphorus cycling in the open waters of the Chesapeake Bay. In: Church,T.M. (Ed.), Marine Chemistry in the Coastal Environment. ACS symposium Series, PA, pp. 664-688.

McDonald, E.T., Cheng, T.R., 1997. A numerical model of sediment transport applied to San Francisco Bay, California. J. Marine Enc. Eng. 4, 1-41.

McLaughlin, D., 1995. Recent developments in hydrological data assimilation. Rev. Geophys. 33, 977-984.

Measures, C.I., Burton, J.D., 1978. Behaviour and speciation of dissolved selenium in estuarine water. Nature 273, 293-295.

Measures, C.I., McDuff, R.E., Edmon, J.M., 1980. Selenium redox chemistry at GEOSECS 1 re-occupation. Earth Planet Sci. Olett. 29, 120.

Menshutkin, V. V., Astrakhantsev, G. P. , Yegorova, N.B. , Rukhovets, L.A., Simo T.L., Petrova, N.A., 1998. Mathematical modeling of the evolution and current conditions of the Ladoga Lake ecosystem. Ecol. Model. 107, 1-24 .

Michel, P., Chiffoleau, J., Averty, B., Auger, D., Chartier, E., 1999. High resolution profiles for arsenic in the Seine Estuary. Seasonal variations and net fluxes to the English Channel. Cont. Shelf Res. 19, 2041-2061.

Miller, G.C., Zepp, R. G., 1979. Photoreactivity of aquatic pollutants sorbed on suspended sediments. Environ. Sci. Technol. 13, 860-863.

Millward, G.E., Moore, R.M., 1982. The adsorption of Cu, Mn and Zn by iron oxyhydrate in model estuarine solution. Water Res. 16, 981-985.

Monirul Qader Mirza, M., 2002. Global warming and changes in the probability of occurrence of floods in Bangladesh and implications. Global Environ. Change 12, 127-138.

Monsen, N.E., 2001. A study of sub-tidal transport in Suisun Bay and the Sacramento-San Joaquin Delta, California. PhD thesis. Stanford Univ.

Motovilov, Y.G, Gottschalk, L., Engeland, K., Rodhe, A., 1999. Validation of a distributed hydrological model against spatial observations. Agric. For. Meteorol. 98, 257-277.

Mwanuzi, F., De Smedt, F., 1999. Heavy metal distribution model under estuarine mixing. Hydrol. Process. 13, 789-804.

Neal, R. H., Sposito, G., Holtzclaw, K.M, Traina, S.J., 1987. Selenite adsorption on alluvial soils: Solution composition effects. Soil Sci. Soc. Am. J. 51, 1165-1169.

Nichols, F.H., Cloern, J.E., Luoma, S.N., Peterson, D.H., 1986. The modification of an Estuary. Science 231, 567-573.

Nival, P., Nival, S., 1976. Particle retention efficiencies of an herbivorous copepod, *Acartia clausi*(adult and copepodite stages): effects on grazing. Limnol. Oceanogr. 21, 24-38.

Nriagu, J.O., Pacyna, J.M., 1988. Quantitative assessment of worldwide contamination of air, water and soils by trace metals. Nature 333, 134-139.

Nyffeler, U.P., Li, Y.H., Santshi, P.H., 1984. A kinetic approach to describe trace-element distribution between particles and solution in natural systems. Geochim. Cosmochim. Acta 48, 1513-1522.

Ohlendorf, H.M., Lowe, R.W., Kelly, P.R., Harvey, T.E., 1986 Selenium and heavy metals in San Francisco diving ducks. J. Wildl. Manage. 50, 64-71.

Omline, M., Brun, R., Reichert, P., 2001. Biogeochemical model of Lake Zuerich: sensitivity, identifiability and uncertainty analysis. Ecol. Model. 141, 105-123.

Oremland, R. S., Hollibaugh, J.T., Maest, M.A., Presser, T.S., Miller, L.G., Culbertson, C.W., 1989. Selenate reduction to elemental selenium, by anerobic bacteria in sediments and cultures: Biogeochemical significance of a novel, sulfate-independent respiration. Appl. Environ. Microbiol. 55, 2333-2343.

Paffenhofer, G.A., 1971. Grazing and ingestion rates of nauplii, copepodids and adults of the marine planktonic copepod *Calanus heloglandicus*. Mar. Bio. 11, 286-298.

Parson, T. R., LeBrasseur, R. J., 1970. The availability of food to different trophic levels in the marine food chain. In: Steel, J.H. (Ed.), Marine Food Chains. Oliver and Boyd, Edinburgh, Scotland, pp. 325-343.

Parsons, T.R., Takahashi, M., Hargrave, B., 1984. In: Biological Oceanographic Processes. Pergamon Press, NY, pp. 147

Paucot, H., Wollast, R., 1997. Transport and transformation of trace metals in the Scheldt Estuary. Mar. Chem. 58, 229-244.

Perrin, C. , Michel, C., Andréassian, V., 2001. Does a large number of parameters enhance model performance? Comparative assessment of common catchment model structures on 429 catchments. J. Hydrol. 242, 275-301.

Peters, G.M., Maher, W.A., Krikowa, F., Roach, A.C., Jeswani, H.K., Barford, J.P., Gomes, V.G., Reible, D.D., 1999. Selenium in sediments, pore waters and benthic infauna of Lake Macquarie, New South Wales, Australia. Mar. Environ. Res. 47, 491-508.

Peterson, D.H., Conomos, T.J., 1975. Implications of Seasonal Chemical and Physical Factors on the Production of Phytoplankton in Northern San Francisco Bay Proceedings of a Workshop on Algae Nutrient Relationships in the San Francisco Bay and Delta, held at Clear Lake, California November 8-10, 1973: The San Francisco Bay and Estuarine Association, pp. 147-165.

Peterson, D.H., Festa, J.F., 1984. Numerical simulation of phytoplankton productivity in partially mixed estuaries. Estuar. Coast. Shelf Sci. 19, 563-589.

Peterson, D.H., Festa, J.F., Conomos, T.J., 1978. Numerical simulation of dissolved silica in the San Francisco Bay. Estuar. Coastal Mar. Sci. 7. 99-116.

Peterson, D.H., Smith, R.E., Hager, S.W., Harmon, D.D., Herndon, R.E., Schemel, L.E., 1985. Interannual variability in dissolved inorganic nutrients in Northern San Francisco Bay Estuary. Hydrobiologia 129, 27-58.

Peterson, D.H., Perry, M.J., Bencala, K.E., Talbot, M.C., 1987. Phytoplankton productivity in relation to light intensity: a simple equation. Estuar. Coast. Shelf Sci. 24, 813-832.

Platt, T., Jassby, A.D., 1976. The relationship between photosynthesis and light for natural assemblages of coastal marine phytoplankton. J. Phycol. 12, 421-430.

Power, M., 1993. The predictive validation of ecological and environmental models. Ecol. Modell. 68, 33-50.

Prandle, D., 1985. On salinity regimes and the vertical structure of residual flows in narrow tidal estuaries. Est. Coast. Shelf Sci. 20, 615-635.

Presser, T.S., Piper, D.Z., 1998. Mass balance approach to selenium cycling through the San Joaquin Valley, sources to river to Bay. In: Grankenberger,W., Engberg, R.A. (Eds.), Environmental Chemistry of Selenium. Marcel Dekker Inc., NY, pp. 153-182.

Price, N.M., Thompson, P.A., Harrison, P.J., 1987. Selenium an essential element for the growth of the coastal marine diatom *Thalassiosira pseudonana* (Bacillariophyceae). J. Phycol. 23, 1-9.

Pritchard, D.W., 1952. Salinity distribution and circulation in the Chesapeake Bay estuaries system. J. Mar. Res. 11, 106-123.

Purkerson, D.G., Doblin, M.A., Bollens, S.M., Luoma, S.N., Cutter, G.A., accepted 2002. Selenium in San Francisco Bay Zooplankton: Potential Effects of Hydrodynamics and Food Web Interactions. Estuaries.

Reamer, D.C., Zoller, W.H., 1980. Selenium biomethylation products from soil and sewage sludge. Science 208, 500-502.

Reinfelder, J.R., Fisher, N.S., 1994. The assimilation of elements in marine planktonic bivalve larvae. Limnol. Oceanogr. 39, 12-20.

Riedel, G.F., Ferrier, D., Sanders, J.G., 1991. Uptake of selenium by fresh-water phytoplankton. Water Air Soil Poll. 57, 23-30.

Riedel, G.F., Sanders, J.G., Gilmour, C.C., 1996. Uptake, transformation, and impact of selenium in freshwater phytoplankton and bacterioplankton communities. Aquat. Microb. Ecol. 11, 43-51.

Robbe, D., Marchandise, P., Gouleau, D., 1985. Heavy metals in the sediments of the Loire Estuary. Water Res. 19, 1555-1563.

Rosenfeld, I., Beath, O.A., 1964. Selenium: Geobotany, biochemistry, toxicity, and nutrition. Academic Press, NY, pp. 159.

Salomons, W., Forstner, U., 1984. Interactions with Ligands, Particulate matter and organisms. In: Metals in the Hydrocycle. Springer-Verlag, Berlin, pp. 5-62.

Sandholm, M., Oksanen, H.E., Pesonen, L., 1973. Uptake of selenium by aquatic organisms. Limn. Oceanogr. 18, 496-498.

Sarathchandra, S.U., Watkinson, J.H., 1981. Oxidation of elemental selenium to selenite by *Bacillus megaterium*. Science 211, 600-601.

Schelkat, C.E., Dowdle, P.R., Lee, B., Luoma, S.N., Oremland, R.S., 2000. Bioavailability of particle-associated Se to the bivalve *Potamocorbula amurensis*. Environ. Sci. and Technol. 34, 4504-4510.

Schlesinger, S., Crosbie, R.E., Gagne, R.E., Innis, G.S., Lalwani, C.S., Loch, J., Sylvester, J., Wright, R.D., Kheir, N., Bartos, D., 1979. Terminology for model credibility: SCS technical committee on model credibility. Simulation 32, 103-104.

Schoellhamer, D.H., 2001. Influence of salinity, bottom topography, and tides on locations of estuarine turbidity maxima in northern San Francisco Bay. In: McAnally, W.H., Mehta, A.J., (Eds.), Coastal and Estuarine Fine Sediment Transport Processes. Elsevier Science B.V., Amsterdam, Netherlands, pp. 343-357.

Schoellhamer, D.H., 2002. Comparison of the basin-scale effect of dredging operations and natural estuarine processes on suspended sediment concentration. Estuaries 25, 488-495.

Schwarz, K., Foltz, C.M., 1957. Selenium as integral part of factor 3 against dietary necrotic liver degeneration. J. Am. Chem. Soc. 79, 3292.

Selleck, R.E., 1968. A model of mixing and dispersion in San Francisco Bay. J. Water Poll. Control Fed. 40, 1873-1886.

Shamberger, R.J., 1983. Biogeochemistry of Selenium. Plenum Press, New York. 334 pp.

Simmons, H.B., 1955. Some effects of upland discharge on estuarine hydraulics. Proc. Am. Soc. Civ. Eng. 81, No. 792.

Smith, P.E., Cheng, R.T., Burau, J.R., Simpson, M.R., 1991. Gravitational circulation in a tidal strait. In: Hydraulic Engineering 1991 Conference Proceedings, WW Division of the American Society of Civil Engineers, Nashville, TN, pp. 429-434.

Sokolova, Y.G., Pilipchuk, M.D., 1973. Geochemistry of selenium in sediments in the N.W. part of the Pacific Ocean. Geokhimiya 10, 1537-1546.

Stadtman, T.C., 1990. Selenium biochemistry. Annu. Rev. Biochem. 59, 111-127.

Starfield, A.M., Beleloch, A.L., 1991. Building models for conservation and wildlife management. Burgess International Group Inc., Endina, MN, pp. 253.

Stumm, W.W., Morgan, J.J., 1981. Aquatic chemistry: an introduction emphasizing chemical equilibria in natural waters. Wiley; Chichester, United Kingdom, 583 pp.

Sunda, W.G., 1988. Trace metal interactions with marine phytoplankton. Biol.

Oceanogr. 6, 411-422.

Takayanagi, K., Belzile, N., 1988. Profiles of dissolved and acid-leachable selenium in a sediment core from the lower St. Lawrence estuary. Mar. Chem. 24, 307-314.

Takayanagi, K., Cossa, D., 1985. Speciation of dissolved selenium in the upper St. Lawrence Estuary. In: Siglo, A.C., Hatteri, A. (Eds.), Marine and Estuarine Geochemistry. Lewis Publishers, Inc., MI, pp. 275-284.

Takayanagi, K., Wong, G.T.F., 1984. Total selenium and selenium (IV) in the James River Estuary and Southern Chesapeake Bay. Estuar. Coast. Shelf Sci. 18, 113-119.

Tamari, Y. 1978. Studies on the state analysis of selenium in sediments. Ph.D. dissertation, Kinki University.

Tebes-Stevens, C.L., Espinoza, F., Valocchi, A.J. 2001. Evaluating the sensitivity of a subsurface multicomponent reactive transport model with respect to transport and reaction parameters. J. Contam. Hydrol. 52, 3-27.

Thompson, J.K. 2000. Two stories of phytoplankton control by bivalves in San Francisco Bay: The importance of spatial and temporal distribution of bivalves. J. Shellfish Res. 19, 612.

Ullman, W.J., Aller, R.C., 1982. Diffusion coefficients in nearshore marine sediments. Limnol. Oceanogr. 27, 552-556.

Uncles, R.J., 1981. A Note on Tidal Asymmetry in the Severn Estuary. Estuar. Coast. Shelf Sci. 13, 419-432.

Uncles, R.J., Bale, A.J., Howland, R.J.M, Morris, A.W., Elliott, R.C.A., 1983. Salinity of surface water in a partially-mixed estuary, and its dispersion at low run-off. Oceanogl. Acta 6, 289-296.

Uncles, R. J., Peterson, D.H., 1996. The long-term salinity field in San Francisco Bay. Cont. Shelf Res. 16, 2005-2039.

van der Sloot, H.A., Hoede, D., Wijkstra, J., Duinker, J.C., Nolting, R.F., 1985. Anionic species of V, As, Se, Mo, Sb, Te, and W in the Scheldt and Rhine Estuaries and the Southern Bight (North Sea). Est. Coastal Shelf Sci. 21, 633-651.

van Geen, A., Luoma, S.N., 1999. The impact of human activities on sediments of San Francisco Bay, California: an overview. Mar. Chem. 64, 1-6.

Vandermeulen, J.H., Foda, A., 1988. Cycling of selenite and selenate in marine

phytoplankton. Mar. Biol. 98, 115-123.

Velinsky, D.J., 1987. The Geochemistry of selenium and sulfur in a coastal salt marsh. PhD thesis. Old Dominion University.

Velinsky, D.J., Cutter, G.A., 1990. Determination of elemental selenium and pyrite-selenium in sediments. Anal. Chim. Acta 235, 419-425.

Velinsky, D.J., Cutter, G.A., 1991. Geochemistry of selenium in a coastal salt marsh. Geochem. Cosmochim. Acta 55, 179-191.

Vidal, J., 1980. Physioecology of zooplankton. Mar. Biol. 56, 111-211.

Walters, R.A., Gartner, J.W., 1985. Subtidal sea level and current variations in the northern reach of San Francisco Bay. Estuar. Coast. Shelf Sci. 21, 17-32.

Weglarczyk, S., 1998. The interdependence and applicability of some statistical quality measured for hydrological models. J. Hydrol. 206, 98-103.

Wehr, J.D., Brown, L.., 1985. Selenium requirement of a bloom forming planktonic alga from softwater and acidified lakes. Can. J. Fish. Aquat. Sci. 42, 1783-1788.

Wendel, A., 1992. Biochemical functions of selenium, Phosphorous, sulfur, silicon. Relat. Elem. 67, 405-415.

Werner, I., Hollibaugh, J.T., 1993. *Potamocorbula amurensis* : Comparison of clearance rates and assimilation efficiencies for phytoplankton and bacterioplankton. Limnol. Oceanogr. 38, 949-964.

Wong, D., Oliveira, L. 1991a. Effects of selenite and selenate on the growth and motility of seven species of marine microalgae. Can. J. Fish. Aquat. Sci. 48, 1193-1200.

Wong, D., Oliveira, L., 1991b. Effects of selenite and selenate toxicity on the ultrastructure and physiology of three species of marine microalgae. Can. J. Fish. Aquat. Sci. 48, 1201-1211.

Wrench, J.J., 1978. Selenium metabolism in the marine phytoplankters *Tetraselmis tetrathele* and *Dunaliella minuta*. Mar. Biol. 49, 231-236.

Wrench, J.J., Measures, C.I., 1982. Temporal variations in dissolved selenium in a coastal ecosystem. Nature 299, 431-433.

Zawislanski, P.T., McGrath, A.E., 1998. Selenium Cycling in Estuarine Wetlands: Overview and New Results from the San Francisco Bay. In: Frankenberger, W.T., Jr.,

Engberg, R.A., (Eds.), Environmental Chemistry of Selenium. Macrcel Dekker, Inc., NY, pp. 223-242.

Zhang, L., Walsh, R.S., Cutter, G.A., 1998 Estuarine cycling of carbonyl sulfide: production and sea-air flux. Mar. Chem. 61, 127-142.

Zhang, P., Sparks. D. L., 1990. Kinetics of selenate and selenite adsorption/desorption at the Geothite/Water interface. Environ. Sci. Technol. 24, 1848-1856.

Zhang Y., Moore, J.N., 1996a. Selenium fractionation and speciation in a wetland sediment. Env. Sci. Technol. 30, 2613-2619.

Zhang, Y., Moore, J.N., 1996b. Reduction potential of selenate in wetland sediment. J. Environ. Qual. 26, 910-916.

Zuwaylif, F.H. 1979. General Applied Statistics Third Edition. Addison-Wesley Publishing Company, California, 384 pp.

Zwolsman, J.J.G., van Eck, J.T.M., 1999. Geochemistry of major elements and trace metals in suspended matter of the Scheldt Estuary, southwest Netherlands. Mar. Chem. 66, 91-111.

APPENDICES

APPENDIX A

Input Data Files for the Model

Table A1
Refinery input for various years

Refinery	Date	Total Se (nmol L^{-1})	Se IV (nmol L^{-1})	Se VI (nmol L^{-1})	Se -II (nmol L^{-1})	R[a]
Chevron	1986	250 ± 120	168 ± 97	52 ± 59	27 ± 38	49.6
Exxon	1986	943 ± 170	734 ± 52	185 ± 173	31 ± 44	7.7
Pacific	1986	97 ± 18	ND	74 ± 39	18 ± 20	0.8
Shell	1986	1784 ± 161	1417 ± 289	266 ± 60	74 ± 105	14.2
Tosco	1986	303 ± 38	27 ± 17	144 ± 106	131 ± 50	9.5
Rodeo	1986	1700 ± 393	1150 ± 90	386 ± 545	156 ± 221	9.0
Chevron	1987	250 ± 120	168 ± 97	52 ± 59	27 ± 38	49.6
Exxon	1987	943 ± 170	734 ± 52	185 ± 173	31 ± 44	7.7
Pacific	1987	97 ± 18	ND	74 ± 39	18 ± 20	0.8
Shell	1987	1784 ± 161	1417 ± 289	266 ± 60	74 ± 105	14.2
Tosco	1987	303 ± 38	27 ± 17	144 ± 106	131 ± 50	9.5
Rodeo	1987	1700 ± 393	1150 ± 90	386 ± 545	156 ± 221	9.0
Chevron	1988	421 ± 169	270 ± 130	85 ± 68	78 ± 79	49.6
Exxon	1988	1439 ± 888	787 ± 608	58 ± 76	580± 749	7.7
Pacific	1988	130 ± 22	68 ± 58	7 ± 6	54 ± 38	0.8
Shell	1988	972 ± 557	613 ± 482	127 ± 151	196 ± 278	14.2
Tosco	1988	245 ± 108	87 ± 70	25 ± 36	128 ± 142	9.5
Rodeo	1999	1172 ± 303	731 ± 318	251 ± 281	161 ± 215	8.2
Chevron	1999	102 ± 3	102 ± 3	217 ± 9	15 ± 13	22.6
Exxon	1999	368 ± 6	23 ± 7	181 ± 5	164± 8	7.2
Pacific	1999	ND	ND	ND	ND	ND
Shell	1999	254 ± 6	109 ± 20	156 ± 9	ND	20
Tosco	1999	107 ± 1	6.3 ± 2	64 ± 20	37 ± 3	15.5
Rodeo	1999	340 ± 4	318 ± 2	8.5 ± 1	14 ± 4	8.2

[a]Average discharge rate of refinery effluent (x 10^6 l d^{-1}). Data obtained from the State of California Water Resources Control Board.
NA = non-detectable (<0.01 nmol L^{-1})

Table A2
Refinery input for years where discharge was not available but total loads were

	1997 (nmol d^{-1})	1998 (nmol d^{-1})
Chevron		
Selenite	3.5	1.5
Selenate	3.1	2.5
Organic selenide	2.7	1.7
Shell		
Selenite	7.8	3.5
Selenate	6.8	6.0
Organic selenide	6.0	4.1
Exxon		
Selenite	7.9	3.6
Selenate	6.8	6.1
Organic selenide	6.1	4.1
Tosco		
Selenite	0.8	0.7
Selenate	0.7	1.0
Organic selenide	0.6	0.8
Rodeo		
Selenite	10.0	3.6
Selenate	9.3	7.0
Organic selenide	8.1	4.8
Total Discharge	79.0	51.0

Table A3
Selenium associated with BEPS for the model

Distance (km)	BEPS Elemental Se (nmol g^{-1})	BEPS SE IV+VI (nmol g^{-1})	BEPS Org. Se -II (nmol g^{-1})
0	1.560	0.664	0.996
14.9768	1.560	0.664	0.996
25.409	1.385	0.740	1.518
27.4511	1.400	0.594	0.891
41.6088	1.255	0.571	0.91775
53.0312	1.5	0.774	1.161
66.1934	1.25	0.664	1.011

Table A4
Bathymetry of the San Francisco Bay

Distance (km)	Depth (m)
0	7.07
3	7.07
7	7.07
10	8.60
13	10.12
16	11.64
20	13.17
23	10.88
26	7.53
29	7.53
32	7.53
35	11.34
38	17.74
41	19.26
44	19.26
47	19.26
50	18.20
53	14.08
56	10.58
59	9.97
62	11.34
66	12.56
69	16.67
72	19.87
79	16.06
82	17.13
85	22.77
98	47.91
101	60.41

Table A5
Initial salinity for the Northern Reach

Distance (km)	$S_{initial}$
0	0.08
3.18	2.10
19.097	1.41
21.62	1.93
26.701	2.80
30.846	5.96
35.713	5.49
41.606	8.01
46.854	9.23
50.003	10.10
53.271	11.48
58.093	13.72
62.466	14.79
68.347	18.53
72.688	20.90
76.664	22.71
83.495	25.00
87.549	26.78
93.236	27.89

APPENDIX B

Sensitivity Analysis for Varying Parameters by Different Percentages

Table B1
Sensitivity analysis of changing parameters by 25 %, 50 %, and 75 % during high flow (December to May) and low flow months (June to November) with dash lines indicate that the model is insensitive to varying that parameter $|S_{c,k}| < 0.15$

Parameter	D ∑Se	D Se IV	D Se VI	D Org. Se –II	Part. ∑Se	Part. Se IV+VI	Part Se O	Part. Org Se-II
High Flow								
c								
+25 %	-	-	-	-	1.07	1.13	1.22	0.81
+50 %	-	-	-	-	1.08	1.12	1.22	0.81
+75 %	-	-	-	-	1.08	1.13	1.22	0.82
k_1								
+25 %	-	-	-	-	-	-	-	-
+50 %	-	-	-	-	-	-	-	-
+75 %	-	-	-	-	-	-	-	-
River Flow								
+25 %	1.00	0.17	2.68	0.15	0.45	0.54	0.33	0.49
+50 %	1.01	0.17	2.68	0.15	0.47	0.54	0.32	0.49
+75 %	1.00	0.18	2.69	0.15	0.46	0.54	0.32	0.48
Refinery								
+25 %	-	-	-	-	-	-	-	-
+50 %	-	-	-	-	-	-	-	-
+75 %	-	-	-	-	-	-	-	-
I_λ								
+25 %	-	-	-	-	-	-	-	0.35
+50 %	-	-	-	-	-	-	-	0.36
+75 %	-	-	-	-	-	-	-	0.34
Low Flow								
c								
+25 %	-	-	-	-	0.84	1.41	1.32	0.18
+50 %	-	-	-	-	0.84	1.42	1.31	0.18
+75 %	-	-	-	-	0.85	1.43	1.32	0.18
k_1								
+25 %	-	-	-	-	-	-	-	0.15
+50 %	-	-	-	-	-	-	-	0.15
+75 %	-	-	-	-	-	-	-	0.15
River Flow								
+25 %	0.21	-0.34	0.39	-	0.96	1.45	1.39	0.22
+50 %	0.22	-0.33	0.39	-	0.97	1.46	1.40	0.22
+75 %	0.23	-0.35	0.39	-	0.95	1.45	1.39	0.22
Refinery								
+25 %	0.33	0.33	0.36	0.28	0.23	-	-	0.36
+50 %	0.33	0.32	0.36	0.27	0.24	-	-	0.38
+75 %	0.33	0.33	0.36	0.29	0.23	-	-	0.37

Table B1 Continued

Parameter	D ∑Se	D Se IV	D Se VI	D Org. Se –II	Part. ∑Se	Part. Se IV+VI	Part Se O	Part. Org Se-II
I_λ								
+25 %	-	-	-	-	0.95	-	-	1.56
+50 %	-	-	-	-	0.95	-	-	1.56
+75 %	-	-	-	-	0.95	-	-	1.56

Table B2

Sensitivity analysis of changing parameters by + 25% and -25 % during high flow months (December to May) and low flow months (June to November) with Dash lines indicate that the model is insensitive to varying that parameter $|S_{c,k}| < 0.15$

Parameter	D ∑Se	D Se IV	D Se VI	D Org. Se –II	Part. ∑Se	Part. Se IV+VI	Part Se O	Part. Org Se-II
High Flow								
c								
+25 %	-	-	-	-	1.07	1.13	1.22	0.81
-25 %	-	-	-	-	1.06	-1.13	-1.22	-0.80
k_4								
+25 %	-	-	-	-	-	-	-	-
-25 %	-	-	-	-	-	-	-	-
River Flow								
+25 %	1.00	0.17	2.68	0.15	0.45	0.54	0.33	0.49
-25 %	-1.01	-0.17	-2.67	-0.14	0.46	-0.53	-0.33	-0.49
Refinery								
+25 %	-	-	-	-	-	-	-	-
-25 %	-	-	-	-	-	-	-	-
I_λ								
+25 %	-	-	-	-	-	-	-	0.35
-25 %	-	-	-	-	-	-	-	-0.36
Low Flow								
c								
+25 %	-	-	-	-	0.84	1.41	1.32	0.18
-25 %	-	-	-	-	0.84	-1.41	-1.32	-0.18
k_4								
+25 %	-	-	-	-	-	-	-	0.15
-25	-	-	-	-	-	-	-	-0.15
River Flow								
+25 %	0.21	-0.34	0.39	-	0.96	1.45	1.39	0.22
-25 %	-0.22	+0.35	-0.39	-	0.95	-1.44	-1.40	-0.20
Refinery								
+25 %	0.33	0.33	0.36	0.28	0.23	-	-	0.36
-25 %	-0.33	-0.33	-0.36	-0.27	0.23	-	-	-0.36
I_λ								
+25 %	-	-	-	-	0.95	-	-	1.56
-25 %	-	-	-	-	0.95	-	-	-1.56

APPENDIX C

Model Validation

Table C1. Observed selenium in North San Francisco Bay for 1987 and 1988

Distance (km)	Salinity	Diss. ΣSe (nmol L^{-1})	Diss. Se IV (nmol L^{-1})	Diss. Se VI (nmol L^{-1})	Diss. Org. Se -II (nmol L^{-1})
8 October 1987					
85	21.36	1.58 ± 0.06	0.94 ± 0.06	ND[a]	0.54 ± 0.08
78	28.18	2.49 ± 0.13	0.91 ± 0.02	0.45 ± 0.06	1.13 ± 0.14
75	26.69	2.26 ± 0.11	1.54 ± 0.05	0.52 ± 0.06	0.20 ± 0.11
70	23.92	3.32 ± 0.29	1.36 ± 0.08	2.00 ± 0.22	ND
67	22.74	2.32 ± 0.09	1.42 ± 0.02	0.43 ± 0.02	0.47 ± 0.09
65	20.46	3.06 ± 0.04	1.42 ± 0.06	1.60 ± 0.20	ND
58	20.48	3.38 ± 0.11	1.56 ± 0.06	0.65 ± 0.10	1.17 ± 0.14
55	17.98	2.98 ± 0.11	1.33 ± 0.09	1.72 ± 0.20	ND
50	15.91	3.02 ± 0.16	1.54 ± 0.09	0.78 ± 0.18	0.70 ± 0.23
48	17.15	3.64 ± 0.13	0.89 ± 0.02	2.76 ± 0.10	ND
42	15.48	2.99 ± 0.19	1.40 ± 0.06	1.82 ± 0.25	ND
40	14.06	3.21 ± 0.22	1.58 ± 0.10	1.26 ± 0.16	0.37 ± 0.26
36	12.01	3.04 ± 0.18	0.67 ± 0.03	2.44 ± 0.15	ND
33	8.48	2.33 ± 0.08	0.49 ± 0.03	1.07 ± 0.03	0.77 ± 0.08
28	6.83	1.80 ± 0.12	0.40 ± 0.01	1.31 ± 0.01	ND
17 December 1987					
85	26.57	1.63 ± 0.07	0.84 ± 0.06	0.44 ± 0.07	0.35 ± 0.08
78	26.23	2.43 ± 0.12	0.39 ± 0.02	1.60 ± 0.10	0.44 ± 0.16
75	25.64	1.48 ± 0.03	0.74 ± 0.04	0.49 ± 0.06	0.25 ± 0.06
70	25.62	2.31 ± 0.07	0.90 ± 0.04	0.56 ± 0.08	0.85 ± 0.10
67	23.63	1.71 ± 0.11	1.13 ± 0.04	0.71 ± 0.10	ND
65	23.95	2.54 ± 0.06	1.26 ± 0.02	0.50 ± 0.06	0.78 ± 0.08
58	23.83	2.61 ± 0.12	1.52 ± 0.01	0.81 ± 0.11	0.28 ± 0.16
55	23.56	2.02 ± 0.03	1.12 ± 0.02	0.88 ± 0.10	ND
50	21.36	1.86 ± 0.06	1.00 ± 0.06	0.90 ± 0.06	ND
48	21.53	3.00 ± 0.15	0.96 ± 0.05	1.36 ± 0.12	0.68 ± 0.19
42	19.65	2.54 ± 0.15	1.26 ± 0.04	1.02 ± 0.18	ND
40	16.36	2.07 ± 0.14	0.91 ± 0.02	0.91 ± 0.09	0.25 ± 0.17
36	13.31	1.98 ± 0.05	1.16 ± 0.02	0.48 ± 0.02	0.34 ± 0.05
28	6.64	1.58 ± 0.07	0.61 ± 0.01	0.72 ± 0.06	0.25 ± 0.09
15 March 1988					
85	30.33	0.96 ± 0.06	0.29 ± 0.01	0.55 ± 0.05	ND
78	29.66	1.61 ± 0.03	0.44 ± 0.03	1.24 ± 0.07	ND
75	28.22	1.54 ± 0.06	0.63 ± 0.03	0.57 ± 0.07	0.34 ± 0.08
70	26.77	1.98 ± 0.03	0.71 ± 0.02	0.78 ± 0.06	0.49 ± 0.06
67	24.73	1.88 ± 0.13	0.67 ± 0.02	0.88 ± 0.04	0.33 ± 0.13
65	24.92	2.12 ± 0.05	0.81 ± 0.06	0.87 ± 0.10	0.44 ± 0.09
58	23.76	2.01 ± 0.14	1.04 ± 0.04	0.96 ± 0.13	ND
55	21.71	2.54 ± 0.05	1.29 ± 0.06	1.19 ± 0.06	ND
50	22.85	2.53 ± 0.15	1.08 ± 0.02	1.00 ± 0.02	0.45 ± 0.15

Table C1 Continued

Distance (km)	Salinity	Diss. ΣSe (nmol L^{-1})	Diss. Se IV (nmol L^{-1})	Diss. Se VI (nmol L^{-1})	Diss. Org. Se -II (nmol L^{-1})
48	22.15	2.11 ± 0.01	1.29 ± 0.03	0.85 ± 0.09	ND
42	20.84	3.18 ± 0.17	1.08 ± 0.02	1.98 ± 0.02	ND
40	16.43	2.83 ± 0.08	1.25 ± 0.08	0.97 ± 0.09	0.61 ± 0.09
36	14.70	2.79 ± 0.09	1.18 ± 0.06	1.57 ± 0.12	ND
33	12.43	2.69 ± 0.17	1.17 ± 0.04	0.81 ± 0.11	0.71 ± 0.20
28	10.68	2.48 ± 0.12	1.12 ± 0.04	1.28 ± 0.12	ND

*ND = non-detectable (<0.01 nmol L^{-1})

Table C2

Model-generated salinity, dissolved selenium and its speciation for October 8 1987

Distance (km)	Salinity	Diss. ΣSe (nmol L^{-1})	Diss. Se IV (nmol L^{-1})	Diss. Se VI (nmol L^{-1})	Diss. Org. Se -II (nmol L^{-1})
1.43	0.67	1.12	0.14	0.64	0.34
4.29	1.62	1.30	0.23	0.70	0.37
7.14	2.57	1.50	0.32	0.77	0.42
10.00	3.59	1.68	0.41	0.82	0.45
12.86	4.52	1.83	0.49	0.86	0.48
15.71	5.32	1.98	0.57	0.90	0.51
18.57	6.38	2.13	0.66	0.92	0.54
21.43	7.56	2.31	0.77	0.95	0.59
24.29	8.69	2.55	0.86	1.05	0.64
27.14	9.73	2.70	0.95	1.06	0.68
30.00	10.66	2.85	1.03	1.10	0.71
32.86	11.40	3.01	1.10	1.17	0.75
35.71	12.03	3.15	1.15	1.23	0.77
38.57	12.82	3.29	1.21	1.27	0.81
41.43	13.76	3.51	1.29	1.38	0.84
44.29	14.93	3.75	1.39	1.49	0.87
50.00	16.62	3.67	1.41	1.39	0.87
52.86	17.60	3.53	1.39	1.29	0.86
55.71	18.88	3.46	1.36	1.25	0.85
58.57	19.99	3.29	1.29	1.17	0.82
61.43	20.97	3.13	1.22	1.12	0.79
64.29	21.86	3.00	1.15	1.08	0.76
67.14	22.69	2.85	1.08	1.02	0.74
70.00	23.46	2.64	1.02	0.91	0.71
72.86	24.24	2.50	0.96	0.85	0.69
75.71	25.00	2.34	0.90	0.77	0.66
81.43	26.48	2.08	0.74	0.74	0.60
84.29	27.28	1.86	0.64	0.65	0.57
87.14	28.06	1.59	0.54	0.52	0.53
90.00	28.77	1.40	0.45	0.45	0.50
92.86	29.45	1.24	0.36	0.40	0.47
95.71	30.09	1.11	0.28	0.38	0.45
98.57	31.18	0.86	0.15	0.30	0.40

Table C3

Model-generated salinity, dissolved selenium and its speciation for December 17, 1987

Distance (km)	Salinity	Diss. ΣSe (nmol L^{-1})	Diss. Se IV (nmol L^{-1})	Diss. Se VI (nmol L^{-1})	Diss. Org. Se -II (nmol L^{-1})
1.43	0.14	1.42	0.09	0.96	0.37
4.29	0.54	1.39	0.13	0.87	0.38
7.14	1.09	1.41	0.18	0.83	0.40
10.00	1.74	1.49	0.25	0.82	0.43
12.86	2.45	1.60	0.31	0.84	0.45
15.71	3.25	1.73	0.38	0.87	0.48
18.57	4.14	1.88	0.46	0.90	0.52
21.43	5.20	2.05	0.55	0.94	0.56
24.29	6.31	2.22	0.65	0.97	0.60
27.14	7.39	2.36	0.74	0.99	0.63
30.00	8.35	2.48	0.83	0.99	0.67
32.86	9.26	2.59	0.91	0.99	0.69
35.71	10.19	2.69	0.99	0.98	0.72
38.57	11.10	2.79	1.07	0.96	0.76
41.43	12.15	2.90	1.16	0.94	0.79
44.29	13.24	2.98	1.24	0.92	0.82
50.00	15.64	2.97	1.28	0.86	0.83
52.86	16.70	2.94	1.29	0.83	0.82
55.71	17.93	2.89	1.29	0.79	0.82
58.57	19.22	2.78	1.24	0.74	0.80
61.43	20.36	2.67	1.20	0.69	0.77
64.29	21.40	2.55	1.15	0.65	0.75
67.14	22.37	2.44	1.10	0.62	0.73
70.00	23.28	2.33	1.04	0.58	0.71
72.86	24.14	2.23	0.99	0.55	0.69
75.71	24.98	2.13	0.93	0.53	0.67
81.43	26.55	1.83	0.76	0.46	0.60
84.29	27.27	1.67	0.67	0.44	0.57
87.14	27.93	1.51	0.57	0.41	0.54
90.00	28.50	1.35	0.47	0.38	0.50
92.86	28.96	1.20	0.37	0.35	0.47
95.71	29.34	1.03	0.26	0.33	0.44
98.57	29.64	0.85	0.15	0.30	0.40

Table C4

Model-generated salinity, dissolved selenium and its speciation for March 15 1988

Distance (km)	Salinity	Diss. ΣSe (nmol L^{-1})	Diss. Se IV (nmol L^{-1})	Diss. Se VI (nmol L^{-1})	Diss. Org. Se -II (nmol L^{-1})
1.43	0.87	0.83	0.16	0.32	0.35
4.29	1.80	1.07	0.25	0.45	0.38
7.14	2.65	1.27	0.33	0.54	0.40
10.00	3.50	1.54	0.41	0.70	0.43
12.86	4.31	1.69	0.48	0.75	0.46
15.71	5.07	1.91	0.55	0.88	0.48
18.57	6.01	2.07	0.64	0.92	0.51
21.43	7.02	2.33	0.73	1.06	0.54
24.29	8.03	2.48	0.81	1.09	0.58
27.14	9.00	2.73	0.90	1.22	0.61
30.00	9.92	2.85	0.98	1.24	0.64
32.86	10.72	2.98	1.04	1.27	0.66
35.71	11.45	3.07	1.11	1.28	0.69
38.57	12.33	3.18	1.18	1.29	0.71
41.43	13.31	3.31	1.26	1.30	0.75
44.29	14.44	3.42	1.35	1.29	0.78
50.00	16.26	3.34	1.32	1.26	0.76
52.86	17.39	3.27	1.28	1.24	0.74
55.71	18.69	3.19	1.26	1.20	0.73
58.57	19.83	3.04	1.18	1.17	0.69
61.43	20.91	2.89	1.10	1.13	0.66
64.29	21.93	2.76	1.03	1.10	0.63
67.14	22.91	2.61	0.97	1.05	0.60
70.00	23.86	2.46	0.91	0.98	0.57
72.86	24.83	2.30	0.85	0.90	0.55
75.71	25.80	2.18	0.80	0.85	0.53
81.43	27.70	1.89	0.64	0.80	0.46
84.29	28.71	1.72	0.55	0.75	0.42
87.14	29.68	1.55	0.47	0.70	0.38
90.00	30.62	1.34	0.39	0.60	0.35
92.86	31.53	1.13	0.31	0.50	0.32
95.71	32.39	0.93	0.24	0.40	0.29
98.57	33.50	0.70	0.15	0.30	0.25

Table C5
Observed data for April 23 1986

Distance (km)	Salinity	Phyto (μg chl L^{-1})	TSM (mg L^{-1})	D Σ Se (nmol L^{-1})	D Se IV (nmol L^{-1})	D Se VI (nmol L^{-1})	D Org. Se - II (nmol L^{-1})	Part. Σ Se (nmol L^{-1})
0	0.09	2.50	20.13	1.41 ± 0.04	0.20 ± 0.02	1.01 ± 0.02	0.2 ± 0.04	0.04 ± 0.01
23.40	0.53	3.92	41.86	2.63 ± 0.02	0.25 ± 0.01	2.26 ± 0.02	ND	0.19 ± 0.01
34.27	2.11	9.21	63.69	2.94 ± 0.18	0.41 ± 0.01	2.38 ± 0.14	ND	0.27 ± 0.02
43.92	6.06	12.16	58.86	2.99 ± 0.13	0.59 ± 0.02	2.31 ± 0.02	ND	0.26 ± 0.01
46.73	7.67	14.37	27.65	2.70 ± 0.17	0.44 ± 0.02	1.53 ± 0.09	0.73 ± 0.17	0.19 ± 0.02
49.87	9.15	13.78	23.90	2.66 ± 0.06	0.60 ± 0.03	1.10 ± 0.02	0.96 ± 0.15	0.15 ± 0.01
52.86	12.30	9.71	13.88	2.61 ± 0.20	0.62 ± 0.02	0.86 ± 0.14	1.13 ± 0.20	0.14 ± 0.01
59.74	14.69	12.28	17.92	1.81 ± 0.08	0.46 ± 0.02	0.96 ± 0.04	0.39 ± 0.08	0.16 ± 0.01
75.28	16.49	12.23	31.64	1.57 ± 0.08	0.48 ± 0.01	0.83 ± 0.02	0.26 ± 0.08	0.16 ± 0.01
81.19	17.67	4.31	25.35	1.71 ± 0.07	0.40 ± 0.02	0.81 ± 0.02	0.50 ± 0.07	0.10 ± 0.01
83.52	20.19	3.12	26.57	1.59 ± 0.04	0.43 ± 0.02	0.72 ± 0.03	0.44 ± 0.05	ND
85.17	20.96	3.20	27.49	1.58 ± 0.07	0.33 ± 0.02	0.92 ± 0.04	0.33 ± 0.07	0.11 ± 0.01
87.59	23.73	4.00	29.91	1.31 ± 0.09	0.36 ± 0.01	0.57 ± 0.02	0.38 ± 0.09	0.09 ± 0.01
91.50	25.74	3.32	17.52	1.22 ± 0.03	0.34 ± 0.01	0.88 ± 0.02	ND	0.09 ± 0.01
96.47	25.72	4.08	24.64	2.13 ± 0.02	0.27 ± 0.02	0.69 ± 0.02	1.17 ± 0.03	0.10 ± 0.01
98.47	26.82	4.72	24.64	1.89 ± 0.04	0.27 ± 0.02	1.00 ± 0.03	0.62 ± 0.07	0.11 ± 0.01

ND = non-detectable (< 0.01 nmol L^{-1})

Table C6
Observed data for September 23 1986

Distance (km)	Salinity	Phyto (μg chl L^{-1})	TSM (mg L^{-1})	D Σ Se (nmol L^{-1})	D Se IV (nmol L^{-1})	D Se VI (nmol L^{-1})	D Org. Se - II (nmol L^{-1})	Part. Σ Se (nmol L^{-1})
0.00	0.07	0.65	28.42	0.61 ± 0.07	0.24 ± 0.01	0.29 ± 0.02	0.08 ± 0.03	0.14 ± 0.01
19.10	0.39	2.20	59.53	1.40 ± 0.05	0.35 ± 0.01	0.49 ± 0.01	0.56 ± 0.05	0.32 ± 0.01
21.62	1.51	2.78	49.24	1.62 ± 0.12	0.35 ± 0.01	0.73 ± 0.01	0.54 ± 0.07	0.34 ± 0.02
26.70	3.61	3.57	42.84	1.85 ± 0.16	0.60 ± 0.03	0.88 ± 0.06	0.37 ± 0.17	0.39 ± 0.02
30.85	5.10	6.87	33.46	2.52 ± 0.07	0.73 ± 0.02	0.91 ± 0.04	0.88 ± 0.07	0.32 ± 0.01
35.72	7.57	6.84	30.71	2.74 ± 0.07	0.83 ± 0.04	0.59 ± 0.05	1.32 ± 0.08	0.29 ± 0.01
41.61	9.65	7.52	18.04	3.64 ± 0.16	1.30 ± 0.04	1.26 ± 0.06	1.08 ± 0.16	0.26 ± 0.03
46.85	11.06	5.46	15.12	3.16 ± 0.09	1.32 ± 0.04	1.06 ± 0.06	0.78 ± 0.09	NS
50.00	11.56	3.06	22.70	2.49 ± 0.09	1.13 ± 0.03	0.70 ± 0.05	0.66 ± 0.10	0.30 ± 0.01
53.27	13.22	4.29	16.20	2.79 ± 0.02	1.01 ± 0.03	0.95 ± 0.11	0.83 ± 0.11	0.16 ± 0.01
58.09	13.89	2.75	16.76	2.66 ± 0.04	1.05 ± 0.02	1.14 ± 0.08	0.47 ± 0.08	0.22 ± 0.01
62.47	17.45	3.13	23.60	2.88 ± 0.07	1.20 ± 0.04	0.90 ± 0.07	0.78 ± 0.09	0.19 ± 0.02
68.35	19.46	4.50	44.16	2.35 ± 0.07	1.00 ± 0.05	0.76 ± 0.07	0.59 ± 0.12	0.28 ± 0.02
72.69	20.97	4.89	63.75	2.75 ± 0.12	1.12 ± 0.01	1.03 ± 0.07	0.60 ± 0.14	NS
76.67	24.01	3.59	31.78	2.11 ± 0.04	0.65 ± 0.02	0.85 ± 0.04	0.61 ± 0.05	0.28 ± 0.01
83.50	27.33	3.69	14.36	1.94 ± 0.05	0.66 ± 0.02	0.76 ± 0.04	0.52 ± 0.06	0.13 ± 0.01
87.59	27.77	4.73	25.60	1.39 ± 0.04	0.42 ± 0.01	0.96 ± 0.05	ND	NS
93.24	31.30	2.44	13.47	1.16 ± 0.01	0.39 ± 0.01	0.21 ± 0.01	0.56 ± 0.01	0.12 ± 0.01
95.26	31.95	2.42	11.96	1.24 ± 0.03	0.46 ± 0.01	0.51 ± 0.03	0.27 ± 0.04	0.08 ± 0.01
97.23	31.58	3.45	10.72	0.90 ± 0.01	0.34 ± 0.01	0.36 ± 0.01	0.20 ± 0.01	0.16 ± 0.01

ND = non-detectable (< 0.01 nmol L^{-1}) and NS = no sample

Table C7

Observed data from November 11 1997 for salinity, phytoplankton, TSM and dissolved selenium and its species

Distance (km)	Salinity	Phyto (μg chl L^{-1})	TSM (mg L^{-1})	D Σ Se (nmol L^{-1})	D Se IV (nmol L^{-1})	D Se VI (nmol L^{-1})	D Org. Se - II (nmol L^{-1})
0.00	0.56	1.75	15.79	1.51 ± 0.07	0.21 ± 0.00	1.74 ± 0.03	ND
11.46	2.79	2.14	19.36	2.14 ± 0.06	0.30 ± 0.04	2.11 ± 0.09	ND
14.39	4.10	0.92	19.44	2.62 ± 0.10	0.34 ± 0.02	1.60 ± 0.07	0.68 ± 0.12
18.70	6.83	1.65	18.14	2.43 ± 0.12	0.39 ± 0.01	1.97 ± 0.03	0.07 ± 0.13
19.27	6.80	2.09	7.593	NS	NS	NS	NS
25.85	9.14	2.25	30.25	2.55 ± 0.06	0.43 ± 0.01	1.44 ± 0.02	0.68 ± 0.06
28.32	9.62	1.44	8.74	2.85 ± 0.07	0.62 ± 0.04	1.41 ± 0.07	0.83 ± 0.09
31.15	12.70	1.38	24.00	2.99 ± 0.06	0.62 ± 0.04	0.83 ± 0.04	1.54 ± 0.06
31.29	13.82	0.95	12.03	2.78 ± 0.12	0.86 ± 0.06	1.01 ± 0.06	0.91 ± 0.12
36.54	15.31	0.93	13.00	2.43 ± 0.18	0.22 ± 0.02	1.03 ± 0.04	1.18 ± 0.18
43.47	19.16	0.64	13.81	2.51 ± 0.03	0.24 ± 0.01	1.60 ± 0.02	0.67 ± 0.03
44.08	16.96	0.84	13.68	2.66 ± 0.05	0.92 ± 0.02	1.48 ± 0.08	0.26 ± 0.09
47.78	18.80	0.58	11.49	2.61 ± 0.09	0.93 ± 0.04	1.02 ± 0.07	0.66 ± 0.11
53.16	21.74	2.20	9.65	2.70 ± 0.04	0.80 ± 0.03	1.15 ± 0.07	0.76 ± 0.07
55.63	22.72	1.09	10.57	2.99 ± 0.03	0.82 ± 0.03	1.14 ± 0.13	1.03 ± 0.13
60.35	25.98	1.38	7.77	4.05 ± 0.05	0.46 ± 0.02	1.90 ± 0.18	1.69 ± 0.19
63.05	26.31	1.57	9.29	2.13 ± 0.03	0.70 ± 0.05	1.15 ± 0.06	0.28 ± 0.04
68.01	26.67	1.15	8.93	1.85 ± 0.02	0.68 ± 0.04	0.96 ± 0.10	0.21 ± 0.09
76.87	28.54	1.37	8.13	1.76 ± 0.07	0.51 ± 0.03	0.99 ± 0.07	0.27 ± 0.10
80.70	29.79	0.81	7.01	1.69 ± 0.08	0.50 ± 0.03	0.58 ± 0.11	0.61 ± 0.13
95.94	31.97	1.49	9.36	1.28 ± 0.02	0.31 ± 0.01	0.60 ± 0.03	0.38 ± 0.03

ND = non-detectable (< 0.01 nmol L^{-1}) and NS = no sample

Table C8
Observed data from November 6 1997 for particulate selenium and its species

Distance (km)	Salinity	Part Σ Se (nmol L^{-1})	Part Se O (nmol L^{-1})	Part Se IV+VI (nmol L^{-1})	Part Org. Se -II (nmol L^{-1})
0.00	0.56	0.11 ± 0.01	0.17 ± 0.00	0.10 ± 0.00	ND
11.46	2.79	0.16 ± 0.00	0.17 ± 0.00	0.02 ± 0.01	ND
14.39	4.10	0.13 ± 0.01	0.07 ± 0.04	0.03 ± 0.01	0.03 ± 0.04
18.70	6.83	0.10 ± 0.01	0.11 ± 0.02	0.07 ± 0.00	ND
19.27	6.80	0.14 ± 0.00	0.09 ± 0.05	0.03 ± 0.01	0.02 ± 0.05
25.85	9.14	0.18 ± 0.00	0.05 ± 0.01	0.06 ± 0.00	0.07 ± 0.01
28.32	9.62	0.18 ± 0.01	0.02 ± 0.01	0.06 ± 0.000	0.10 ± 0.02
31.15	12.70	0.22 ± 0.00	0.08 ± 0.00	0.07 ± 0.000	0.07 ± 0.00
31.29	13.82	0.12 ± 0.02	0.10 ± 0.00	0.02 ± 0.01	ND
36.54	15.31	0.10 ± 0.01	0.05 ± 0.00	0.04 ± 0.00	0.01 ± 0.01
43.47	19.16	0.14 ± 0.02	0.01 ± 0.00	0.06 ± 0.05	0.08 ± 0.05
44.08	16.96	0.11 ± 0.00	0.03 ± 0.02	0.01 ± 0.01	0.07 ± 0.02
47.78	18.80	0.10 ± 0.01	0.08 ± 0.00	0.05 ± 0.01	ND
53.16	21.74	0.15 ± 0.02	0.02 ± 0.01	0.04 ± 0.00	0.10 ± 0.02
55.63	22.72	0.13 ± 0.00	0.04 ± 0.00	0.06 ± 0.01	0.04 ± 0.1
60.35	25.98	0.10 ± 0.00	0.04 ± 0.00	0.02 ± 0.00	0.04 ± 0.00
63.05	26.31	0.16 ± 0.02	0.01 ± 0.01	0.01 ± 0.00	0.14 ± 0.02
68.01	26.67	0.12 ± 0.01	0.05 ± 0.01	0.05 ± 0.00	0.02 ± 0.01
76.87	28.54	0.08 ± 0.01	0.01 ± 0.00	ND	0.07 ± 0.01
80.70	29.79	0.08 ± 0.01	0.02 ± 0.00	0.56 ± 0.01	ND
95.94	31.97	0.10 ± 0.03	0.04 ± 0.00	0.04 ± 0.00	0.02 ± 0.02

ND = non-detectable (< 0.01 nmol L^{-1})

Table C9

Model-generated salinity, TSM, phytoplankton, dissolved and particulate selenium for April 23, 1986

Distance (km)	D ΣSe (nmol L^{-1})	D Se IV (nmol L^{-1})	D Se VI (nmol L^{-1})	D Org. Se -II (nmol L^{-1})	Phyto (µg L^{-1})	TSM (mg L^{-1})	Part ΣSe (nmol L^{-1})	Salinity
1.43	1.08	0.12	0.63	0.33	2.23	36.80	0.10	0.01
4.29	1.36	0.13	0.91	0.33	3.13	38.10	0.11	0.02
7.14	1.59	0.14	1.10	0.34	3.88	37.94	0.11	0.05
10.00	1.81	0.16	1.28	0.38	4.47	37.10	0.12	0.07
12.86	2.10	0.18	1.49	0.43	4.99	35.37	0.12	0.11
15.71	2.45	0.21	1.74	0.49	5.42	33.05	0.12	0.15
18.57	2.72	0.24	1.93	0.55	5.74	31.67	0.11	0.20
21.43	2.64	0.25	1.85	0.54	6.22	34.37	0.12	0.32
24.29	2.64	0.27	1.82	0.55	6.71	37.90	0.13	0.48
27.14	2.64	0.30	1.78	0.56	7.21	43.62	0.15	0.69
30.00	2.64	0.33	1.74	0.57	7.70	51.77	0.18	0.98
32.86	2.65	0.37	1.69	0.59	8.22	62.48	0.21	1.36
35.71	2.67	0.42	1.64	0.61	8.67	72.47	0.24	1.78
38.57	2.68	0.46	1.59	0.63	9.02	79.66	0.26	2.16
41.43	2.70	0.50	1.55	0.65	9.34	85.73	0.28	2.59
44.29	2.69	0.53	1.50	0.66	9.66	89.36	0.29	3.13
50.00	2.59	0.55	1.37	0.67	10.35	87.62	0.32	4.73
52.86	2.55	0.56	1.32	0.67	10.56	82.10	0.31	5.42
55.71	2.50	0.57	1.26	0.67	10.71	71.22	0.30	6.19
58.57	2.41	0.55	1.19	0.67	10.82	58.14	0.28	7.21
61.43	2.32	0.54	1.13	0.66	10.84	47.01	0.26	8.36
64.29	2.24	0.53	1.06	0.65	10.75	38.39	0.25	9.65
67.14	2.15	0.52	1.00	0.63	10.54	32.19	0.24	11.05
70.00	2.06	0.50	0.94	0.62	10.21	27.83	0.23	12.58
72.86	1.97	0.49	0.88	0.61	9.79	24.79	0.22	14.18
75.71	1.87	0.46	0.81	0.59	9.27	22.46	0.22	15.90
81.43	1.62	0.39	0.69	0.55	7.99	18.94	0.19	19.43
84.29	1.51	0.36	0.63	0.52	7.27	17.51	0.18	21.15
87.14	1.38	0.32	0.56	0.50	6.37	16.02	0.16	23.06
90.00	1.24	0.27	0.49	0.47	5.29	14.45	0.13	25.15
92.86	1.10	0.23	0.42	0.45	4.08	12.80	0.10	27.27
95.71	0.95	0.18	0.35	0.42	2.94	11.16	0.06	29.14
98.57	0.85	0.15	0.30	0.40	2.20	10.00	0.03	30.25

Table C10

Model-generated salinity, TSM, phytoplankton, dissolved and particulate selenium for April 23, 1986

Distance (km)	D ΣSe (nmol L^{-1})	D Se IV (nmol L^{-1})	D Se VI (nmol L^{-1})	D Org. Se -II (nmol L^{-1})	Phyto (µg L^{-1})	TSM (mg L^{-1})	Part ΣSe (nmol L^{-1})	Salinity
1.43	1.14	0.09	0.69	0.35	2.12	29.49	0.06	0.11
4.29	1.34	0.12	0.84	0.38	2.89	30.00	0.28	0.44
7.14	1.48	0.16	0.91	0.40	3.67	45.00	0.42	0.89
10.00	1.60	0.21	0.96	0.43	4.42	50.00	0.51	1.47
12.86	1.73	0.27	1.00	0.46	4.97	52.00	0.51	2.04
15.71	1.85	0.33	1.03	0.49	5.34	50.00	0.52	2.59
18.57	2.00	0.40	1.08	0.53	5.71	45.00	0.51	3.32
21.43	2.11	0.48	1.08	0.55	6.04	41.00	0.46	4.23
24.29	2.17	0.57	1.05	0.56	6.28	37.00	0.41	5.20
27.14	2.23	0.65	1.01	0.57	6.43	33.00	0.38	6.14
30.00	2.28	0.72	0.97	0.58	6.52	30.00	0.36	7.03
32.86	2.33	0.79	0.94	0.59	6.56	27.00	0.35	7.76
35.71	2.37	0.84	0.92	0.61	6.58	24.00	0.35	8.44
38.57	2.43	0.91	0.90	0.62	6.59	22.00	0.35	9.26
41.43	2.52	1.00	0.87	0.64	6.58	20.00	0.36	10.25
44.29	2.62	1.10	0.85	0.67	6.55	18.00	0.36	11.44
50.00	2.63	1.15	0.81	0.68	6.48	14.00	0.36	13.30
52.86	2.62	1.16	0.79	0.67	6.41	13.54	0.36	14.41
55.71	2.59	1.16	0.76	0.67	6.31	13.19	0.36	15.82
58.57	2.51	1.13	0.73	0.65	6.21	12.90	0.35	17.08
61.43	2.42	1.09	0.70	0.63	6.10	12.64	0.35	18.23
64.29	2.33	1.05	0.67	0.62	5.98	12.41	0.34	19.31
67.14	2.24	1.00	0.64	0.60	5.85	12.19	0.32	20.34
70.00	2.15	0.95	0.62	0.58	5.70	11.99	0.31	21.32
72.86	2.06	0.90	0.59	0.57	5.54	11.79	0.29	22.32
75.71	1.97	0.85	0.56	0.56	5.35	11.59	0.27	23.32
81.43	1.73	0.71	0.50	0.51	4.89	11.21	0.22	25.32
84.29	1.58	0.62	0.47	0.49	4.59	11.00	0.19	26.42
87.14	1.43	0.53	0.44	0.47	4.26	10.80	0.16	27.51
90.00	1.29	0.44	0.41	0.45	3.88	10.61	0.13	28.53
92.86	1.16	0.36	0.37	0.43	3.46	10.43	0.10	29.51
95.71	1.04	0.27	0.34	0.42	3.00	10.26	0.07	30.43
98.57	0.85	0.15	0.30	0.40	2.20	10.00	0.03	31.76

Table C11

Model-generated salinity, TSM, phytoplankton, dissolved and particulate selenium and its speciation for November 6, 1997 fot the re

Distance (km)	D ΣSe (nmol L^{-1})	D Se IV (nmol L^{-1})	D Se VI (nmol L^{-1})	D Org. Se -II (nmol L^{-1})	Phyto (µg L^{-1})	TSM (mg L^{-1})	P. ΣSe (nmol L^{-1})	P. Se O (nmol L^{-1})	P. Se IV+VI (nmol L^{-1})	P. Org. Se -II (nmol L^{-1})	Salinity
1.43	1.64	0.08	1.15	0.40	1.61	18.15	0.06	0.02	0.03	0.02	0.70
4.29	1.66	0.10	1.13	0.42	1.63	18.09	0.09	0.04	0.03	0.02	1.53
7.14	1.68	0.12	1.11	0.46	1.63	18.02	0.13	0.07	0.03	0.03	2.32
10.00	1.73	0.15	1.08	0.50	1.62	17.63	0.18	0.11	0.04	0.04	3.17
12.86	1.78	0.18	1.05	0.55	1.60	17.12	0.21	0.13	0.04	0.04	3.93
15.71	1.83	0.20	1.03	0.59	1.57	16.81	0.23	0.14	0.05	0.05	4.59
18.57	1.91	0.25	1.01	0.66	1.52	16.47	0.26	0.15	0.05	0.05	5.48
21.43	2.02	0.30	0.98	0.75	1.44	16.01	0.27	0.16	0.05	0.06	6.52
24.29	2.14	0.35	0.95	0.84	1.36	15.62	0.26	0.15	0.05	0.06	7.54
27.14	2.27	0.40	0.94	0.93	1.27	15.34	0.24	0.13	0.05	0.06	8.48
30.00	2.40	0.45	0.92	1.02	1.18	15.14	0.22	0.11	0.04	0.07	9.34
32.86	2.51	0.49	0.92	1.10	1.10	15.00	0.21	0.10	0.04	0.07	10.02
35.71	2.60	0.52	0.91	1.17	1.03	14.90	0.20	0.10	0.04	0.07	10.61
38.57	2.73	0.57	0.91	1.26	0.94	14.77	0.20	0.09	0.04	0.07	11.34
41.43	2.90	0.62	0.91	1.37	0.83	14.61	0.20	0.08	0.04	0.07	12.26
44.29	3.20	0.71	0.91	1.58	0.71	14.39	0.19	0.08	0.04	0.08	13.45
50.00	3.27	0.75	0.90	1.62	0.61	14.06	0.18	0.07	0.04	0.08	15.20
52.86	3.23	0.76	0.89	1.58	0.62	13.86	0.18	0.06	0.03	0.08	16.20
55.71	3.13	0.77	0.87	1.50	0.63	13.57	0.18	0.06	0.03	0.08	17.57
58.57	2.96	0.74	0.82	1.40	0.65	13.31	0.17	0.06	0.03	0.08	18.80
61.43	2.79	0.71	0.77	1.31	0.71	13.07	0.17	0.06	0.03	0.08	19.89
64.29	2.63	0.68	0.72	1.23	0.78	12.84	0.17	0.05	0.03	0.08	20.88
67.14	2.48	0.64	0.68	1.16	0.86	12.62	0.16	0.05	0.03	0.08	21.81
70.00	2.34	0.61	0.64	1.09	0.94	12.41	0.16	0.05	0.03	0.08	22.68
72.86	2.20	0.57	0.61	1.03	1.02	12.20	0.15	0.05	0.03	0.08	23.56
75.71	2.08	0.54	0.57	0.96	1.11	11.98	0.15	0.05	0.03	0.07	24.44
81.43	1.80	0.46	0.51	0.83	1.27	11.54	0.13	0.04	0.03	0.06	26.16
84.29	1.64	0.41	0.47	0.76	1.38	11.29	0.12	0.04	0.02	0.06	27.13
87.14	1.48	0.36	0.44	0.69	1.49	11.03	0.10	0.03	0.02	0.05	28.09
90.00	1.34	0.31	0.40	0.62	1.61	10.80	0.09	0.03	0.02	0.04	28.98
92.86	1.20	0.27	0.37	0.56	1.74	10.57	0.07	0.02	0.02	0.03	29.79
95.71	1.07	0.22	0.35	0.50	1.88	10.36	0.06	0.02	0.01	0.02	30.55

Table C11 Continued

Distance (km)	D ΣSe (nmol L^{-1})	D Se IV (nmol L^{-1})	D Se VI (nmol L^{-1})	D Org. Se -II (nmol L^{-1})	Phyto (µg L^{-1})	TSM (mg L^{-1})	P. ΣSe (nmol L^{-1})	P. Se O (nmol L^{-1})	P. Se IV+VI (nmol L^{-1})	P. Org. Se -II (nmol L^{-1})	Salinity
98.57	0.85	0.15	0.30	0.40	2.20	10.00	0.03	0.01	0.01	0.01	31.80

APPENDIX D

Predictive Simulations

Table D1

High flow conditions (April) with flow from Vernalis for the San Joaquin River with no Delta removal effect and 38 mol d^{-1} of refinery input (57 % as selenate)

Distance (km)	D ΣSe (nmol L^{-1})	D Se IV (nmol L^{-1})	D Se VI (nmol L^{-1})	D Org. Se -II (nmol L^{-1})	Phyto (µg L^{-1})	TSM (mg L^{-1})	P. ΣSe (nmol L^{-1})	P. Se O (nmol L^{-1})	P. Se IV+VI (nmol L^{-1})	P. Org. Se -II (nmol L^{-1})	Salinity
1.43	0.50	0.11	0.00	0.39	1.75	35.19	0.09	0.04	0.03	0.03	0.00
4.29	0.50	0.11	0.02	0.38	1.95	34.22	0.09	0.04	0.03	0.03	0.02
7.14	0.54	0.11	0.06	0.37	2.19	33.80	0.09	0.04	0.03	0.03	0.05
10.00	0.62	0.11	0.13	0.38	2.45	34.14	0.09	0.03	0.03	0.03	0.10
12.86	0.72	0.12	0.21	0.39	2.67	35.39	0.09	0.04	0.03	0.03	0.17
15.71	0.84	0.13	0.30	0.41	2.85	37.37	0.10	0.04	0.03	0.03	0.27
18.57	1.00	0.14	0.42	0.44	3.05	41.54	0.11	0.04	0.03	0.04	0.41
21.43	1.18	0.15	0.55	0.48	3.22	47.79	0.13	0.05	0.04	0.04	0.60
24.29	1.38	0.17	0.69	0.52	3.33	54.64	0.15	0.05	0.05	0.05	0.83
27.14	1.56	0.18	0.83	0.55	3.38	60.73	0.18	0.06	0.06	0.06	1.11
30.00	1.73	0.20	0.95	0.59	3.35	65.38	0.20	0.07	0.07	0.06	1.42
32.86	1.88	0.21	1.05	0.62	3.28	68.31	0.22	0.07	0.07	0.07	1.74
35.71	2.01	0.22	1.14	0.64	3.17	71.40	0.23	0.08	0.08	0.07	2.09
38.57	2.15	0.23	1.24	0.67	2.99	75.41	0.25	0.08	0.08	0.08	2.52
41.43	2.30	0.24	1.35	0.71	2.80	78.93	0.27	0.09	0.09	0.09	3.05
44.29	2.45	0.26	1.45	0.74	2.63	77.97	0.28	0.10	0.10	0.09	3.69
50.00	2.58	0.26	1.56	0.75	2.63	69.07	0.29	0.10	0.10	0.10	4.98
52.86	2.64	0.27	1.61	0.76	2.70	65.78	0.30	0.10	0.10	0.10	5.85
55.71	2.66	0.27	1.64	0.75	2.74	56.77	0.30	0.10	0.10	0.10	6.92
58.57	2.65	0.27	1.64	0.75	2.78	47.87	0.30	0.10	0.09	0.10	7.98
61.43	2.62	0.27	1.62	0.74	2.92	41.16	0.30	0.10	0.09	0.11	9.10
64.29	2.58	0.27	1.58	0.73	3.09	36.36	0.30	0.10	0.09	0.11	10.30
67.14	2.51	0.26	1.53	0.71	3.22	32.93	0.30	0.10	0.09	0.11	11.58
70.00	2.42	0.26	1.47	0.69	3.31	30.37	0.30	0.10	0.09	0.11	12.94
72.86	2.32	0.25	1.40	0.67	3.37	28.25	0.30	0.10	0.09	0.11	14.41

Table D1 Continued

Distance (km)	D ΣSe (nmol L^{-1})	D Se IV (nmol L^{-1})	D Se VI (nmol L^{-1})	D Org. Se -II (nmol L^{-1})	Phyto (µg L^{-1})	TSM (mg L^{-1})	P. ΣSe (nmol L^{-1})	P. Se O (nmol L^{-1})	P. Se IV+VI (nmol L^{-1})	P. Org. Se -II (nmol L^{-1})	Salinity
75.71	2.21	0.24	1.32	0.65	3.39	26.33	0.29	0.10	0.09	0.10	15.99
81.43	1.94	0.22	1.11	0.60	3.34	22.74	0.27	0.09	0.08	0.09	19.42
84.29	1.78	0.21	1.00	0.57	3.26	20.83	0.25	0.09	0.07	0.09	21.36
87.14	1.61	0.20	0.87	0.54	3.14	18.85	0.22	0.08	0.07	0.08	23.39
90.00	1.43	0.19	0.74	0.50	2.97	16.81	0.19	0.07	0.06	0.07	25.49
92.86	1.25	0.18	0.60	0.47	2.76	14.69	0.15	0.05	0.04	0.05	27.67
95.71	1.07	0.17	0.47	0.44	2.53	12.57	0.10	0.04	0.03	0.03	29.84
98.57	0.85	0.15	0.30	0.40	2.20	10.00	0.03	0.01	0.01	0.01	32.50

Table D2

Low flow conditions (November) with flow from Vernalis for the San Joaquin River with no Delta removal effect and 38 mol d^{-1} of refinery input (57 % as selenate)

Distance (km)	D ΣSe (nmol L^{-1})	D Se IV (nmol L^{-1})	D Se VI (nmol L^{-1})	D Org. Se -II (nmol L^{-1})	Phyto (µg L^{-1})	TSM (mg L^{-1})	P. ΣSe (nmol L^{-1})	P. Se O (nmol L^{-1})	P. Se IV+VI (nmol L^{-1})	P. Org. Se -II (nmol L^{-1})	Salinity
1.43	1.25	0.08	0.83	0.34	1.57	18.00	0.05	0.02	0.01	0.02	0.24
4.29	1.48	0.09	1.01	0.38	1.58	26.72	0.21	0.06	0.10	0.05	0.73
7.14	1.60	0.10	1.09	0.41	1.58	30.73	0.27	0.08	0.13	0.06	1.29
10.00	1.69	0.12	1.14	0.43	1.57	31.35	0.28	0.08	0.13	0.07	1.94
12.86	1.75	0.13	1.17	0.45	1.55	29.85	0.25	0.07	0.12	0.06	2.61
15.71	1.80	0.14	1.20	0.47	1.52	28.37	0.24	0.07	0.11	0.07	3.27
18.57	1.86	0.15	1.22	0.49	1.47	26.34	0.22	0.06	0.09	0.06	4.12
21.43	1.92	0.16	1.25	0.51	1.40	23.67	0.19	0.05	0.07	0.06	5.06
24.29	1.97	0.18	1.26	0.53	1.32	21.16	0.16	0.04	0.06	0.06	6.04
27.14	2.01	0.19	1.28	0.55	1.22	19.30	0.14	0.03	0.05	0.06	7.02
30.00	2.05	0.20	1.29	0.57	1.12	18.04	0.13	0.03	0.04	0.06	7.97
32.86	2.08	0.21	1.29	0.58	1.03	17.25	0.12	0.03	0.04	0.06	8.79
35.71	2.10	0.21	1.30	0.59	0.95	16.74	0.12	0.02	0.04	0.06	9.53
38.57	2.12	0.22	1.30	0.61	0.85	16.23	0.12	0.02	0.03	0.06	10.44

Table D2 Continued

Distance (km)	D ΣSe (nmol L^{-1})	D Se IV (nmol L^{-1})	D Se VI (nmol L^{-1})	D Org. Se -II (nmol L^{-1})	Phyto (µg L^{-1})	TSM (mg L^{-1})	P. ΣSe (nmol L^{-1})	P. Se O (nmol L^{-1})	P. Se IV+VI (nmol L^{-1})	P. Org. Se -II (nmol L^{-1})	Salinity
41.43	2.15	0.23	1.30	0.62	0.74	15.73	0.11	0.02	0.03	0.06	11.47
44.29	2.18	0.24	1.30	0.64	0.64	15.21	0.11	0.02	0.03	0.06	12.67
50.00	2.11	0.24	1.25	0.62	0.59	14.54	0.11	0.02	0.03	0.06	14.53
52.86	2.05	0.23	1.21	0.60	0.61	14.21	0.11	0.02	0.03	0.06	15.68
55.71	1.96	0.23	1.14	0.58	0.63	13.83	0.11	0.02	0.03	0.06	17.04
58.57	1.87	0.23	1.07	0.57	0.64	13.52	0.11	0.02	0.03	0.06	18.21
61.43	1.78	0.22	1.01	0.55	0.69	13.24	0.10	0.02	0.03	0.06	19.31
64.29	1.71	0.22	0.95	0.54	0.77	12.98	0.10	0.02	0.03	0.06	20.36
67.14	1.63	0.22	0.89	0.52	0.85	12.73	0.10	0.02	0.03	0.05	21.38
70.00	1.57	0.21	0.84	0.51	0.93	12.49	0.09	0.02	0.03	0.05	22.36
72.86	1.50	0.21	0.79	0.50	1.01	12.24	0.09	0.02	0.02	0.05	23.35
75.71	1.43	0.20	0.74	0.49	1.09	11.99	0.08	0.02	0.02	0.05	24.34
81.43	1.29	0.19	0.63	0.47	1.27	11.50	0.07	0.01	0.02	0.04	26.24
84.29	1.21	0.18	0.57	0.45	1.38	11.24	0.07	0.01	0.02	0.03	27.26
87.14	1.13	0.18	0.51	0.44	1.50	10.99	0.06	0.01	0.02	0.03	28.25
90.00	1.06	0.17	0.46	0.43	1.63	10.74	0.05	0.01	0.01	0.02	29.22
92.86	0.99	0.16	0.41	0.42	1.78	10.50	0.04	0.01	0.01	0.02	30.17
95.71	0.93	0.16	0.36	0.41	1.94	10.28	0.04	0.01	0.01	0.01	31.06
98.57	0.85	0.15	0.30	0.40	2.20	10.00	0.03	0.01	0.01	0.01	32.27

Table D3
High flow conditions (April) with flow from Vernalis for the San Joaquin River with Delta removal effect and 38 mol d^{-1} of refinery input (57 % as selenate)

Distance (km)	D ΣSe (nmol L^{-1})	D Se IV (nmol L^{-1})	D Se VI (nmol L^{-1})	D Org. Se -II (nmol L^{-1})	Phyto (µg L^{-1})	TSM (mg L^{-1})	P. ΣSe (nmol L^{-1})	P. Se O (nmol L^{-1})	P. Se IV+VI (nmol L^{-1})	P. Org. Se -II (nmol L^{-1})	Salinity
1.43	0.50	0.11	0.00	0.39	1.77	35.19	0.09	0.03	0.03	0.03	0.00
4.29	0.55	0.11	0.05	0.39	2.01	33.92	0.09	0.03	0.03	0.03	0.02
7.14	0.67	0.11	0.15	0.41	2.29	32.82	0.09	0.03	0.03	0.03	0.05
10.00	0.87	0.13	0.30	0.44	2.60	31.84	0.09	0.03	0.03	0.03	0.09
12.86	1.13	0.14	0.49	0.50	2.89	31.05	0.09	0.03	0.03	0.03	0.14
15.71	1.44	0.16	0.71	0.57	3.15	30.41	0.09	0.03	0.03	0.03	0.21
18.57	1.88	0.18	1.02	0.67	3.45	29.52	0.09	0.03	0.03	0.03	0.30
21.43	1.94	0.19	1.07	0.68	3.59	33.10	0.10	0.03	0.03	0.03	0.45
24.29	1.95	0.19	1.09	0.67	3.68	38.65	0.12	0.04	0.04	0.04	0.65
27.14	1.96	0.19	1.10	0.67	3.70	45.07	0.13	0.04	0.04	0.04	0.89
30.00	1.96	0.19	1.11	0.66	3.66	51.44	0.16	0.05	0.05	0.05	1.17
32.86	1.97	0.20	1.11	0.66	3.57	56.56	0.17	0.06	0.06	0.05	1.45
35.71	1.97	0.20	1.12	0.65	3.45	61.75	0.19	0.06	0.06	0.06	1.77
38.57	1.98	0.20	1.13	0.65	3.26	68.83	0.21	0.07	0.07	0.06	2.18
41.43	2.00	0.20	1.15	0.65	3.05	76.84	0.23	0.08	0.08	0.07	2.68
44.29	2.02	0.21	1.16	0.65	2.85	81.46	0.25	0.09	0.09	0.07	3.29
50.00	1.97	0.20	1.14	0.63	2.78	78.40	0.27	0.09	0.09	0.08	4.54
52.86	1.94	0.20	1.13	0.61	2.81	77.66	0.29	0.10	0.10	0.08	5.39
55.71	1.89	0.20	1.10	0.59	2.80	68.38	0.29	0.10	0.10	0.09	6.44
58.57	1.83	0.20	1.06	0.58	2.80	57.01	0.29	0.09	0.09	0.09	7.49
61.43	1.77	0.19	1.02	0.56	2.90	47.70	0.29	0.09	0.09	0.09	8.61
64.29	1.71	0.19	0.98	0.55	3.02	40.85	0.29	0.09	0.09	0.09	9.80
67.14	1.66	0.19	0.93	0.54	3.11	36.03	0.30	0.09	0.09	0.09	11.08
70.00	1.60	0.19	0.89	0.52	3.18	32.62	0.30	0.09	0.09	0.09	12.44
72.86	1.54	0.18	0.84	0.51	3.23	29.98	0.29	0.09	0.09	0.09	13.92
75.71	1.48	0.18	0.79	0.50	3.25	27.75	0.29	0.09	0.09	0.09	15.51
81.43	1.34	0.17	0.68	0.48	3.20	23.84	0.27	0.08	0.08	0.08	18.97
84.29	1.26	0.17	0.62	0.46	3.13	21.81	0.25	0.08	0.08	0.08	20.95
87.14	1.18	0.17	0.56	0.45	3.03	19.71	0.23	0.07	0.07	0.07	23.03

Table D3 Continued

90.00	1.10	0.16	0.50	0.44	2.88	17.51	0.20	0.06	0.06	0.06	25.20
92.86	1.02	0.16	0.44	0.43	2.70	15.21	0.15	0.05	0.05	0.05	27.45
95.71	0.94	0.15	0.38	0.41	2.49	12.88	0.10	0.03	0.03	0.03	29.71
98.57	0.85	0.15	0.30	0.40	2.20	10.00	0.03	0.01	0.01	0.01	32.50

Table D4

Low flow conditions (November) with flow from Vernalis for the San Joaquin River with Delta removal effect and 38 mol d^{-1} of refinery input (57 % as selenate)

Distance (km)	D ΣSe (nmol L^{-1})	D Se IV (nmol L^{-1})	D Se VI (nmol L^{-1})	D Org. Se -II (nmol L^{-1})	Phyto (µg L^{-1})	TSM (mg L^{-1})	P. ΣSe (nmol L^{-1})	P. Se O (nmol L^{-1})	P. Se IV+VI (nmol L^{-1})	P. Org. Se -II (nmol L^{-1})	Salinity
1.43	1.30	0.08	0.86	0.35	1.62	18.00	0.05	0.02	0.01	0.02	0.21
4.29	1.60	0.10	1.10	0.39	1.71	31.84	0.24	0.07	0.12	0.05	0.58
7.14	1.80	0.12	1.25	0.43	1.80	39.80	0.33	0.09	0.16	0.07	0.98
10.00	1.99	0.14	1.38	0.47	1.88	42.88	0.36	0.10	0.18	0.08	1.44
12.86	2.15	0.16	1.48	0.51	1.95	41.85	0.36	0.10	0.17	0.09	1.91
15.71	2.30	0.17	1.58	0.55	2.00	40.26	0.35	0.09	0.17	0.09	2.35
18.57	2.50	0.19	1.70	0.61	2.07	37.29	0.33	0.09	0.15	0.09	2.91
21.43	2.54	0.21	1.72	0.62	1.98	33.44	0.30	0.07	0.13	0.09	3.68
24.29	2.55	0.22	1.72	0.61	1.85	28.57	0.25	0.06	0.11	0.09	4.54
27.14	2.56	0.22	1.72	0.62	1.71	24.21	0.22	0.05	0.08	0.08	5.41
30.00	2.57	0.23	1.71	0.63	1.56	21.00	0.19	0.04	0.07	0.08	6.28
32.86	2.59	0.24	1.70	0.64	1.43	19.03	0.17	0.03	0.06	0.08	7.05
35.71	2.60	0.25	1.70	0.65	1.31	17.84	0.16	0.03	0.05	0.08	7.75
38.57	2.61	0.25	1.69	0.66	1.16	16.77	0.15	0.03	0.04	0.08	8.62
41.43	2.62	0.26	1.68	0.68	1.00	15.73	0.14	0.03	0.04	0.08	9.62
44.29	2.63	0.27	1.67	0.70	0.85	14.66	0.14	0.02	0.03	0.08	10.81
50.00	2.54	0.27	1.59	0.68	0.75	13.50	0.13	0.02	0.03	0.08	12.68
52.86	2.47	0.27	1.54	0.66	0.75	13.08	0.13	0.02	0.03	0.08	13.85
55.71	2.36	0.26	1.46	0.64	0.73	12.65	0.12	0.02	0.03	0.08	15.27

Table D4 Continued

Distance (km)	D ΣSe (nmol L^{-1})	D Se IV (nmol L^{-1})	D Se VI (nmol L^{-1})	D Org. Se -II (nmol L^{-1})	Phyto (µg L^{-1})	TSM (mg L^{-1})	P. ΣSe (nmol L^{-1})	P. Se O (nmol L^{-1})	P. Se IV+VI (nmol L^{-1})	P. Org. Se -II (nmol L^{-1})	Salinity
58.57	2.26	0.26	1.38	0.62	0.73	12.35	0.12	0.02	0.03	0.08	16.50
61.43	2.16	0.25	1.30	0.61	0.77	12.12	0.12	0.02	0.03	0.07	17.67
64.29	2.06	0.25	1.22	0.59	0.83	11.93	0.11	0.02	0.03	0.07	18.80
67.14	1.96	0.24	1.15	0.57	0.90	11.75	0.11	0.02	0.02	0.07	19.91
70.00	1.87	0.24	1.08	0.56	0.97	11.60	0.11	0.02	0.02	0.07	20.98
72.86	1.78	0.23	1.00	0.54	1.04	11.44	0.10	0.01	0.02	0.06	22.08
75.71	1.68	0.22	0.93	0.53	1.12	11.28	0.09	0.01	0.02	0.06	23.18
81.43	1.48	0.21	0.78	0.50	1.29	10.97	0.08	0.01	0.02	0.05	25.33
84.29	1.37	0.20	0.69	0.48	1.40	10.81	0.07	0.01	0.02	0.04	26.49
87.14	1.26	0.19	0.61	0.46	1.52	10.64	0.06	0.01	0.02	0.04	27.63
90.00	1.16	0.18	0.53	0.45	1.65	10.48	0.06	0.01	0.01	0.03	28.75
92.86	1.06	0.17	0.46	0.43	1.79	10.33	0.05	0.01	0.01	0.02	29.84
95.71	0.97	0.16	0.39	0.42	1.95	10.19	0.04	0.01	0.01	0.02	30.87
98.57	0.85	0.15	0.30	0.40	2.20	10.00	0.03	0.01	0.01	0.01	32.27

Table D5

High flow conditions (April) with 2000 flow from San Joaquin River and 38 mol d^{-1} of refinery input (57 % as selenate)

Distance (km)	D ΣSe (nmol L^{-1})	D Se IV (nmol L^{-1})	D SeVI (nmol L^{-1})	Dorg. Se -II (nmol L^{-1})	Phyto (µg L^{-1})	TSM (mg L^{-1})	P. ΣSe (nmol L^{-1})	P. Se O (nmol L^{-1})	P. Se VI+VI (nmol L^{-1})	P. Org. Se -II (nmol L^{-1})	Salinity
1.43	0.50	0.11	0.00	0.39	1.75	35.19	0.09	0.04	0.03	0.03	0.00
4.29	0.49	0.10	0.01	0.37	1.95	34.22	0.09	0.04	0.03	0.03	0.02
7.14	0.50	0.10	0.04	0.36	2.19	33.80	0.09	0.04	0.03	0.03	0.05
10.00	0.54	0.11	0.07	0.36	2.45	34.14	0.09	0.03	0.03	0.03	0.10
12.86	0.59	0.11	0.12	0.36	2.67	35.39	0.09	0.04	0.03	0.03	0.17
15.71	0.66	0.11	0.17	0.37	2.85	37.37	0.09	0.04	0.03	0.03	0.27
18.57	0.75	0.12	0.24	0.39	3.05	41.54	0.11	0.04	0.03	0.03	0.41
21.43	0.85	0.13	0.32	0.40	3.22	47.79	0.12	0.05	0.04	0.04	0.60
24.29	0.96	0.13	0.40	0.42	3.33	54.64	0.14	0.05	0.05	0.04	0.83

Table D5 Continued

Distance (km)	D ΣSe (nmol L^{-1})	D Se IV (nmol L^{-1})	D Se VI (nmol L^{-1})	D Org. Se -II (nmol L^{-1})	Phyto (µg L^{-1})	TSM (mg L^{-1})	P. ΣSe (nmol L^{-1})	P. Se IV+VI (nmol L^{-1})	P. Se O (nmol L^{-1})	P. Org. Se -II (nmol L^{-1})	Salinity
27.14	1.07	0.14	0.48	0.44	3.38	60.73	0.16	0.06	0.05	0.05	1.11
30.00	1.17	0.15	0.56	0.46	3.35	65.38	0.18	0.07	0.06	0.05	1.42
32.86	1.26	0.16	0.62	0.48	3.28	68.31	0.20	0.07	0.07	0.06	1.74
35.71	1.34	0.16	0.68	0.50	3.17	71.40	0.21	0.08	0.07	0.06	2.09
38.57	1.43	0.17	0.74	0.52	2.99	75.41	0.23	0.08	0.08	0.07	2.52
41.43	1.53	0.18	0.81	0.54	2.80	78.93	0.25	0.09	0.08	0.07	3.05
44.29	1.64	0.19	0.88	0.57	2.63	77.97	0.26	0.10	0.09	0.08	3.69
50.00	1.71	0.19	0.95	0.57	2.63	69.07	0.27	0.10	0.09	0.08	4.98
52.86	1.74	0.19	0.98	0.57	2.70	65.78	0.28	0.10	0.09	0.08	5.85
55.71	1.74	0.19	0.99	0.56	2.74	56.77	0.28	0.10	0.09	0.08	6.92
58.57	1.73	0.19	0.98	0.56	2.78	47.87	0.28	0.10	0.09	0.08	7.98
61.43	1.71	0.19	0.97	0.55	2.92	41.16	0.28	0.10	0.09	0.09	9.10
64.29	1.68	0.19	0.95	0.54	3.09	36.36	0.28	0.10	0.09	0.09	10.30
67.14	1.64	0.19	0.92	0.53	3.22	32.93	0.28	0.10	0.09	0.09	11.58
70.00	1.60	0.19	0.89	0.53	3.31	30.37	0.28	0.10	0.09	0.09	12.94
72.86	1.55	0.18	0.85	0.52	3.37	28.25	0.27	0.10	0.08	0.08	14.41
75.71	1.50	0.18	0.81	0.51	3.39	26.33	0.27	0.10	0.08	0.08	15.99
81.43	1.36	0.18	0.70	0.48	3.34	22.74	0.25	0.09	0.08	0.08	19.42
84.29	1.28	0.17	0.64	0.47	3.26	20.83	0.23	0.09	0.07	0.07	21.36
87.14	1.20	0.17	0.58	0.46	3.14	18.85	0.20	0.08	0.06	0.06	23.39
90.00	1.12	0.16	0.52	0.44	2.97	16.81	0.17	0.07	0.05	0.05	25.49
92.86	1.04	0.16	0.45	0.43	2.76	14.69	0.14	0.05	0.04	0.04	27.67
95.71	0.95	0.16	0.38	0.42	2.53	12.57	0.09	0.04	0.03	0.03	29.84
98.57	0.85	0.15	0.30	0.40	2.20	10.00	0.03	0.01	0.01	0.01	32.50

Table D6

Low flow conditions (November) with 2000 flow from San Joaquin River and 38 mol d^{-1} of refinery input (57 % as selenate)

Distance (km)	D ΣSe (nmol L^{-1})	D Se IV (nmol L^{-1})	D Se VI (nmol L^{-1})	D Org. Se -II (nmol L^{-1})	Phyto (µg L^{-1})	TSM (mg L^{-1})	P. ΣSe (nmol L^{-1})	P. Se O (nmol L^{-1})	P. Se VI+VI (nmol L^{-1})	P. Org. Se -II (nmol L^{-1})	Salinity
1.43	1.23	0.08	0.81	0.34	1.58	18.00	0.05	0.02	0.01	0.02	0.24
4.29	1.43	0.09	0.97	0.37	1.60	26.72	0.19	0.06	0.08	0.05	0.73
7.14	1.52	0.10	1.04	0.39	1.61	30.73	0.24	0.08	0.10	0.06	1.29
10.00	1.58	0.11	1.07	0.41	1.61	31.35	0.25	0.08	0.10	0.06	1.94
12.86	1.62	0.12	1.08	0.42	1.60	29.85	0.23	0.07	0.09	0.06	2.61
15.71	1.66	0.13	1.10	0.43	1.57	28.37	0.22	0.07	0.09	0.06	3.27
18.57	1.70	0.14	1.11	0.45	1.52	26.34	0.20	0.06	0.08	0.06	4.12
21.43	1.74	0.15	1.12	0.47	1.45	23.67	0.17	0.05	0.06	0.06	5.06
24.29	1.78	0.16	1.13	0.49	1.37	21.16	0.14	0.04	0.05	0.06	6.04
27.14	1.82	0.17	1.14	0.50	1.28	19.30	0.13	0.03	0.04	0.05	7.02
30.00	1.86	0.18	1.15	0.52	1.17	18.04	0.12	0.03	0.04	0.05	7.97
32.86	1.89	0.19	1.16	0.54	1.08	17.25	0.11	0.03	0.03	0.05	8.79
35.71	1.92	0.20	1.17	0.55	1.00	16.74	0.11	0.02	0.03	0.05	9.53
38.57	1.95	0.20	1.18	0.57	0.89	16.23	0.11	0.02	0.03	0.05	10.44
41.43	1.98	0.21	1.19	0.58	0.77	15.73	0.11	0.02	0.03	0.05	11.47
44.29	2.03	0.22	1.20	0.61	0.67	15.21	0.10	0.02	0.03	0.06	12.67
50.00	1.98	0.22	1.16	0.59	0.62	14.54	0.10	0.02	0.03	0.06	14.53
52.86	1.93	0.22	1.13	0.58	0.64	14.21	0.10	0.02	0.03	0.06	15.68
55.71	1.86	0.22	1.08	0.56	0.65	13.83	0.10	0.02	0.03	0.06	17.04
58.57	1.78	0.22	1.02	0.55	0.67	13.52	0.10	0.02	0.03	0.05	18.21
61.43	1.71	0.22	0.96	0.54	0.72	13.24	0.10	0.02	0.03	0.05	19.31
64.29	1.65	0.21	0.91	0.53	0.80	12.98	0.10	0.02	0.03	0.05	20.36
67.14	1.58	0.21	0.86	0.52	0.88	12.73	0.09	0.02	0.03	0.05	21.38
70.00	1.52	0.21	0.81	0.51	0.95	12.49	0.09	0.02	0.02	0.05	22.36
72.86	1.46	0.20	0.76	0.50	1.03	12.24	0.09	0.02	0.02	0.05	23.35
75.71	1.40	0.20	0.72	0.49	1.12	11.99	0.08	0.02	0.02	0.04	24.34
81.43	1.27	0.19	0.61	0.46	1.30	11.50	0.07	0.01	0.02	0.04	26.24
84.29	1.19	0.18	0.56	0.45	1.40	11.24	0.06	0.01	0.02	0.03	27.26
87.14	1.12	0.18	0.51	0.44	1.52	10.99	0.06	0.01	0.02	0.03	28.25
90.00	1.05	0.17	0.45	0.43	1.65	10.74	0.05	0.01	0.01	0.02	29.22
92.86	0.99	0.16	0.40	0.42	1.79	10.50	0.04	0.01	0.01	0.02	30.17

Table D6 Continued

Distance (km)	D ΣSe (nmol L^{-1})	D Se IV (nmol L^{-1})	D Se VI (nmol L^{-1})	D Org. Se -II (nmol L^{-1})	Phyto (µg L^{-1})	TSM (mg L^{-1})	P. ΣSe (nmol L^{-1})	P. Se IV+VI (nmol L^{-1})	P. Se O (nmol L^{-1})	P. Org. Se -II (nmol L^{-1})	Salinity
95.71	0.93	0.16	0.36	0.41	1.95	10.28	0.03	0.01	0.01	0.01	31.06
98.57	0.85	0.15	0.30	0.40	2.20	10.00	0.03	0.01	0.01	0.01	32.27

Table D7

High flow conditions (April) with 2000 flow for both river and no refinery inputs

Distance (km)	D ΣSe (nmol L^{-1})	D Se IV (nmol L^{-1})	D Se VI (nmol L^{-1})	D Org. Se -II (nmol L^{-1})	Phyto (µg L^{-1})	TSM (mg L^{-1})	P. ΣSe (nmol L^{-1})	P. Se O (nmol L^{-1})	P. Se VI+VI (nmol L^{-1})	P. Org. Se -II (nmol L^{-1})	Salinity
1.43	0.50	0.11	0.00	0.39	1.75	35.19	0.09	0.04	0.03	0.03	0.00
4.29	0.49	0.10	0.01	0.37	1.94	34.22	0.09	0.04	0.03	0.03	0.02
7.14	0.50	0.10	0.03	0.36	2.17	33.80	0.09	0.04	0.03	0.03	0.05
10.00	0.53	0.11	0.07	0.36	2.41	34.14	0.09	0.03	0.03	0.03	0.10
12.86	0.57	0.11	0.11	0.36	2.62	35.39	0.09	0.04	0.03	0.03	0.17
15.71	0.63	0.11	0.15	0.36	2.80	37.37	0.09	0.04	0.03	0.03	0.27
18.57	0.70	0.11	0.21	0.37	2.98	41.53	0.10	0.04	0.03	0.03	0.41
21.43	0.78	0.12	0.28	0.38	3.14	47.79	0.12	0.05	0.04	0.04	0.60
24.29	0.87	0.12	0.35	0.39	3.24	54.64	0.14	0.05	0.05	0.04	0.83
27.14	0.94	0.13	0.41	0.40	3.28	60.73	0.16	0.06	0.05	0.05	1.11
30.00	1.01	0.13	0.47	0.41	3.25	65.38	0.18	0.07	0.06	0.05	1.42
32.86	1.07	0.14	0.51	0.42	3.18	68.31	0.20	0.07	0.06	0.06	1.74
35.71	1.12	0.14	0.55	0.43	3.07	71.40	0.21	0.08	0.07	0.06	2.09
38.57	1.17	0.14	0.59	0.43	2.90	75.41	0.22	0.08	0.07	0.06	2.52
41.43	1.22	0.15	0.63	0.44	2.71	78.93	0.24	0.09	0.08	0.07	3.05
44.29	1.27	0.15	0.67	0.45	2.54	77.97	0.25	0.10	0.08	0.07	3.69
50.00	1.33	0.15	0.72	0.46	2.54	69.07	0.27	0.10	0.09	0.08	4.98
52.86	1.36	0.16	0.75	0.46	2.61	65.78	0.27	0.10	0.09	0.08	5.85
55.71	1.39	0.16	0.77	0.46	2.64	56.77	0.27	0.10	0.09	0.08	6.92
58.57	1.40	0.16	0.78	0.46	2.68	47.87	0.27	0.10	0.09	0.08	7.98

Table D7 Continued

Distance (km)	D ΣSe (nmol L^{-1})	D Se IV (nmol L^{-1})	D Se VI (nmol L^{-1})	D Org. Se -II (nmol L^{-1})	Phyto (µg L^{-1})	TSM (mg L^{-1})	P. ΣSe (nmol L^{-1})	P. Se IV+VI (nmol L^{-1})	P. Se O (nmol L^{-1})	P. Org. Se -II (nmol L^{-1})	Salinity
61.43	1.40	0.16	0.78	0.46	2.82	41.16	0.27	0.10	0.09	0.08	9.10
64.29	1.40	0.16	0.77	0.46	2.98	36.36	0.27	0.10	0.09	0.08	10.30
67.14	1.38	0.16	0.76	0.46	3.10	32.93	0.27	0.10	0.09	0.08	11.58
70.00	1.36	0.16	0.74	0.46	3.20	30.37	0.27	0.10	0.08	0.08	12.94
72.86	1.33	0.16	0.71	0.45	3.26	28.25	0.27	0.10	0.08	0.08	14.41
75.71	1.29	0.16	0.68	0.45	3.29	26.33	0.26	0.10	0.08	0.08	15.99
81.43	1.21	0.16	0.61	0.44	3.25	22.74	0.24	0.09	0.08	0.07	19.42
84.29	1.16	0.16	0.56	0.43	3.18	20.83	0.22	0.09	0.07	0.07	21.36
87.14	1.10	0.16	0.52	0.43	3.07	18.85	0.20	0.08	0.06	0.06	23.39
90.00	1.04	0.16	0.47	0.42	2.91	16.81	0.17	0.07	0.05	0.05	25.49
92.86	0.98	0.16	0.42	0.41	2.72	14.69	0.14	0.05	0.04	0.04	27.67
95.71	0.92	0.15	0.36	0.41	2.50	12.57	0.09	0.04	0.03	0.03	29.84
98.57	0.85	0.15	0.30	0.40	2.20	10.00	0.03	0.01	0.01	0.01	32.50

Table D8

Low flow conditions (November) with 2000 flow for both river and no refinery inputs

Distance (km)	D ΣSe (nmol L^{-1})	D Se IV (nmol L^{-1})	D Se VI (nmol L^{-1})	D Org. Se -II (nmol L^{-1})	Phyto (µg L^{-1})	TSM (mg L^{-1})	P. ΣSe (nmol L^{-1})	P. Se O (nmol L^{-1})	P. Se VI+VI (nmol L^{-1})	P. Org. Se -II (nmol L^{-1})	Salinity
1.43	1.22	0.08	0.81	0.33	1.58	18.00	0.05	0.02	0.01	0.02	0.24
4.29	1.39	0.08	0.95	0.36	1.60	26.72	0.18	0.06	0.07	0.04	0.73
7.14	1.44	0.09	0.99	0.37	1.61	30.73	0.23	0.08	0.09	0.06	1.29
10.00	1.46	0.09	1.00	0.37	1.61	31.35	0.23	0.08	0.09	0.06	1.94
12.86	1.46	0.10	0.99	0.37	1.60	29.85	0.22	0.07	0.08	0.06	2.61
15.71	1.45	0.10	0.98	0.38	1.57	28.37	0.20	0.07	0.08	0.06	3.27
18.57	1.44	0.11	0.96	0.38	1.52	26.34	0.18	0.06	0.07	0.05	4.12
21.43	1.42	0.11	0.93	0.38	1.45	23.67	0.15	0.05	0.06	0.05	5.06
24.29	1.40	0.11	0.91	0.38	1.37	21.16	0.13	0.04	0.05	0.04	6.04

Table D8 Continued

Distance (km)	D ΣSe (nmol L^{-1})	D Se IV (nmol L^{-1})	D Se VI (nmol L^{-1})	D Org. Se -II (nmol L^{-1})	Phyto (µg L^{-1})	TSM (mg L^{-1})	P. ΣSe (nmol L^{-1})	P. Se IV+VI (nmol L^{-1})	P. Se O (nmol L^{-1})	P. Org. Se -II (nmol L^{-1})	Salinity
27.14	1.38	0.12	0.88	0.38	1.28	19.30	0.11	0.03	0.04	0.04	7.02
30.00	1.36	0.12	0.86	0.37	1.17	18.04	0.10	0.03	0.03	0.04	7.97
32.86	1.34	0.12	0.84	0.37	1.08	17.25	0.09	0.03	0.03	0.04	8.79
35.71	1.32	0.13	0.82	0.37	1.00	16.74	0.09	0.02	0.03	0.04	9.53
38.57	1.30	0.13	0.80	0.37	0.89	16.23	0.09	0.02	0.03	0.04	10.44
41.43	1.27	0.13	0.77	0.37	0.77	15.73	0.09	0.02	0.03	0.04	11.47
44.29	1.25	0.13	0.74	0.37	0.67	15.21	0.08	0.02	0.03	0.04	12.67
50.00	1.20	0.14	0.69	0.37	0.62	14.54	0.08	0.02	0.02	0.04	14.53
52.86	1.18	0.14	0.67	0.37	0.64	14.21	0.08	0.02	0.02	0.04	15.68
55.71	1.15	0.14	0.63	0.37	0.65	13.83	0.08	0.02	0.02	0.04	17.04
58.57	1.12	0.14	0.61	0.37	0.67	13.52	0.08	0.02	0.02	0.04	18.21
61.43	1.10	0.15	0.58	0.37	0.72	13.24	0.08	0.02	0.02	0.04	19.31
64.29	1.08	0.15	0.55	0.37	0.80	12.98	0.08	0.02	0.02	0.04	20.36
67.14	1.05	0.15	0.53	0.37	0.88	12.73	0.07	0.02	0.02	0.03	21.38
70.00	1.03	0.15	0.51	0.38	0.95	12.49	0.07	0.02	0.02	0.03	22.36
72.86	1.02	0.15	0.49	0.38	1.03	12.24	0.07	0.02	0.02	0.03	23.35
75.71	1.00	0.15	0.47	0.38	1.12	11.99	0.06	0.02	0.02	0.03	24.34
81.43	0.96	0.15	0.42	0.38	1.30	11.50	0.06	0.01	0.02	0.03	26.24
84.29	0.94	0.15	0.40	0.39	1.40	11.24	0.05	0.01	0.02	0.02	27.26
87.14	0.92	0.15	0.38	0.39	1.52	10.99	0.05	0.01	0.01	0.02	28.25
90.00	0.90	0.15	0.36	0.39	1.65	10.74	0.04	0.01	0.01	0.02	29.22
92.86	0.89	0.15	0.34	0.39	1.79	10.50	0.04	0.01	0.01	0.01	30.17
95.71	0.87	0.15	0.32	0.40	1.95	10.28	0.03	0.01	0.01	0.01	31.06
98.57	0.85	0.15	0.30	0.40	2.20	10.00	0.03	0.01	0.01	0.01	32.27

Table D9

High flow conditions (April) with 2000 flow for both river and 99 mol d^{-1} total discharge with 57 % as selenate

Distance (km)	D ΣSe (nmol L^{-1})	D Se IV (nmol L^{-1})	D Se VI (nmol L^{-1})	D Org. Se -II (nmol L^{-1})	Phyto (µg L^{-1})	TSM (mg L^{-1})	P. ΣSe (nmol L^{-1})	P. Se O (nmol L^{-1})	P. Se VI+VI (nmol L^{-1})	P. Org. Se -II (nmol L^{-1})	Salinity
1.43	0.50	0.11	0.00	0.39	1.75	35.19	0.09	0.04	0.03	0.03	0.00
4.29	0.49	0.10	0.01	0.37	1.94	34.22	0.09	0.04	0.03	0.03	0.02
7.14	0.51	0.11	0.04	0.37	2.17	33.80	0.09	0.04	0.03	0.03	0.05
10.00	0.55	0.11	0.08	0.36	2.41	34.14	0.09	0.03	0.03	0.03	0.10
12.86	0.61	0.11	0.12	0.37	2.62	35.39	0.09	0.04	0.03	0.03	0.17
15.71	0.68	0.12	0.18	0.38	2.80	37.37	0.09	0.04	0.03	0.03	0.27
18.57	0.78	0.13	0.25	0.40	2.98	41.53	0.11	0.04	0.03	0.03	0.41
21.43	0.90	0.14	0.34	0.42	3.14	47.79	0.12	0.05	0.04	0.04	0.60
24.29	1.02	0.15	0.43	0.44	3.24	54.64	0.15	0.05	0.05	0.04	0.83
27.14	1.15	0.16	0.52	0.47	3.28	60.73	0.17	0.06	0.06	0.05	1.11
30.00	1.27	0.18	0.60	0.50	3.25	65.38	0.19	0.07	0.06	0.05	1.42
32.86	1.38	0.19	0.67	0.53	3.18	68.31	0.20	0.07	0.07	0.06	1.74
35.71	1.49	0.20	0.74	0.55	3.07	71.40	0.21	0.08	0.07	0.06	2.09
38.57	1.61	0.21	0.81	0.58	2.90	75.41	0.23	0.08	0.08	0.07	2.52
41.43	1.75	0.23	0.90	0.61	2.71	78.93	0.25	0.09	0.09	0.07	3.05
44.29	1.88	0.25	0.98	0.65	2.54	77.97	0.26	0.10	0.09	0.08	3.69
50.00	2.01	0.26	1.09	0.66	2.54	69.07	0.27	0.10	0.09	0.08	4.98
52.86	2.09	0.26	1.16	0.67	2.61	65.78	0.28	0.10	0.09	0.08	5.85
55.71	2.13	0.26	1.19	0.67	2.64	56.77	0.28	0.10	0.09	0.09	6.92
58.57	2.11	0.26	1.18	0.66	2.68	47.87	0.28	0.10	0.09	0.09	7.98
61.43	2.07	0.26	1.16	0.65	2.82	41.16	0.28	0.10	0.09	0.09	9.10
64.29	2.03	0.25	1.13	0.64	2.98	36.36	0.28	0.10	0.09	0.09	10.30
67.14	1.98	0.25	1.10	0.63	3.10	32.93	0.28	0.10	0.09	0.09	11.58
70.00	1.92	0.24	1.06	0.62	3.20	30.37	0.28	0.10	0.09	0.09	12.94
72.86	1.86	0.24	1.02	0.60	3.26	28.25	0.28	0.10	0.09	0.09	14.41
75.71	1.80	0.24	0.97	0.59	3.29	26.33	0.27	0.10	0.08	0.09	15.99
81.43	1.59	0.22	0.83	0.55	3.25	22.74	0.25	0.09	0.08	0.08	19.42
84.29	1.48	0.21	0.75	0.52	3.18	20.83	0.23	0.09	0.07	0.07	21.36
87.14	1.36	0.20	0.66	0.50	3.07	18.85	0.21	0.08	0.06	0.07	23.39
90.00	1.24	0.18	0.58	0.47	2.91	16.81	0.18	0.07	0.05	0.06	25.49
92.86	1.11	0.17	0.49	0.45	2.72	14.69	0.14	0.05	0.04	0.04	27.67

Table D9 Continued

Distance (km)	D ΣSe (nmol L^{-1})	D Se IV (nmol L^{-1})	D Se VI (nmol L^{-1})	D Org. Se -II (nmol L^{-1})	Phyto (µg L^{-1})	TSM (mg L^{-1})	P. ΣSe (nmol L^{-1})	P. Se IV+VI (nmol L^{-1})	P. Se O (nmol L^{-1})	P. Org. Se -II (nmol L^{-1})	Salinity
95.71	0.99	0.16	0.40	0.43	2.50	12.57	0.09	0.04	0.03	0.03	29.84
98.57	0.85	0.15	0.30	0.40	2.20	10.00	0.03	0.01	0.01	0.01	32.50

Table D10

Low flow conditions (November) with 2000 flow for both river and 99 mol d^{-1} total discharge with 57 % as selenate

Distance (km)	D ΣSe (nmol L^{-1})	D Se IV (nmol L^{-1})	D Se VI (nmol L^{-1})	D Org. Se -II (nmol L^{-1})	Phyto (µg L^{-1})	TSM (mg L^{-1})	P. ΣSe (nmol L^{-1})	P. Se O (nmol L^{-1})	P. Se VI+VI (nmol L^{-1})	P. Org. Se -II (nmol L^{-1})	Salinity
1.43	1.25	0.08	0.82	0.34	1.58	18.00	0.05	0.02	0.01	0.02	0.24
4.29	1.47	0.10	0.99	0.38	1.60	26.72	0.20	0.06	0.09	0.05	0.73
7.14	1.59	0.12	1.07	0.41	1.61	30.73	0.26	0.08	0.12	0.06	1.29
10.00	1.68	0.13	1.11	0.43	1.61	31.35	0.27	0.08	0.12	0.07	1.94
12.86	1.76	0.15	1.14	0.46	1.60	29.85	0.25	0.07	0.11	0.07	2.61
15.71	1.82	0.17	1.17	0.48	1.57	28.37	0.24	0.07	0.10	0.07	3.27
18.57	1.90	0.19	1.20	0.51	1.52	26.34	0.22	0.06	0.09	0.07	4.12
21.43	1.99	0.22	1.24	0.54	1.45	23.67	0.19	0.05	0.07	0.07	5.06
24.29	2.08	0.24	1.27	0.57	1.37	21.16	0.17	0.04	0.06	0.07	6.04
27.14	2.17	0.26	1.30	0.60	1.28	19.30	0.15	0.03	0.05	0.07	7.02
30.00	2.26	0.29	1.33	0.63	1.17	18.04	0.14	0.03	0.04	0.07	7.97
32.86	2.33	0.30	1.36	0.66	1.08	17.25	0.14	0.03	0.04	0.07	8.79
35.71	2.39	0.32	1.39	0.69	1.00	16.74	0.14	0.02	0.04	0.07	9.53
38.57	2.47	0.34	1.42	0.71	0.89	16.23	0.13	0.02	0.04	0.07	10.44
41.43	2.56	0.36	1.45	0.75	0.77	15.73	0.13	0.02	0.04	0.07	11.47
44.29	2.65	0.38	1.48	0.79	0.67	15.21	0.13	0.02	0.04	0.08	12.67
50.00	2.67	0.39	1.50	0.78	0.62	14.54	0.13	0.02	0.04	0.08	14.53
52.86	2.67	0.38	1.51	0.77	0.64	14.21	0.13	0.02	0.04	0.08	15.68
55.71	2.64	0.38	1.49	0.77	0.65	13.83	0.13	0.02	0.03	0.08	17.04
58.57	2.54	0.38	1.41	0.75	0.67	13.52	0.13	0.02	0.03	0.08	18.21

Table D10 Continued

Distance (km)	D ΣSe (nmol L^{-1})	D Se IV (nmol L^{-1})	D Se VI (nmol L^{-1})	D Org. Se -II (nmol L^{-1})	Phyto (µg L^{-1})	TSM (mg L^{-1})	P. ΣSe (nmol L^{-1})	P. Se IV+VI (nmol L^{-1})	P. Se O (nmol L^{-1})	P. Org. Se -II (nmol L^{-1})	Salinity
61.43	2.42	0.37	1.34	0.72	0.72	13.24	0.13	0.02	0.03	0.08	19.31
64.29	2.32	0.35	1.26	0.70	0.80	12.98	0.12	0.02	0.03	0.07	20.36
67.14	2.22	0.34	1.20	0.68	0.88	12.73	0.12	0.02	0.03	0.07	21.38
70.00	2.13	0.33	1.13	0.66	0.95	12.49	0.12	0.02	0.03	0.07	22.36
72.86	2.03	0.32	1.07	0.64	1.03	12.24	0.11	0.02	0.03	0.06	23.35
75.71	1.94	0.31	1.00	0.63	1.12	11.99	0.10	0.02	0.03	0.06	24.34
81.43	1.82	0.29	0.92	0.60	1.20	11.75	0.10	0.02	0.03	0.06	25.29
84.29	1.68	0.27	0.84	0.57	1.30	11.50	0.09	0.01	0.02	0.05	26.24
87.14	1.53	0.25	0.74	0.54	1.40	11.24	0.08	0.01	0.02	0.04	27.26
90.00	1.25	0.21	0.56	0.48	1.65	10.74	0.06	0.01	0.02	0.03	29.22
92.86	1.12	0.19	0.48	0.46	1.79	10.50	0.05	0.01	0.01	0.02	30.17
95.71	1.00	0.17	0.40	0.43	1.95	10.28	0.04	0.01	0.01	0.02	31.06
98.57	0.85	0.15	0.30	0.40	2.20	10.00	0.03	0.01	0.01	0.01	32.27

Table D11

Low flow conditions (November) with drought flow (1977) for both river and 99 mol d^{-1} total discharge with 57 % as selenate

Distance (km)	D ΣSe (nmol L^{-1})	D Se IV (nmol L^{-1})	D Se VI (nmol L^{-1})	D Org. Se -II (nmol L^{-1})	Phyto (µg L^{-1})	TSM (mg L^{-1})	P. ΣSe (nmol L^{-1})	P. Se O (nmol L^{-1})	P. Se VI+VI (nmol L^{-1})	P. Org. Se - II (nmol L^{-1})	Salinity
1.43	1.75	0.32	0.80	0.64	1.15	10.05	0.04	0.01	0.01	0.01	1.00
4.29	1.85	0.37	0.85	0.64	1.21	13.06	0.04	0.02	0.01	0.01	6.98
7.14	2.50	0.48	1.28	0.74	1.09	11.12	0.09	0.01	0.02	0.05	9.58
10.00	2.88	0.53	1.54	0.80	1.05	9.58	0.12	0.01	0.03	0.08	11.04
12.86	3.17	0.57	1.74	0.85	1.04	8.54	0.14	0.01	0.03	0.10	12.05
15.71	3.37	0.59	1.89	0.89	1.06	7.91	0.15	0.01	0.04	0.11	12.72
18.57	3.53	0.61	2.00	0.92	1.08	7.55	0.17	0.01	0.04	0.12	13.21
21.43	3.70	0.62	2.11	0.97	1.13	7.22	0.17	0.01	0.04	0.13	13.67
24.29	3.72	0.64	2.11	0.97	1.01	7.30	0.19	0.01	0.04	0.14	14.75

Table D11 Continued

Distance (km)	D ΣSe (nmol L^{-1})	D Se IV (nmol L^{-1})	D Se VI (nmol L^{-1})	D Org. Se -II (nmol L^{-1})	Phyto (µg L^{-1})	TSM (mg L^{-1})	P. ΣSe (nmol L^{-1})	P. Se IV+VI (nmol L^{-1})	P. Se O (nmol L^{-1})	P. Org. Se -II (nmol L^{-1})	Salinity
27.14	3.71	0.65	2.08	0.98	0.87	7.50	0.20	0.01	0.05	0.14	15.90
30.00	3.70	0.67	2.05	0.98	0.76	7.71	0.20	0.01	0.05	0.15	16.95
32.86	3.70	0.68	2.03	0.99	0.66	7.90	0.21	0.01	0.05	0.15	17.87
35.71	3.70	0.68	2.01	1.00	0.59	8.06	0.21	0.01	0.05	0.15	18.61
38.57	3.70	0.69	2.00	1.01	0.53	8.19	0.21	0.01	0.05	0.15	19.23
41.43	3.70	0.69	1.98	1.02	0.47	8.34	0.20	0.01	0.05	0.14	19.97
44.29	3.70	0.70	1.97	1.04	0.41	8.50	0.20	0.01	0.05	0.14	20.76
50.00	3.69	0.70	1.94	1.05	0.35	8.67	0.20	0.01	0.05	0.14	21.64
52.86	3.55	0.67	1.88	1.01	0.35	8.91	0.19	0.01	0.05	0.13	22.92
55.71	3.47	0.64	1.85	0.98	0.38	9.05	0.18	0.01	0.05	0.12	23.67
58.57	3.33	0.62	1.77	0.95	0.42	9.19	0.17	0.01	0.05	0.12	24.53
61.43	3.14	0.59	1.65	0.90	0.45	9.30	0.17	0.01	0.04	0.11	25.24
64.29	2.95	0.55	1.54	0.86	0.52	9.40	0.16	0.01	0.04	0.11	25.87
67.14	2.77	0.52	1.43	0.82	0.60	9.48	0.15	0.01	0.04	0.10	26.46
70.00	2.61	0.49	1.33	0.78	0.69	9.55	0.14	0.01	0.04	0.09	27.01
72.86	2.46	0.47	1.25	0.75	0.77	9.61	0.13	0.01	0.04	0.09	27.52
75.71	2.32	0.44	1.16	0.72	0.86	9.66	0.12	0.01	0.03	0.08	28.02
81.43	2.18	0.41	1.08	0.69	0.96	9.72	0.11	0.01	0.03	0.07	28.51
84.29	2.02	0.38	0.98	0.66	1.06	9.76	0.10	0.01	0.03	0.07	28.97
87.14	1.84	0.35	0.88	0.62	1.17	9.80	0.09	0.01	0.03	0.06	29.42
90.00	1.66	0.31	0.77	0.57	1.30	9.84	0.08	0.01	0.02	0.05	29.89
92.86	1.32	0.25	0.57	0.50	1.58	9.91	0.06	0.01	0.02	0.03	30.80
95.71	1.16	0.21	0.48	0.47	1.75	9.94	0.05	0.01	0.01	0.02	31.24
98.57	0.85	0.15	0.30	0.40	2.20	10.00	0.03	0.01	0.01	0.02	32.27

VITA

Shannon L. Meseck

EDUCATION

Doctor of Philosophy in Oceanography
Dept. of OEAS, ODU, Norfolk, Virginia 23529 — Dec. 2002

Bachelor of Science in Chemistry and Environmental Science
Dept. of Science, State University of New York at Plattsburgh,
Plattsburgh, New York, 12901 — May 1997

TALKS

Meseck, S.L., L.C., Cutter, and G.A. Cutter. Biogeochemistry of selenium in the San Francisco Bay: Sediment cycling. 2000 Ocean Sciences Meeting, San Antonio, TX (USA), Jan 24-28 2000.

Meseck, S.L., and G.A. Cutter. Biogeochemical cycle of selenium in the San Francisco Bay: A modeling approach. ASLO 2001: American Society of Limnology 2001 Aquatic Sciences Meeting, Albuquerque, NM (USA), Feb. 12-16 2001.

Meseck, S.L. Biogeochemical cycle of selenium in the San Francisco Bay. DISCO XVII. Dissertations Symposium on Chemical Oceanography. May 5-10, 2002.

Meseck and G.A. Cutter. Modeling the biogeochemical cycle of selenium in the San Francisco Bay. 7th International Estuarine Biogeochemistry Symposium. Grimstad, Norway, May 28-30 2002.

POSTERS

Mullikin, S.U., M.A. Doblin, S.L. Meseck, and G.A. Cutter. Estuarine biogeochemistry of selenium: Elemental ratios in food web components. ASLO 2001: American Society of Limnology 2001 Aquatic Sciences Meeting, Albuquerque, NM (USA), Feb. 12-12, 2001.

HONORS AND AWARDS

2002 Recipient of Jacques S. Zaneveld Scholarship, ODU
1999 Recipient of the Maritime Scholarship, ODU
1996 Phi Kappa Phi National Honor Society